Cork Open Research Archive
Cartlann Taighde Oscailte Chorcaí

Title	Mass transfer analysis of gas exchange through microperforated packaging films
Authors	Viana Ramos, Andresa
Publication date	2017
Original Citation	Viana Ramos, A. 2017. Mass transfer analysis of gas exchange through microperforated packaging films. PhD Thesis, University College Cork.
Type of publication	Doctoral thesis
Rights	© 2017, Andresa Viana Ramos. - http://creativecommons.org/licenses/by-nc-nd/3.0/
Download date	2025-06-13 10:10:49
Item downloaded from	https://hdl.handle.net/10468/5421

University College Cork, Ireland
Coláiste na hOllscoile Corcaigh

Ollscoil na hÉireann, Corcaigh
The National University of Ireland, Cork
UNIVERSITY COLLEGE CORK
School of Engineering
Department of Process & Chemical Engineering

Mass Transfer Analysis of Gas Exchange through Microperforated Packaging Films

Andresa Viana Ramos

The thesis is presented to the National University of Ireland in fulfilment of the requirements for the Degree of Doctor of Philosophy (PhD), with the supervision of

Dr. Jorge C. Oliveira

Dr. Maria J. de Sousa Gallagher

Head of Department: Prof Edmond Byrne

September, 2017

DECLARATION

I hereby declare that the present dissertation is my own work and has not been submitted to another degree neither at the University College Cork nor elsewhere. Where the work of others was necessary to build an argument, it was acknowledged and referenced properly.

Andresa Viana Ramos

“Make no mistake, I only achieve

simplicity with enormous effort.

As long as I have questions and no

answers I’ll keep on writing.”

Clarice Lispector

ACKNOWLEDGEMENTS

I would like to acknowledge the financial support provided by the Coordenação de Aperfeiçoamento de Pessoal de Nivel Superior (CAPES), on process number 0449-14-8. The financial support of the Department of Agriculture, Food and the Marine to the projects “Development of Risk assessment tools of package/ product systems for a safe and sustainable food chain” and “Innovative process technology for the fresh produce industry” was also essential to this work and is also recognised.

I would like to express my deepest gratitude to Dr. Jorge Oliveira, for accepting me as his PhD student. I do not have enough words to express my gratitude for all your support, and all the knowledge you have shared with me. This thesis would not be possible without your visionary thinking and your valuable guidance. I have learned a lot from you over these years I have been under your supervision and I am very thankful for this opportunity you gave me.

I would like to thank Dr. Maria de Sousa Gallagher for all the guidance, help and encouragement during my PhD. You have been always very supportive to me and I appreciate all your effort.

Many thanks to the staff of the Department of Process and Chemical Engineering. Without their help and support this work would not be possible. I also would like to thank all the lectures of the Department, who have

always been very kind and supportive not only to me but to all the students in the department.

I would like to thank specially Dr. Denis Ring for your support over this years. I am really grateful for all the opportunities you gave me and the support with the analysis of X-ray diffraction of my samples, which could not be done without your help. I also would like to thank Dr. Abina Crean and Ms. Maryam Mohammadpour for the help with this analysis.

Many thanks to Ms. Fiona Burch and to Avoncourt Packaging Ltd for kindly providing the plastic trays I used in my experiments.

To my family, for the support and encouragement over all these years of study. To my mom, who never let me desist from anything, and to my uncle for paying my English course when I was still a teenager.

To my dear friend Luiz, for being by my side during this journey since college. I am very fortunate for having your friendship and I am very glad we could experience all of that together, I could not have had better company.

To Dr. Edwin Rojas, for giving the opportunity to work with you when I was only starting college and introducing me to the research and for everything I learned from you. I am also thankful to Dr. Veronica Calado and Dr. Carlos Piler for all I have learned during my masters. This thesis is also a reflex of everything I have learned from you. To Dr. Bernardo Costa and Dr Nathália Melo, because if I decided to pursue a PhD I was also inspired by your passion on Food Engineering and due to all I have learned from you. To my friend Dr. Clitor Souza, whose dedication was also an inspiration to me. I really appreciate all the support you have given me and your friendship over these years.

To my dear friends Alejandra, Dr. Lourdes Moralez-Oyervides, Dr. Julio Montanez-Saenz, Rita, Tank, Bárbara, Aoife, Margarida and Dr. Fuweng Zhang for your support and companionship during my PhD; I have learned a lot from all of you. My special thanks to Dr. Julio for introducing me to the experimental procedures in lab when I started my PhD. Also, to my friend Dr. Kashub Tumwesigye, with whom I have spent about two years sharing the office, the labs and many valuable thoughts over our research, and I am very thankful for this valuable time we spent together and for your friendship.

To the UCC Language Centre and to their English teachers, for the opportunity of studying English in UCC, which was essential to the development of this work.

To Mr Aaron Swartz and Ms. Alexandra Elbakyan, for their effort on making science accessible to all.

Finally, to all those who directly or indirectly have collaborated to the development of this work.

ABSTRACT

The primary purpose of this work was to provide robust tools for the design of perforated packaging based on rigorous mathematical methods. A dimensionless correlation was established based on the identification of the variables affecting mass transfer through perforations. It was proved that the diameter of the perforation is the most important parameter. Air velocity and temperature (via its effect on viscosity and density of air) and diffusivity of gases through air are also relevant to this analysis. The Buckingham$-\Pi$ Theorem was applied to identify the dimensionless numbers that provide a dimensionless correlation availing of the principle of dynamic similarity to predict the mass transfer coefficients of both oxygen and water vapour through perforations. As films tend to be much more permeable to water than to oxygen, a study on the effect of water (humidity) on films was also performed. It was found that diffusion and hence permeability can be significantly affected by the water content of the films and therefore the humidity of the atmospheres that the films are exposed to on both sides. A methodology was applied combining the William, Landel and Ferry and the Gordon-Taylor equations with the isotherm of water sorption to obtain the correct effective permeability of films during storage depending on the relative humidity. A methodology was also developed to analyse leakage flow in sealed packages in order to identify the relevant parameters that influence their variability and provide the most robust sealing conditions.

The results on this thesis provide substantial data and rigorous mathematical approaches for a more efficient and accurate packaging design to achieve maximum shelf life.

FOREWORD

Recent reports from the Food and Agriculture Organization of the United Nations suggest that one third of all food produced in the world is lost or wasted, in different stages of the Food Value Chain. Fresh and minimally processed fruits and vegetables are highly perishable and likely to reach great losses on mass and nutritional value during storage to the point of being improper for consumption. However, the normally short shelf-life of these produce can be extended by managing the contents of oxygen, carbon dioxide and relative humidity during storage.

An atmosphere rich in carbon dioxide and poor in oxygen, with suitable relative humidity to minimise water loss by drying (transpiration), is known to be effective for the extension of shelf life of a large number of commodities and there is extensive data in literature on the adequate atmosphere conditions for different products. Every product has a range of concentrations for each gas where the oxygen must be below a certain amount in order to avoid fermentation and carbon dioxide cannot be above a level where it causes damage to the produce or changes in flavour. At the same time, relative humidity should be planned in order to avoid quality loss due to excessive drying. It should be noted that a respiring product will always emit water vapour as a result of respiration; if, however, it also loses its liquid water by evaporation (drying), it will shrivel, lose excessive weight and the appearance of a fresh product.

As soon as the commodity is packed, it is possible to establish the best conditions within the range of gas concentrations that can extend the shelf life to the maximum possible. Engineering packaging design consists in establishing the product and package parameters that combine to equilibrate the packaging permeability and the respiration of the product at protective atmosphere conditions. The internal atmosphere controls the respiration rate (as quantified by various Michaelis-Menten type of models, uninhibited, competitively inhibited, uncompetitively inhibited, etc.) and also the influx of oxygen via the concentration gradient established with the outside *circa* 21%. The lower the oxygen concentration the lower the respiration rate and the higher the gradient and thus the influx of oxygen. As a result, the rate of oxygen consumption stabilizes with the gas entering the package at the desired concentration provided that the package has been designed properly. Similarly, water and carbon dioxide released by respiration also equilibrate with the loss through the package to the outside atmosphere.

Almost all plastic films used to pack these commodities have lower permeability to oxygen, carbon dioxide and even water vapour than the rates of oxygen consumption, carbon dioxide and water release. Hence, the result in terms of humidity is water condensation inside the package which stimulates mould growth and even fermentation, leading to a rapid loss of quality and worse occurs with oxygen, as when it falls below a level that depends on the product anoxia sets in, which could lead to the growth of dangerous pathogens in case the product was contaminated with them.

In order to avoid this problem, macroperforated films have been used to pack fresh commodities. Although they work as a way to eliminate excess water vapour and carbon dioxide and introduce oxygen into the package, it is an underused technology. The perforation profile could be planned to control the composition of the gases inside the package to a protective atmosphere that extends shelf life.

However, this technology lacks reliable data on mass transfer through both films and perforations. The literature on mass transport through perforations is confusing and conflicting. Each work calculates the phenomenon using a different equation and adopting a different principle, from adjusting the diffusivity with a concept named effective length, to giving results that relate the permeability to the area of the each perforation (and as a result, the data is valid only to each specific area). As the films are thin enough for the effect of diffusion to be insignificant, the air flow can be assumed to be mainly due to convective mass transfer. Besides, the mathematical models proposed in literature have another inconvenient that is the lack of dynamic similarity, which makes them useless under conditions other than those applied to the data used on the model development.

In addition, permeability of plastic films are normally obtained under conditions determined by standard methodologies (ASTM). It means that oxygen permeability of many films in literature are determined at 23°C and 0% of relative humidity, and between 23 and 37°C, normally 25°C, and a relative humidity gradient of 90% (or more) for water vapour permeability. Both the inner and outer atmospheres of actual produce packages are far from these conditions, which means that there is little information on barrier properties of plastic films under the real conditions of use of the materials to pack fruits and vegetables, and if they influence the mass transfer properties, a proper design cannot be achieved with these parameters, effective values must be determined.

A final aspect also relevant to the design of modified atmosphere packaging is that seals usually have some leakage. If all the planning is based on the mass transfer through the film and the perforation but there is great variability in the sealing, the design can be compromised by excessive gas transfer through the seal. On the other hand, if the permeance through the seal is a constant parameter, it can be incorporated in the design and the combination film - perforations (if needed) - seal provide the required overall permeance. In this case, it might be more efficient to identify the sealing settings that minimise the variability of the effective permeability of the packages.

Microperforations are a powerful tool to design packages that can prolong shelf life of fresh and minimally processed fruits and vegetables but it is necessary to avail of a better understanding of the mass transfer processes in plastic films and microperforations. This thesis was structured as follows:

1. Analysis of mass transfer through perforations:

Mass transfer through perforations has been quantified in various ways, but most have limited applicability because they do not obey the principle of dynamic similarity. They are reviewed in chapter 2. The first objective of this work was to establish dimensionless correlations involving the relevant parameters using the proper and rigorous method of Π Buckingham Theorem in order to obtain a model able to predict the permeability due to perforations with wide applicability.

In order to apply this model, it is necessary to define which parameters have a significant influence on permeability and this is the specific objective of the fist experimental work described in chapter 3: Determination of the mass transfer coefficient through package perforations and analysis of the most influential parameters.

The next chapter then provides a substantial analysis of experimental data with variation of the parameters previously established to be more relevant, applying Π Buckingham Theorem and determining the best dimensional correlation fitting all data for oxygen transfer. One assumption used in chapter 4 was that the mass transfer coefficient would not depend on the oxygen gradient itself. Chapter 5 then assesses this assumption, determining the value of a variable mass transfer coefficient depending on the concentration gradient. Finally, Chapter 6 presents the experimental data and establishes the dimensionless correlations for water vapour transport.

2. Effect of water on mass transport through plastic films:

The permeability of microperforated films may be modulated by the film itself and therefore determining the effective permeability of polymeric film packages (including its sealing) is equally important. However, there is an over-reliance on accurate ASTM methods, which are presented as material testing tools, but do not necessarily provide the true (or effective) permeability of a package in its actual conditions of use. This is mostly for two reasons: the effect of the humidity (water) in the molecular mobility through the polymer and the fact that seals usually have a significant influence too.

The effect of water content, which will change from the original film to whatever will result from its exposition to the inner and outer package atmospheres (where the inner is bound to be quite humid), can be very significant especially for biobased films. In general, it will be for films with high water vapour permeability. Chapter 7 provides a fundamental approach to the quantification of the impact of relative humidity on the modified atmospheres for two biobased films, Polylactic acid (PLA), the most common of them, and NVS, a new market proposition of the Innovia Packaging Group by using polymer science concepts,.Namely, the WLF and Gordon-Taylor equations are combined with sorption isotherms, resulting in a more fundamentally-based model able to describe permeance through films under any set of humidity conditions.

3. Mass transfer through packaging seals:

A final study is provided on the relevance of seals in the effective permeability of a package. From a practical point of view, the fact that seals may influence the effective permeability due to a non-negligible gas transfer through them is not a problem; provided that it can be quantified, it can be handled just like the permeability through the film itself and through the perforations. The problem that needs to be considered is its variability. Whereas films are fairly homogeneous and perforations can be made accurately with precision (with laser perforation systems), the hermeticity (in permeance) of seal will depend on the operation of the packaging machine and thus can potentially vary from package to package. Chapter 8 applies the Taguchi robust design engineering method to illustrate how a packaging machine can be tuned to operate under the conditions that give minimum variability of the effective package permeability, as influenced by the seals.

This PhD was supported by a grant awarded by the *Coordenação de Aperfeiçoamento de Pessoal de Nível Superior* - Brazil (CAPES) under the process number 0449-14-8, with the research costs met by two projects provided by the Fund Institutional Research Measure (FIRM) of the Department of Agriculture, Food and the Marine, namely “Development of Risk assessment tools of package/ product systems for a safe and sustainable food chain” and “Innovative process technology for the fresh produce industry”, and part of the research work was included in one or the other.

Papers for peer-reviewed journals:

- A meta-study providing a unified analysis of the design engineering methods for modified atmosphere packaging with perforated films for optimum oxygen and carbon dioxide balance (Chapter 2)

- Effect of hydrodynamic conditions and geometric aspects on the permeance perforated packaging films (Chapter 3)

- Dimensionless correlations for estimating the permeability of perforated packaging films to oxygen (Chapter 4)

- Analysis of the influence of the oxygen concentration gradient on the permeance of perforated packaging films (Chapter 5)

- Determination of the mass transfer of water vapour through microperforated packaging films (Chapter 6)

- Analysis of plasticizing and antiplasticizing effects of humidity on the permeability of biobased films to water vapour (Chapter 7)

Chapter 8 was written with a similar format but it is not planned to submit it for publication.

Posters presented in Conferences:

- Ramos, A. V., Oliveira, J. C., Sousa-Gallagher, M. J. Impact of the packing arrangement during storage on the Modified Atmosphere Packaging performance of microperforated packages. In: 4th International Meeting on Material/Bioproduct Interaction – MATBIM. Porto, 2017.

- Ramos, A. V., Oliveira, J. C., Sousa-Gallagher, M. J. Determination of the permeance to water vapour of microperforated packaging films. In: 4th International Meeting on Material/Bioproduct Interaction – MATBIM. Porto, 2017.

- Oliveira, J. C., Ramos, A. V., Sousa-Gallagher, M. J. Influence of relative humidity on the effective permeability of packages resulting from the plasticising effect of water in the polymeric structure. In: 4th International Meeting on Material/Bioproduct Interaction – MATBIM. Porto, 2017.

- Ramos, A. V., Sousa-Gallagher, M. J., Oliveira, J. C. Using dimensionless analysis to describe the permeability of perforated packaging films. In: IUFoST, 2016.

- Ramos, A. V., Sousa-Gallagher, M. J., Oliveira, J. C. Effect of Stacking During Storage on the Permeability of Perforated Packaging Films. In: IUFoST, 2016.

- Ramos, A. V., Sousa-Gallagher, M. J., Oliveira, J. C. Effect of air velocity, perforation diameter and position on the permeability of perforated packaging films .In: 1st Brazil Ireland Science Week, Dublin, Ireland, 2015.

- Ramos, A. V., Sousa-Gallagher, M. J., Oliveira, J. C. Dimensionless Correlations for Estimating the Permeability of Perforated Packaging Films. In: 44th Annual Food Research Conference, 2015.

THESIS STRUCTURE

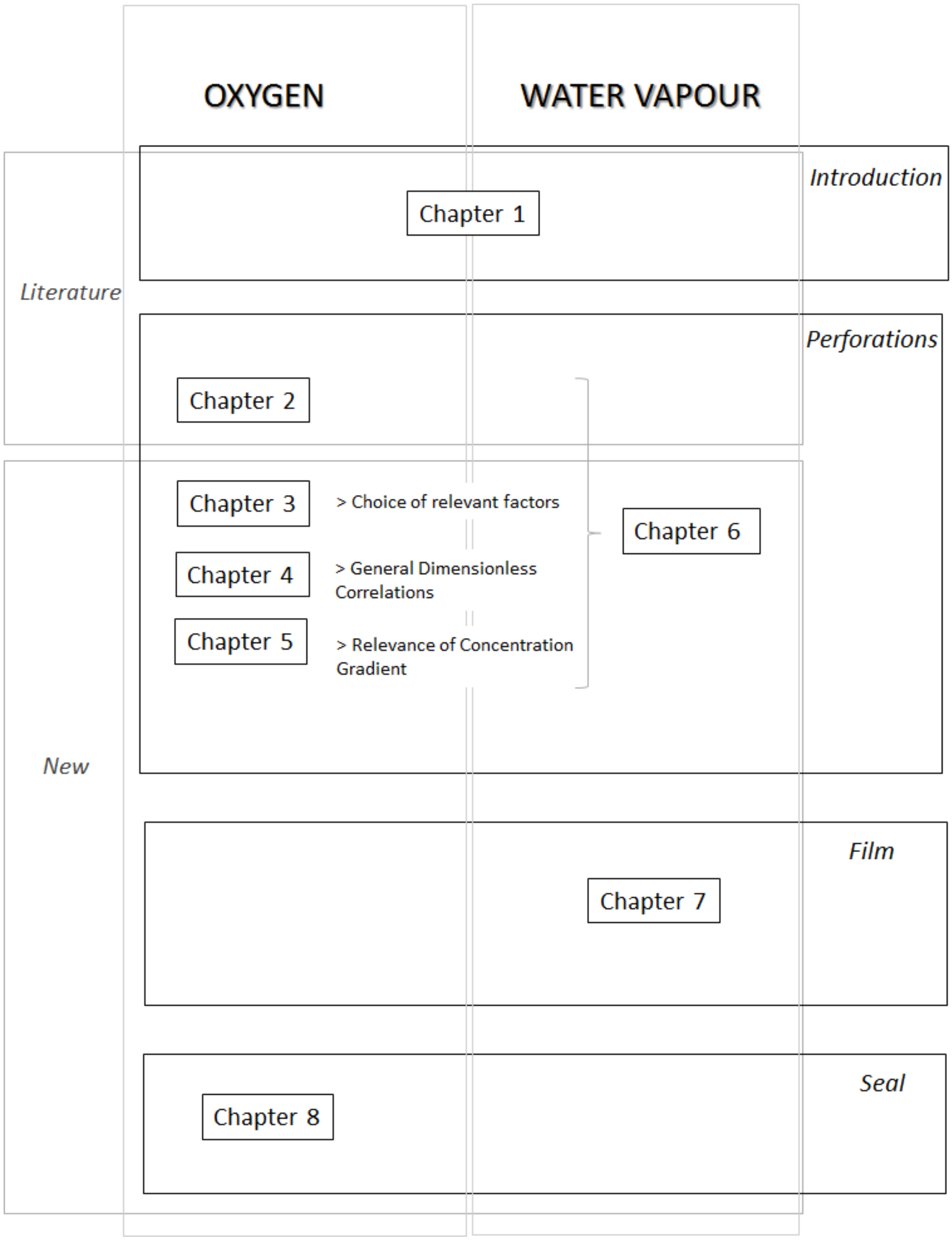
OXYGEN
WATER VAPOUR
Introduction
Chapter 1
Literature
Perforations
Chapter 2
Chapter 3
> Choice of relevant factors
Chapter 4
> General Dimensionless Correlations
Chapter 5
> Relevance of Concentration Gradient
Chapter 6
New
Film
Chapter 7
Seal
Chapter 8

TABLE OF CONTENTS

Declaration i

Acknowledgements iii

Abstract vi

Foreword viii

Thesis Structure xviii

Table of Contents xix

List of Tables xxvi

List of Figures xxix

1. Literature Review 1

Abstract 1

1.1. Preamble 3

1.2. Water in Food Packaging 11

1.3. Water Adsorption-Desorption in Films 12

1.3.1. Water Vapour Permeability and Diffusivity in Films ... 23

1.4. Mathematical approach of water plasticization in films .. 30

1.5. Oxygen and Carbon Dioxide 34

1.6. Mass Transfer through Perforations 42

1.7. Dimensionless Correlations In Mass Transfer Analysis . 50

2. A meta-study providing a unified analysis of the design engineering methods for modified atmosphere packaging with perforated films for optimum oxygen and carbon dioxide balance 59

Abstract 59

2.1. Introduction 61

2.1.1. Permeability of an unperforated film 66

2.1.2. Advantages of perforating a package 72

2.1.3. Mass transfer through perforated films 76

2.2. Review of methods proposed and data reported 81

2.2.1. Lumped capacity model and overall transmission rates 81

2.2.2. Hydrodynamic flow models 93

2.2.3. Diffusional models using Stefan-Maxwell's equations 98

2.2.4. Diffusional methods using Fickian diffusion with constant diffusivity 105

2.2.5. Dimensionless correlation for mass transfer coefficients 115

2.2.6. Methods solving the fundamental equations of mass and momentum transfer... 123

2.3. Packaging design engineering 126

2.4. Conclusion 139

3. Effect of hydrodynamic conditions and geometric aspects on the permeance perforated packaging films 141

Abstract 141

3.1. Introduction 143

3.2. Materials and Methods 146

3.2.1. Experimental Procedure 146

3.2.2. Effect of air velocity, perforation diameter and position of perforation 147

3.2.3. Effect of temperature, number and diameter of perforations 148

3.2.4. Effect of area of perforation on mass transfer coefficient 149

3.2.5. Effect of the distance between perforations on mass transfer coefficient 149

3.2.6. Effect of different atmospheres in oxygen transfer through the packaging 150

3.2.7. Effect of packing arrangement during storage on the Modified Atmosphere Packaging performance of microperforated packages 150

3.2.7.1. Effect of the position in stacking on the package permeance 151

3.2.7.2. Effect of the position of the perforation on the package permeance 151

3.2.8. Determination of film permeance 152

3.3. Results and Discussion 154

3.3.1. Effect of different parameters on the mass transfer coefficient 154

3.3.2. Influence of the distance between perforations........ 165

3.3.3. Effect of storage conditions during storage on mass transfer coefficient 166

3.3.3.1. Effect of the position in stacking on the package permeance 166

3.3.3.2. Effect of the position of the perforation on the package permeance 167

3.3.4. Effect of atmosphere composition on mass transfer coefficient 168

3.4. Conclusion.. 171

4. Dimensionless Correlations for Estimating the Permeability of Perforated Packaging Films to Oxygen... 172

Abstract 172

4.1. Introduction... 174

4.2. Materials and Methods 177

4.2.1. Experimental procedure 177

4.2.2. Determination of Mass Transfer Coefficient 178

4.2.3. Dimensionless Correlations 180

4.3. Results and discussion 182

4.4. Conclusion 190

5. Analysis of the influence of the oxygen concentration gradient on the permeance of perforated packaging films 192

Abstract 192

5.1. Introduction 194

5.2. Materials and Methods 196

5.2.1. Experimental Procedure 196

5.2.2. Determination of average and variable permeances 198

5.2.3. Dimensionless Correlations 201

5.3. Results and Discussion 204

5.4. Conclusion 212

6. Determination of the mass transfer of water vapour through microperforated packaging films 213

Abstract 213

6.1. Introduction 215

6.2. Experimental set up 216

6.3. Results and discussion using models for water vapour fluxes through packaging perforations suggested in literature 219

6.4. Development of new models using dimensionless numbers 224

6.5. Conclusions 241

7. Analysis of plasticizing and antiplasticizing effects of humidity on the permeability of biobased films to water vapour 243

Abstract 243

7.1. Introduction 245

7.2. Materials and Methods 249

7.2.1. Mathematical methods 249

7.2.1.1. Quantification of WVP 249

7.2.1.2. Data analysis to determine variable diffusion coefficients 255

7.2.2. Experimental methods 257

7.2.2.1. Materials 257

7.2.2.2. Experimental procedures 258

7.3. Results and discussion 262

7.3.1. Sorption isotherms at 5°C 262

7.3.2. Water diffusivity through the polymers at 5°C 266

7.3.2.1. Results for NVS 266

7.3.2.2. Results for PLA 271

7.3.3. Water vapour permeance under different conditions of use 280

7.4. Conclusion 285

8. Maximising the conformity of the effect of seal leakage in the effective permeance of packages 287

Abstract 287

8.1. Introduction 289

8.2. Materials and Methods 292

8.2.1. Experimental procedure 292

8.2.2. Statistical analysis 294

8.3. Results and discussion 295

8.4. Conclusion 302

9. Conclusions and Recommendations 303

9.1. General Conclusions 303

9.2. Future Work 306

References 308

LIST OF TABLES

Table 1.1 - Common Isotherm Models 14

Table 1.2 – Use of isotherms to describe isotherms of adsorption in films 20

Table 1.3– Water Vapour Permeability reported for different materials 27

Table 1.4– Permeability to Oxygen (P_{O2}) and to Carbon Dioxide (P_{CO2}) of different materials 36

Table 1.5– Impact of Mass Flux Trough the Perforations ($nperf$) on Total Mass Flux through Perforated Films ($ntotal$) 49

Table 3.1– Mass Transfer Coefficients (K, in $m\cdot s^{-1}$; average of 2 repeats) of Perforated Films with different perforation diameters (in μm), air velocities (in $m\cdot s^{-1}$) and distances from edge (in cm), and with $P_{film} = 1.11\cdot 10^{-8}$ cm/s 156

Table 3.2– Mass Transfer Coefficient (K, $m^2\cdot s^{-1}$, average of 2 repeats) of Perforated Films with different number of holes (X_1) and diameter of perforations ($X_{2,}$ in μm), air velocity of 2.7 m/s at 5, 10 and 15ºC. 159

Table 3.3- Mass Transfer Coefficient (K, in $\cdot m^{-2}\cdot s^{-1}$, average of 3 replicates) of Perforated Films with different number of perforations, diameter (in μm) and area of perforation (in cm^2), with air velocity of 2.7 m/s 162

Table 3.4– Mass Transfer Coefficient (K) of Perforated Films with different distances between two perforations (average of 3 replicates) 165

Table 3.5- Permeance (Pa) and Mass Transfer Coefficient (K) through microperforated films at different positions of the stacking 166

Table 3.6- Mass Transfer Coefficient through films perforated in different positions 168

Table 3.7- Mass Transfer Coefficient of oxygen through microperforated films flushed with different atmosphere compositions 170

Table 4.1– Parameters of the dimensionless correlations 182

Table 4.2– Mass Transfer Coefficient (K) obtained by applying different mathematical models 190

Table 5.1 – Model fitting results with least squares regression 206

Table 6.1- Goodness of fit (coefficient of determination) of 3 empirical models for the convection mass transfer coefficient in microperforations obtained with the 94 experimental data points 226

Table 6.2– Design of PLA packages for tomatoes and peaches 240

Table 7.1– Model parameters and goodness of fit of the sorption curves of PLA and NVS at 5 ^{o}C 263

Table 7.2 - WLF and Gordon-Taylor parameters obtained by least squares regression of average diffusivities of water through NVS and PLA at 5°C 267

Table 7.3 – Water Vapour Permeability of PLA previously stored at different Relative Humidity (RH) conditions at 5˚C (in g · m^{-2} · day^{-1}, average of 3 replicates) 276

Table 8.1 Effective permeance (Pa) of sealed packages with different sealing conditions. 296

LIST OF FIGURES

Figure 1.1 – Occurrence of isotherm models on literature referred by the Web of Science (Thomson-Reuters 2017), where bars indicate the total number of citations, diamonds mark the number of citations since 2016 and triangles refer to total number of citations in works related to films only. . 17

Figure 1.2 - Modified atmospheres that can be generated by cherry tomatoes following the respiration rate model of Sousa, Oliveira, and Sousa-Gallagher (2017) packed in Polypropylene, High Density Polypropylene, Chitosan or PLA films with permeabilities according to Mastromatteo et al. (2012), Ullsten and Hedenqvist (2003), Cerqueira et al. (2012) and Żenkiewicz and Richert (2008) both influenced by temperature, for storage at 5°C. The straight lines give all possible atmospheres for each film if unperforated. The symbols indicate atmosphere compositions of a package with 150 cm^2 of exposed area of 30 μm thick film and 250 g of cherry tomatoes, from unperforated (points on top of the respective line) to increasing number of perforations of 100 μm diameter (each additional perforation is one further point). 45

Figure 2.1. Sketch of the main phenomena involved in package design. The headspace volume is exaggerated in the picture for clarity purposes. C_e is the external concentration and C_h that in the headspace, with i denoting oxygen or carbon dioxide. 65

Figure 2.2 - Sketch of the mass transfer movements through a perforated film. 1 and 3 are convection movements (inner and outer, respectively), 2a is diffusion of a dissolved gas in a plastic film and 2b is diffusion/hydrodynamic/convective flow through a gas mix of varying composition from the headspace modified atmosphere to normal air. 77

Figure 2.3 - . Influence of the perforation length to diameter ratio on the ratio between the global mass transfer parameter K obtained with simple diffusion through the perforation across otherwise stagnant air of normal composition and the K value reported by the various authors for their own experimental data for (a) oxygen and water vapour (Lange et al, 2000) and (b) carbon dioxide. Data for very low L/d_h ratios is not shown (very high y-axis values). The straight lines are added just to help visualise tendencies. 86

Figure 2.4. Logarithmic plot of the ratio of lumped capacity model global mass transfer K parameter between that due to diffusion through stagnated normal air and that reported by the various authors as a function of the length to diameter ratio of the perforation(s) for (a) oxygen and water vapour (Lange et al. 2000), (b) carbon dioxide. The dotted lines are added just to help visualise tendencies.. 90

Figure 2.5. Mass transfer coefficients extracted from the data reported by several authors for perforations of various diameters, with smaller diameters in fig. a and bigger ones in fig. b. The first letter indicates the literature reference as in the legend of fig. 4 and the second letter the gas, with O for oxygen, C for carbon dioxide and W for water vapour. 92

Figure 2.6 - Sketch of the molecular movements conceived to obtain a limit Sherwood number of 2 for diffusion through stagnated air defining Sh with the perforation diameter. Full arrows indicate radial movements and dotted arrows axial movements parallel to the perforation length. 109

Figure 2.7 - Mass transfer coefficients at 20 ^oC predicted by the dimensionless correlations for oxygen moving into a flat surface at different positions (x, in cm) from the edge in the direction of the air flow, using the physical properties of normal air and a density gradient for the Grashof number caused by density difference to a modified atmosphere saturated in water vapour, with 15% carbon dioxide and 5% oxygen. 122

Figure 2.8 - Modified atmospheres that can be generated by strawberries following the respiration rate model of Hertog et al. (1999) packed in EVA, LDPE or Saran films with permeabilities according to Exama et al. (1993), both influenced by temperature, for storage at 10 ^oC (a) and 20 ^oC (b). The dashed lines give all possible atmospheres for each film if unperforated, depending on temperature, film thickness and area to weight ratio of the package. The symbols indicate atmosphere compositions of a package with 20x10 cm^2 of exposed area of 25 μm films and 300 g of strawberries, from unperforated (points on top of the respective line) to increasing number of perforations of 0.1 mm diameter (each additional perforation is one further point). 130

Figure 3.1–Position of the Perforation (Dashed circles represent the situation where 5 perforations were used) (a) and disposition of the containers (b) 147

Figure 3.2– Result of the Analysis of Variance of the mass transfer coefficient for diameter, distance and air velocity for a single perforation at 10°C, showing the portions of the raw sums of squares explained by each effect (total number of points = 30, total SS = 0.0103), where light grey denotes statistically significant effects ($p < 0.05$), dark grey marginally significant effects ($0.1 > p > 0.05$) and black non-significant effects ($p > 0.1$) 157

Figure 3.3– Result of the Analysis of Variance of the mass transfer coefficient for diameter, temperature and number of perforations, with 2.7 m/s air velocity, showing the portions of the raw sums of squares explained by each effect (total number of points = 54, total SS = 2.4483), where light grey denotes statistically significant effects ($p < 0.05$), dark grey marginally significant effects ($0.1 > p > 0.05$) and black non-significant effects ($p > 0.1$) 160

Figure 3.4 - Representation of flow path through a pore. Adapted from Meidner and Mansfield (1968). 164

Figure 4.1- Observed versus predicted values of the mass transfer coefficient determined by Buckingham π- Method (a) and Sherwood Correlation (b). 185

Figure 4.2- Comparison of the predictions of eq. 4.7 (open symbols) and eq. 4.9 (closed symbols) with the experimental values obtained in the validation trial 186

Figure 5.1 - Plots to obtain instant values of the permeance for the 2 replicates at 10°C with 0.76 m/s air velocity for perforations of (a) 270 μm, (b) 450 μm and (c) 750 μm. Polynomial fits (equations and R^2 indicated next to the lines) are shown in full lines, with the dotted lines showing the best straight line (the slope of which is the average permeance) 205

Figure 5.2 - Diagnosis plot of the dimensionless correlation of eq. 5.11 with the parameters of table 5.1. 207

Figure 5.3 - Influence of the concentration gradient on the mass transfer coefficient in two replicate experiments at 10ºC and 0.76 m/s air velocity for perforations of 270 μm (filled spheres), 450 μm (shaded squares) and 750 μm (open triangles). The horizontal dotted lines indicate the average mass transfer coefficient and the full lines the model predictions of eq. 5.11. 209

Figure 6.1 –Mass Transfer Coefficient (K) predicted by the 6 models compared to the experimental results in the validation set of experiments. Legend: (◊) Eq. 6.3, (Δ) Eq. 6.4, (□) using the end correction proposed by Lee et al. (2000),. 223

Figure 6.2 –Diagnosis plots of the Sherwood correlation (a) and K/v (b) fitting 227

Figure 6.3 –Mass Transfer Coefficient (K) of the validation set of experiments predicted by the proposed models. Legend: (▲) Eq. 6.8, (◊) Eq. 6.9, (♦) Eq. 6.10. 228

Figure 6.4– K values obtained by the proposed dimensionless correlations (♦) 270 μm at 5ºC, (◊) 270 μm at 10ºC, (■) 450 μm at 5ºC, (□) 450 μm at 10ºC, (▲) 750 μm at 5ºC, (∆) 750 μm at 10ºC. 229

Figure 6.5– Mass transfer coefficients obtained initially ignoring the effect of velocity on the saturation point at (♦) 270 μm at 5°C, (◊) 270 μm at 10ºC, (▲) 750 μm at 5°C, (∆) 750 μm at 10°C, and obtained with the correction of the saturation point from the cooling effect of velocity denoted by (●) and (○) on both graphs for 5 and 10°C, respectively. 233

Figure 6.6 – Diagnosis plot of experimental data obtained in the 3rd set of experiments with different internal humidities and the predictions made with eq. 6.10 (●) and with eq. 6.17 (○) 237

Figure 7.1 - Sorption isotherms of (a) PLA (▲) and (b) NVS (■) films at 5°C. Open symbols are experimental data for desorption and full symbols for adsorption; the lines show fits of Park's model (joint adsorption-desorption for PLA and for NVS, solid line for adsorption and dashed line for desorption).. 262

Figure 7.2 - Experimental average diffusivities (symbols) of water through NVS at 5°C and model predictions (lines). (a) average diffusivities; (b) variable diffusivity diagnosis plot; (c) variation of individual and average (from 0) diffusivities (full and dashed lines, respectively, on the left y-axis) and glass transition temperature (dash-dot line, on the right y-axis) with the water content of NVS. 270

Figure 7.3 - Experimental average diffusivities (symbols) of water through PLA at 5 ºC and model predictions (lines) for $a_w \leq 0.95$. (a) average diffusivities; (b) variable diffusivity diagnosis plot; (c) variation of average and individual diffusivities (full and dashed lines, respectively, on the left y-axis) and glass transition temperature (dash-dot line, on the right y-axis) with the water content of PLA; the constant diffusivity for this range of water contents is also shown as a dotted line. 272

Figure 7.4– X-ray pattern of PLA films conditioned to different relative humidity conditions by storage over 15 days 278

Figure 7.5 - Water Vapour Transmission Rates of NVS at 5˚C obtained experimentally (full spheres for 50%-90% humidity gradient and open squares for 75%-100%), predicted by the model for the dryer side at 0% RH (full line), 50% RH (dashed line) and 75% RH (dotted line), with wetter side on the x-axis, and obtained with ASTM E36 method at 5°C (dash-dot line). 282

Figure 8.1- Normal plots of dispersion effects Fi, where T is the Temperature, F is Force and t is the time. 300

1. LITERATURE REVIEW

ABSTRACT

Food packaging design requires comprehensive knowledge of the product to be packed, the packaging material and their interactions. For fresh and minimally processed fruits and vegetables, there are various aspects that need to be quantified properly. On the product side the key issue is that the vegetable tissues keep respiring after harvesting and therefore they consume the ambient oxygen and release carbon dioxide and water vapour. Furthermore, water loss may also occur by evaporation depending on the relative humidity of the environment and the phase equilibrium between product and air. Hence, the key issue in the case of the package is permeability to gases in order to avoid anoxia and water condensation inside the package. For some products sensitive to carbon dioxide, elevated concentrations of this gas may also be detrimental to quality. On the other hand, appropriate barrier properties of the packaging material will establish an equilibrium between gas consumption/production and transfer through the package, establishing a protective atmosphere that can extend the shelf life of the produce significantly. Hence, engineering packaging design consists in defining the package factors that will work with the specific product to generate the optimum atmosphere for that product to reach maximum shelf life under its appropriate storage conditions. As

packaging films tend to present low permeability to carbon dioxide and oxygen and the ratio between the permeabilities is normally greater than the respiration quotient of the produce, an alternative to manipulate the permeability ratio of the film is to perforate the packages. However, such perforations will necessarily need to be very small, and possibly in a small number too, as gas transfer through a perforation will inevitably have a high rate. Availing of accurate kinetic models of the phenomena will therefore enable the packaging design engineer to establish the correct perforation profile that will meet the necessities of the specific product and additional package details, such as sizes and actual packaging material(s) to be used. Perforations will also an important bearing on water vapour transport through the package and the resulting relative humidity of the internal package atmosphere, which is desired to be sufficiently high to limit evaporative water loss from the product, but without reaching saturation which would lead to condensation, accumulation of liquid water, and consequent quality loss due to mould growth, loss of texture and stimulating detrimental microbial activity. This introductory chapter reviews the state of the art knowledge of the main aspects on the oxygen, carbon dioxide and water vapour permeability of films and of the relevant mathematical models of gas permeability through perforated films.

1.1. PREAMBLE

Plants absorb nutrients and water from the soil and their main metabolic activities are photosynthesis and respiration. Chemical changes in the vegetable tissues after harvesting are due to respiration and fermentation, aerobic and anaerobic oxidation respectively. Both processes involve energy consumption, and as a result, quality loss. The organic substrates accumulated during growth are oxidized to carbon dioxide (CO_2) and water. The energy necessary for all the metabolic activities in detached plant parts came from aerobic respiration whereby cells completely oxidize molecules such as carbohydrates, organic acids, proteins and fats to produce energy, in addition to water and CO_2; the energy produced during respiration is mainly conserved in the form of ATP (Adenosine triphosphate) or lost as heat (Damodaran, Parkin, and Fennema 2007).

Oxygen (O_2) serves as the final electron acceptor in respiration, while on fermentation, complete oxidation does not occur and electrons are instead passed on to other molecules within the cell. When carbohydrates are used for respiration, about 1 mole of CO_2 is produced for each mole of O_2 consumed. (Nelson and Cox 2013). In this case, the overall equation for respiration, normally expressed as the glucose oxidation, is presented as follows (Chitarra and Chitarra 2005):

$$C_6H_{12}O_6 + 6O_2 + ADP + Pi \rightarrow 6CO_2 + 6H_2O + 673\ \text{kcal} + 38\ ATP \qquad (1.1)$$

Respiration is directly related to transpiration, which is the main factor responsible for decreasing product weight. Unfortunately, there is much confusion on what transpiration is and how it relates to product weight loss. Respiration produces water vapour, which is released by the plant to the surrounding atmosphere. On the other hand, the product contains significant amounts of liquid water as well, and thus it would normally dry and lose water by evaporation inevitably, unless the atmosphere is humid. This is to say that if there was no respiration at all, the product would still release water to the atmosphere from the drying process. Therefore, the release of water vapour from a plant occurs both because of respiration (which produces water vapour out of the oxidation of a substrate) and drying (which produces water vapour by the simple evaporation of liquid water). If transpiration is the name given to the production of water vapour by a plant, then it is the sum of these two effects.

On the other hand, water loss due to drying is not the sole factor causing weight loss, because the substrate (a soluble solid) is converted to gases (carbon dioxide and water vapour) by the respiration. Although under normal conditions the water lost by evaporation causes much of the weight loss, the substrate loss is not necessarily negligible. Thus, if transpiration is equated to weight loss, it is not just the effect of drying either, but a combination of both respiration and drying effects.

The liquid water loss due to drying results from the gradient of water vapour pressure between the tissue and the surrounding air (Romero, 1987, Becker and Fricke, 1996). Chitarra and Alves (2001) named transpiration as the effect of all physiological activities that culminate in production of water vapour by the plant. However, other authors also determine transpiration rates from measuring weight loss (Bovi et al. 2016, Caleb et al. 2016), and in this case the measurement is not the same because the relation between the substrate weight loss and the water vapour produced by respiration can vary significantly depending on what the substrate effectively is (for instance, in the case of fructose or glucose, 1 mole of sugar produces 6 moles of water vapour). When the loss of weight due to substrate conversion is neglected and all the water vapour production is equated to the loss of water by drying, then transpiration is being used to term only the drying process, and not the totality of water production.

These differences matter particularly with packaging, because a package that hinders water vapour transmission to the environment will be creating a saturated environment inside the package and thus, there should occur no drying and hence no more loss of liquid water and no more weight loss due to it. Yet, the plant will continue to produce water vapour due to respiration, which results in condensation and the accumulation of liquid water in the package (and also, some weight loss due to the substrate loss). Thus, a proper and accurate quantification of the phenomena should distinguish between the different effects: water vapour produced by respiration, water vapour produced by evaporation of liquid water, weight loss due to conversion of substrate, weight loss due to loss of liquid water by evaporation, and, when applicable, condensation of water vapour in a saturated environment.

Water lost due to drying impacts quality significantly; losses of just 3 to 6% are sufficient to reduce turgidity and cause permanent damage on the integrity of the vegetable tissues, and appearance begins to be significantly affected (Chitarra and Alves 2001, Ben-Yehoshua and Rodov 2002).

However, in packaged products, water produced by respiration may be a significant quality problem, because if the package is too impermeable to water vapour the saturated environment causes a continuous condensation of this water vapour, and the liquid water thus created will lead to mould or yeast growth and rapid deterioration. Thus, the ideal package should hinder water vapour transfer sufficiently to create a high humidity environment inside the package such that there is little water loss due to drying, but be sufficiently permeable to allow the excess water vapour produced by respiration to transfer out, that is, water vapour permeability has to strike a perfect balance between production and mass transfer.

Despite the fact that stomata are the most important path for gases through plant tissues, studies with various types of fruits and vegetables also showed that CO_2, ethylene and water vapour could be released not only through the stomata, but also by cuticle, lenticels, hydathodes, the stem scar or other injured areas (Ben-Yehoshua and Cameron 1989, Pantastico 1975, Chitarra and Alves 2001).

Water loss in fruits and vegetables is strongly dependent on the conditions of their stomata, on the opening and closing of the pores. These organelles are determinant to the gas exchange through the membrane of the commodity, even considering that the percentage of opened stomata decreases significantly after harvesting. Also, stomata opening may depend on the ambient conditions, such as relative humidity, temperature and light/darkness (Ben-Yehoshua and Cameron 1989).

Regulation of transpiration is strongly dependent on the response of stomata to vapour pressure difference and temperature. Because the former may vary in the atmospheric air with the latter, it can be difficult to distinguish the effect of each of them on transpiration; however, when both effects are separated, it is possible to observe that the mass transport through the stomata increases with temperature, and the rise occurs for temperatures above the optimum for photosynthesis in plants on the field (Schulze and Hall 1982). Gas exchange through the stomata is particularly problematic on leaves, as the large number of stomata in their tissue are the main cause of water loss for these products, together with the large area-volume ratio. For these vegetables, the ideal conditions of storage must be followed with rigor in order to keep their quality and avoid food loss (Cantwell and Reid 1993, Ben-Yehoshua and Rodov 2002).

Water loss during storage is a constant on postharvest technology. A good refrigeration system is very important to reduce the internal heat of fruits and vegetables, present as field and vital heat. The former consists of the ambient heat absorbed by the plant tissues and the heat produced by the rapid respiration due to the physiological stress of the harvesting, and because of that rapid cooling is very important immediately after harvest. Vital heat is produced during respiration and is responsible for the water loss due to evapotranspiration during storage (Chitarra and Chitarra 2005).

The less efficient the refrigeration, the more water condensation on the product surface due to the internal heat. Any malfunction such as insufficient ventilation or temperature fluctuations can increase the loss of water (Rodov et al. 2010). The effect of temperature is related to the relative humidity. In the field, crops exposed to high temperatures and high relative humidity tend to suffer less than plants under limiting water conditions (Wahid et al. 2007). Refrigeration reduces the temperature and consequently the respiration rate, which leads to an extend shelf life as it slows loss of nutrients and proliferation of microorganisms. However, refrigeration should be just enough to remove vital heat and not affect the ambient humidity necessary to avoid transpiration (Silva, Finger, and Corrêa 2000).

Transpiration as a normal drying process is simply the evaporation of the product’s liquid water to water vapour to the surrounding air. It may involve 3 stages: (i) water transport from inside the commodity to its surface,

(ii) evaporation from the surface and (iii) convective mass transfer to the surrounding atmosphere (Rennie and Tavoularis 2009).

The evaporation of liquid water occurs due to the water vapour pressure gradient between the surface and the air. If there was only water and air, then drying would occur until the partial pressure of water vapour in the air equals its vapour pressure, that is, the relative humidity reaches 100%. However, when there is also a food product, the water is in fact the solvent of various solutes, and therefore the equilibrium water-air is not the same as the pure water. The equilibrium partition of water between food and atmosphere will be reached for relative humidities less than 100%, as the relative humidity is calculated for liquid water / air equilibrium. As drying progresses and the liquid water concentration decreases, the vapour pressure decreases and thus the equilibrium will progressively evolve to even lower relative humidities. The entire range of equilibrium points is well described by the respective desorption isotherm, which theoretically could go up to 100% relative humidity (the same as a water activity of 1), but in practice due to the presence of the solutes the humidity of the atmosphere in a package is below 100% (usually 95 to 98%, depending on the product, and typically lower for vegetables than fruits).

As respiration releases heat, the temperature of a commodity will inevitably be somewhat higher than that of the surrounding air. Even if this difference is often neglected in many calculations, it implies that the vapour pressure at equilibrium just below the surface of the product will always be above that of the surrounding air, so the product would continuously lose liquid water, even if it then condenses in the atmosphere (Becker and Fricke 1996).

Besides, not all the weight loss during storage is due to water loss, which is a common mistake in literature. As respiration implies nutrient depletion, part of the weight loss is related to the loss of substrates. Hence, in order to determine the correct amount of water loss it is necessary to observe how much water is released. A complete discussion of transpiration routes and water loss was put forward by Ben-Yehoshua and Rodov (2002). Determination of water loss in fruits has been reported in literature by discounting the loss of CO_2 from the respiratory activity (Ben-Yehoshua, Burg, and Young 1985).

Water constitutes 80-95% of the weight of fresh commodities such as fresh fruits and vegetables. Water is also responsible to provide the turgor desired in horticultural products, due to its low compressibility. In this case, small losses (<1% of weight) can deplete the quality, affecting the physical aspect, texture and nutritional characteristic (Damodaran, Parkin, and Fennema 2007). Water loss in minimally processed fruits and vegetables is highly affected by peeling and cutting due to their effect on respiration rate. Hence, the quality control of fruits and vegetables demands an efficient storage system.

1.2. WATER IN FOOD PACKAGING

As water is so critical to storage, it is crucial to understand its impact on food packaging. From the point of view of water effect, there are two main groups of materials involved in packing fresh and minimally processed fruits and vegetables: hydrophilic and hydrophobic materials, i.e. those highly affected by water molecules and those where water molecules have no to very little effect on their structure.

Equilibrium in hydrophobic films obeys Henry's Law, meaning that the concentration of gas in the polymer is directly proportional to the gas partial pressure, and the Henry constant of proportionality is named Solubility. In this case, there are no strong polymer–penetrant interactions and no specific interactions between the penetrant molecules. Only small portions of water are absorbed (Van Krevelen and Te Nijenhuis 2009). Henry's law applies to other gases such as Oxygen, but the interactions with water vapour and organic gases have more complex behaviour, which is highly observed in hydrophilic materials, whose polymer-water interactions are strong and determinant to the water transport. As a result, films such as ethyl cellulose can be more than a thousand times more permeable to water than Polyethylene or Polyvinylalcohol, three hundred times more than polypropylene or twenty times more than polystyrene (Metz et al. 2005).

Water concentration in hydrophilic polymers depends on the water adsorption-desorption behaviour and may be quantified by isotherms.

These curves allow to understand the polymer-water interactions and its influence on water vapour concentration in the polymer.

1.3. WATER ADSORPTION-DESORPTION IN FILMS

Isotherms give information not only on the relationship between water vapour pressure and water content in the material but also on the character of the water-water and water-surface relations, providing acquaintance with the porosity of the material (Gregg and Sing 1983, Teixeira, Coutinho, and Gomes 2001, Van Krevelen and Te Nijenhuis 2009). Likewise, different isotherm equations can be found in literature with applications in many areas, and of course can be applied to other adsorbates than water (Zeller, Saleeb, and Ludescher 1998, Lucas et al. 2004). Their ability to describe water adsorption-desorption is related to the shape of the isotherm, which in turn describes how water is absorbed by the material (van den Berg and Bruin 1981, Al-Muhtaseb, McMinn, and Magee 2002). Isotherms can be classified in different types, where the main 5 types can be found at Brunauer et al. (1940), extended to 6 on a IUPAC classification (Sing et al. 1985) and subsequently supplemented by 2 (Thommes et al. 2015) or 3 (Rouquerol et al. 2013) more subgroups. A classification into shapes (C, L, S and H) is sometimes used and can be found in the work of Giles, Smith, and Huitson (1974).

When the adsorption-desorption process follows Henry's law, the graphical representation of the isotherm presents a linear relationship with pressure and is observed in the sorption of permanent gases at moderate pressures. To some extent, a linear isotherm will always be verified at sufficiently law water contents, which was subsequently explored by Park (1986) Other main isotherm profiles are characterized as Langmuir adsorption, Flory–Huggins type and Brunauer, Emmett and Teller (BET) isotherm. Langmuir adsorption characterises a unimolecular adsorption, i.e. the surface can take up only one layer of adsorbed gas. Thus, after an eventual earlier linear region, as water activity increases the water content levels off to a maximum limit. The Flory–Huggins type describes a situation when the solubility coefficient increases continuously with water content. It presents a preference for formation of penetrant pairs and clusters and is observed when the penetrant acts as a swelling agent for the polymer without being a real solvent. An example is water in relatively hydrophobic polymers containing also some polar groups. BET type is classic of hydrophilic materials, and is a combination of Langmuir and Flory–Huggins types (Van Krevelen and Te Nijenhuis 2009).

There are many equations developed to describe isotherms and they have been extensively described in literature (van den Berg and Bruin 1981, Basu, Shivhare, and Mujumdar 2006, Foo and Hameed 2010). A list of common sorption models is shown in Table 1.1.

.

Table 1.1 - Common Isotherm Models

$X_{BET} = \frac{X_m \cdot C \cdot a_w}{(1 - a_w) \cdot (1 + C \cdot a_w - a_w)}$	X_m: monolayer water content, C: energy difference between the upper layers and the monolayer	Brunauer, Emmett, and Teller (1938)
$X_{GAB} = \frac{Q_m \cdot C \cdot K \cdot a_w}{(1 - K \cdot a_w) \cdot (1 - K \cdot a_w + C \cdot K \cdot a_w)}$	X_m: water content sorbed in the first layer, K: associated to water sorbed molecules on multi-layer and C: Guggenheim constant which corresponds to the total sorption heat of the first sorbed lay	van den Berg (1985)
$\frac{X_L}{X_m} = \frac{C_L \cdot a_w}{1 + C_L \cdot a_w}$	C_L: kinetic constant related to the sorption in the first layer, Q_L: moisture content d.b. based on non-soluble dry matter, Q_m: moisture content d.b. at monolayer coverage based on non-soluble dry matter	Langmuir (1918)
$X_{Le} = \frac{F}{(1 - a_w)^G} + \frac{F}{(1 - a_w)^H}$	F, G, G, H are parameters obtained by fitting into the data	Lewicki (1998)
$X_O = c_1 \left(\frac{a_w}{1 - a_w} \right)^{c_2}$	c_1 and c_2 are model constants	Oswin (1946)
$X_{Pa} = \frac{A_L \cdot b_L \cdot a_w}{1 + b_L \cdot a_w} + K_H \cdot a_w + K_a \cdot K_H \cdot {a_w}^n$	A_L: the Langmuir capacity constant, gives the extension of the internal pore surfaces per unit volume, b_L: Langmuir affinity parameter, k_H : Henry's solubility coefficient, k_a : equilibrium constant for the clustering reaction, n: the mean number of water molecules per cluster	Park (1986)
$X_{Pa2} = \frac{A_L \cdot b_L \cdot a_w}{1 + b_L \cdot a_w} + K_H \cdot a_w + n \cdot K_a \cdot {K_H}^n \cdot {a_w}^n$	Park model is presented in literature in slightly different forms (Q_{Pa2} and Q_{Pa3}), both with good fitting to data from different authors and materials, without however indicate where these modifications come from.	In: Charlon et al. (2017)
$X_{Pa3} = \frac{A_L \cdot b_L \cdot a_w}{1 + b_L \cdot a_w} + K_H \cdot a_w + K_a \cdot {a_w}^n$		In: Gouanvé et al. (2006), Wolf et al. (2016)
$Q_{Pe} = K_1 {a_w}^{n_1} \cdot K_2 {a_w}^{n_2}$	K_1, K_2, n_1 and n_2 are constants obtained from mathematical fitting.	Peleg (1993)
$X_{VR} = \frac{X_m \cdot C \cdot K \cdot a_w}{(1 - K \cdot a_w) \cdot (1 - K \cdot a_w + C \cdot K \cdot a_w)} + \frac{C \cdot K \cdot K_2 \cdot {a_w}^2}{(1 - K \cdot a_w) \cdot (1 - a_w)}$	Q_m: monolayer moisture content, C the Guggenheim constant and k a constant whose value generally lies between 0.7 and 1.	Viollaz and Rovedo (1999) (sometimes named Modified GAB)

a_w is the water activity and Qx are the water content in dry basis calculated by the x different models

Evidently, not all equations will fit well any specific case, and sometimes equations may be valid only in given regions of water activity. BET equation, for example, is sometimes applied in a range of water activity up to 0.65 (Biliaderis, Lazaridou, and Arvanitoyannis 1999, Akanbi, Adeyemi, and Ojo 2006, Villalobos, Hernández-Muñoz, and Chiralt 2006, Saberi et al. 2016). Equations like those proposed by Oswin (1946) and Viollaz and Rovedo (1999) cannot be used at 100% mathematically and GAB equation might underestimate water content of materials subjected to a water activity greater than 0.93 (Basu, Shivhare, and Mujumdar 2006).

GAB equation is one of the most used equations for describing water adsorption. A simple research on Web of Science Core Collection (Thomson-Reuters 2017) showed 799 papers published on the matter since 1989, appearing 50 times in 2016. Of these, 73 refer also to “film”, occurring since 1993 (Thomson-Reuters 2017).

GAB model, Guggenheim-Anderson-De Boer according to van den Berg (1981), is a modification of BET model for isotherms. BET was proposed by Brunauer, Emmett, and Teller (1938) and it provides a sigmoidal curve that assumes a multilayer profile where the first molecule (monolayer) on a site has a much stronger interaction with the sorbent than the second and following layers (van den Berg 1985). It is probably the most used equation on the study of isotherms, with over 1000 occurrences on Web of Science (Thomson-Reuters 2017); however, BET is frequently bettered by other models in terms of goodness of fit and range of applicability. In fact, it has been observed that GAB parameters are more meaningful to the phenomenon and provide a better value for the monolayer than BET model (Timmermann, Chirife, and Iglesias 2001), as BET tends to provide smaller values at low water activities and greater values at high water activities than those obtained experimentally (Mc and Teller 1951). As a result, the monolayer value provided by GAB is often greater than the one obtained via BET equation (Suriyatem et al. 2015). Other GAB-like equations have also been developed but appear less frequently in literature, such as those proposed by Timmermann and Chirife (1991) and Viollaz and Rovedo (1999).

Extra information on the materials can be obtained using the data from the isotherms. Knowing the monolayer moisture content, it is possible to determine the water binding properties of particulate materials applying a model proposed by Labuza (1968) and used by other authors (Cassini, Marczak, and Noreña 2006, Rosa, Moraes, and Pinto 2010). According to Brunauer, Emmett, and Teller (1938), knowing the volume of gas adsorbed on the first layer, the surface area of the adsorbent is obtained by multiplying the number of molecules required to form a unimolecular layer by the average area occupied by each molecule on the surface. Also, Larotonda et al. (2005) deduced a mathematical model that gives solubility from the GAB equation.

Other models that often appear together with the GAB equation, offering good fit to different sets of data, are the Oswin, Peleg and Park equations (Basu, Shivhare, and Mujumdar 2006, Aguirre-Loredo, Rodriguez-Hernandez, and Velazquez 2017, Wolf et al. 2016, Suppakul et al. 2013). Figure 1.1 shows the occurrence of BET, GAB, Oswin and Peleg models in literature in publications referenced by the Web of Science website in 2017 (Thomson-Reuters 2017) and it can be seen that the BET equation appeared more often on literature, but GAB was more frequent in papers related to films.

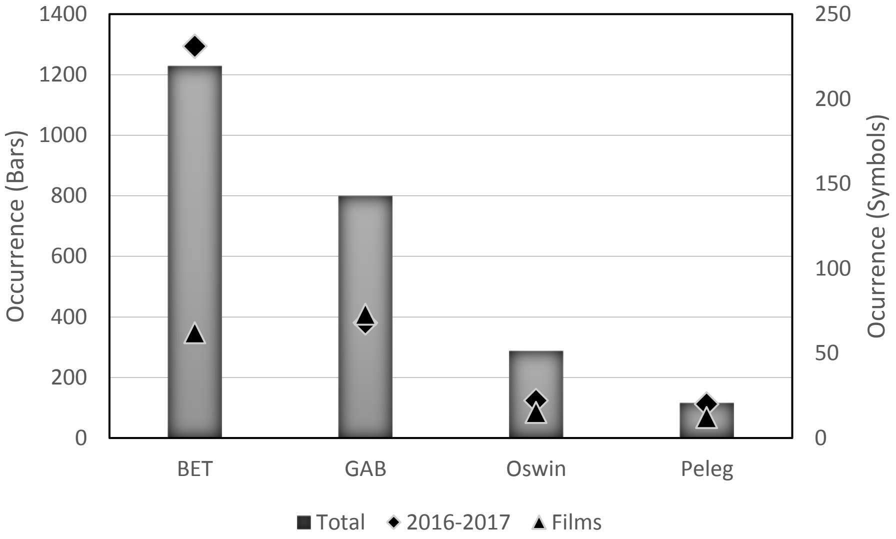

Figure 1.1 – Occurrence of isotherm models on literature referred by the Web of Science (Thomson-Reuters 2017), where bars indicate the total number of citations, diamonds mark the number of citations since 2016 and triangles refer to total number of citations in works related to films only.

Oswin (1946) developed a mathematical relation that could be applied to packaging studies, as according to the author equations previously published could not be used on the study of packaging life. Peleg (1993) proposed a semi-empirical four parameter model to describe sigmoid moisture sorption isotherms that tends to fit as well as or better than the GAB model, but whose parameters have no physical meaning. Peleg equation tends to present a good fit to different sets of data from different materials (Galus and Lenart 2013).

According to Lewicki (1998), GAB and Peleg models fail when water activity is 1, as they predict a finite solution. Hence they developed a model from the BET equation that led to an equation consisting of two functions subtracted from each other that assumes two processes occurring in parallel, where the first one occurs at higher water activities and the second part prevails at low vapour pressure. Their equation predicts infinite adsorption at a water activity of 1 and surpassed GAB's ability to predict data correctly in their studies, but did not present a better performance than Peleg equation. This model consists on a three-parameter equation, and subsequently the same author published another work where a two-parameter model was put forward (Lewicki 2000), but this time it was not compared to Peleg's, only to the GAB equation.

Park (1986) proposed a model that incorporates the effect of Henry's law or Flory-Huggins-type sorption complicated by a Langmuir-type sorption on internal pore surfaces at low activities and at higher vapour pressures by clustering. It resulted in an equation that can be applied to both hydrophilic and hydrophobic polymers and whose parameters have physical meaning, indicating the equilibrium constant for the clustering reaction, the Henry's law solubility coefficient of monomeric water, the measure of the extent of the internal pore surfaces per unit volume of membrane, and the Langmuir sorption parameter. Park equation assumes that a different phenomenon takes place depending on the water content, and therefore each term of the equation has greater effect on a specific range of water activity (Detallante et al. 2001, Alix et al. 2009).

Table 1.2 shows a list of published papers that included the water sorption properties of different films, the models used by the authors (equation chosen as better is written in bold). It can be seen that GAB equation appears constantly and it is sometimes bettered by other models cited above. Nevertheless, GAB generally offers good fit to the data and the difference to the best model in each case tends to be very small.

Table 1.2 – Use of isotherms to describe isotherms of adsorption in films

Material	Temperature (°C)	Model	Reference
Methylcellulose	9, 15, 20, 25, 35	**GAB,** BET	de la Cruz, Torres, and Martín-Polo (2001)
Ethylcellulose			
Sodium Caseinate	25	Park	Colak et al. (2015)
Pullulan-Starch*	25	**GAB,** BET	Biliaderis, Lazaridou, and Arvanitoyannis (1999)
Cassava Starch - PBAT	25	GAB	Brandelero, Grossmann, and Yamashita (2013)
Cassava Starch			
Peanut Protein	25	**BET**, GAB, Smith, Henderson	Jangchud and Chinnan (1999)
Alginate - Pectin	25	Peleg	Galus and Lenart (2013)
Wheat Gluten	25	**GAB**, *Kuhn*, Smith, Oswin, Halsey, Flory-Huggins	Roy et al. (2000)
Bitter Cassava	10, 20, 30	Ferro-Fontan, GAB, Halsey, Henderson, Modified BET, **Peleg**, Smith	Tumwesigye, Oliveira, and Sousa-Gallagher (2017)
Polylactic acid	10.5, 20, 40	Flory-Huggins	Oliveira et al. (2006)
Polylactic acid	40	Flory-Huggins	Cairncross et al. (2006)

Material	Temperature (°C)	Model	Reference
Chitosan	15-30	BET, **GAB**, Henderson, Halsey, **Oswin** and their modifications	Aguirre-Loredo, Rodriguez-Hernandez, and Velazquez (2017)
Pea Starch	5,15, 25, 40	BET, GAB, Peleg, Oswin, Ferro-Fontan, Henderson, **Lewicki***, Iglesias-Chirife, Flory-Higgins	Saberi et al. (2016)
Rice Starch Carboxymethyl Chitosan	25	Lewicki, BET, GAB, Oswin, **Peleg**	Suriyatem et al. (2015)
PHBV- Wheat Straw Fibers	20	Park, **GAB**	Wolf et al. (2016)
Cassava	30	Lewicki, **GAB**, Oswin, Peleg	Suppakul et al. (2013)
Amaranth Flour	30, 40	GAB	Tapia-Blácido, Sobral, and Menegalli (2013)
Chicken Feather Keratin	20,35	BET, **GAB**, Smith, Iglesias-Chifrite	Martelli et al. (2006)
Lignocellulose-based	20	GAB, **Park**	Muraille et al. (2015)
WPI- Sodium Caseinate	2, 25, 40	Peleg	Lei et al. (2014)
PSB-based PSBA-based	25	**Park, Feng**	Charlon et al. (2017)

Material	Temperature (°C)	Model	Reference
Polyamide	25	Park	Follain et al. (2016)

*3-parameter equation (Lewicki 1998).

PHBV is Poly(3-hydroxybutyrate-co-3-hydroxyvalerate), PBAT is Poly(butylene adipate-co-terephthalate), WPI is Whey Protein Isolate, PSB is Poly(butylene succinate) and PSBA is Poly[(butylene succinate)-co-(butylene adipate)]

1.3.1. Water Vapour Permeability and Diffusivity in Films

Different expressions are traditionally used for permeability of water vapour. At constant temperature and in steady state, a most common empirical expression is:

$$\dot{m}_w = P_{a,w} \cdot A \cdot p_s \cdot \left(h_{r,2} - h_{r,1}\right) \tag{1.2}$$

where $\dot{m}$ is expressed usually in mass per unit of time (e.g. g/s), $P_{a,w}$is the permeance of the film to water vapour, p_s the saturation pressure of water vapour in air, A is the area of the film exposed and h_r is the relative humidity of the atmosphere, with subscript 1 for one side and 2 for the other side. These are equal to the water activities of the atmosphere.

Water vapour transmission rate is usually expressed in mass per unit of time, and the most common units used in literature make no conversions to the values measured, so usual units of permeance of water vapour are g/(m^2.bar.day) and other combinations of units of mass over area, pressure and time. For a film composed by a single polymer, it is better to define permeability (P), the permeance per unit of thickness of the film, giving:

$$m_{\dot{W}} = \frac{P_W}{L}.A.p_S.\left(h_{r,2} - h_{r,1}\right) \tag{1.3}$$

where L is the thickness of the film and P_w the permeability.

This shows that the result is actually just the same as Fick’s 1st law, so if one can assume that the entire process occurred in steady state, the relation between permeability and molecular diffusion can be established. Diffusion occurs in the film between one surface and the other due to the gradient of concentrations that results from equilibrium with the two different atmospheres. Fick's 1st law for a constant diffusion coefficient and dilute concentrations is:

$$m\dot{_W} = \frac{D_W}{\delta} . A . \left(C_{f,2} - C_{f,1}\right) \tag{1.4}$$

where D_W is the diffusivity of liquid water through the polymeric matrix and C_f denotes the concentration of liquid water in the polymer (not in the air), where using the concentration in units of mass per volume (e.g. g/mL) gives the mass flow rate $\dot{m}_w$ in mass per unit of time, with the units of diffusivity being area per time (e.g. cm^2/s). The use of concentration in the film is however not desirable. If the film/air equilibrium obeyed Henry's law, then one could state that

$$p_W = S \cdot C_f \tag{1.5}$$

where p_W is the partial pressure of water vapour in the air (= $p_s . h_r$) and S the solubility. Replacing this result in Fick's law and then comparing with eq. 1.2 gives the often cited result that permeability equals molecular diffusivity times solubility ($P = D \cdot S$), which Doty, Aiken, and Mark (1944) derived. However, this is only valid if solubility is the same on both sides, that is, if Henry's law is valid up to the maximum concentration in the problem. This issue is very important because with water vapour this is rarely the case, the sorption isotherms are not linear in the range of relative humidities of interest and therefore one needs to be careful when relating permeability with diffusion.

This would be more complex for multilayer materials, with more than one polymer, which in fact is the case of most films as often there is at least one layer of some adhesive to improve sealing. In this case one would need to consider not only the two different diffusivities/permeabilities to compose the permeance, but also the equlibrium at the interfaces between the two different polymers.

If the film is made of a single polymer, then the permeance is equal to the permeability divided by the thickness of the film. However, most commercial films have at least a layer of some adhesive, and are rarely single polymer, so permeance may be a better variable to work with in practice.

Traditionally, standard methodology such as ASTM 96 (1995) has been applied to the analysis of water permeability of films, sometimes with modifications. The original methodology suggests a humidity gradient of 50% either with chamber kept at 50% and the relative humidity inside either at 0 or 100%, on a temperature between 21 and 32°C, suggesting the highest one as a better choice. The main modification of the methodology in practice is related to the relative humidity, as often in literature and in industry authors prefer to use a high gradient, such as 90 or even 100%, normally at 25°C (37 °C is also common in the US, being 100 ºF) (Gontard et al. 1994). It may be noted that in practice the polymer/gas and produce/gas equilibrium may imply that saturation is less than 100%, if taken as p_W / p_{total}.

However, there is a main issue that should be considered in the studies of water vapour permeability of films and their application on design of food packaging and that has not received due attention. Neither the conditions proposed by ASTM 96 (1995) nor a gradient of 100% are the normal storage conditions of fruits and vegetables. In fact, temperature recommended for storage also tend to be significantly lower than 21°C, which means that data obtained at the standard ASTM conditions may not reflect the performance of the material during use. Same argument is valid for the analysis of sorption isotherms, since frequently data is generated at 25°C, as seen in Table 1.2. As a result, Permeability of different films in literature are obtained in different conditions, as can be seen in Table 1.3.

Table 1.3– Water Vapour Permeability reported for different materials

Material	$H_{r,1}$	$h_{r,2}$	T (°C)	P_w x 10^5 (cm^2/s)	P_w x 10^{10} ($g \cdot cm^{-1} \cdot s^{-1} \cdot KPa^{-1}$)	Reference
OPP	0	100	25	0.002	0.001	Rubino et al. (2001)
	0	100	35	0.003	0.002	
PP	10	100	23	0.011	0.008	Mastromatteo et al. (2012)
PLA	10	100		0.138	0.101	Żenkiewicz and Richert (2008)
	40	90	10	0.029	0.022	Auras et al. (2003)
			20	0.026	0.019	
			30	0.023	0.017	
			37.8	0.022	0.015	
Polyethylene	0	33	25*	0.018	0.013	Bilck, Grossmann, and Yamashita (2010)
	33	64		0.035	0.025	
	64	97		0.126	0.091	
Wheat flour/PLA	0	60	25	9.255	6.720	Abdillahi et al, 2013
Sodium Caseinate	0	30		1.928	1.400	Colak et al, 2015
	0	45		6.197	4.500	
	0	70		58.531	42.500	
Peanut Protein	0	50	37.8	2.127	1.481	Jangchud & Chinnan, 1999
Chitosan	0	50	25	14.158	10.280	Caner et al, 1998
	100	0	20	11.279	8.330	Cerqueira et al, 2012
	76.9	22.5	30	104.098	74.340	Ferreira et al, 2016
Cassava Starch	0	33	25*	4.001	2.905	Bilck, Grossman and Yamashita, 2010
	33	64		7.093	5.150	
	64	97		13.294	9.653	
	2	32.8	25	0.453	0.329	Brandelero et al, 2013
	32.8	64.5		1.199	0.870	
	64.4	90		3.269	2.374	
	100	0		2.301	1.670	Vicentini, 2003
Cassava Flour	100	0		12.423	9.020	Ramos, Carvalho, and Calado (2014)
Taro Flour	100	0		10.122	7.350	
Potato Starch	53	100		30.827	22.384	Moreno et al, 2015
FucoPol	76.9	22.5	30	18.904	13.500	Ferreira et al, 2016

*Refered as ASTM 96 (1995) but not fully specified, so it was assumed 25°C as it is the most common

Brandelero, Grossmann, and Yamashita (2013) and Bilck, Grossmann, and Yamashita (2010) observed that films under the same relative humidity gradient but different relative humidity inside (h_1) and outside (h_2) (e.g. $h_{r,1}$: 30%, $h_{r,2}$: 60% and $h_{r,1}$: 60%, $h_{r,2}$: 90%) presented different permeability to water, and permeability was greater at higher relative humidity conditions. It suggests that water vapour permeability is dependent on the water content of the films.

It is very important to notice that both adsorption and desorption isotherms should be obtained in order to calculate the diffusivity through the film from Eq.1.2. However, it is not easy to find data in literature on desorption isotherms of plastic films. All the papers cited in Table 1.2, e.g., give information on adsorption isotherms of but none of them mentioned desorption and therefore it is not known if hysteresis can lead to significant differences in a film depending on whether it has reached a given equilibrium from dryer or from wetter.

The fact that $P = S \cdot D$ does not apply to all cases, and sometimes apply just for a range of water activity has been known for a while. Hauser and McLaren (1948) observed that Henry's law held for vinyl polymers, rubber hydrochloride, and cellulose acetate materials when the relative humidity was below 50%, but under other conditions diffusion could not be calculated from this simple relation.

Larotonda et al. (2005) proposed an equation that describes solubility by differentiating GAB equation in terms of water activity and dividing the result by the water vapour saturation pressure. This equation has been applied in literature by other authors, such as Brandelero, Grossmann, and Yamashita (2013), Abdillahi et al. (2013) and Bilck, Grossmann, and Yamashita (2010). However, this approach generated a very cumbersome equation that might not be practical. Besides, this equation is only valid when GAB equation applies, which works fine in most cases, but there are situations where the GAB model does not provide a good fit. Also, the equation proposed calculates a single value of solubility valid for a specific equilibrium point only at the film surface in contact with the gas, but not the remaining of the film.

This problem could be easily solved mathematically by using the the isotherm in equation 1.2 with the mass flux obtained on the same method applied to determine permeability. It was precisely what Roy et al. (2000) did when determining the solubility of their films by multiplying the ratio between moisture content and partial pressure of water vapour by the density of the dried film (transforming the water content from gram of water per gram of dried film in grams of water per cubic meters).

Depending on the properties of the material, water passes from one side to the other due to the relative humidity gradient. This gas exchange is commonly measured in terms of permeability, which represents the resistance to the water movement between outer and inner atmospheres.

Water diffusion through a film occurs due to the existence of a concentration gradient. Diffusivity is the measure of how well the permeant moves through the polymer. Hence, permeability measures how fast the permeant concentration increases on the side of lower humidity, diffusivity describes what happens in the polymer (Cussler 2009, Han and Scanlon 2014).

Some authors, such as Colak et al. (2015) , determines the diffusivity from the isotherm. However, as stated by Van Krevelen and Te Nijenhuis (2009) diffusivity can only be determined from the isotherms if the gas diffusion is only dependent on temperature (and thus not on concentration or time). As previously shown, water vapour diffusivity of films is dependent on the gas concentration and therefore should be calculated from Eq. 1.4.

Interactions package-food, and package-ambient typically result in mass transfer that occurs as absorption, permeation and diffusion. Not only water, but also monomers, additives and solvents can migrate from package to food and to the environment through diffusion. Food fats and colorants can be absorbed by package and flavours can permeate, going into or out of the package.

1.4. MATHEMATICAL APPROACH OF WATER PLASTICIZATION IN FILMS

Water can have either act a plasticizing or an antiplasticizing effect on the polymeric matrix. Water molecules can form hydrogen bonds between themselves or with polar groups of hydrophilic polymers. As a result, the isotherm can present different forms depending on the strength and nature of these interactions, which in turn depend on the characteristics of the polymer and on the vapour pressure (Giles, Smith, and Huitson 1974, Sing et al. 1985).

Antiplasticizing effects frequently appear on mechanical tests. Some films present an increase of tensile strength with an increase of water concentration when exposed to small quantities of the plasticizer, or decreasing elongation at break under the same conditions (Chang, Cheah, and Seow 2000, Chang, Abd Karim, and Seow 2006). Water fills the molecular spaces within the polymeric matrix and in case some affinity (covalent, polar, hydrogen bonds) with the polymer molecule entraps the water molecules, it could lead to an increased rigidity, reduces molecular mobility that decreases the free volume and therefore increases structural order by promoting the reorganization of the molecular chains. Hence, the unusual changes on the mechanical properties, and also on glass transition temperature and crystallinity of the polymer (Chaudhary, Adhikari, and Kasapis 2011).

Accumulation of water within the polymer pores is known as clustering, and Park (1986) considered in his isotherm equation the clustering at high water activities by incorporating the work of Zimm and Lundberg (1956) and Lundberg (1972) on clustering functions. It happens when water-water interactions are stronger than water-polymer interactions, typical of polymers that are not very hydrophilic and do not have many polar groups (Almenar and Auras 2010, Van Krevelen and Te Nijenhuis 2009, Siparsky et al. 1997).

Du et al. (2012), observed that in films such as polylactic acid (PLA) the water molecules tend to be adsorbed in the vicinity of other water molecules in the polymer and form clusters instead of simply be adsorbed by the polymer in a water-polymer bond. It is also known that PLA adsorbs low quantities of water, despite the fact that it is a polymer with polar groups on its chains (Auras, Harte, and Selke 2004, Auras et al. 2003, Holm, Ndoni, and Risbo 2006). Antiplasticizing effect of plasticizer in small concentrations on the crystallinity of polymers has been argued by Lourdin, Bizot, and Colonna (1997) for Polyvinyl chloride (PVC), with effect also on mechanical and dynamic mechanical analysis (Mascia 1978, Guerrero 1989).

Increasing water content decreases the tensile strength of the amorphous phase to a point when the overall modulus starts decreasing in value (Guerrero 1989). Then, the water acts as a normal plasticizer, increasing the chain mobility and the free volume. As a result, the glass transition temperature and tensile strength are lowered by the increase on plasticizer content, while elongation at break increases. The plasticising effect of water in polymers is widely explored in literature. Also, mathematical models have been proposed to correlate plasticizer content and the properties of the materials.

An equation was put forward by Gordon and Taylor (1952) correlating the glass transition temperature (Tg) with the fractions of both components and Wood (1958) came to the same conclusions.

$$T_g = \frac{(w_1 \cdot T_{g_1} + k \cdot w_2 \cdot T_{g_2})}{(w_1 + k \cdot w_2)} \tag{1.6}$$

where w_1 and w_2 are the mass fractions of components with glass transition temperatures T_{g1} and T_{g2}, respectively, and k is a material constant.

This equation has been used not only to calculate a single Tg for a copolymer but also to study the effect of plasticizer content on Tg of a polymer. A modification of this equation also allows to study the effect of a third compound on Tg (Chaudhary, Adhikari, and Kasapis 2011, Goldstein 1985, Gontard and Ring 1996). Gordon-Taylor equation is widespread in literature, but there are slightly different equations that have been used in literature (Kwei 1984, Jenckel and Heusch 1953).

William, Landel and Ferry (WLF) equation was proposed to study the effect of temperature on viscosity, mechanical and electrical relaxations of amorphous polymers and other supercooled, glass-forming liquids polymers (Williams, Landel, and Ferry 1955).Applied to molar diffusion:

$$log \frac{D_w}{D_{w,g}} = \pm \frac{C_1 (T - T_g)}{C_2 + T - T_g} \tag{1.7}$$

This type of equation has been used for a variety of properties that depend on molecular mobility and relaxation times, including diffusivity as in eq. 1.7, and appears in literature to analyse the viscoelastic behaviour of hydrophilic films (Schnell and Wolf 2001). Biliaderis, Lazaridou, and Arvanitoyannis (1999), Lazaridou and Biliaderis (2002) and Kristo and Biliaderis (2006) used this model to fit data from DMTA analysis and hence study the E'.

Despite the fact that this equation is normally used on the study of viscoelastic properties, it has been successfully applied on the study of gas transport through films, such as on the study of Kinetics of Seed Viability Loss (Sun 1997), water diffusivity on drying kinetics (Räderer, Besson, and Sommer 2002) and permeability to ethylene of wheat gluten films (Paz et al. 2005).

Gordon-Taylor equation (G-T) describes the dependence of Tg on plasticizer content and WLF equation relates the kinetics of a phenomenon that correlates relaxation time with the Tg of the material, and therefore both equations are often used in literature (Sun 1997, Lazaridou and Biliaderis 2002, Merenga and Katana 2010). A more robust analysis could be carried out by combining both theories, as shown by Räderer, Besson, and Sommer (2002) on the study of water diffusivity.

1.5. OXYGEN AND CARBON DIOXIDE

Unlike water and organic gases, O_2 and CO_2 follow Henry's law and their adsorption is linearly dependent on pressure. As a result, permeability can be assumed as the product of Solubility and Diffusivity for single layer materials. However, it should be noticed that solubility of CO_2 in polymers tends to be much greater than O_2. Their ration, P_{CO_2}/P_{O_2}, is known as the permeability ratio β, which is a critical parameter in packaging design, as it can be shown that the equilibrium atmosphere depends on this ratio, regardless of the individual values for each gas. While this value may vary between 2 and 8, it is around 3-4 for most films (Van Krevelen and Te Nijenhuis 2009). Hence, films tend to present higher permeability to carbon dioxide than to oxygen, as can be seen in Table 1.4.

From Table 1.4 it is possible to observe that there is more information in literature on permeability to Oxygen than to Carbon Dioxide. Considering that films in Table 1.4 differ on conditions of processing, presence of plasticiser and analysis, it is possible to say that biobased and non-biodegradable materials presented similar resistance to oxygen.

Table 1.4– Permeability to Oxygen (P_{O2}) and to Carbon Dioxide (P_{CO2}) of different materials

Material	Test Conditions	$P_{O2} \times 10^9$ (cm^2/s)	$P_{CO2} \times 10^9$ (cm^2/s)	β	Reference
HDPE	50-75% RH, 25°C	5.45	80.62	14.78	Ullsten and Hedenqvist (2003)
LDPE	50-75% RH, 25°C	20.82	60.41	2.90	Ullsten and Hedenqvist (2003)
PP	-	1.38	3.58	2.59	Mastromatteo et al. (2012)
	50% RH, 15°C	2.35	-		Hong and Krochta (2003)
PET	0% RH, 23°C	0.18	-		Laufer et al. (2013)
APET	50% RH, 23°C	0.71	-		Abdillahi et al. (2013)
PLA	50% RH, 23°C	1.00	-		Abdillahi et al. (2013)
	-	2.95	30.61	10.37	Zenkiewicz and Richert, 2008
PS/EVOH/PE	50% RH, 23°C	$2.31\cdot10^{-7}$	-		Abdillahi et al. (2013)
Wheat flour/PLA	50% RH, 23°C	0.55	-		Abdillahi et al. (2013)
Sodium Caseinate	35% RH, 23°C	0.05	-		Colak et al. (2015)
	50% RH, 23°C	0.13	-		
	75% RH, 23°C	1.46	-		
Peanut Protein	0% RH, 30°C	6.92	-		Jangchud and Chinnan (1999)
Chitosan	0% RH, 25°C	0.83	-		Caner, Vergano, and Wiles (1998)
	-	3333.33	-		Swain et al. (2014)
	-	5.86	19.95	3.41	Cerqueira et al. (2012)
	55% RH, 30°C	5.92	34.13	5.76	Ferreira et al. (2016)
	-	5.48	-		Fajardo et al. (2010)
Cassava Starch	75% RH, 23°C	0.50	-		Souza et al. (2012)
Potato Starch	53% RH, -	0.16	-		Moreno, Atarés, and Chiralt (2015)
FucoPol	55% RH, 30°C	4.86	14.83	3.05	Ferreira et al. (2016)
Alginate/ Apple Puree	50% RH, 25°C	0.12			Rojas-Graü et al. (2007)
Banana Flour	50% RH, 25°C	0.47	-		Sothornvit and Pitak (2007)

It should be noticed that all the results in Table 1.4 were originally reported in quite diverse units. For oxygen and carbon dioxide as the variables that are normally measured experimentally are the volumetric fractions, it is usual to write the permeance/permeability equation with volumetric flow rates. This gives for permeability:

$$\dot{v}_W = \frac{P_W}{\delta}.A.p.(y_2 - y_1) \tag{1.8}$$

where $\dot{v}_W$ comes in units of volume per time and y is the volumetric fraction (which is equal to the molar fraction for a gas). Units of permeability in literature usually continue to cite the individual units of each of the measured variables, for instance, mL.mm/(m^2.atm.day), and various similar combinations. As oxygen and carbon dioxide obey Henry's law, in this case one can safely state that this is the same as

$$\dot{n}_W = \frac{D_W.S}{\delta}.A.p.(y_2 - y_1) \tag{1.9}$$

Where $\dot{n}_W$ is the molar flow rate. It would be better to use molar flow rates because they do not depend on pressure or temperature, whereas volumetric flow rates do. However, the latter are the norm in packaging literature

As the volume of a gas depends on pressure, volumetric units of permeability need to specify whether they refer to a reference temperature and pressure (STP being the most common, 273.15 K and 1 atmosphere), or they refer to the temperature at which the permeability was determined. The influence of temperature on the units of permeability is a cumbersome and unfortunate consequence of selecting volumetric flow rates as a reference.

In order to avoid this problem, this thesis uses permeability of oxygen and carbon dioxide in units of square length per unit of time, permeance and mass transfer coefficient in units of length per time. Results in mole were converted by multiplying the results per temperature (T, in Kelvin) and R (universal gas constant, in $m^3 \cdot atm \cdot K^{-1} \cdot mol^{-1}$ or $m^3 \cdot Pa \cdot K^{-1} \cdot mol^{-1}$, depending on the pressure used by the authors). Permeability to O_2 and CO_2 in $g \cdot Pa^{-1} \cdot s^{-1} \cdot m^{-1}$ were converted to $cm^2 \cdot s^{-1}$ by passing grams to moles of gas (from the molar mass) and then multiplying per R · T.

The permeance (or permeability) of a film can be determined experimentally very easily by creating a modified atmosphere in one side of the film and then allow it to equilibrate as a result of the transfer through the film. Most typically, a tight container with the film on top is in contact with the normal atmosphere (which will have approximately 21% of oxygen and 0.1% of carbon dioxide), and the atmosphere inside is flushed (for instance, 0% oxygen and 20% carbon dioxide). The gas composition inside the container will evolve to atmospheric over time. A simple mass balance with n referring to the number of moles of gas inside the container at a given time t gives:

$$variation = transfer$$

and

$$\frac{\mathrm{dn}}{\mathrm{dt}} = \text{molar flow rate through film}$$

$$V\frac{dC}{dt} = P_aA(C_e - C) \tag{1.10}$$

where V is the container volume, C the molar concentration of gas inside the container and C_e that outside (assumed constant). Using molar fractions:

$$V\frac{dy}{dt} = P_aA(y_e - y) \tag{1.11}$$

If permeance is constant, then integration gives:

$$y_t = y_e - (y_e - y_0) \cdot e^{-\frac{P_a \cdot A \cdot t}{V \cdot l}} \tag{1.12}$$

Note that the permeability obtained from equation 1.8 appears in units of square length per unit of time. Equation 1.12, or similar approaches that consider permeance (Pa = P/l) or that makes area implicit (P” = P · A), are usually applied when using multilayer films or in the study of permeability of perforated films (Fonseca et al. 2000, Montanez et al. 2010a).

It is interesting to consider what would happen if the container was a food package with a given quantity of a commodity respiring. There would be a rate of consumption or production of the gas in addition to the transfer through the film, so the mass balance would be:

$$V\frac{dC}{dt} = P_a A(C_e - C) + R_m.w \qquad (1.13)$$

where R_m is the molar rate of production of gas (using the standard nomenclature in chemical reaction engineering, rates of reaction are positive for products and negative for reagents) per unit of product weight (moles per unit of time and weight), and w its weight. Thus, one will reach steady state when the two terms balance:

$$P_a A(C^* - C_e) = R^*{}_m.w \qquad (1.14)$$

where the * is used to denote concentration at equilibrium (respiration rate may vary with concentration of gases, hence a * is also used to clearly note that the equality refers only to equilibrium conditions). It is usual in literature to consider volumetric rates of respiration (if so, and as already noted, it is critical to clarify the temperature and pressure that the volume refers to). With R denoting a volumetric rate of production, e.g. mL/(hour.kg):

$$P_a A(y^* - y_e) = R^*.w \tag{1.15}$$

Let us now consider the case of both oxygen and carbon dioxide. There will be a system of two equations giving the atmosphere composition at equilibrium (note that oxygen is a reagent, so the rate is negative):

$$P_{a,O} A\left({y^*}_O - y_{O,e}\right) = -{R^*}_O.w \tag{1.16}$$

$$P_{a,C} A\left({y^*}_C - y_{C,e}\right) = {R^*}_C.w \tag{1.17}$$

Dividing the two equations, and with the ratio of permeance of carbon dioxide to that of oxygen being the permeability coefficient β, and the ratio of respiration rate of carbon dioxide to that of oxygen being the respiratory quotient Q:

$$\beta \frac{({y^*}_C - y_{C,e})}{(y_{O,e} - {y^*}_O)} = Q^* \tag{1.18}$$

Therefore, if the respiratory quotient does not vary with the gas composition (a common occurrence, even when individual rates depend on gas composition), the relation between carbon dioxide and oxygen compositions at equilibrium is given by a simple straight line with a slope that depends only on the ratio between permeabilities and rates of respiration and not on their individual values:

$$y^*{}_C = y_{C,e} + \frac{Q^*}{\beta}\left(y_{O,e} - y^*{}_O\right) \tag{1.19}$$

As the concentration of carbon dioxide in the outside air is bound to be very small,

$$y^*{}_C \approx \frac{Q^*}{\beta}\left(y_{O,e} - y^*{}_O\right) \tag{1.20}$$

1.6. MASS TRANSFER THROUGH PERFORATIONS

An efficient packaging design balances both respiration profile of produce and package permeability, as the respiration rate equals the mass transfer through the package at equilibrium. Permeability to O_2 of most plastic materials are around 2 to 8 times lower than to CO_2. It means that these materials would be preferable for products less tolerant to CO_2 such as apples and mangoes (Hussein, Caleb, and Opara 2015, Finnegan 2014). However, products such as lettuce and tomatoes require an atmosphere of similar levels of O_2 and CO_2, or richer in carbon dioxide (Ballantyne, Stark, and Selman 1988, Tumwesigye et al. 2017). Besides, many products benefit from high levels of CO_2 as it reduces respiration rates of many fresh and minimally processed fruits, inhibits ethylene action and may also be beneficial to inhibit the growth of moulds, fungi and many pathogens (Chitarra and Chitarra 2005, Beaudry 1999). Ethylene is a volatile compound produced by fruits and vegetables that is responsible for activating the ripening process and stimulating respiratory activity of fruits and vegetables. Therefore, high levels of CO2 may help prolonging shelf life of products by reducing the respiratory activity(Eskin and Hoehn 2013).

The ratio of production of carbon dioxide to consumption of oxygen is known as the respiratory quotient, and varies between 0.8 and 1 for most products under aerobic conditions (values above 1 typically indicate anaerobic fermentation). It depends essentially on the composition of the substrate begin oxidised by the respiration process - for instance, sugars such as glucose and fructose would have a ratio of 1 (Guillaume, Guillard, and Gontard 2010). A compilation of optimum atmospheres for different products can be found in Mahajan et al. (2005). Therefore, the mass transfer fluxes out of the package should be around the same (would be equal if respiratory quotient was 1). However, carbon dioxide is escaping from the package much faster than oxygen is entering for most films simply because it has a much higher solubility in them than oxygen does. Much lower permeability ratios would be required to achieve an environment much richer in carbon dioxide than in oxygen. Hence, an alternative to the problem would be the utilization of perforated films. Another reason to use perforated films is that some products have too high respiration rates compared to the mass transfer process through films and in those cases the package would reach anoxia quickly.

The permeability ratio of a perforated package will go from 2-8 to 0.8 when the package is excessively perforated. In order to achieve the optimum compositions for the different products, that is, the atmosphere composition necessary to maintain the initial product quality and extend the shelf-life of the products, it is necessary to find the correct area of perforation. Mir and Beaudry (2016) show the expansion of the feasible concentrations that packages can achieve with perforations in a useful visual form in CO_2 versus O_2 plots. A similar plot is shown in figure 1.2, comparing different films and the ideal package conditions for cherry tomatoes based on respiration data provided by Sousa, Oliveira, and Sousa-Gallagher (2017), assuming a package area of 150 cm^2 with a diameter of perforation of 110 μm and 250 g of produce stored at 5°C. Mass transfer coefficient was calculated from the permeance of perforated films obtained by Mastromatteo et al. (2012) and the permeability of the films can be found in Table 1.4. Results show that cherry tomatoes would reach the ideal conditions if packed in PLA films without perforations, which confirms the results obtained by Tumwesigye et al. (2017), who observed that the cherry tomatoes could be packed with unperforated films.

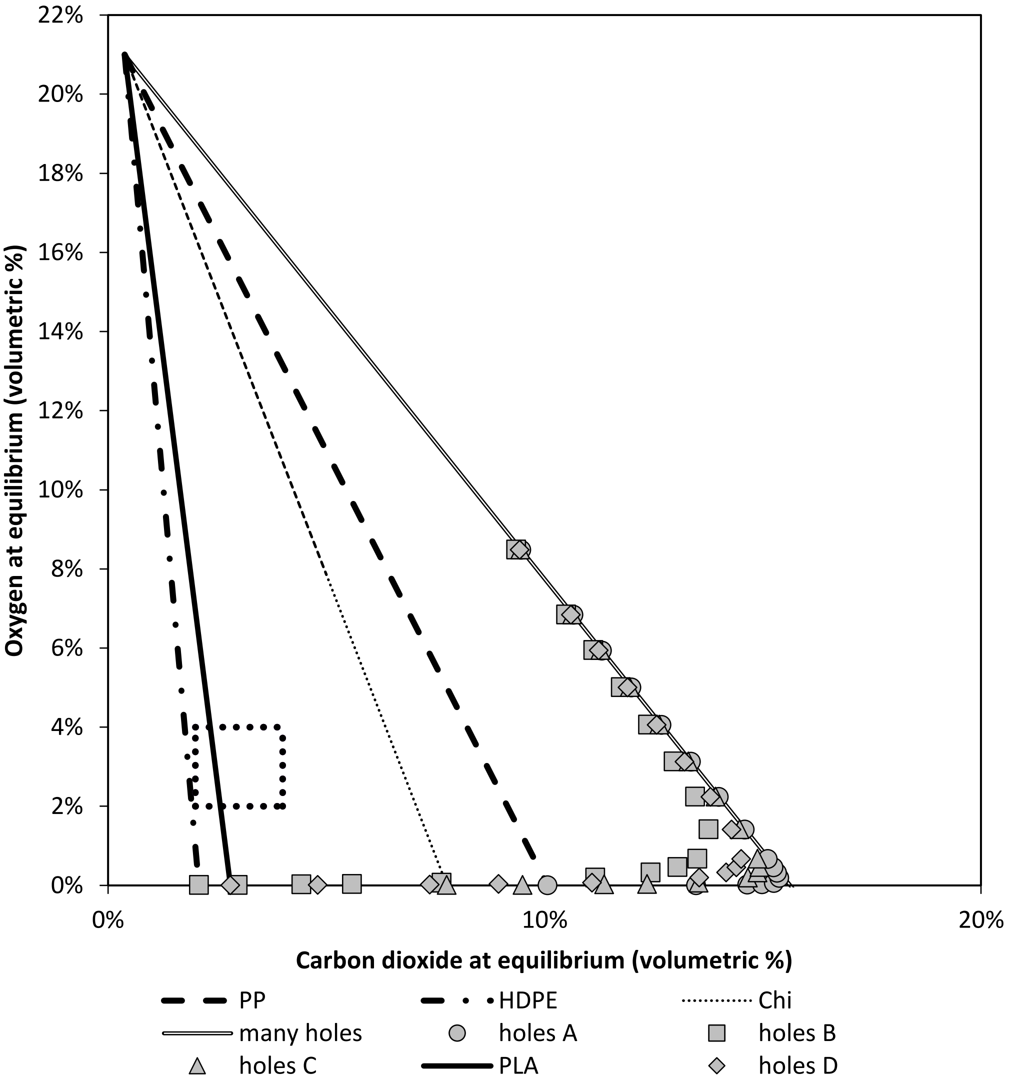

Figure 1.2 - Modified atmospheres that can be generated by cherry tomatoes following the respiration rate model of Sousa, Oliveira, and Sousa-Gallagher (2017) packed in Polypropylene, High Density Polypropylene, Chitosan or PLA films with permeabilities according to Mastromatteo et al. (2012), Ullsten and Hedenqvist (2003), Cerqueira et al. (2012) and Żenkiewicz and Richert (2008) both influenced by temperature, for storage at 5°C. The straight lines give all possible atmospheres for each film if unperforated. The symbols indicate atmosphere compositions of a package with 150 cm^2 of exposed area of 30 μm thick film and 250 g of cherry tomatoes, from unperforated (points on top of the respective line) to increasing number of perforations of 100 μm diameter (each additional perforation is one further point).

For perforated films, total mass transfer is the sum of two processes that occur in parallel: (i) the mass transfer through the polymeric film; (ii) the mass transfer through the perforation. The total flux through a film can be described by the product of Permeance, Area of film and the difference between gas concentration on the ambient outside and inside. This total flux can is equal to the sum of the flux within the film and through the perforations. Hence:

$$\mathrm{P}_a \, \mathrm{A} \, (c_e - c) = P_{af} \cdot \left(\mathrm{A} - A_p\right) \cdot (c_e - c) + K \cdot A_p \cdot (c_e - c) \quad (1.21)$$

P_a is the effective permeance of the whole film with its perforations. $P_{a,f}$ is the permeance of the unperforated film, K is the mass transfer coefficient through the perforation, A_p is the total area of perforations. The mass transfer coefficient through a perforation is equal to the permeance due to it. Permeance of the whole system and permeance of the film without perforations can be determined experimentally. Thus, the mass transfer coefficient through the perforations may be calculated as follows:

$$K = \mathrm{P}_a \cdot \frac{\mathrm{A}}{A_p} - P_{film} \cdot \left(\frac{\mathrm{A}}{A_p} - 1\right) \quad (1.22)$$

Water vapour permeability through perforations has not received much attention perhaps mainly for two reasons: (i) most research in fruits and vegetables provide data on weight loss but very few divide this in water loss and substrate loss, and thus are not truly measuring water transport and (ii) the permeability to water vapour of films is usually much greater than to oxygen and carbon dioxide, difference even more significant for biobased materials (check Table 1.3 and Table 1.4 for data on permeability of different films). Tumwesigye et al. (2017), for example, studied two different films with different number of perforations stored at two different relative humidities, but did not explore the effect of water permeability of film and perforation on their results, and only speculated a possible relation between relative humidity and weight loss. Mistriotis et al. (2016) designed perforated packages for cherry tomatoes and peaches knowing their water transpiration rate, but totally disregarded the amount of water that passes through the perforations assuming water flows mainly through the polymer, without however providing proof of this assumption.

In order to evaluate the relative importance of mass transfer through the perforations on the total water vapour flux through the film, data on water vapour permeability through perforated Polypropylene (PP) provided by Mastromatteo et al. (2012) was used to calculate the mass flux through a package by applying Eq. 1.21 (it should be noted that the total flux on the ratio n_{perf} / n_{total} is a sum of the mass flux through the perforations and through the film). Calculations were made supposing a packaging area of 150 cm^2, made of Polypropylene (PP), Poly(lactic acid) (PLA) or Chitosan. These films represent low, medium and high water permeabilities, respectively. Results are shown in Table 1.5, indicating that the water flux through the perforation is only small enough to be negligible when the film is very permeable to water (Chitosan). On films with medium and low permeability to water, however, the flux through the perforations can be responsible for great part of the transport through the package. Larger perforations or a higher number of perforations will provide an even greater impact on the total flux, which tend to affect also films more permeable to water. These results indicate that a proper design of perforated films should consider the water transfer through both film and perforations.

Table 1.5– Impact of Mass Flux Trough the Perforations ($\dot{n}_{perf}$) on Total Mass Flux through Perforated Films ($\dot{n}_{total}$)

Diameter of perforations (μm)	Number of Holes	$K \cdot A_{perf}$ (cm^3/s)	$\dot{n}_{perf}/\dot{n}_{total}$ (%)		
			PP*	PLA**	Chitosan***
50	1	7.22E-04	11.25	2.54	0.001
50	2	1.22E-03	17.65	4.23	0.002
50	4	7.44E-03	56.64	21.19	0.014
50	10	1.29E-02	69.40	31.83	0.025
70	1	8.43E-04	12.90	2.96	0.002
70	2	1.66E-03	22.59	5.67	0.003
70	4	7.97E-03	58.31	22.36	0.015
70	10	1.37E-02	70.63	33.11	0.026
90	2	1.79E-03	23.96	6.09	0.003
90	4	8.16E-03	58.90	22.78	0.016
90	10	1.80E-02	75.98	39.44	0.035
110	1	2.97E-04	7.22	1.58	0.001
110	2	3.16E-03	35.71	10.26	0.006
110	4	8.71E-03	60.48	23.95	0.017
110	10	2.08E-02	78.53	42.96	0.040

*Polypropylene, data from Mastromatteo et al. (2012), **Poly(lactic acid), permeability from Żenkiewicz and Richert (2008), ***Chitosan, data from Ferreira et al. (2016).

Mass transfer through perforations was studied by Emond, Chau and co-workers (Emond et al. 1991, Emond 1992, Emond et al. 1998) and further applied by other authors such as Silva et al. (1999), Fonseca et al. (2000), and Montanez et al. (2010a) in the context of perforated-mediated modified atmosphere packaging where they used a perfectly impermeable container, with just a few plugs of a given diameter and length that would control the mass transfer rate. These were cylinders that could have a few mm of length, and generally had a high length to diameter ratio.

However, research in literature may contain imprecisions on the study of perforated films or plugs. Emond et al. (1991) studied the mass transfer coefficient of macroperforated films through relatively thick films (approx.. 0.1, 0.7 and 1.2 cm thick). In spite of starting their analysis from an approach similar to Eq. 1.4, the authors decided to consider not the mass transfer coefficient but a term they called effective permeability, which was the permeability from Eq. 1.4 multiplied by area and divided by thickness. It means that the authors did not discount the area from their coefficient K, and there is an obvious influence of the diameter of the perforation that is simply due to the area available for mass transfer. As a result, all the data obtained by this approach are only valid for those specific areas. Therefore, mathematical models proposed by authors that adopted this methodology such as González et al. (2008), Montanez et al. (2010a), Fonseca et al. (2000) and Techavises and Hikida (2008) are only valid for the same areas used in the original works.

1.7. DIMENSIONLESS CORRELATIONS IN MASS TRANSFER ANALYSIS

Some studies on perforated films have tried to establish mathematical models that describe the phenomenon. Fonseca et al. (2000)

proposed a model relating what they called mass transfer coefficient (including the area) to diameter and length of their tubes. González et al. (2008) proposed an equation that relates an oxygen transmission rate (actually a permeance that also includes the area) with area of perforation. Mahajan, Rodrigues, and Leflaive (2008), from the model proposed by Fonseca et al. (2000) and the Arrhenius equation, obtained a model relating water vapour transmission rates of tubes not only to the diameter and length of their tubes but also to the time, temperature, tortuosity and porosity of their materials. Techavises and Hikida (2008) put forward a quadratic equation relating the diameter of perforation with their effective permeability (also incorporating the area within the result). Mastromatteo et al. (2012) proposed an empirical model with 2 fitted parameters in an attempt to develop a model that considers the perforation and the film similar to eq. 1.22.

Regardless of how accurate the calculations were, the main issue regarding these models is that they do not avail of the principle of dynamic similarity, and therefore tend to be only valid to their own set of data. Thus, it comes as no surprise that these models have not been actually applied by other authors. One correlation for each set of data is a problem of empirical functions that are not written in terms of dimensionless correlations, as they do not avail of the principle of dynamic similarity.

Dimensionless numbers are used by engineers as a tool to reproduce projects in a different scale (scale up or down). Data obtained in lab scale can be applied to larger processes by establishing the similarities between the parameters. The principle of similarity states that the dimensionless number has the same effect regardless of the individual values of the properties that compose it. This topic has great interest to Chemical and Food Engineers, and has been explored in literature such as in the works of Astarita (1997), de Souza Mendes (2007), Ignacio (2013) and Delaplace et al. (2015b). Extensive lists of dimensionless numbers and details of their physical meaning can be found in the work of Ruzicka (2008) and Delaplace et al. (2015a).

The Sherwood number (Sh) is a dimensionless quantity that includes the mass transfer coefficient and gives the relationship between the convective mass transport over the boundary layer with transport purely due to diffusion (Delaplace et al. 2015a, Ruzicka 2008). It can be calculated as a function of other dimensionless numbers, and in the case of forced convection normally appears as:

$$Sh = \beta_1 + \beta_2 \cdot Re^{\beta_3} \cdot Sc^{\beta_4} \tag{1.23}$$

Sh is given by the relationship $K \cdot L \cdot D^{-1}$, Reynolds number as $\rho \cdot v \cdot L \cdot \mu^{-1}$, and Schmidt number $\mu \cdot D^{-1} \cdot \rho^{-1}$, where L is the characteristic length, v the fluid velocity, and μ, ρ and D are the viscosity, density and diffusivity of the fluid, respectively. Parameters β_i are found in literature for many situations and can also be obtained by data regression. Oliveira and

Oliveira (2010) provide an extensive list of values that β_i have been assigned in literature.

The Reynolds (Re) number is one of the most important dimensionless numbers in Engineering. It was proposed by British physicist Osborne Reynolds to characterize the flow of liquids in cylindrical ducts and has been used in Fluid Mechanics to study the fluid flow and identify its regime (laminar, transitory or turbulent) (Delaplace et al. 2015b). For natural convection, the Reynolds number on eq. 1.23 is replaced by the Grashof number (Gr), which includes the buoyancy effect. The Schmidt number (Sc) relates viscosity, density and diffusivity, and appears when the transport rate is sufficient to affect the flow (Ruzicka 2008).

Examples of successful application of correlations for the Sherwood number in literature can be found in the study of mass transfer in membranes (Gekas and Hallström 1987, Lee, Amy, and Cho 2004). Metz (2003) applied this type of correlation to describe water vapour transport through membranes. In their work, the authors included a ratio between length of flow and hydraulic diameter, raised to another parameter β_i. This term can be particularly useful to us as L/d affects the mass flux and determines if only the convective mass transfer is relevant or diffusion has great effect on the flow.

Rennie and Tavoularis (2009) used the study of Becker, Misra, and Fricke (1996) on transpiration of fruits and vegetables and applied a Sherwood relation to calculate the air film mass transfer coefficient, which is related to the air flow surrounding the respiring commodity. The authors also studied the produce temperature by using the interfacial convective Nusselt number (Nu) and the gas mixture temperature in the package with another correlation , analogue of 1.23 for heat transfer, that relates Nu with the Reynolds and Prandtl (Pr) number. Despite the fact that their work is on perforated packages, the authors did not present a model that can be applied directly on the calculation of mass transfer through perforations. However, it gives an indication that the use of dimensionless numbers on packaging technology can be a useful tool for food packaging design.

The suitability of a correlation depends, as mentioned before, on the physics of the phenomenon, and hence an established model such as the Sherwood correlation may not be the most adequate to all situations. The underlying principles should be verified. The proper methodology is known as the Buckingham-Π Theorem that can be used to determine which dimensionless numbers are suitable for a specific phenomenon. Vaschy (1892) wrote a paper on similarities in physics and Buckingham (1914) developed the theory and provided proof of its applicability, and thus it is also called Vaschy–Buckingham theorem. Besides the original work of Buckingham (1914), it is possible to find information on this theory in other works in literature, such as Curtis, Logan, and Parker (1982), Geankoplis (1993), Ignacio (2013) , Delaplace et al. (2015c) and Debongnie (2016). It has been applied to describe a wide variety of phenomena such as microrobots propulsion inspired by the motility mechanism of bacteria

(Behkam and Sitti 2004), extrudate expansion in a twin-screw food extruder (Cheng and Friis 2010) or even in Operations Management (Miragliotta 2011).

The Buckingham- Π method begins by listing the important variables in the particular physical problem. It states that n independent dimensionless groups, named Π's, can be determined by the relationship between q quantities (parameters or variables) whose units are defined in terms of u fundamental units or dimensions, where n is obtained from q – u.

Exemplifying, consider a hypothetical situation where the mass transfer coefficient through perforations (K) depends on temperature, diameter of perforation (d) and thickness of film (L). Temperature affects the mass transfer by its effect on diffusivity (D), density (ρ) and viscosity (μ) of the fluid. This totals 6 variables. The units for the fluid properties are $\delta^2 \cdot t^{-1}$, $M \cdot \delta^{-3}$ and $M \cdot \delta^{-1} \cdot t^{-1}$, respectively (where δ is the unit of Length, t time and M mass). Diameter of perforation and film thickness have units of length (δ) and the mass transfer coefficient (K) is expressed as $\delta \cdot t^{-1}$. With q = 6, there are just 3 fundamental units (u = 3), therefore 3 dimensionless numbers are necessary (n = q – u = 3).

The procedure to establish the 3 dimensionless groups (or Π's) consists in choosing as many primary variables as there are dimensions (3 in this case), and then find the dimensionless groups formed by these 3 variables and each one of the others. Different groups will result from the choice of 3 primary variables; they must include all 3 dimensions, and the desired property should be left aside.

In this case, a particularly interesting combination is obtained by choosing as primary variables ρ, d and D. Thus, the 3 groups will be composed by:

- $\Pi_1 = \rho^a\, d^b\, D^c\, K$

Dimensions: $M^a\, \delta^{-3a}\, \delta^{b}\, \delta^{2c}\, \delta^{-c}\, \delta\, t^{-1}$

For this group to be dimensionless:

a=0,

-3a+b+2c+1=0, b=1

-c-1=0 , c=-1

Hence,

$$\Pi_1 = \rho^0\, d^1\, D^{-1}\, K \quad \therefore \ \Pi_1 = \frac{K \cdot d}{D}$$

- $\Pi_2 = \rho^a\, d^b\, D^c\, \mu$

Dimensions: $M^a\, \delta^{-3a}\, \delta^{b}\, \delta^{2c}\, t^{-c}\, M\, \delta^{-1}\, t^{-1}$

Then:

a = -1

-3a+b+2c-1=0, b = 0

-c = 1, c=-1

Hence,

$\Pi_2 = \rho^{-1} d^0 D^{-1} \mu \therefore \Pi_2 = \frac{\mu}{\rho \cdot D}$

- $\Pi_3 = \rho^a d^b D^c L$

Dimensions: $M^a \delta^{-3a} \delta^b \delta^{2c} t^{-c} \delta$

For this group to be dimensionless:

a=0,

-3a+b+2c+1=0, b=-1

-c=0 , c=0

Hence,

$\Pi_3 = \rho^0 d^{-1} D^0 L \therefore \Pi_3 = \frac{L}{d}$

Thus, one can propose $\Pi_1 = f(\Pi_2, \Pi_3)$

Note that Π_1 is the Sherwood number when the characteristic dimension is the diameter, Π_2 is the Schmidt number, and Π_3 is a ratio between thickness and diameter, and therefore when temperature (and hence viscosity, density and diffusivity), diameter of perforation and thickness of film are the only variables important to the matter, a correlation similar to the Sherwood correlation presented in eq. 1.23 with the ratio L/d instead the Reynolds number would be suitable for the analysis. However, it has been said that air velocity is a constant on food packaging and probably with great effect on the mass transfer coefficient, and likewise other parameters such as gas concentration might also be relevant to the matter. Hence, this model might not apply to those circumstances, and is shown here just to illustrate the principle.

2. A META-STUDY PROVIDING A UNIFIED ANALYSIS OF THE DESIGN ENGINEERING METHODS FOR MODIFIED ATMOSPHERE PACKAGING WITH PERFORATED FILMS FOR OPTIMUM OXYGEN AND CARBON DIOXIDE BALANCE

ABSTRACT

The use of perforation systems has expanded the applicability of modified atmosphere packaging, as perforated films allow for higher carbon dioxide concentrations and may also permit to use a same film and modulate its permeability by perforating the correct number of holes of the appropriate dimension. Research publications on this topic apply different approaches needlessly and some of the models suggested and conclusions proposed are not correct. The quantification of the gas exchange through perforated packages for oxygen and carbon dioxide is reviewed in this communication with a view to provide a unified analysis of methods used and a meta-analysis of data reported to date. The effective permeability of a perforated package is approximately what would be expected from dimensionless correlations for mass transfer from flat planes for perforation diameters of around 1mm and bigger. For smaller perforations the effective permeability increases significantly with decreasing diameters. The concentration gradient across the package is also relevant. Even small

differences in values of mass transfer coefficients have a dramatic effect on the result.

2.1. INTRODUCTION

Modified atmosphere packaging is a shelf life extension technique that could be described as an example of chemical reactions being slowed down by excess concentrations of their products and lower concentrations of their reagents. Many food products are not stable throughout their shelf life and the metabolisms taking place are often related to oxidative processes, where oxygen is being consumed and carbon dioxide and water vapour are being produced. While the most studied of these is the respiration of fresh fruits and vegetables, many other products consume and produce gases in the same way and can be considered in the same manner (Rodriguez-Aguilera and Oliveira 2009) The senescence of the vegetable tissues is strongly inhibited by lowering temperature, which is the most influential controlling factor of the rate of chemical reactions. Secondly, as respiration consumes oxygen and releases carbon dioxide and water vapour, if the environment surrounding the product is poor in oxygen and rich in the other two gases, the degradation rate may be further reduced and shelf life is extended. The phenomenological reasons for this effect are varied, depending on the product and on the specific metabolisms involved, including inhibitory effect of CO_2, possible acidification of the intercellular space by CO_2, but is not universal (some products do not benefit significantly from modified atmospheres). Water vapour would involve not only respiration but also transpiration, which essentially is the loss of water due to drying. While water vapour (humidity) is of crucial importance to the quality and value of a product and the establishment of optimum atmospheres for a wide variety of commodities (Rodriguez-Aguilera and Oliveira 2009), the modified atmosphere packaging design for fresh fruits and vegetables has been done very often by considering oxygen and carbon dioxide alone (Mannapperuma et al. 1989, Paul and Clarke 2002, Sousa-Gallagher and Mahajan 2013). Although this work is focused on oxygen and carbon dioxide alone, it is stressed that water vapour is a crucial element to be considered adequately as well in modified atmosphere packaging.

Respiration is not the only phenomenon of interest for shelf life; microbial growth may be of paramount importance particularly when considering safety issues. In fact, extending the shelf life with modified atmospheres has raised concerns that pathogens might thus have time to grow and vegetable products might not be spoiled, but be effectively dangerous (Sivertsik, Rosnes, and Bergslien 2002). This implies that the oxygen content desired is not zero, or even too close to zero, as anaerobic phenomena and fermentations could set, hence, there is usually a minimum and maximum oxygen content desired for maximum preservation that depends on the product (Beaudry 1999). High carbon dioxide concentrations also inhibit the growth of many pathogens, such as salmonella, but not others like *Clostridium botulinum* that can grow in depleted oxygen environments (Sivertsik, Rosnes, and Bergslien 2002).

Therefore, high carbon dioxide may be beneficial for shelf life also from the safety point of view. Conversely, excess carbon dioxide may induce chilling injuries or lead to off-flavours and off-aromas, which means that there is also a window of desirability for the concentration of this gas, with a minimum and a maximum recommended for each product. Plots of carbon dioxide versus oxygen recommended concentration windows are a useful way of summarising this information (Mannapperuma et al. 1989, Mahajan et al. 2005).

Perforated films expand the potential of modified atmosphere packaging, as will be quantified later. The permeability of a perforated film obviously depends strongly on the perforated area, and therefore finding the optimum film for a particular product becomes complex. Several studies in literature use a simple trial and error approach: try a number of films with different perforations, and see which one seems to work better for a product (Cliffe-Byrnes, Mc Laughlin, and O'Beirne 2003, Amorós et al. 2008, Ramin and Khoshbakhat 2008, Kartal, Aday, and Caner 2012). With a wide variety of choices of packaging films and number and size of perforations, the almost endless combinations possible make this approach very inefficient. Furthermore, respiration rates may change significantly between different product batches, so even if one solution proves good enough by trial and error for a particular batch, there is no assurance that it will be suitable for another.

Therefore, designing a package that will provide an optimum performance because it will maintain a gas composition inside it within the optimum window for both gases is an excellent example of applying engineering concepts for the design of optimised food systems. It involves quantifying the respiration rate of the product (kinetics of the consumption of oxygen and production of carbon dioxide and water vapour) and the rate of exchange of these gases through the package to the outside atmosphere (mass transfer phenomena) to predict the composition inside the package at equilibrium and thus ensure that it sits inside the optimum window of oxygen and carbon dioxide concentrations for the specific products. At this stage, it is assumed that the storage conditions (temperature and relative humidity) are constant throughout. This paper focuses on oxygen and carbon dioxide, while noting that water vapour, and possibly ethylene, should then also be considered.

A simple mass balance can be applied to engineer the design of a package. In steady state, the concentration of any gas inside the package is constant, and so it must be such that the respiration rate equals the rate of mass transfer across the film for every gas, as depicted in fig. 2.1.

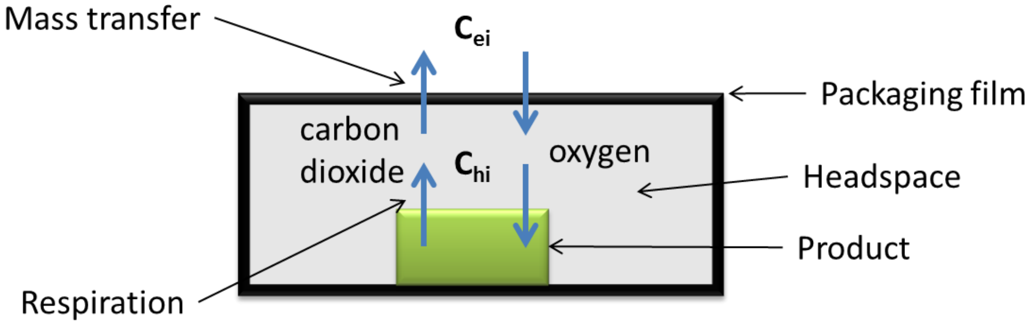

Figure 2.1. Sketch of the main phenomena involved in package design. The headspace volume is exaggerated in the picture for clarity purposes. C_e is the external concentration and C_h that in the headspace, with i denoting oxygen or carbon dioxide.

When a film is perforated, the latter will be composed by two mass fluxes in parallel: through the film and through the perforations. The mass flux through perforations has not always been dealt with properly, though. Different approaches and models have been proposed, some are perfectly correct but may be too complex to be used efficiently in practice, and others are actually grossly wrong, with some inaccuracies in between that have brought needless complexity and confusion to the area.

The purpose of this chapter is to provide what pharmacology designates a meta-study, that is, a global analysis of a variety of specific studies published to date with the purpose of establishing a clearer and unbiased view, and thus reach conclusions of wide applicability with greater confidence.

A second objective of the work is to provide evidence for the importance of a proper determination of mass transfer coefficients for the case of perforated films, and suggest a suitable approach that uses the principal of dynamic similarity to maximise the comparability of data and the accuracy of estimates.

2.1.1. Permeability of an unperforated film

Any model results from statements regarding the phenomena that it describes and it is therefore crucial to understand the phenomena involved. In a package composed by a plastic film, the rate of the mass transfer process involves a series of steps. For a gas flowing outwards (e.g. carbon dioxide): (i) movement of gas molecules inside the package towards its inside surface; (ii) absorption of the gas molecules by the packaging film; (iii) diffusion of the absorbed molecules in the solid state film towards the outside surface; (iv) desorption of the gas molecules back to the gas phase on the outside interface; (v) movement of the molecules away from the surface towards the bulk air. Obviously, the reverse steps occur for gas flowing into the package (e.g. oxygen). The movement of the absorbed gas within the polymeric film is such a slow process that it effectively controls the rate of exchange. Although steps i and v (the resistance to the movement of molecules in the boundary layers adjacent to both sides of the film) may interfere somewhat, they are usually not relevant except in rather extreme conditions. Metz (2003) determined the resistances to mass transfer on both boundary layers for water vapour, inside a test cell, but with exceptions such as this, quantifying mass transfer across a polymeric film has been largely reduced to determining what is called the permeability of the films. In spite of it being a simple example of mass transfer theory, it originated in empirical approaches that created its own jargon. Thus, one refers to a permeability, a permeance, or a gas transfer rate (e.g. OTR, CTR) of a packaging film rather than a diffusion coefficient of a gas in a polymer (and possible convection resistance terms, such as in Metz, 2003). Nomenclature in this area can be somewhat confusing and units common in practice are not even consistent, so care must be exerted when using a literature value (Finnigan 2009)).

A simple mass transfer approach for the molecular movement of a dissolved gas through a polymeric film in steady state is based on Fick's 1st law, considering that the film is a flat surface and that only the net molecular movement perpendicular to it needs to be quantified:

$$n_i = -D_{f,i} A_f \frac{dC_{si}}{dl} = -D_{f,i} A_f \frac{p}{R_g T} \frac{dy_{si}}{dl} \tag{2.1}$$

where i denotes oxygen or carbon dioxide, n_i is the molar flow rate, $D_{f,i}$ is the diffusivity of the gas dissolved in the film moving through it, A_f is the film area perpendicular to the gas movement, C_s is the concentration of the gas dissolved in the film and y_s its molar fraction, with p and T being the total pressure and absolute temperature, respectively, and R_g the ideal gas constant. The hydrodynamic term of the mass transfer equation can be neglected because the gas in the film will be very dilute (that is, the net flux is equal to the flux by pure diffusion).

An empirical determination of the gas flux through the package leads to a simple definition of permeability, which can be related to diffusivity. In practice, permeability is not expressed in consistent units (such as SI). The permeability of a film to oxygen and to carbon dioxide quoted in literature and in manufacturer's material data sheets usually refer to measurements made with volumetric flow rates, as in equation 2.2:

$$\dot{V}_i = -P_i A_f \frac{(y_{i,e} - y_{i,i}) p_t}{L} \qquad (2.2)$$

where $\dot{V}_i$ is the volumetric flow rate of gas through the film, P_i is the permeability to gas i, p_t the total pressure (most usually 1 bar), L the total thickness of the film and y the volumetric fraction of gas i in the gas phase at the outside of the package (subscript e) and in the inside (subscript i). P_i/L is also known as the permeance, and $P_i \cdot p_t/L$ as the gas transmission rate. The minus sign defines the orientation of the axis from inside out. It follows that if the diffusivity in the film is constant, if the boundary mass transfer resistances on both sides of the package are negligible compared to diffusion in the film, if the absorption/desorption is instantaneous compared to diffusion and if y_s and y are related by a same partition coefficient on both sides (which means that the equilibrium of the gas in the two phases is linear), equation 2.1 and 2.2 are the same, and then permeability P is simple equal to diffusivity D_f times the partition coefficient that relates y_s with y (minus conversions from molar to volumetric flow rates, of course). The partition coefficient (relation between the concentration of a molecule in the two different phases, gas and film) is the solubility of the gas in the film, and hence the simple result that the permeability is equal to the diffusivity times the solubility (Sullof 2002) is obtained. Note also that a linear relationship between y and y_s is assumed in the integration of equation 2.1 (that is, solubility is considered independent of concentration).

It is evident that if one or both convection mass transfer resistances on either side of the film are relevant, then P will be an empirical parameter that integrates all resistances and thus will not be equal to the diffusivity in the film multiplied by the solubility (minus unit conversions). In such case, the exact value of permeability in an experimental determination could be affected by the hydrodynamic conditions prevailing in the experiment (i.e., stagnant air, normal circulating air, forced air circulation). It is also obvious that if solubility would not be independent of concentration this relationship would not be so simple. Henry's law is widely used to describe the partition coefficient (solubility) in films (Sullof 2002, Guillaume, Guillard, and Gontard 2010), which would indeed meet this criterion, but it is known that gas adsorption on solids follows sigmoidal-type isotherms (BET, GAB) that are not linear. As the concentrations are very dilute, Henry's law is likely to be a good approximation - James (2007) cites that this will be the case for solubilities up to 0.2% at pressures not exceeding atmospheric. However, this neglects the plasticising effect of water which will bring additional problems in the case of films with high water permeability (thus high water solubility), as the data collected by James (2007) shows.

An important word of caution is given on the units of permeability. Common units of permeability simply list each of the components of equation 2.2, for instance, cm^3.mil/(atm.day.m^2) is a common unit, even though the mil (a thousandth of an inch) is not even a unit of the same system as the other length dimensions. As pointed out by Finnigan (2009), the use of inconsistent and empirical approaches to units has led to chaos and confusion in this area, so it is important to be sure that data is used in the proper units. The volume of a gas depends on pressure, and therefore, volumetric units of permeability such as 10^{-10} cm^3.cm/(cm^2.cm Hg.s) (a unit known as the Barrer) or similar ones need to specify whether they refer to a reference temperature and pressure (STP being the most common, 273.15 K and 1 atmosphere), or they refer to the temperature at which the permeability was determined. The influence of temperature on the units of permeability is a cumbersome and unfortunate consequence of selecting volumetric flow rates as a reference, as in eq. 2.2 - with molar or mass permeabilities in eq. 2.1, this problem would not occur (the latter is actually the norm for water vapour permeability). In order to avoid this problem, this paper will use an apparent diffusivity, which is equal to the real diffusivity multiplied by the solubility, in units of square length per unit of time, which refers to the integration of equation 2.1 and conversion of concentration to molar fraction:

$$n_i = -\frac{D_{ai}A_f}{L}\frac{(y_{i,e}-y_{i,i})P_t}{R_gT} \tag{2.3}$$

where R_g is the ideal gas constant and D_a the apparent diffusivity (equal to D_f times solubility if surface resistances are negligible and solubility is independent of concentration). The difference between D_a and permeability P defined in units such as the Barrer is just the conversion from volumetric to molar flow rate (with the ideal gas law, multiplying by the molar volume equal to R_gT/p_t suffices, but note that T must be interpreted correctly, depending on the reference of the permeability units used), and unit conversions.

A final and extremely important point needs to be made if using literature data of permeability. Material data sheets and ASTM standard methods widely used typically provide permeability values for a given temperature (23°C is the most common) and for films exposed to 0% of relative humidity. That is due to the most widely used method consisting in measuring the rate of gas transfer through the film with both sides in contact with pure gas (oxygen or carbon dioxide in one side and nitrogen in the other). It can be expected that many films will have very different permeabilities to these standard values at real conditions of use, because typically the environment inside a package is saturated in water vapour. The completely dried films of the standard method may have vastly different permeabilities. Water plasticises polymeric structures, that is, it decreases their glass transition temperature and increases the molecular mobility. Therefore, as films that are highly permeable to water also imply that they have high solubilities of water, they will be significantly changed by humidity. Massey (2003) provides values for permeabilities of some films at various relative humidities measured with ASTM methods, and it can be seen that some have permeabilities that are hundreds to thousands of times higher with saturated humidity compared to totally dried environments.

Water is a very important factor in packaging design, which is not addressed further in this paper. In relation to oxygen and carbon dioxide permeabilities, the most important point at this stage is to note that values for film permeabilities used in packaging design must refer to the temperature and relative humidity conditions that the package will be designed for, and standard values of permeability may give totally wrong estimates if real conditions differ significantly from the references.

Therefore, due to the uncertainty on the actual effective permeabilities of films used in published studies with perforations, the data that can be used with confidence in this meta-study are those obtained with perforations in otherwise impermeable materials, where all flux occurs through the perforations.

2.1.2. Advantages of perforating a package

The equilibrium composition of the gas inside a package depends on the ratio of permeabilities to carbon dioxide and oxygen, as will be demonstrated later. This statement is however intuitive, as it was stated that the respiration rate equals the mass transfer through the package at equilibrium. The ratio of production of carbon dioxide to consumption of oxygen is known as the respiratory quotient (R_Q), and varies between 0.8 and 1 for most products. It depends essentially on the composition of the substrate begin oxidised in the respiration process - for instance, sugars such as glucose and fructose would have a ratio of 1 (Guillaume, Guillard, and Gontard 2010). Values over 1 usually indicate that there is some fermentation activity occurring. Therefore, the mass transfer fluxes out of the package should be around the same (would be equal if R_Q=1). However, carbon dioxide dissolves much more than oxygen does in almost any type of medium (even in water, due to the formation of carbonic acid) and as permeability is the product of diffusivity by solubility, it is not surprising that the ratio of permeability to carbon dioxide to permeability of oxygen is high - for most films it varies from around 2 to 8 (Exama et al. 1993, Massey 2003). The concentration gradients can vary somewhat, depending on the ideal gas composition, but are not too different either (for instance, 10% oxygen and 10% carbon dioxide or 5% oxygen and 15% carbon dioxide imply gradients that are about the same). Therefore, carbon dioxide is escaping from the package much faster than oxygen is entering for most films simply because it has a much higher solubility in them than oxygen does. Much lower permeability ratios would be required to achieve an environment much richer in carbon dioxide than in oxygen.

With the significant increase of fresh cut products brought about by consumer demands for convenience, there has been a significant market growth for products that are not properly packed in any of the usual films because they would benefit from elevated carbon dioxide content, which is not generated with polymeric films (Exama et al. 1993). Cut products have high respiration rates for two reasons: they have much higher surface area / volume ratios, and the cut cells respond to injury with increased respiratory activity. Inhibition of the respiration rate by carbon dioxide can counteract this effect, so many cut products wold benefit from atmospheres that are not provided by any polymeric film (a compilation of optimum atmospheres for a variety of such products can be found in Mahajan et al. (2005)). Whole berries also benefit from elevated carbon dioxide concentrations (Beaudry 1999), and high carbon dioxide is also beneficial to inhibit the growth of many pathogens (Sivertsik, Rosnes, and Bergslien 2002). The ratio of mass transfer of carbon dioxide to oxygen in air itself is actually lower than 1 (around 0.8, depending on temperature) and therefore a package where mass transfer would be totally mediated by movement in air would have a much lower permeability ratio than polymeric films. If both mass transfer through the film and through air are important, an intermediate effect will be found. Therefore, the permeability ratio of a perforated package will go from 2 to 8, depending on the film, to 0.8 when the package is excessively perforated. Finding the correct area of perforation would ensure the build-up of sufficient carbon dioxide to achieve optimum compositions for many products. Mir and Beaudry (2016) show this expansion of the feasible concentrations that packages can achieve with perforations in a useful visual form in CO_2 versus O_2 plots that will also be used later in the quantitative part of this work.

Therefore, it is even possible to use a same film (preferably very cheap), and modulate its permeability with perforations depending on the product. Laser perforations are excellent for this purpose, able to drill very small holes (less than 100 micron is possible), or bigger ones, as required (Renault, Souty, and Chambroy 1994). The engineering challenge in this case is obvious: not enough perforations and the package is too impermeable, will lead to excessive oxygen depletion, anoxia and not only quality, but potentially even serious safety problems; too many perforations and the inside atmosphere is little different from normal, with rapid degradation and loss of the product.

It is also obvious even before any quantification is done that the choice of polymer to be perforated is important. A very impermeable film with even a single small perforation will already have a permeability ratio close to that through air (0.8) because most of the gas exchange will occur through the perforation. Therefore, it is necessary to avail of a balance between the two fluxes in order to have some control of the effective permeability of a perforated film by simply changing the area of perforations.

A final important point about perforations which is obvious from a safety point of view is that a perforated package will no longer avail of a barrier against post-packaging microbial contamination. However, if this is considered to be an unnecessary additional hazard, it can be eliminated by using a multilayer film with a very permeable unperforated layer, plus the perforated one, where the former is just ensuring a full microbial barrier and the latter totally controls the gas exchange rate. The minimum requirement would be a simple highly permeable label covering the perforated area. It is not more complicated to design a multilayer system, as the overall resistance is simply the combination of resistances in series. There are also suggestions of adding antimicrobial agents to eliminate this problem in perforated packages (for instance, US Patent 6110479 (Blaney, Cartwright, and Strack 2000)).

2.1.3. Mass transfer through perforated films

For perforated films, total mass transfer is the sum of two processes that occur in parallel, as depicted in figure 2.2: (i) the mass transfer through the polymeric film; (ii) the mass transfer through the perforation(s). The former is composed by the 5 steps mentioned in the previous section, and largely controlled by the diffusion in the film (step 2a in figure 2.2). It is quantified by the permeability of the polymer (eq. 2.3).

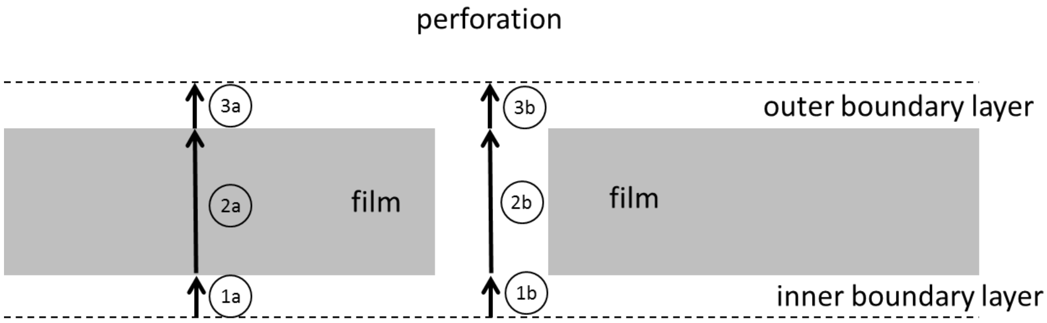

Figure 2.2 - Sketch of the mass transfer movements through a perforated film. 1 and 3 are convection movements (inner and outer, respectively), 2a is diffusion of a dissolved gas in a plastic film and 2b is diffusion/hydrodynamic/convective flow through a gas mix of varying composition from the headspace modified atmosphere to normal air.

Mass transfer through perforations was studied by Emond, Chau and co-workers (Emond et al. 1991, Emond et al. 1998) and further applied by other authors (e.g. Montanez et al. (2010a), Fonseca et al. (2000), (Silva et al. 1999)) in the context of perforated-mediated modified atmosphere packaging where the concept being developed was to use a perfectly impermeable container, with just a few plugs of a given diameter and length that would control the mass transfer rate. These were cylinders that could have a few mm of length, and generally had a high length to diameter ratio. In this case, there are just 3 steps: (i) movement of the molecules in the inner space towards the edge of the tube on the inside; (ii) diffusion through the tube to the other edge; (iii) movement of the molecules from the edge of the tube to the bulk of the air outside. Step ii is much faster than diffusion through a solid phase polymer and so in this case it is not necessarily true that diffusion will control. Therefore, variability in the external convection currents can affect the overall gas exchange rate significantly. This was noted by Kirkland, Clarke, and Paul (2008), that proposed to consider the external hydrodynamic conditions as a parameter that defines the effective permeability of a perforated package, and Ghosh and Anantheswaran (2001) also provide experimental evidence of the relevance of air velocities by comparing static and flow-through measurements. Montanez et al. (2010b) also provided correlations considering air velocity, although they do not discount the effect of temperature and gas composition due simply to differences in diffusivities in other physical properties.

There have been different approaches proposed to quantify this movement: (i) a lumped capacity model, as in the original work by Emond et al. (1991), (ii) diffusional-based models (Fick and Stephan-Maxwell), (iii) a hydrodynamic flow approach, (iv) the full solution of the 3-dimensional mass and momentum transfer equations, solved numerically. The phenomena is the same and therefore they must all be related. Instead of proposing new models as some authors try to do, it is more helpful to do the opposite and reduce all approaches to a same view of what has to be the same phenomena. In order to understand the links and the errors that have occurred in some applications it is a good starting point to begin exactly where chemical engineering does when describing this phenomena, and then relate everything to this basis.

The simplest chemical engineering approach is to consider diffusion and external convection as resistances in series and therefore the reciprocal of the overall resistance (effective permeability of a perforation) is the sum of the reciprocals of the three resistances (Paul and Clarke 2002, Metz 2003). The diffusion equation might not be the same because the diffusional movement is not in a dilute media (oxygen concentration goes up to 21%, and so can carbon dioxide). The proper equation of mass transfer (Marrero and Mason 1972) includes both pure diffusional and hydrodynamic movement (which in a sense relates velocities to a stationary frame of reference with relative velocities):

$$n_i = -D_i A_h \frac{p}{R_g T} \frac{dy_i}{dl} + y_i \sum_{j=1}^{4} n_j \qquad (2.4)$$

where A_h is the cross sectional area of the perforation(s), given their diameter d_h and number n_h, D_i is the effective diffusivity of gas i through the gas mix in the perforation and n_j are the molar flow rates of all moving gases (oxygen, carbon dioxide, water vapour, and nitrogen). However, equation 2.4 can be reduced to pure diffusion because the situation must be equimolar counter diffusion, that is, the net sum of all flow rates must be zero. The pressure on both sides of the film is the same, or the package would shrink or inflate. It is of course possible that pressure differentials would occur, but such packages would then show sufficient deformations to be saleable, so for situations of practical interest, the total number of moles remains the same and the hydrodynamic term must therefore cancel. Paul and Clarke (2002) initially considered that the sum of fluxes is not zero, obtaining a more general expression, and stated that this sum will be equal to what they term a convective flux $\hat{Q}$ per unit area. However, in the final steps of their mathematical development (from their equation 10 to 11) they make this term equal to zero as well.

Equation 2.4 applies between the two surfaces of the film, and is then combined with Newton's equation quantifying the resistance to mass transfer on the boundary layers of the two surrounding atmospheres on both sides:

$$n_i = k_i A_h \frac{p}{R_g T}\left(y_{i,0} - y_{i,h}\right) \tag{2.5}$$

$$n_i = k_e A_h \frac{p}{R_g T}\left(y_{i,e} - y_{i,L}\right) \tag{2.6}$$

where k_i and k_e are the mass transfer coefficients on the inner and outer boundary layers, respectively, $y_{i,h}$ is the molar fraction of gas i in the headspace volume inside the package (assumed perfectly mixed), $y_{i,0}$ is the molar fraction of gas i at the inner edge of the hole (position l=0), $y_{i.L}$ the fraction at the other edge (position l=L, the thickness of the film or length of perforation tube), and $y_{i,e}$ the fraction in the outside bulk atmosphere, assumed perfectly mixed. With the hydrodynamic term in equation 2.4 cancelled due to equimolar counter diffusion, the equality of the molar flow rate in equations 2.4 to 2.6 results in the overall sum of resistances in series:

$$n_i = -A_h \frac{p}{R_g T} \frac{(y_{i,e} - y_{i,i})}{\frac{L}{D_i} + \frac{1}{k_c}} \tag{2.7}$$

where k_c is the effective overall mass transfer coefficient that combines the two film resistances ($1/k_c = 1/k_i + 1/k_e$).

2.2. REVIEW OF METHODS PROPOSED AND DATA REPORTED

2.2.1. Lumped capacity model and overall transmission rates

Several authors pooled various factors into one single parameter, as in Emond et al's original approach (Emond et al. 1991, Silva et al. 1999, Fonseca et al. 2000, Emond et al. 1998, Ghosh and Anantheswaran 2001, Mahajan, Rodrigues, and Leflaive 2008, Techavises and Hikida 2008, Montanez et al. 2010a, b). More recently, authors working with perforated films instead of long tube insertions have used comparable approaches (González et al. 2008). The correlations proposed in these works are often cited as possibilities for perforated films (e.g. Guillaume, Guillard, and Gontard (2010)). However, although there is nothing wrong originally, the applications and usefulness for perforated films have incorrections or pointless expressions, as can be seen by comparing results with equation 2.7 and analysing the data of the authors themselves. The permeation model is determined by flushing one side of the film in a hermetic container of volume V with a given composition and allowing it to exchange to a normal atmosphere over a period of time. A first order model is then applied to describe the unsteady state evolution of concentration:

$$-V\frac{dy_i}{dt} = K\left(y_{i,e} - y_{i,i}\right) \tag{2.8}$$

The authors cited have termed the K constant as the mass transfer coefficient. However, comparing to eq. 2.7, that is not what it is, and this imprecision of nomenclature has consequences in applying this concept to perforated films. Ghosh and Anantheswaran (2001), working only with oxygen, preferred to call this K parameter the oxygen transmission rate OTR, which is not exactly what it is either, for the same reason that K is not the standard mass transfer coefficient, which is the fact that the area of flow is not being individualised. Applying the pseudo-steady state assumption, the mass balance simply states that in unsteady state the molar flow rate of the equivalent steady state condition of the respective instant is equal to the variation of concentration on the flushed side. Pseudo steady-state assumptions are very common in mass transfer problems because diffusion is so much slower than other processes (Bird, Stewart, and Lightfoot 2007). Thus, the second hand side of eq. 2.8 is simply equal to the molar flow rate n_i with the pseudo steady state assumption. It is for this reason that Fonseca et al. (2000) also termed the first order model as the lumped capacity model (which is the same as Newton’s law applied to mass transfer). However, it should properly be written by individualising the area of flow as in Newton's equation, that is:

$$-V\frac{dy_i}{dt} = K_m A_h \left(y_{i,e} - y_{i,i}\right) \qquad (2.9)$$

Comparing to eq. 2.7 it is evident that the first-order model parameter is the same as an overall mass transfer rate that is equal to the sum of the resistances to diffusion inside the tube (or perforation) and the film resistances, so:

$$K = K_m A_h = \frac{A_h}{\frac{L}{D_i}+\frac{1}{k_c}} \qquad (2.10)$$

The publications referred to in this area usually go on to develop empirical correlations for K as a function of the length and diameter of the plugs (Emond et al. (1991) and Emond et al. (1998) used additive correlations and Fonseca et al. (2000) and Montanez et al. (2010a and b) multiplicative correlations, while none have used dimensionless correlations). Authors working with perforated films then suggest these as possibilities for perforated films (e.g., Ghosh and Anantheswaran (2001); Guillaume, Guillard, and Gontard (2010)). That is clearly not so. The first issue is that as Emond and Chau and later authors did not discount the area from their coefficient K, there is an obvious influence of the diameter of the perforation that is simply due to the area available for mass transfer.

Secondly, with plugs the length to diameter ratio is high. As this ratio increases and the two resistances sum, resistance by diffusion becomes overwhelming and convection mass transfer may become irrelevant. Therefore, a feature of these correlations that must be hidden somewhere is that K will just become equal to D_iA/L when L/d is sufficiently large. However, the geometry of perforations in films is completely different, L/d is usually much lower than 1, and therefore the convective mass transfer resistance should be much more important in perforated films than they are in the plug implements. The L/d ratio has been known to be an important parameter actually since the 1960's, as a result of work done on the diffusion of gases from leafy structures with micropores in the development of plant physiology biophysics (Meidner and Mansfield 1968). L/d is the reciprocal of the dimensionless parameter δ defined by Chung, Papadakis, and Yam (2003). Metz (2003) also proposed a correlation that added the L/d ratio to dimensionless correlations, defining the Sherwood number with d, but proposed that d would be an hydraulic diameter that is not clearly defined.

Fonseca et al. (2000), Ghosh and Anantheswaran (2001), González et al. (2008) and Techavises and Hikida (2008) have conveniently provided tables of data in their publications, the former for plug implements of L/d_h ratios between 0.6 and 2.1 and the latter two for perforations in a film, with L/d_h ratios between 0.16 and 0.85 in the first case and between 0.0024 and 0.006 in the second. Techavises and Hikida (2008) used a slight variation of eq. 2.8, with partial pressure, and termed the coefficient the effective permeability; their effective permeability is therefore K divided by the total pressure. Montanez et al. (2010a and b) have also provided graphs for plug implements, from where the values of K can be read, and although this will be less precise than using the actual values, they can also be used, with L/d_h ratios between 0.6 and 4. According to eq. 2.10, the values of K should tend to D_iA/L as L/d increases (minus volumetric to molar unit conversions). The values published in all these papers were obtained for different temperatures, different velocities of circulation of the surrounding air, in different chambers and containers and perforations of very different dimensions (d from 0.012 to 41.1 mm and L from 0.049 to 17.1 mm), yet, as figs. 2.3 and 2.4 show, all data can be pooled together quite coherently. These figures are also showing already data from authors that used other mathematical approaches and that will be reviewed later in this text.

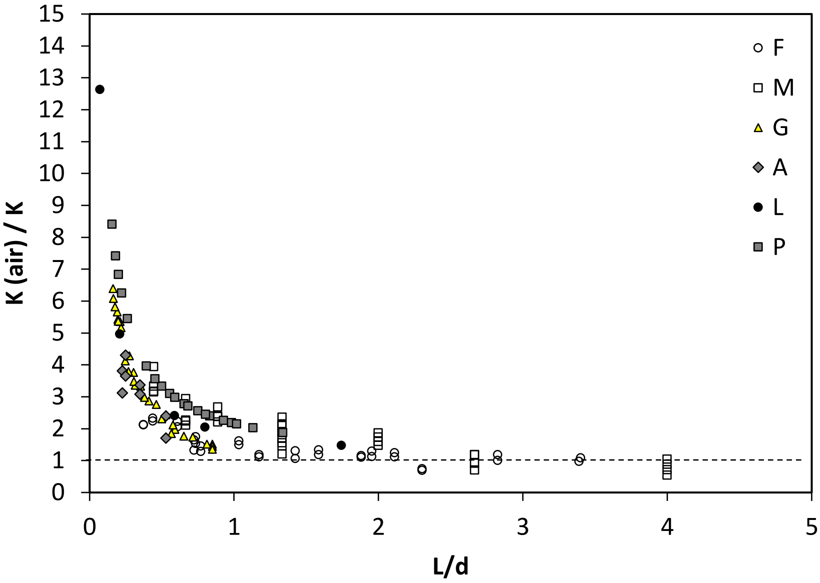

(a)

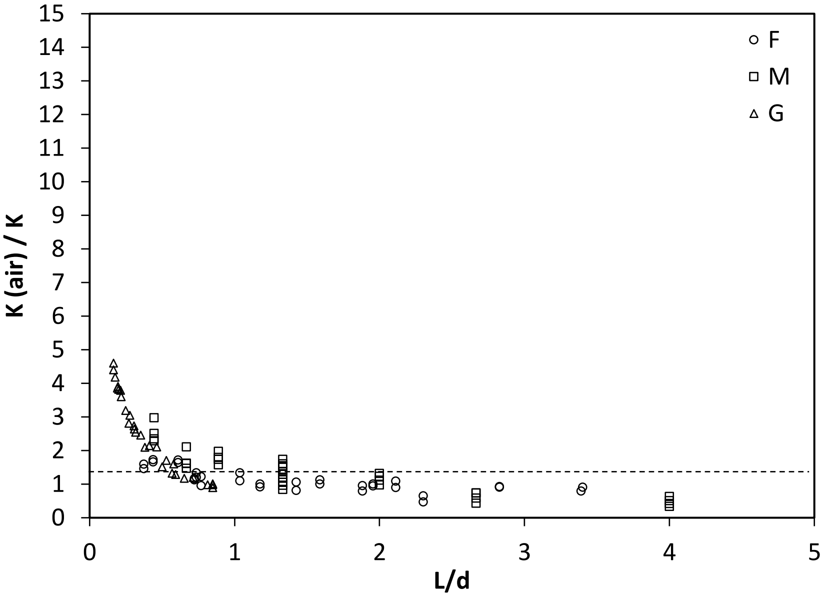

(b)

Figure 2.3 - . Influence of the perforation length to diameter ratio on the ratio between the global mass transfer parameter K obtained with simple diffusion through the perforation across otherwise stagnant air of normal composition and the K value reported by the various authors for their own experimental data for (a) oxygen and water vapour (Lange et al, 2000) and (b) carbon dioxide. Data for very low L/d_h ratios is not shown (very high y-axis values). The straight lines are added just to help visualise tendencies. F - Fonseca et al. (2000), M - Montanez et al. (2010), G - Gonzalez et al. (2008), A - Ghosh and Anantheswaran (2001), L - Lange et al. (2000), P - Paul and Clarke, 2002

Figures 2.3 and 2.4 show the ratio of the K value (the overall transfer rate) obtained with the diffusivity of the respective gas (oxygen or carbon dioxide) in stagnated air at the temperature in question for each specific data point (the data from the authors cited varies from 5 to 23°C) and the K value given by the authors of the publications reviewed. The values for diffusivity of oxygen, carbon dioxide and water vapour in air were obtained from literature (Marrero and Mason 1972), for 1 atm and as a function of temperature (different temperatures for different authors and data points). In spite of the differences between geometries, dimensions, temperatures, gas compositions, hydrodynamic conditions, and even mathematical models that were being validated, the data agree particularly well between Fonseca et al. (2000), Ghosh and Anantheswaran (2001), Gonzalez et al. (2008) and Techavises and Hikida (2008), with Paul and Clarke (2002) and Montanez et al. (2010b) agreeing between themselves and being slightly above the others, and Rodriguez-Aguilera et al. (2010) few points are slightly below. Although the data of Lange et al. (2000) are for water vapour, they agree particularly with the oxygen data of Fonseca et al. (2000), Ghosh and Anantheswaran (2001), Gonzalez et al. (2008) and Techavises and Hikida (2008).

This excellent agreement between different authors is very significant, because the actual values of L and of d are very different, yet the L/d_h ratio brings them together. It is obvious from fig. 2.3 that the K values of this approach using the lumped capacity model become approximately the values inferred from the diffusivity of the gases in air for L/d greater than unity. Thus, correlations of K for L/d greater than 1 are somewhat pointless. Correlations for L/d lower than 1 may be useful for providing values from where the mass transfer coefficients can be obtained, once diffusion and flow area are separated. A simple mathematical handling would reveal that the ratio of the K value that would be obtained using air diffusivities to that obtained experimentally is equal to $1+1/Sh_L$, this being the Sherwood number defined with the thickness of the film as characteristic dimension ($Sh_L=k_cL/D$) - dimensionless numbers and mass transfer coefficients will be discussed later when using diffusional models. Thus, $1/Sh_L$ is tending to zero (as D is becoming much bigger than k_c)

It is noted that there is some uncertainty as to the precise value of effective diffusivity that should be used. This will be discussed in more detail when analysing the diffusional models. At this stage it is sufficient to note that diffusivity in air taken from literature refers to gas molecules of oxygen or carbon dioxide moving in otherwise stagnated molecules of the other gases in normal air concentrations (21% oxygen, 79% nitrogen, and almost no carbon dioxide). The effective diffusivity of gases depends on the composition of the gas mix (Marrero and Mason 1972). For instance, the oxygen diffusivity in air used in fig. 2.3, at 20˚C is 0.203 cm^2/s, while at this temperature that of oxygen in nitrogen is 0.202, and that of oxygen in carbon dioxide is 0.159 cm^2/s. The diffusivities that should be used in equation 2.10 must refer to the gas mix in the perforation, which has much more carbon dioxide than normal air (and thus is lower than in normal air, which is why some data points in fig. 2.3 are below 1). Furthermore, all molecules are moving, which increases the collisions. Therefore, D_i is not the same as diffusion through stagnated normal air, but how different is it and how can it be calculated? Determining an effective diffusivity of each gas through the gas mix in the perforation could, of course, be done precisely by fitting data points with equation 2.10, and obtaining both D_i and k_i. However, this would provide an apparent value that is in fact an average that depends on the specific composition of the gas inside the package, which in turn depends on the effective permeability of the perforated film and on the dimensions of the perforation - this will be shown later when discussing Stefan-Maxwell's diffusion model.

Fig. 2.3 in a normal scale does not show data for very low L/d_h ratios; for scale reasons these are better seen in fig 2.4 that uses a log scale. This is mostly because Techavises and Hikida (2008) and Rodriguez-Aguilera and Oliveira (2009) reported data for very small film thickness with relatively large diameters, so the L/d ratio is small and the K_{air}/K ratio approaches infinity due to the very small L.

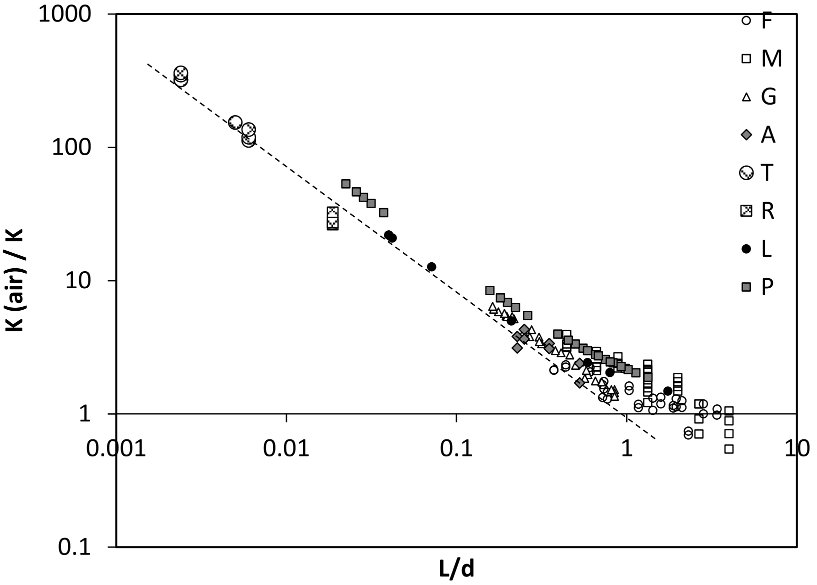

(a)

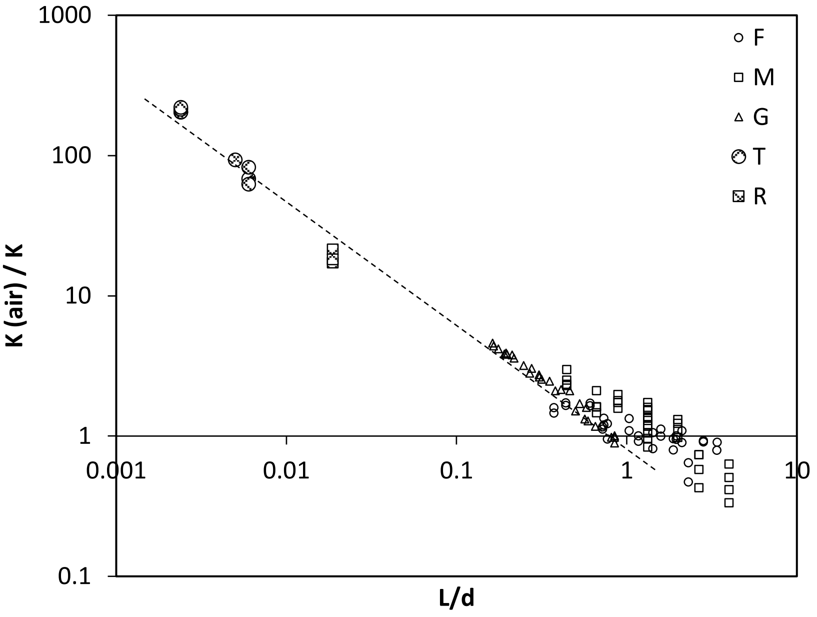

(b)

Figure 2.4. Logarithmic plot of the ratio of lumped capacity model global mass transfer K parameter between that due to diffusion through stagnated normal air and that reported by the various authors as a function of the length to diameter ratio of the perforation(s) for (a) oxygen and water vapour (Lange et al. 2000), (b) carbon dioxide. The dotted lines are added just to help visualise tendencies.

F - Fonseca et al. (2000), M - Montanez et al. (2010b), G - Gonzalez et al. (1998), A - Ghosh and Anantheswaran (2001), T - Techavises and Hikida, 2008, R - Rodriguez-Aguilera et al. (2009), L - Lange et al. (2000), P - Paul and Clarke, 2002

Therefore, they require a logarithmic scale to be pooled with the other data and the approximate linearity of fig 2.4 up to L/d = 1 suggests a power-law relationship between the effective permeability ratio and the L/d ratio, and it is noted that power laws are typical functions in dimensionless correlations. It is also noted that this implies that $1/Sh_L$ is tending to zero according to a power exponent of L/d. The deviation from the straight line as L/d goes beyond 1 is mostly due to the uncertainty of the values of D, as discussed previously, which is magnified in log scales when approaching zero.

The proper mass transfer coefficients, k_c, obtained by applying equation 2.10 to the data of the authors cited are shown in fig. 2.5. There are many factors that may influence k_c and the diffusivity values used were those in normal air, which is imprecise as discussed earlier, but fig. 2.5 already shows the most important feature: the order of magnitude for a variety of conditions. Also, the data suggests that an important parameter is the diameter of the perforations, as there is a clear tendency for k_c to increase with decreasing diameters. The data were separated in two figures covering different scales of d because the mass transfer coefficients for the very small perforations are much bigger. These are from González et al. (2008) and Ghosh and Anantheswaran (2001), which also agree with those from Lange et al. (2000) for the same dimensions around 0.2 mm.

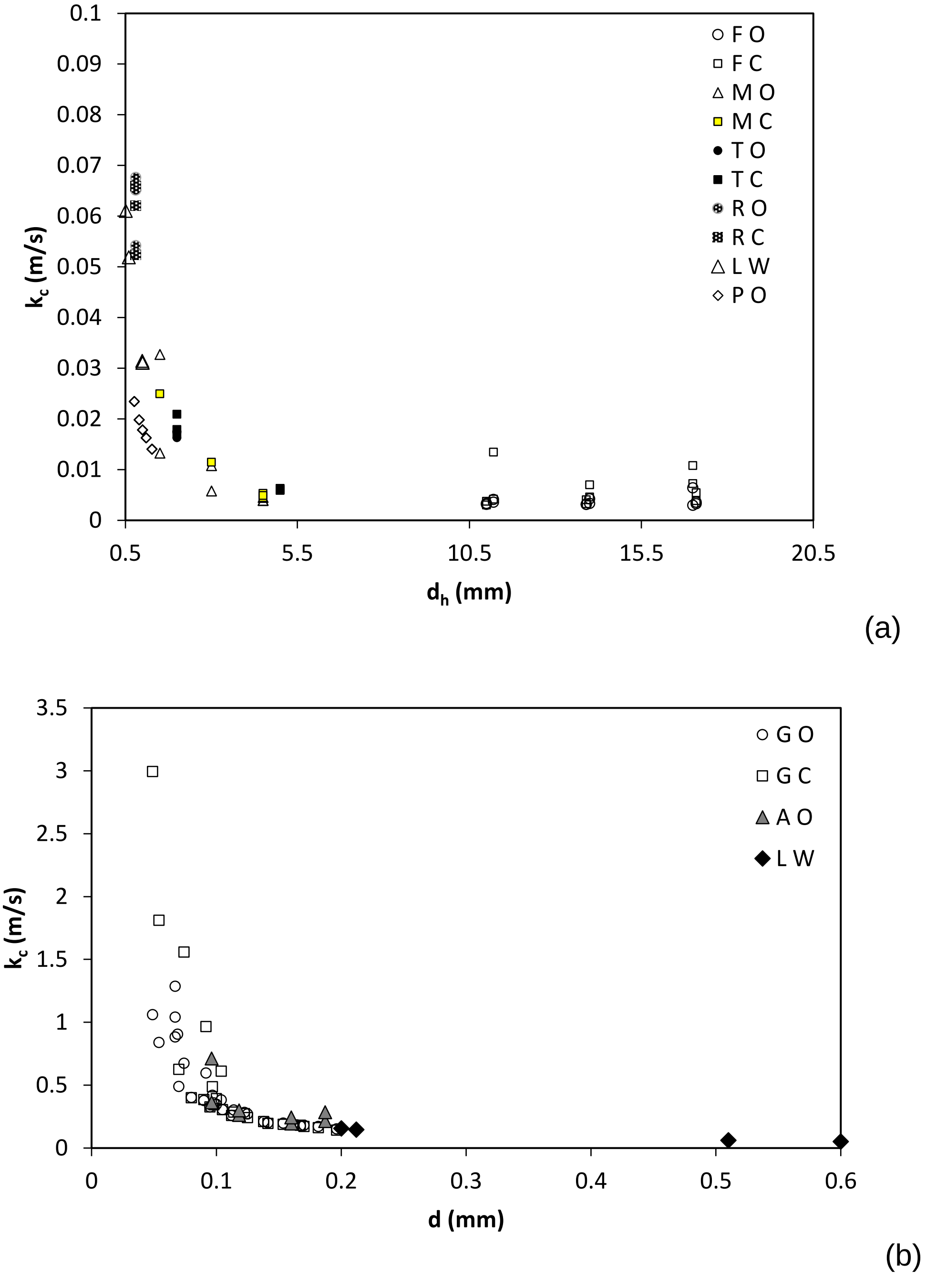

Figure 2.5. Mass transfer coefficients extracted from the data reported by several authors for perforations of various diameters, with smaller diameters in fig. a and bigger ones in fig. b. The first letter indicates the literature reference as in the legend of fig. 4 and the second letter the gas, with O for oxygen, C for carbon dioxide and W for water vapour.

It is noted that the plug implements studied in Fonseca et al. (2000) and Montanez et al. (2010a and b) come out of the surface of the lid by about half its length. Therefore, the hydrodynamic conditions surrounding the outlet of the implements are different from those than one would find in perforated films, where there are no protrusions sticking out of the film surface. Notwithstanding, the mass transfer coefficients are in line with all others and a tendency for k_c to decrease with increasing diameter. The k_c values that can be calculated from Techavises and Hikida (2008) are for perforated films, but with perforations of dimensions close to those of the plugs used by Fonseca et al. (2000) and Montanez et al. (2010), and yet are very much in line with the overall pattern, in spite of the L values being far smaller.

2.2.2. Hydrodynamic flow models

Gonzalez-Buesa et al. (2009, 2013) have taken a different approach, considering that the flow of both gases can be described by Poiseuille's equation for hydrodynamic laminar flow (Foust 1980). Other authors (Del-Valle et al. 2003) found this approach useful, but considered that this term can be added to the pure diffusion equation, so that a hydrodynamic flow caused by a total pressure imbalance adds to the diffusional flow. Poiseuille's law is:

$$\dot{V}_i = -\frac{{d_h}^2}{32\mu}\frac{dp_t}{dl} \tag{2.11}$$

Alas, using Poiseuille’s equation cannot provide a suitable phenomenological model for 2 reasons. The most obvious one is that Poiseuille’s equation describes a completely different phenomenon. The hydrodynamic flow it refers to is caused by a gradient of the total pressure and all molecules move in the same direction, from the higher to the lower pressure. All of them would have the same parabolic velocity profile, as laminar flow is assumed, and in the same direction. Counter flow movements of the different gases would disturb a laminar movement and therefore the basic assumption of Poiseuille's equation is not met. Furthermore, if there was a pressure differential, the package would deform, and hence this is not the type of flow that is occurring in packages, as Chung, Papadakis, and Yam (2003) have noted, and only mass transfer with its opposite flows should be considered. A partial pressure gradient causes a molecular movement with a pure diffusion and a hydrodynamic term as eq. 2.4 describes, where molecules are moving in opposite directions and colliding with each other - this is not the hydrodynamic flow rate provided by total pressure differentials. The net hydrodynamic terms are however balancing themselves out at equilibrium (or the package would not be saleable, as explained before). A detailed scientific discussion on the reason to neglect pressure differentials in general and adopt equation 2.4 as an exact result can be found in Marrero and Mason (1972). Even if this was not the case, however, and there was indeed a significant pressure differential in an inflated package, there is a second reason why Poiseuille's equation cannot be used, especially in perforated films, which is that it assumes fully developed flow, that is, it neglects end effects at both ends. It is known from fluid mechanics that this assumption is reasonable for L/d values of more than 20, or maybe more than 10 if one would be generous with precision (Foust et al. 1980). That is far from being the case in perforated films (where d_h is actually bigger than L), and even in the plugs used in perforation mediated modified atmosphere. Poiseuille's equation would not be applicable even if there was an imbalance in total pressure on both sides and there was no concentration gradient causing opposite movements. The approach of correcting it by adding an apparent length (Foust et al., 1980) is not suitable for such low L/d_h ratios because a fully developed flow will actually never occur at all (one cannot correct a marginal effect onto a phenomena if the phenomena never existed in the first place). The appropriate way to analyse a situation with an imbalance of pressures on both sides would actually be simply to write eq. 2.4 for all moving gases in terms of number of moles (oxygen, water vapour, carbon dioxide and nitrogen), consider the actual resulting pressures and solve the set of equations jointly. Techavises and Hikida (2008) have done this, for instance.

González-Buesa et al. (2013) have actually determined real hydrodynamic flow rates in test cells by causing a total pressure imbalance on both sides of a film and measuring the gas flow rates. That part of the work is totally correct; it just is measuring something that is not what happens in packages, so when those authors apply the concept to a package, the model would not fit. Based on a previous work (Gonzalez-Buesa et al, 2009), an empirical model is used to describe the actual gas transfer rate. The authors note that Poiseuille's equation neglects end effects and determine an apparent diameter of the perforations that makes the model fit the data, and then verify that the adjusted Poiseuille's equation and the empirical gas transfer model give the same result. Therefore, in the end what is done is to fit data points to a model that has an adjustable parameter, but as the model does not describe the phenomena in question, using that or a polynomial or some sort would be just as good: the result is an empirical model anyway that can only be applied for the conditions that it was determined for, it has no predictive potential with certainty. Something similar can be said about Del Valle et al. (2003) results: the fact that a model adjusts itself to experimental data by allowing some parameter to be whatever is needed to fit data does not prove that the model is phenomenologically correct - any empirical model will do that equally well. Notwithstanding, these results are useful, as they actually show that the diameter of the perforations does influence the mass transfer rates beyond its obvious effect in terms of mass transfer area, as found also in the analysis of the lumped capacity model approach. The empirical model proposed by Gonzalez-Buesa et al. (2009) for perforations in the range of 50 to 200 microns is a volumetric transmission rate in units of mL/day, that is, it compares with the K of the lumped capacity model and is not discounting the effect of the diameter on the area of flow. Converting units leads to the following result relating Gonzalez-Buesa's model with eq. 2.7:

$$K_m = \left(\frac{4}{\pi}\right)^{1-a_2} \cdot \frac{a_1 \cdot 10^4}{d^{(2-2a_2)} \cdot 864} \qquad (2.12)$$

where a_1 and a_2 are parameters of the model fit provided by Gonzalez-Buesa et al. (2009). Using the model proposed by these authors to generate the gas flow rates, and then comparing to the diffusional model in the same way that was done for the lumped capacity model data, provides results that fit perfectly the data of Gonzalez et al (2008) shown in figs. 2.3 and 2.5. As the authors are actually the same, this is not surprising, as the data sets may be the same or include same points. Curiously, although L/d_h of 1 would be a slight extrapolation of their model (from the limit of validity of 50 micron to 40 micron, which is the thickness of the film quoted), it would correspond to a ratio between transmission measured and that due to the diffusivity of air exactly equal to 1. Therefore, these authors have also found that the mass transfer coefficient increases with decreasing diameter of perforations, which contradicts their own assumption that only the total area of flow matters, and that the diameter does not influence the flux. They also found that as L/d_h increases, the mass transfer through a perforation becomes equal to that predicted by simple diffusion through air, and this is reached at L/d_h approximately equal to unity. This shows very well the importance of discounting the area of flow from the model parameters and assessing the data properly - all data in fig. 2.5 are suggesting that smaller diameters have lower mass transfer resistances, and hence, a larger number of perforations of a smaller diameter have a greater permeability than a smaller number of perforations of a bigger diameter even though their total areas of perforation may be the same.

2.2.3. Diffusional models using Stefan-Maxwell's equations

The first distinction that needs to be made regarding methods that consider molecular diffusion is between an approach based on the simple application of Fick's law (equation 2.4) and the irreversible thermodynamics approach of Stefan-Maxwell's method. Both have been used to describe mass transfer through perforated films. Paul and Clarke (2002), who used the former, note that Stefan-Maxwell equations are complex to solve and there is no need for complicating what can be solved easily, while Renault, Souty, and Chambroy (1994) and Rennie and Tavoularis (2009), who used the latter, state that Stefan-Maxwell must be used as the diffusional coefficients in Fick's law are not correct for multicomponent diffusion. Authors that discuss this subject tend to see the two approaches as being different, as they originate in completely different approaches and statements of scientific laws. While that is true, the fact remains that the phenomena are the same, and therefore the two models should be compared (it should be possible to convert one result into the other).

It is important to have clear ideas about this. Fick's law can be applicable, its problem to describe the diffusion of multiple gases through open pores is that the effective diffusion coefficient D varies with the composition of the gas and also depends on whether other molecules are moving or not, and can be very cumbersome to determine with precision (Marrero and Mason 1972, Whitaker 2009). Even if it could be determined with accuracy, Fick’s multicomponent diffusivity is therefore not a constant parameter but a variable that depends on the specifics of the problem (concentration gradients, geometries, fluxes), in which case Fick’s equations (in their differential form) of Stefan-Maxwell’s would be equally complex (actually, Stefan-Maxwell’s is somewhat easier to solve numerically). Relating Fick and Stefan-Maxwell equations can be very complex, but ideal gas mixes have a variety of simplifications that make the relationship easier to handle, and that can therefore be used to test whether a constant effective Fickian diffusivity may be sufficiently accurate, or whether it would bring unacceptable errors. It is noted that for binary diffusion Stefan-Maxwell's equations reduce to Fick's 2nd law (Taylor and Krishna 1993) and that although the binary diffusion coefficients of Stefan-Maxwell's and Fick's equations are not exactly the same theoretically, they can be taken as such for all practical purposes (Marrero and Mason, 1972). For each gas, the Stefan-Maxwell expression for an ideal gas mixture at perfect isothermal conditions can be reduced to (Taylor and Krishna, 1993, see chapter 6):

$$\frac{A_h p}{R_g T}\frac{dy_i}{dl} = \frac{y_i n_1 - y_1 n_i}{D_{i,1}} + \frac{y_i n_2 - y_2 n_i}{D_{i,2}} + \frac{y_i n_3 - y_3 n_i}{D_{i,3}} \qquad (2.13)$$

where $D_{i,j}$ are the binary diffusion coefficients of gas i in gas j. The subscript i denotes the gas for which the mass balance is being written, and 1, 2 and 3 denote the other 3 gases (considering only the movements of oxygen, carbon dioxide, nitrogen and water vapour). Comparing to eq. 2.4 for all gases leads to the relationship between Fick's effective diffusivity of a gas in a gas mix and the binary diffusion coefficients that is perfectly applicable to this mixture of gases (oxygen, carbon dioxide, nitrogen and water vapour, Taylor and Krishna, 1993):

$$D_i = \frac{n_i - y_i(n_i + n_1 + n_2 + n_3)}{\frac{y_i n_1 - y_1 n_i}{D_{i,1}} + \frac{y_i n_2 - y_2 n_i}{D_{i,2}} + \frac{y_i n_3 - y_3 n_i}{D_{i,3}}} \qquad (2.14)$$

This relation can be further elaborated noting that the sum of the 4 fluxes is zero (equimolar counter diffusion), leading to:

$$D_i = \frac{1}{\left(\frac{y_1}{D_{i,1}} + \frac{y_2}{D_{i,2}} + \frac{y_3}{D_{i,3}}\right) - \frac{y_i}{n_i}\left(\frac{n_1}{D_{i,1}} + \frac{n_2}{D_{i,2}} + \frac{n_3}{D_{i,3}}\right)} \qquad (2.15)$$

It is noted that if the gas i is fairly diluted (y_i is very small):

$$D_{i,diluted} \cong \frac{1}{\left(\frac{y_1}{D_{i,1}}+\frac{y_2}{D_{i,2}}+\frac{y_3}{D_{i,3}}\right)} \tag{2.16}$$

Wilke (1950) has also proved that even if the gas is not diluted, equation 2.13 also reduces to equation 2.15 for fluxes through otherwise stagnated gas mixes (all n_i but the one in question being zero), provided that the molar fractions to be used are the i-free fractions (that is, $y_1' = y_1/(1-y_i)$ instead of y_1, etc. Equation 2.15 might be applicable only to water vapour in this case, because 100% relative humidity, which is the maximum amount of water in air, corresponds to molar fractions of 1 to 2 %, depending on temperature. For oxygen and carbon dioxide eq. 2.15 would need to be used and then Fick's 2nd law or Stefan-Maxwell would be equally complex: both would require solving the 4 equations simultaneously and actually, the result is the same for the simplified assumptions under which equation 2.14 is valid (no temperature gradient, ideal mix, constant total molar concentration, and thus, zero net flux).

This implies that Renault, Souty, and Chambroy (1994), Lee and Renault (1998) and Rennie and Tavoularis (2009) are correct in stating that Stefan-Maxwell's equations are the appropriate solution of this problem because they do not depend on the use of a parameter (diffusivity) that is actually not a constant. However, Paul and Clarke (2002) may also be correct in stating that this increased precision is a minor benefit and that a constant effective Fickian diffusion can be used. For high L/d_h ratios, where the resistance to mass transfer is dominated by the diffusion inside the pore, it would be important to be precise, and then the increased complexity of Stefan-Maxwell, or the proper use of Fick's law with a variable diffusion coefficient, might be required. In fact, the experimental data obtained by Renault et al. (1994) and its citations to own earlier work would suggest this. Those authors found that for $L=d_h$ the resistance to convection was about the same as that of diffusion. From fig. 2.3 it can be seen that for $L=d_h$ all other authors found the overall resistance equal to what would be estimated from diffusion in stagnated air. However, Renault et al. (1994) did not work with the diffusivities in stagnated air, but with the real binary diffusivities with the Stefan-Maxwell model. This suggests that Fickian average constant diffusivities that would be calculated by fitting mass fluxes to equation 2.4 would be about half of those through stagnated air for perforations of the dimensions used by Renault et al. (1994) in their experimental work, with thickness L of the order of a few dozen μm. This would be a much bigger difference that might be expected from the differences in the binary diffusion coefficients, but it is just a very broad assessment of broad comparisons.

Montanez et al. (2010a), who worked with plug implements of high L/d_h ratio, provide evidence of the influence of gas composition on effective permeabilities, although they used a single parameter that did not individualise the effect of temperature on diffusivity and convective resistance, and as the correlations proposed are not dimensionless they can only be applied to the specific set of conditions under which they were determined.

Notwithstanding, all this suggests that a more precise quantitative analysis might be needed before deciding whether Stefan-Mawell's increased precisions is necessary or not. Taking a typical scenario for perforated packages, with a perforation of a given diameter and length and an internal composition of 7.5% oxygen and 17.5% carbon dioxide (the remaining being nitrogen) evolving to an outside atmosphere of 21% oxygen and 0.38% carbon dioxide (thus neglecting water vapour completely, for simplification, as it is less than 2% in both cases), at 10 ^{o}C, equation 2.4 was solved numerically for oxygen, carbon dioxide and nitrogen jointly, with equation 2.15 giving the effective diffusivity values as a function of the gas composition at every point of the discretization of the l domain from 0 to L (divided in 1000 points), using one-sided finite differences. The 3 molar fluxes n_O, n_C and n_N (oxygen, carbon dioxide and water vapour) were obtained from the boundary conditions that at l=L the normal air concentrations of 21% and 0.38% for carbon dioxide should be found and also that the sum of the 3 fluxes would be zero. The simulation was run for perforations of L=25 μm and d_h=0.1 mm; L=3 mm and d_h=0.1 mm and L=3 mm and d_h=1 mm. In each case, equation 2.7 was then used to obtain the average (apparent) constant Fickian diffusion by fitting the integrated results of equation 2.4 with a constant diffusivity for each flux. The Fickian constant diffusivities thus obtained for the 2 scenarios were, respectively, 0.1786, 0.1785 and 0.1785 cm^2/s for oxygen and 0.1490, 0.1490 and 0.1490 cm^2/s for carbon dioxide. These compare with the diffusivities through stagnated air (without water vapour), given by equation 2.16 (using the respective gas-free molar basis), of 0.1810 cm^2/s and 0.1491 cm^2/s for carbon dioxide. Therefore, there is a small difference between the apparent, average (constant), Fickian diffusivity for oxygen and that through stagnated air - whether this is of sufficient importance will be assessed in section 3 of this paper, with a quantitative example. However, there is virtually no difference between the various scenarios tested, suggesting that the main issue may be to use a representative value for a situation of molecular counterfluxes involving higher carbon dioxide contents rather than a stagnated gas mix with almost no carbon dioxide.

Therefore, one can agree with Paul and Clarke (2002) that the increased accuracy of Stefan-Maxwell's method is not worth the increased complexity. However, it may be necessary to use a more appropriate diffusivity than the value in stagnated air. This will be discussed in more detail in the last section of this paper. In fact, with convection resistance being more important than diffusion in perforated films with small thickness compared to diameter, Fick's model is much easier to use. Lee and Renault (1998) addressed the problem by simply considering an effective length greater than the real length; the difficulties with this approach are discussed in the next section. Combining convection resistance with diffusion with

Stefan-Maxwell approach properly is more cumbersome than with Fick's law (details can be found in Whitaker, 2009).

2.2.4. Diffusional methods using Fickian diffusion with constant diffusivity

Several authors have used Fick's law combining diffusion through the perforation and convection effects on the two surfaces (Lange et al., 2000, Paul and Clarke, 2002, Chung et al., 2003, Rodriguez Aguillera et al., 2009, Mastromatteo et al., 2012). However, they have not expressed it exactly as in equation 2.7, but by defining an apparent length of perforation L_e that corrects the diffusional expression to account for the convection resistances on both sides. This means that equation 2.4 was used, but with L replaced by $L+L_e$. The relation between L_e and k_c is therefore obvious:

$$k_c = \frac{D}{L_e} \tag{2.17}$$

which also implies that the result is the same as describing convection mass transfer using the boundary layer concept, with L_e being the thickness of the boundary layer (that is, the distance from the surface at which the concentration of the gas is approximately equal to that in the perfectly agitated bulk volume). These authors then go on to relate L_e with parameters of the system, so it can be estimated, and all propose that L_e is simply a function of the diameter of the perforations, and of the same type, but with slightly different parameters. Generally, it is suggested that (Chung, Papadakis, and Yam 2003):

$$L_e = \varepsilon d_h \tag{2.18}$$

with ε being a constant, and with Fishman, Rodov, and BenYehoshua (1996) and Ghosh and Anantheswaran (2001) proposing a value of 0.5 , Lange et al. (2000) a value of 5/6 (app. 0.8) for stagnated air and 3/7 (app. 0.4) under air movement. Renault et al. (1994) propose a value of 1.1 and Paul and Clarke (2002) suggest a value of 7/6 (app. 1.2) from a theoretical development, which is then validated experimentally. Rodriguez-Aguilera et al. (2009) obtained a value of 0.4 by fitting the model to experimental data and Mistriotis et al. (2016) obtained a value of 0.3 by numeric simulations, and 0.43 experimentally. Considering that the phenomenon is the same, it is obvious that the variability between 0.4 and 1.2 is hiding the fact that other parameters must also be important (such as the air velocities, as suggested by Chung et al., 2003), but there is an inherent problem in this simple correlation, which is that it must have a limit of applicability as it provides a physically impossible extrapolation result: that the wider the perforation, the greater the resistance. Fig. 2.4 already shows that indeed many authors have found that smaller perforations may have lower resistances (that is, they provide greater permeability), but there has to be a levelling off of the decrease of permeability with increasing diameters, followed by a reversal, as when the perforation will be wide enough, the resistance will actually be zero. Obviously, that will be outside of the range of interest, but the levelling off effect must exist, which is also very clear from fig. 2.5, and equation 2.17 does not provide for it.

It is therefore crucial to understand where these suggestions come from. There are essentially two theoretical approaches, besides simple data regression. Values of 0.5 and 1.1 (7/6 to be exact) were actually both obtained by assuming that the velocity profile of the gases emerging out of a perforation is a perfect circle. Considering that molecules move axially up to that point and from it onwards there is just movement by diffusion through the surrounding (otherwise unstirred) air in the radial direction, there will be pure diffusion in spherical coordinates from the half-spheres defined by the circular velocity profile, as depicted in fig. 2.6. The value of 0.5 comes from noting that the Sherwood number has a limit value of 2 for diffusion from a spherical surface (Bird, Stewart, and Lightfoot 2007), defining the Sherwood number as $k_c.d_h/D$, and therefore if movement is radial from the spherical surface outwards and it occurs by diffusion alone (no natural convection), L_e is half of the diameter. The value of 7/6 was obtained by Paul and Clarke (2002). They also noted that the Sherwood number is 2 with these assumptions, although they termed it the Nusselt number, which is not truly appropriate, as Nusselt is the corresponding dimensionless number for heat transfer (it is important to be clear about dimensionless numbers and their meaning; for instance, Leonardi, Baille, and Guichard (2000) use a dimensionless correlation tending to a Sh value of 2 for stagnated air, but then define Sh as if it was the Nusselt number - that is, with the thermal conductivity instead of mass diffusivity; therefore their number is neither Sh nor Nu, and is not even dimensionless). Paul and Clarke (2002) however go further than this and consider both ends of the perforation and that the boundary conditions will never be a perfectly stagnated environment, and consider diffusion over an equivalent length to quantify this convective disturbance. They then define this equivalent length from the ratio between the volume and the cross section area of an "apparent" cylinder that would have the same volume as the real cylinder (length L) plus the two spherical surfaces of diameter equal to d_h. Thus, the result they obtain in the end, L_e=7/6 is a consequence of assuming that the equivalent length corresponds to this geometrical analogy, but there is no physical nor phenomenological reason to consider why it should be so. The value of 0.8 (10/12 to be more exact) is obtained from the derivation proposed by Heiss (1949) and used by Lange et al. (2000), which is similar to that of Paul and Clarke (2002) in considering "apparent" cylinders, but a different assumption about its volume leads to a different end result of 10/12.

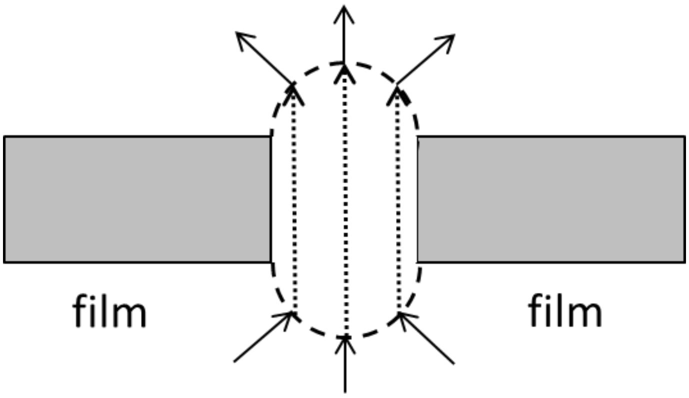

Figure 2.6 - Sketch of the molecular movements conceived to obtain a limit Sherwood number of 2 for diffusion through stagnated air defining Sh with the perforation diameter. Full arrows indicate radial movements and dotted arrows axial movements parallel to the perforation length.

Experimental fitting was used by Renault, Souty, and Chambroy (1994), that actually did not obtain an equivalent length, but rather an equivalent area of perforations (which made more sense to them as they used films with a large number of microperforations difficult to detect experimentally). They report values of the area obtained by model fitting to the real area averaging 0.43, and refer to Renault's original thesis work (1988) as an expected result for $L=d_h$. Thus, Chung, Papadakis, and Yam (2003) converted this result to equivalent length giving the value of $\varepsilon=1.1$, which interestingly is quite close to that suggested by Paul and Clarke (2002). However, Renault et al. (1994) actually refer to their difficulty of being sure that all microperforations were identified in all films tested experimentally, and suggest that a value of 0.5 for the area ratio is more appropriate (lower were attributed to difficulty in identifying all pores with SEM), which would imply $\varepsilon=1$, although it must be noted that Renault et al.

(1994) are only claiming this value for L approximately equal to d_h. Rodriguez-Aguilera et al. (2009) worked with larger and longer perforations, and their data fitting resulted in ε=0.4, which is closer to the suggestion of Fishman, Rodov, and BenYehoshua (1996).

There are some problems with this approach. One is already obvious from comparing the work of different authors: the uncertainty as to what would constitute an equivalent length leads to different results. It is highly unlikely that molecules will move axially up to the point marked by a spherical surface and then radially (for $\varepsilon = 0.5$) or with an apparent cylindrical length accounting for the convection terms (ε = 10/12 or 7/6). None of the molecules are moving in otherwise stagnated environments. There is at least natural convection, and the movement of the other molecules themselves, with the turbulence caused by collisions due to the counterflows likely to disturb this simplest scenario even further. Notwithstanding, it is often found that simplified assumptions can generate models that are applicable in practice. The experimental validation provided by the authors that proposed these models confirms that this was their case, but as different authors propose fairly different values, and all were experimentally validated, it follows that either the precision between 0.4 and 1.2 as the value of ε is irrelevant, or then the different results come from fitting what is in the end an empirical model with different sets of conditions of other influential parameters, and possibly over different ranges of values of L, d_h and A_h. Paul and Clarke (2002) validated ε=7/6 for L between 28.4

and 1020 μm and d_h between 762 and 1270 μm (actual combinations not specified) for oxygen at 25 ^oC, Lange et al. (2000) validated ε=10/12 for the L/d_h combinations (in μm) of 42/200, 43/600, 42/1000, 370/212, 408/510, 584/990 for water vapour at 30 ^oC, and Rodriguez-Aguillera et al. (2009) obtained ε=0.4 for L of 0.015 mm with d_h of 0.8 mm for 1, 2 and 3 perforations, for oxygen and carbon dioxide, all at 20 ^oC (other L and d_h values reported were for plugs with high L/d_h ratio). Using equations 2.10, 2.16 and 2.17, it is possible to calculate the overall K value similar to the lumped capacity model parameter that each correlation is predicting, so as to compare the values obtained by these authors, and also relate them to those reported by authors that used a different mathematical approach. All these data points are shown in figs. 2.3, 2.4 and 2.5. It is noted that they are obtained from the ε value proposed by each respective author (they are not the actual experimental data points because these were not provided in the publications), and that in the case of Paul and Clarke (2002), as the exact combinations of L and d_h tested were not reported, several possible combinations are shown (it is thus possible that some were not actually tried by the authors). These data also show the feature that a global parameter approaches the value of diffusivity through the gas mix as L/d_h approaches unity (fig. 2.3), and that the perforation diameter influences the convection resistance, with resistance increasing with the diameter (fig. 2.5), but levelling off for wider diameters. As figures 2.3 to 2.5 show that the results of the authors that used different values of ε do not match perfectly, the actual value of ε between 0.4 and 1.2 does matter, so the differences must be due to differences in the other parameters that are likely to have been different in the work of the various authors (actual air velocities, temperatures, dimensions, etc.). It is noted that these differences are of the same order of magnitude of differences of results obtained by the authors that were previously reviewed. Figure 2.5 shows a clear relevance of the diameter of the perforation on the convective resistance, but other factors are also important, which is why there is the spread observed.

Mastromatteo et al. (2012) provide a variation of this approach, suggesting an exponential function of d_h^2 instead of eq. 2.17 This would solve the problem of resistance increasing with the diameter, as this effect will level off as diameter increases with an exponential function, and would fit data such as González et al. (2008) well, although as it is not a dimensionless correlation the parameters of Mastromatteo et al. (2012) do not fit the data of Gonzalez et al. (2008), the model would need to be re-fitted to the other set of data. One correlation for each set of data is a problem of empirical functions that are not written in terms of dimensionless correlations, as they do not avail of the principle of dynamic similarity.

The original work of physiology biophysics is quite relevant to the design of packages and deserves to be considered further, because it provides a very comprehensive analysis both theoretical and experimental of the movement of gases from micropores to surrounding air. Nobel (1974) shows the result of applying chemical engineering mass transfer analysis of convection resistance for gases flowing parallel over a flat plane, which leads to the result that the thickness of the boundary layer (L_e) varies with the position from the edge of the plane, and the average is proportional to the square root of the ratio between the length of the plane in the direction of the flow and the wind velocity. The constant of proportionality obtained by the theoretical development assuming that the wind moves in laminar flow over the flat plane (Meidner and Mansfield, 1968) is 0.6 in the cgs system of units (cm.s$^{-0.5}$), but experimental data obtained in wind tunnels cited by Nobel (1974) provided a better fit with the value of 0.4. Those experimental data also show that the exponent of this relationship may actually vary quite significantly depending on the size and actual shape of the plane. Noting that the stomata physiology work was performed with leaves, which are smaller and less flat than packages, it is uncertain that the empirical modifications of parameters would be similar, so the best result to apply to packages would be the theoretical result:

$$L_e = f\left(\frac{x}{v}\right)^a \tag{2.19}$$

with the theoretical values being a = 0.5 and f = 0.6 cm.s$^{-0.5}$. This expression would predict an infinite boundary layer for still air, but still air does not exist, the limit is natural convection. Nobel (1974) specifies that "still air" for equation 2.17 corresponds to velocities of 10 cm/s. The air circulation velocities measured by Montanez et al. (2010a) inside storage rooms as a result of the operation of the temperature control fans are of the order of 20 cm/s. For a flat plane of 20 cm of length (a typical value for a package), this would imply that L_e would be around 0.6 to 0.8 cm. This would be an extremely substantial value, completely overwhelming the importance of diffusion through the pore (as L is of the order of microns). Furthermore, it is independent of the diameter of the pore. From eq. 2.16, this would suggest k_c values of the order of 0.25 cm/s for oxygen, which are of the order of magnitude of those shown in fig. 2.5 for flow from packages with larger perforations (over 5 mm); smaller perforations generally have much higher values of k_c. Stomata pores are of the order of 10 to 100 microns, which means that this expression would suggest k_c values around 100 times smaller (L_e values 100 times bigger) than those in fig. 2.5 (obtained by Ghosh and Anantheswaran, 2001 and Gonzalez et al., 2008). This could be explained simply by the difference in surface roughness and shape of leaves compared to fairly flat package tops, but is also likely due to the fact that the type of diffusional flow from the stomata is much milder (the concentration gradients are smaller than in modified atmosphere packages at equilibrium) and thus they disturb the surrounding air flow at the boundary layer less. Although the expressions are therefore not applicable directly, the method is perfectly correct, and what needs to be done for packages is to develop experimental studies to determine the correlations that apply to their case (longer and flatter planes with greater fluxes through the perforations).

This work elucidates that eq. 2.18, whatever the value of ε, is not the most suitable approach. Parameters such as the actual size of the package (at least its length in the air flow direction) and velocity of the circulating air must be considered, as Nobel (1974) shows. Allan-Wojtas et al. (2008) also speculated that the viscosity of air must have an influence, when explaining an anomaly in their data (that the intercept of the gas transmission rate versus area of perforation straight line was significantly higher than the value given by the permeability of the unperforated film). Therefore, the most appropriate procedure is to go back to basics, and define an approach based on mass transfer analysis of the movement of gases over packages, taken as flat planes, and applicable to this situation.

2.2.5. Dimensionless correlation for mass transfer coefficients

The standard approach of chemical engineering is to establish dimensionless correlations, as these are likely to benefit from the principle of dynamic similarity (Bird, Stewart, and Lightfoot 2007). None of the work reviewed up to this point on mass transfer through perforated packages proposed dimensionless correlations, with the exception of Metz (2003) that proposed adding L/d_h raised to some power to expressions of the type of eq. 2.19. The limitation of expressions such as eq. 2.18, 2.19, or the correlations for K that do not discount the mass transfer area of Emond et al. (1991) or Fonseca et al. (2000) is that because they do not involve relations between dimensionless numbers each of which quantifies a ratio between different phenomena or forces at play, they do not ensure dynamic similarity. This has proved to be a most useful concept (Bird, Stewart, and Lightfoot 2007), which allows to predict results for completely different individual values of the relevant parameters, provided that their dimensionless ratios are within their range of applicability. Therefore, dimensionless correlations have a much wider applicability. It is particularly relevant in this case to overcome the problem of eq. 2.18 being applicable only up to a given value of d_h, above which the effect of d_h on permeability must level off. That limit is likely to be a different value of d_h depending on the other relevant parameters, but it is expectable that a dimensionless number may provide an objective limit of applicability. Also, dimensionless correlations are likely to bring in power exponents which will provide the level off effect and extend regions of applicability. This is the appropriate procedure to bring all data together and make joint sense of everything instead of having each publication providing a new equation, as has been the case.

There are some dimensionless correlations that have already been used in chemical engineering to quantify the mass transfer convection resistance of molecules moving perpendicularly out of flat planes for natural convection, and also for forced convection with a stream of air moving parallel to the surface. These correlations are valid for quantifying convection from an unperforated film, but it is not known if they would apply to perforations, because the bigger molecular fluxes involved and the turbulence caused by the counterflow movements may interfere significantly. Notwithstanding, they also provide suggestions for dimensionless numbers that may be relevant. From the experimental measurements of rate of evaporation from a liquid surface or from the sublimation rate of a volatile solid surface into a controlled air-stream, correlations are available that have been found to satisfy the equations obtained by theoretical analysis of boundary layers (Baehr and Stephan 2006):

- isothermal laminar flow over a flat plate at position x from the edge of the plate in the direction parallel to the flow

$$Sh_x = 0.664{Re_x}^{0.5}Sc^{1/3} \tag{2.20}$$

valid for $Re_x < 3x10^5$ and for $0.6 < Sc < 2500$

- isothermal turbulent flow over a flat plate at position x from the edge of the plate in the direction parallel to the flow
-

$$Sh_x = 0.036{Re_x}^{0.8}Sc^{1/3} \tag{2.21}$$

valid for $3x10^5 < Re_x < 1x10^8$ and for $0.6 < Sc < 2500$

For natural convection, the best that can be done is to use the heat and mass transfer analogy and postulate the mass transfer equivalent of the heat transfer correlations, which give (Baehr and Stephan 2006):

- isothermal natural convection over a flat horizontal plate for flow from the plate outwards:

$$Sh_{\delta} = 0.54(Gr \times Sc)^{1/4} \qquad (2.22)$$

valid for $1x10^4 < Ra < 1x10^7$

$$Sh_{\delta} = 0.15(Gr \times Sc)^{1/3} \qquad (2.23)$$

valid for $1x10^7 < Ra < 1x10^{11}$

- isothermal natural convection over a flat horizontal plate for flow from the top towards the plate:

$$Sh_{\delta} = 0.27(Gr \times Sc)^{1/4} \qquad (2.24)$$

valid for $1x10^5 < Ra < 1x10^{10}$

where the dimensionless numbers Sh (Sherwood), Re (Reynolds), Sc (Schmidt) and Gr_m (Grashof for mass transfer) are:

$$Sh_x = \frac{k_c x}{D}$$

$$Sh_\delta = \frac{k_c \delta}{D}$$

$$Re_x = \frac{\rho v x}{\mu}$$

$$Sc = \frac{\mu}{\rho D}$$

$$Gr_m = \frac{g\rho^2\delta^3}{\mu^2}\left|\frac{\rho}{\rho_s} - 1\right|$$

with x being the distance from the edge of the plate in the direction of the flow, D the diffusivity of the gas in question in the gas mix, k_c its mass transfer coefficient, δ is the ratio of the surface area to the perimeter of the plate, v is the average velocity of the circulating air with ρ and μ being its density and viscosity, respectively, and ρ_s is the density of the gas mix at the surface of the plate. Ra, the Rayleigh number, is the product between Grashof and Schmidt numbers. There is an obvious difficulty in using the Grashof number, which is that the density of the gas mix at the surface of the plane is unknown. The density of the gas mix depends on its composition, which is not known unless k_c would be known. If the resistance to diffusion through the perforation would be negligible compared to the resistances to convection on both ends, and if both would be regarded the same, then ρ_s could be calculated as the density of the modified atmosphere in the package headspace. This implies that the mass transfer coefficient for natural convection would depend on the actual concentration gradients. It is noted that while this is the only option to quantify the Grashof number without any further analysis, it may overestimate it. However, it usefully brings in a dependence of the mass transfer coefficient on the gradient across the package.

In order to compare what these correlations would suggest with the values obtained from the literature review discussed previously, the following scenario was considered: oxygen transferring from normal air into a package with 20 cm of length and 10 of width, at different positions from the edge, for an internal gas composition of 100% relative humidity, 15% carbon dioxide, 5% oxygen and remaining made up by nitrogen, at 20 ^{o}C, and with air circulation velocities from 0 (natural convection) to different values up to 2 m/s. Under those conditions the Schmidt number was at the edge of validity (0.6), the Reynolds number was always in the laminar range (2.47 x10^4 was the maximum value) and the Rayleigh number was within validity except for x lower than 4 cm. The results are summarised in fig. 2.7. The mass transfer coefficient k_c for natural convection varied with the distance from the edge between around 0.002 and 0.003 m/s, which is exactly the order of magnitude of the smaller mass transfer coefficients reported for large perforations (see fig. 2.5) and also the value predicted for “still air” with eq. 2.19 regarding leaves. As the velocity of air increases to 0.2 m/s (which is the air velocity reported by Montanez et al. (2010a) for their storage room) k_c increases to around 0.01 m/s, which is exactly the range of values reported by Montanez et al. (2010) for oxygen (see fig. 2.5) with their wide perforations. Therefore, the dimensionless correlations suggest that the convective mass transfer resistance found with perforations wider than 1 mm is exactly what is expected from all the work done in chemical engineering for mass transfer by convection from flat plates. However, lower diameters have been giving much lower resistances (higher k_c) to all authors that have worked with small perforations - even extremely high air velocities would not justify the high values of k_c of perforations of 0.2 mm and less (see fig. 2.5a). This concurs with the suggestion that the turbulence caused by the movement through the perforations disturbs the boundary layer quite significantly, and explains why smaller perforations give lower resistances: the greater the net velocities of the moving molecules coming into and out of the perforations, the greater the turbulence and hence the higher the value of k_c. Thus, the hypothesis that the concentration gradient across the package may influence the convective resistance that was already raised when analysing the Grashof number would justify that the mass transfer coefficients from the biophysics plant physiology work on leaves are much smaller than those found by Gonzalez et al. (2008) and Ghosh and Anantheswaran (2001) in microperforated packages with perforations of similar dimension to the leaf micropores. The fact that these correlations also fit the data suggested by the independent work carried out in plant physiology, where the thickness of the boundary layer was considered to vary with the air velocity and distance from the edge of the leaf, but not with the size of the pores (see eq. 2.18), further stresses that if the fluxes out of the pores would not disturb the boundary layer significantly, then the mass transfer coefficients from a pore or from a film would be similar.

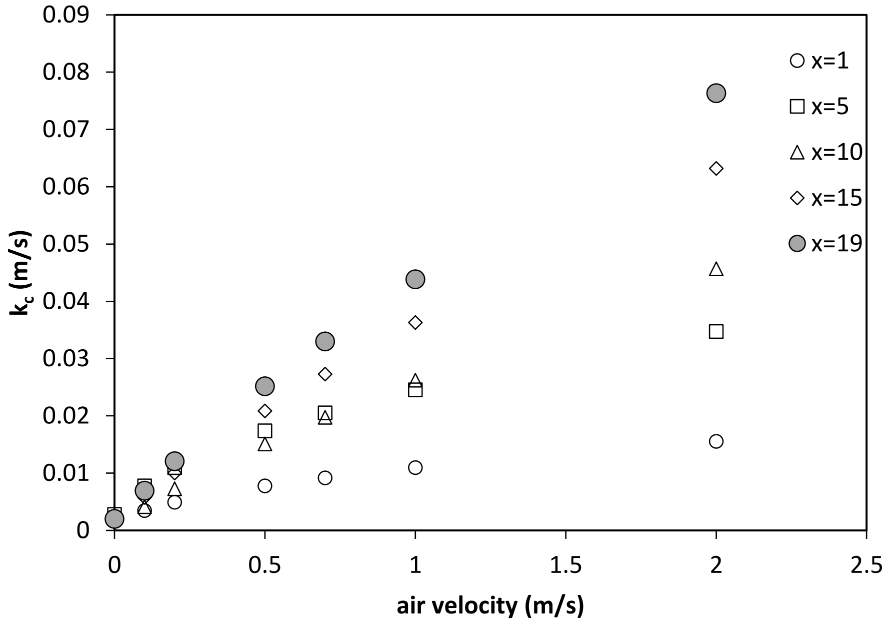

Figure 2.7 - Mass transfer coefficients at 20 ^{o}C predicted by the dimensionless correlations for oxygen moving into a flat surface at different positions (x, in cm) from the edge in the direction of the air flow, using the physical properties of normal air and a density gradient for the Grashof number caused by density difference to a modified atmosphere saturated in water vapour, with 15% carbon dioxide and 5% oxygen.

The results shown in figs. 2.5 and 2.7 suggest that this is the case for perforations greater than 1 mm and therefore, the existing correlations seem to suffice for wider perforations. This leads to the curious conclusion that the correlations proposed by Emond et al. (1991), Fonseca et al. (2000) and Montanez et al. (2010a) could be replaced by equations 2.4 and 2.17-19 for d_h greater than 1 mm. For smaller perforations, however, more work is needed to develop dimensionless correlations for mass transfer coefficients that will certainly be showing the importance of the diameter of the perforation and the gradient of concentrations across the package, in an effect that levels off and becomes negligible as the perforation size increases.

2.2.6. Methods solving the fundamental equations of mass and momentum transfer

If convection mass transfer resistance through the boundary layer is of critical importance to designing perforated packages, then dimensionless correlations would not be the most accurate way of addressing the problem. With the availability of strong computing power, it is possible to solve complex expressions numerically with a good level of precision and the full set of fundamental equations of motion, that is, the hydrodynamic terms in 3 dimensions and the diffusional terms in 3 dimensions could be used. The hydrodynamic equations (Navier-Stokes) are a set of 3 equations with partial derivatives for 3 components of velocity in the 3 axis, and thus the full problem is defined by a set of 6 partial differential equations. Xanthopoulos, Koronaki, and Boudouvis (2012) have solved that problem, assuming Fick's law with the diffusivities of gases in stagnated air. They compared the total flux from a film that is not fully impermeable, and where there is a balance between the flux through the film and through the pores; for the case studies analysed, the former varied between 5 to 15% of the total, with the film being polypropylene. Rennie and Tavoularis (2009a) used Stefan-Maxwell's equations and also added the energy (temperature) balance, which Fennir, M. (1997) also used. When solving the problem with the full set of fundamental equations, one could consider that it is a minor added complexity to consider temperature and this would provide an even more precise result. All methods mentioned previously assume perfect isothermal conditions. However, it is evident that this cannot be the case in reality because respiration releases heat, therefore, even in steady state the temperature of the product must be somewhat higher than its surroundings. Notwithstanding, the temperature difference may well be irrelevant as a few degrees are unlikely to change physical properties noticeably, which is likely to be the case considering that all authors reviewed before obtained perfect fits considering isothermal conditions. However, even small temperature differences may influence the fluxes through the perforations, so this is an issue that deserves further attention in the determination of the convective mass transfer coefficients. In the case of Fennir, M. (1997) work, the temperature balance was important because the author was measuring respiration rates with accuracy by analysing variations of compositions in containers.

While this approach can provide accurate results, it is still a very complex endeavour and requires significant computing time and advanced skills of the designer. It is therefore not very efficient to assist packaging design in real time and real conditions of practice, where both generally lack.

As will be shown in the next section, packaging design using unidimensional Fick's law with mass transfer coefficients provided by dimensionless correlations gives a very easy method to determine the optimum area of perforations for any particular batch of products and packaging film, and therefore can be implemented in practice with minor difficulty and used by designers with basic skills. The chemical engineering work on mass transfer operations (Bird, Stewart, and Lightfoot 2007, Foust 1980) has proved that this approach provides results that are quite adequate, in spite of the relatively high level of uncertainty in using constant values of k_c and of D, for a very wide range of problems of chemical engineering. However, it is important that the dimensionless correlations provide results that are as accurate as possible. The importance of accurate values for k_c is analysed in the next section.

Numerical solutions of the fundamental equations have a crucial role to play in providing a good assessment of dimensionless correlations and their parameters, and link fundamental phenomenological with practice results. This is exactly how this area has evolved in chemical engineering, for instance, the correlations in equations 2.20 and 2.21 have been found to correspond with good accuracy to the results inferred from a fundamental analysis of boundary layer movements (Baehr and Stephan, 2006), while those of equations 2.22 to 2.23 have not yet been addressed in the same way, so their application has a much higher level of uncertainty. If researchers solve the problem of permeability of perforated packages by numerical solution of the fundamental equations to study in particular the boundary layer surrounding the perforations, and from this work test and propose dimensionless correlations, this would give a much greater confidence in the application of these tools to packaging design. Furthermore, it would be possible to study a variety of scenarios individualising different effects (such as distance between packs due to distance between trays in palettes, differences in hydrodynamic conditions resulting from different storage environments, effect caused by fans on temperature controlled rooms, etc).

It is noted that if a fundamental approach is taken to give an accurate description of reality, then either Stefan-Maxwell equation should be used, or the diffusion coefficient for each gas (in the mix at any point of the space) should be considered variable, according to eq. 2.16.

2.3. PACKAGING DESIGN ENGINEERING

The design of a perforated package, that is, the determination of the ideal area of perforation for a given film, package and product, is simple by using Fick’s law with constant diffusivity and a convection mass transfer parameter. Combining equations 2.3 and 2.7 gives an effective, or apparent, permeability for a film as a function of its perforations, defined also by Mastromatteo et al. (2012). It is proposed to use the term apparent diffusivity instead of permeability for a question of consistency of units, as discussed before:

$$n_i = -\frac{D_{ei}A}{L}\frac{(y_{i,e}-y_{i,i})p_t}{R_gT} \qquad (2.25)$$

where A is the whole area of package exposed to air (film plus perforations) and D_e the effective diffusivity of a perforated package, which is equal to:

$$D_{ei} = D_{ai} + \left(\frac{1}{\frac{1}{D_i}+\frac{1}{L\times k_{ci}}} - D_{ai}\right)\frac{A_h}{A} \qquad (2.26)$$

It is reminded for clarity that D_i is the effective diffusivity of gas i through air in the perforation (taken as a constant, and that is likely to be lower than that through normal stagnated air), D_{ai} is the apparent diffusivity of gas i through the polymeric film, which is equal to its real diffusivity multiplied by the solubility (taken to be constant), and D_{ei} is the effective diffusivity of the perforated package, which is equal to its effective permeability upon conversion of units by comparison between eqs. 2.2 and 2.25.

At steady state, the diffusional fluxes of eq. 2.25 for oxygen and carbon dioxide equal their consumption and production (respectively) from the respiration rate. Designating R_i as the respiration rate in moles of gas consumed or produced per unit of time and of mass of product gives a set of 2 equations:

$$\frac{D_{eO}A}{L}\frac{\left(y_{O,e}-y_{O,i}\right)P_t}{R_gT} = (-R_O)w \qquad (2.27)$$

$$\frac{D_{eC}A}{L}\frac{\left(y_{C,i}-y_{C,e}\right)P_t}{R_gT} = R_Cw \qquad (2.28)$$

where O denotes oxygen and C carbon dioxide and w is the weight of the product inside the package. It is noted that as oxygen is consumed R$_O$ is negative (using the standard chemical reaction engineering notation of negative rates for reagents and positive for products), so the quantity -R$_O$ is positive, and it is also noted that the minus sign for carbon dioxide was removed by switching the inner and outer molar fractions in the numerator. In this way, all values in equations 2.27 and 2.28 are positive. Dividing eq. 2.28 by 2.27 gives:

$$y_{C,i} = y_{C,e} + \frac{{R_C}/{(-R_O)}}{{D_{eC}}/{D_{eO}}}\left(y_{O,e}-y_{O,i}\right) \qquad (2.29)$$

The ratio of the effective diffusivity of carbon dioxide to that of oxygen is the same as the ratio of the effective permeabilities, which is known as β. The ratio of the respiration rates of carbon dioxide to oxygen is known as the respiratory quotient, R_Q, thus, if the respiratory quotient is constant, eq. 2.29 defines a straight line in a carbon dioxide versus oxygen plot:

$$y_{C,i} = y_{C,e} + \frac{R_Q}{\beta}\left(y_{O,e} - y_{O,i}\right) \qquad (2.30)$$

For instance, taking typical polymeric films (EVA, LDPE and Saran were chosen, providing a spread of different permeabilities and β values - Exama et al., 1993; Mahajan et al., 2006), with A_h=0 (no perforations), and using the respiration rate model of strawberries proposed by Hertog et al. (1999) gives the 3 dashed lines in fig. 2.8, for storage temperatures of 10 ^{o}C (fig 2.8a) or 20 ^{o}C (fig 2.8b). The model proposed by Hertog et al (1999) does not require R_Q to be constant, so the lines are not straight. They only deviate significantly from a straight line, however, for low concentrations of oxygen because under those conditions the strawberries would be fermenting, and this portion of the lines (below 5% oxygen) is of no practical interest (the packages would be inflated and unsaleable and the product could be a health hazard). To avoid confusing the graph with regions of no interest, the lines shown in fig. 2.8 are extrapolations for oxygen concentrations below 2% (the original model would start increasing carbon dioxide content abnormally, as in those conditions it is essentially describing fermentation, not respiration).

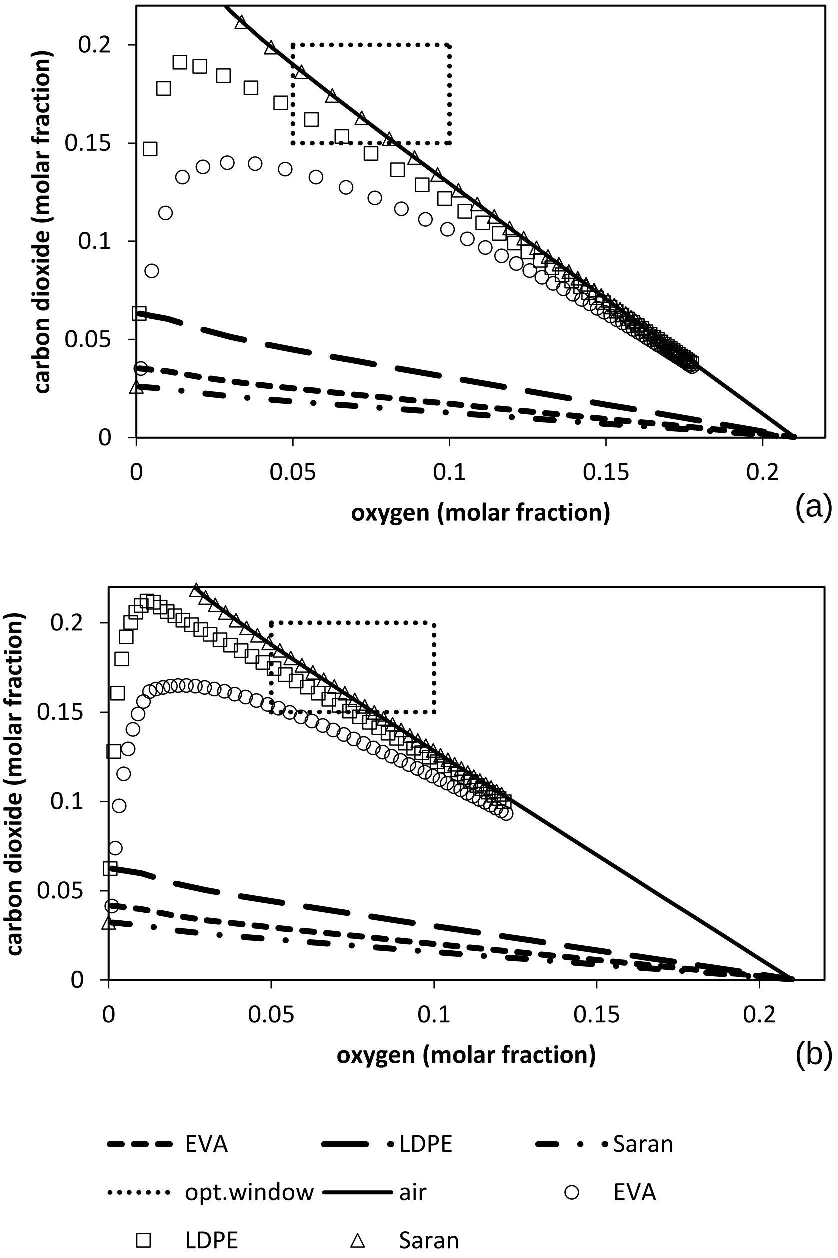

Figure 2.8 - Modified atmospheres that can be generated by strawberries following the respiration rate model of Hertog et al. (1999) packed in EVA, LDPE or Saran films with permeabilities according to Exama et al. (1993), both influenced by temperature, for storage at 10 ^{o}C (a) and 20 ^{o}C (b). The dashed lines give all possible atmospheres for each film if unperforated, depending on temperature, film thickness and area to weight ratio of the package. The symbols indicate atmosphere compositions of a package with 20x10 cm^2 of exposed area of 25 μm films and 300 g of strawberries, from unperforated (points on top of the respective line) to increasing number of perforations of 0.1 mm diameter (each additional perforation is one further point).

Any package using these films will lead to a modified atmosphere at equilibrium somewhere along the respective line, whatever the thickness of the film, the area exposed, the temperature of storage and the weight of product packed. The optimum gas composition for storage of strawberries is also shown as a dotted rectangle, and therefore, no film would give optimum conditions, whatever the characteristics of the package.

The exact location within the line can be calculated easily by handling equations 2.26 and 2.29 together with the respiration rate model. To illustrate the effect of package characteristics, fig. 2.8 shows the composition of a modified atmosphere for 300 g of strawberries that would respire exactly as those of Hertog et al. (1999) stored at 10 ^oC (a) or 20 ^oC (b) in a pack with a 20x10 cm^2 exposed film of 25 μm thickness - this implies that the effect of humidity on permeability is being neglected (an issue that will be discussed in part 2 of this work). The effect of temperature on the permeability of the films was considered, using the activation energies from Exama et al. (1993), and thus the lines are different for different temperatures, as figs. 2.8 a and b show. It can be seen from equations 2.29 and 2.30 that if temperature increases, as the activation energy of the respiration rate model is higher than that of the films, the location of the modified atmosphere would slide along the line to the left (as respiration increases more than permeation does), although it is noted that the lines themselves would change somewhat too, because temperature affects both the permeability and the respiration rate ratios due to the activation energies for oxygen and for carbon dioxide being different in both cases. Using a thicker film and using a lower ratio A/w would also move the location of the points to the left - sliding to the right would result from lower temperature, thinner films or bigger A/w ratios. The individual values of A and w do not matter, only their ratio, according to eqs. 2.28 and 2.30 - this is because the respiration rate models proposed in literature do not consider any effect of the surface area and grouping/packing of the different individual pieces of strawberries within a package. It can be seen that all 3 films are so impermeable for a package of those characteristics, that all of them would be totally inappropriate for these strawberries, as the package would tend to anoxia and fermentation would set. It would be possible to have oxygen concentrations of 5 to 10% only if using excessively thin films and/or too high A/w ratios, but even in those cases, the carbon dioxide content would still be quite low, as one wold be sliding along the dotted lines.

Perforating the package will modify the permeability, increasing it overall and also lowering the value of β (eq. 2.29), therefore, the corresponding atmospheres will be providing points further up and further to the right in fig. 2.8. Fig. 2.8 shows the location of the modified atmospheres for different numbers of perforations of 100 μm each using for gas diffusivity the values for diffusion across stagnated air and a mass transfer coefficient equal to the diffusivity divided by 50 μm, which is the prediction from Fishman et al. (1996) for ε=0.5 (this corresponds to a k_c value of 0.38 m/s for oxygen and 0.30 m/s for carbon dioxide at 10 ^oC, which are just slightly lower than the values of data points in fig. 2.5, of around 0.4 m/s). The data tend to the full line in fig. 2.8, which is given by the ratio of the respiratory quotient to the permeability ratio β of the perforations (diffusion and convection through air), which is evident from the equations. Saran is the most impermeable film (0.086 and 0.710 $mL.mil.m^{-2}.atm^{-1}.hr^{-1}$ for oxygen and carbon dioxide, respectively, at 10°C, from Exama et al. 1993), and thus even one single perforation is enough to bring the modified atmosphere composition to the line drawn for air (this point is outside the scale of fig. 2.8, being of no practical interest). In effect, using a Saran film or a fully impermeable material would give the same result in this case. It is noted that for strawberries, as the line for air actually crosses the optimum window, this is a very good option, so a good package for strawberries would be the cheapest container that is gas impermeable, with the suitable number of perforations (10 would give the point closest to the center of the window of fig. 2.8 for Saran) - however, it is reminded that this conclusions is based on the oxygen and carbon dioxide balance only, and is neglecting water and humidity. LDPE (permeabilities of 110 and 0.710 $mL.mil.m^{-2}.atm^{-1}.hr^{-1}$ for oxygen and carbon dioxide, respectively, at 10 ^{o}C, from Exama et al., 1993) with 8 perforations would be estimated to provide a similar result, while EVA, being very permeable to carbon dioxide (158 and 945 $mL.mil.m^{-2}.atm^{-1}.hr^{-1}$ for oxygen and carbon dioxide, respectively, at 10 ^{o}C) would not allow a sufficient build up of carbon dioxide at 10°C to reach the optimum window with this type of package (it could however reach it by increasing the thickness to 60 μm, for instance). It is noted that these observations apply to films with the properties of those tested by Exama et al. (1993): specific films can vary significantly depending on a variety of characteristics, among various suppliers, even if they would all be called LDPE, for instance.

In order to assess the importance of the accuracy in diffusivity and in mass transfer coefficients, fig. 2.9 shows what happens to a given prediction as these values change. Figure 2.9a shows just the importance of diffusivity and of mass transfer coefficients for the same perforation size of 100 μm, comparing 4 different methods of estimating the mass transfer coefficients. The full symbols show the results obtained using the diffusivities of oxygen and carbon dioxide through normal stagnated air and the open symbols using gas diffusivities 80% lower for oxygen and 90% lower for carbon dioxide (this is a difference expected from the analysis of Stefan-Maxwell's method discussed earlier). The circles show the result using Fishman et al. (1996) suggestion for equivalent length, the squares the result with Paul and Clarke's (2002) derivation with $\varepsilon = 7/6$, the triangles the result of $k_c = 0.4$ m/s, which is the approximate value in fig. 2.5a for both gases, due essentially to Gonzalez et al. (1998) and Ghosh and Anantheswaran (2001) data, and the diamond shapes show the results with the dimensionless correlations that neglect the influence of the hydrodynamic disturbances in the boundary layer near the perforations (eqs. 2.20 to 2.24) for air circulation velocities of 1 m/s.

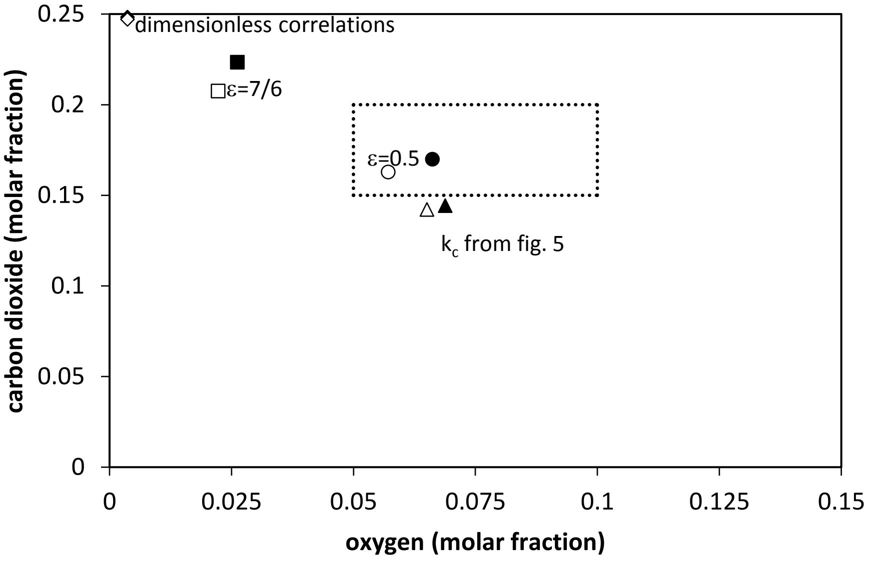

(a)

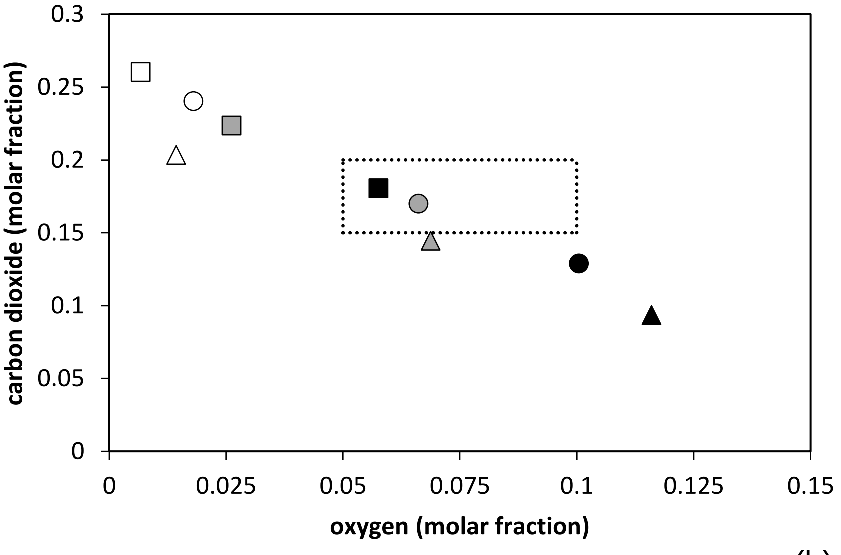

(b)

Figure 2.9. Variation of the composition of modified atmospheres for 300 g of strawberries following the respiration rate model of Hertog et al. (1999) packed in a package with a 20·10 cm^2 area of a 25 μm thick Saran film at 10°C predicted by assuming different values for the diffusivity of the gases through the perforations and the mass transfer coefficients.

a) with 10 perforations of 100 μm each, full symbols indicating the use of the diffusivity of gases in stagnated normal air and open symbols diffusivities 80% lower than that. Estimates of the mass transfer coefficients according to the method indicated on the graph (circles for ε=0.5, squares for ε=7/6, triangles for values taken from fig. 2.5 and diamonds for values from eqs. 2.20 to 2.25)

b) using diffusivity of gases in stagnated normal air and the same total area of perforations, but different number and sizes of perforations. Full symbols for 40 of

50 μm each, shaded symbols 10 of 100 μm and open symbols 1 of 316 mm. Mass transfer coefficients estimated with ε=0.5 (circles), ε=7/6 (squares) and taken from fig. 2.5 (triangles).

It can be seen that the diffusivity can affect significantly the predictions from the distances between the open and closed symbols. However, as previously found, the most important issue may be to use a diffusivity that relates to a situation of each gas moving across a mix of diffusional flows, and not across a stagnated mix, and for higher carbon dioxide concentrations that in normal air. Fig. 2.9 shows that this may be a relevant difference. The most important effect, however, is that of the mass transfer coefficients. Even a difference between 0.4 and 0.38 to 0.30 between Fishman, Rodov, and BenYehoshua (1996) suggestion and the data of fig. 2.5 provides quite significant differences. Using Paul and Clarke (2002) value for this package and product would provide a completely different result (the corresponding k_c values being 0.16 and 0.13 m/s for oxygen and carbon dioxide, respectively, for diffusivities through stagnated air), and the most different would be the one considering the mass transfer coefficient to be equal to that from a flat plane (dimensionless correlations and plant biophysiology correlations, giving k_c values of 0.03 m/s). Unsurprisingly, the smaller the mass transfer coefficient, the further to the left the location is in the graph, as lower k_c means greater resistance to mass transfer, so the effective permeability of a perforated film increases with k_c. The consequence regarding the package design is that if one was using the broad k_c values from fig. 2.5, the result would suggest one or two more perforations than the results with ε=0.5, while taking the Paul and Clarke (2002) value of ε=7/6 would suggest using many more perforations.

Fig. 2.9b shows the relevance of the size of perforations. In this case, all data points were obtained with the diffusivities in normal stagnated air, and the perforation size and number was varied. The shaded symbols show the same points as in fig. 2.9a for 100 μm perforations, which with 10 perforations gives a total area of 0.0785 mm^2. This same area can be obtained with 1 perforation of 316 μm which would lead to the full symbols, the 10 perforations of 100 μm as in fig. 2.9a (shaded symbols), and with 40 perforations of 50 μm (open symbols). The circles are the predictions using ε=0.5, the squares with ε=7/6, and the triangles the k_c values from fig. 2.5 (which are around 1.2 and 1.7 m/s for 50 μm for oxygen and carbon dioxide, respectively, according to the data from González et al. (2008), and both around 0.1 m/s for 0.3 mm). Fig. 2.9b shows a rather dramatic effect of the size of the perforations, whatever the method of quantifying the convection resistance.

Both fig 2.9a and 2.9b show that estimating the mass transfer coefficient is a key issue for a proper design of perforated packages, and that the existing data is insufficient. The significant influence of even small variations in k_c raises a particular problem with the use of perforated films in practice. As air circulation velocities are bound to affect the mass transfer coefficients significantly, the permeability of a perforated package may effectively change with changes in the hydrodynamic conditions surrounding the package. This is a significant hindrance because in real-life distribution chains these are likely to vary from store houses, to transportation vehicles, to store displays. Therefore, it is noted that the possibility of covering the perforations with a highly permeable label raised for safety reasons (preventing microbial contamination) would also offer an alternative that would result in a more robust performance. This would break the velocity profile and minimise the disturbance at the boundary layers, and although increasing the total resistance, it would make the system more predictable and less prone to variations caused by differences in the surrounding hydrodynamic conditions.

2.4. CONCLUSION

There have been several authors addressing the packaging design with perforated films and proposing a variety of different methods and models. However, all data can be pooled together and are quite consistent when seen under a same light. A mass transfer analysis considering a constant Fickian diffusion and a mass transfer coefficient is a simple and effective way to quantify the situation with sufficient precision, although it would be more appropriate that the diffusivity values are representative of diffusion through perforations, which may be somewhat smaller than the diffusivities of the gases through stagnated air.

The composition of a modified atmosphere at equilibrium estimated by any method depends significantly on the actual values of the mass transfer coefficient (or equivalent length, if that parameter would be preferred to quantify the convective resistances). All data analysed actually shows quite clearly that the diameter of the perforations influences these resistances very significantly, especially for perforations of less than 1 mm diameter, and therefore, broad suggestions that the only parameter that matters is the total area of perforations are not correct. The analysis of the data indicate that the disturbance of the boundary layer by the molecular counterflows through the perforations increases the mass transfer coefficient significantly (lower the resistance), and therefore the greater the concentration gradient across the package and the smaller the diameter, the higher the effective permeability of a perforated package. No correlation proposed to date to quantify the convective resistance is satisfactory, either because it does not consider the actual conditions of perforation counterflows and their effect on the boundary layer, and thus underestimate the mass transfer coefficient significantly (that is, they suggest lower permeabilities than reality), or because they do not benefit of any dynamic similarity and are only valid for the set of data used to generate them.

It is therefore urgent to develop appropriate dimensionless correlations to estimate the mass transfer coefficients, which will need to consider the surrounding air velocities, diameter and length of the perforations (thickness of the film), geometry and dimensions of the surface, and concentration gradient across the package.

3. EFFECT OF HYDRODYNAMIC CONDITIONS AND GEOMETRIC ASPECTS ON THE PERMEANCE PERFORATED PACKAGING FILMS

ABSTRACT

Modified atmosphere packaging (MAP) is applied to extend shelf-life of fresh and minimally processed produce. It ensures a protective gas composition inside the package as a result of the interplay between product respiration and package permeability. Commonly used films, such as Oriented Polypropylene (OPP), are too impermeable to gases for successful MAP for products with moderate to high respiration rates, which has led to perforated systems. In order to design the perforation profile to ensure MAP targets for extended shelf life it is necessary to evaluate which parameters affect the mass transfer through the perforations significantly. Perforations (270, 450 and 750 μm diameter) were made in an OPP film with the inner atmosphere initially flushed to high carbon dioxide and no oxygen and allowed to equilibrate to atmospheric conditions under different temperatures and circulating air velocities, considering also different locations for the perforations. The oxygen concentration was measured with a non-intrusive method, providing the data for calculation of the resulting permeance. The results obtained showed that the perforation diameter is the most important parameter and can even be more significant than the total area of perforation (and therefore the number of perforations). Air

velocity around the package and storage temperature were also relevant. Stacking during storage risks blocking perforations and therefore it is recommended to pierce trays on the sides in order to ensure better robustness. The package gas composition itself also affected mass transfer due to the interplay of oxygen flux with other gas fluxes, with particular relevance to the case of water vapour.

3.1. INTRODUCTION

Modified atmosphere is a technology used to prolong the shelf life of fresh and minimally processed food. It consists in manipulating the levels of gases (generally O_2, CO_2, N_2 and water vapour creating an atmosphere composition different to that of normal air. Modified atmosphere packaging (MAP) ensures a protective gas composition inside the package as a joint result of the respiration of the product itself and the permeability of the package. It typically contains an inert gas (nitrogen) combined with carbon dioxide which has an antimicrobial activity, and low levels of oxygen (Spencer 2005).

Atmosphere is not constant in all MAP products and will change according to the permeability of the packaging material, the microbiological activity and respiration of the food itself. Successful MAP requires raw materials to have a low microbiological count and strict temperature control throughout the process (Fellows 2009).

Oriented polypropylene (OPP) is a commonly used packaging film that has low permeability to water vapour (WV), O_2 and CO_2. As OPP is too impermeable to gases, it results in excessive humidity build-up leading to condensation and early mould development and even dangerous anoxia conditions and for this reason such films are now commonly micro or macroperforated to increase their permeability.

In order to design the perforation profile to ensure MAP targets to extend shelf life while avoiding anoxia, it is necessary to quantify appropriately the permeability of a perforated package. A main problem that has not received sufficient attention to date is that the effective permeability of perforations is much more dependent on factors such as the hydrodynamic movements outside the package than would be the case in a non-perforated film and therefore the importance of all relevant parameters for this particular case needs to be assessed comprehensively.

Air movement is actually essential to prolong the shelf life of fresh fruits and vegetables as it assists in liberating the respiration heat during storage. Temperature differentials due to this heat release would increase the water vapour pressure difference near the surface of the product and thus increase evaporative water loss (transpiration). The air movement should be enough to prevent large temperature gradients forming without affecting the water vapour pressure around the produce (DeELL, Prange, and Peppelenbos 2003).

There have been different propositions on how to quantify the permeance of a package due to perforations, as shown in Chapter 2. Most of these consider only one parameter, such as the perforation diameter, or a few, with empirical expressions that do not obey the principle of dynamic similarity - this means that their applicability is limited to the range of values used in the experimental set of data used to derive the correlations for each of these parameters.

Gas flows through perforations have been extensively studied in various chemical engineering applications and a simple yet powerful approach to quantify these fluxes is to determine the convection mass transfer coefficients and relate them to the relevant system parameters with dimensionless correlations, which due to the principle of dynamic similarity would be amenable for scale up and much wider application. In order to establish widely applicable correlations it is necessary to obtain a significant amount of experimental data and therefore it is advantageous to establish first which system parameters are more influential and need to be considered with greater care in the development of these correlations. Montanez et al. (2010b) observed that there is air movement in storage rooms as a result of the cooling equipment. The impact of this on the mass transfer coefficient of packaging films was analysed, but their study was focused on the specific characteristics of their own storage room. As the hydrodynamic conditions affect the gas exchange through the perforations, it is necessary to study this effect by obtaining results that could be applied to different storage conditions, and hence the relevance of dimensionless correlations.

Also, food containers are commonly stacked in order to save space during storage. This will create different hydrodynamic conditions depending on where and how individual packages are positioned, which could impact on their permeability. A particular concern would be regions of such stagnated conditions that the packages would reach anoxia.

Therefore, it is important to evaluate the effect of stacking on the mass transfer coefficients.

The purpose of this work was to assess the importance of some parameters that are found in chemical engineering correlations of comparable scenarios: the dimension of the perforations, the number of perforations, the average surface velocity of air on the outside of the package, the distance between the hole and the edge of the package in the direction of the air flow and the temperature of storage. It was also desired to analyse the effect of different storage stacking options on the mass transfer coefficient.

3.2. MATERIALS AND METHODS

3.2.1. Experimental Procedure

Hermetic containers with an open top where a $7.85 \cdot 10^{-3}$ m^2 oriented polypropylene (OPP) film could be hermetically crimped were used. The containers were flushed with 20-23% v/v of CO_2 and the balance with N_2 and kept in a walk-in controlled temperature cold room maintained within 1°C of the set temperature.

The O_2 concentration inside the containers was measured using a Fiber Optic Oxygen Transmitter (Presens, Germany). This device uses an optical probe to determine the inner concentrations without disturbing the inner atmosphere, from colorimetric changes in spots glued to the inner surface of the film, across its transparency.

3.2.2. Effect of air velocity, perforation diameter and position of perforation

In order to evaluate the effect of air velocity, diameter of perforation and distance from the edge, the films were perforated with a needle making one single perforation of the defined diameter at the defined location (3 options for each: 270, 450 and 750 μm diameters, and locations (x) at 2.5, 5 and 7.5 cm from the edge). A fan located next to the packages was set at different speeds and the average air velocity over the package surface measured, giving 3 different conditions: 0, 2.7 and 4 m/s. The experiments were performed at 10°C.

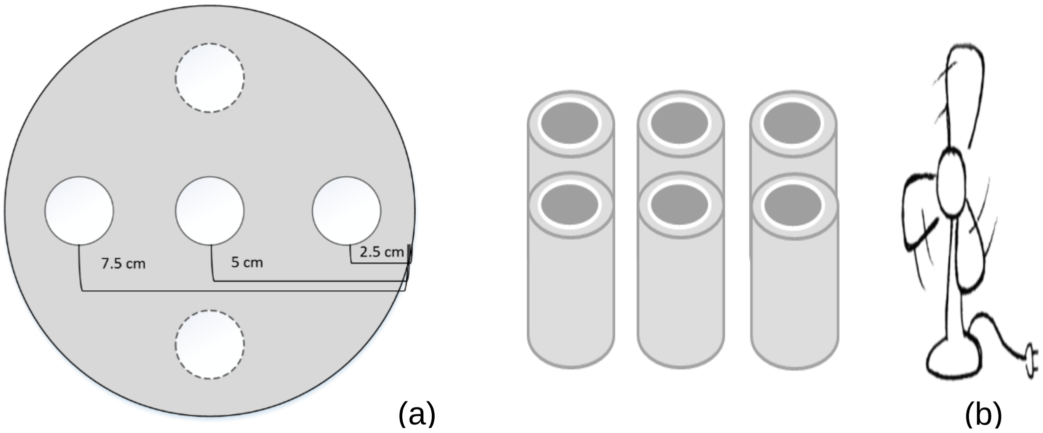

(a) (b)

Figure 3.1–Position of the Perforation (Dashed circles represent the situation where 5 perforations were used) (a) and disposition of the containers (b)

The experimental runs were performed with all the combinations of the 3 levels of the 3 factors, and the combination of centre values was replicated 3 times, in a total of 30 experiments (see table 3.1 for details). The data was analysed with Statistica software for Windows v. 8.0 (Tulsa, USA), with a factorial Analysis of Variance with a significance level of 95%. In order to avoid the elimination of some results that could be important to explain some observed phenomena, results with $0.05 < p < 0.1$ were called marginally significant and also considered for the analysis (Montgomery 2013).

3.2.3. Effect of temperature, number and diameter of perforations

The effects of temperature (5, 10 and 15 ºC), number of perforations (1, 3 or 5) and hole diameter (270, 450 or 750 μm) on the permeability of films were analysed with two replicate experimental runs of all the combinations of a 3^3 full factorial design, in a total of 27 experiments. A fan was used to create an average air velocity of 2.7 m/s, in order to create external turbulence (the mid-point of air velocity studied earlier). Fig 3.1 shows the locations of the perforations (Fig 3.1.a) and the arrangement of containers relative to the fan (Fig 3.b).

3.2.4. Effect of area of perforation on mass transfer coefficient

Perforated films with different diameter and number of perforations, but similar areas of perforation were analysed in order to determine if the total area of perforation being obtained in different ways affects the mass transfer coefficient, these results were compared with mass transfer coefficient of films with same diameter of perforation but different total perforated area. The experiments were performed in triplicate, at 10°C, and analysed according to Tukey’s multiple range test at a confidence interval of 95% to determine the significant differences between group samples.

3.2.5. Effect of the distance between perforations on mass transfer coefficient

Films with two perforations (diameter: 750 μm each) with different distances between them (0.1, 0.2, 0.3, 0.5, 1.0, 1.5, 2.5 and 5 cm) were analysed. The experiments were performed in triplicate and the mass transfer coefficients were analysed according to Tukey’s multiple range test at a confidence interval of 95% to determine the significant differences between group samples.

3.2.6. Effect of different atmospheres in oxygen transfer through the packaging

Small containers (volume: 226.2 cm^3) with an opened top (area: 44.2 cm^2) fitted with OPP hermetically crimped were flushed with different gas compositions. Films were singly perforated with a 750 μm-diameter needle. Five different atmosphere conditions inside the containers were evaluated: i) 20% CO_2 and 80% N_2; 0% RH; ii) 20% CO_2 and 80% N_2; 53% RH, iii) 20% CO_2, 80% N_2; RH ambient, iv) 20% CO_2 and 80% N_2; 100% RH and v) 100% N_2; RH ambient.

The containers were kept in a cold room at 5°C and 80±3% ambient RH, with air velocity of 2.7 m/s. The RH inside the containers was controlled as follows: calcium anhydride ($CaCl_2$ – 0% RH), saturated solution $Mg(NO_3)_2$ (52.9% RH) and water (100% RH). Experiments were performed in triplicate and the mass transfer coefficients were analysed according to Tukey's multiple range test at a confidence interval of 95% to determine the significant differences between group samples.

3.2.7. Effect of packing arrangement during storage on the Modified Atmosphere Packaging performance of microperforated packages

OPP films were hermetically crimped on small containers (v 226.2 cm3) and flushed with a mix of N_2:CO_2 (80:20). All films were single perforated with a surgical needle (diameter: 0.750 mm) and kept at 5ºC. A fan was used to keep the air velocity at 0.8 m/s around the boxes, creating a constant air movement representative of storage in cold rooms.

All experiments were performed in triplicate. Significant differences were assessed with a one-way Analysis of Variance, with post-hoc analysis using Tukey's Honest Significant Difference multiple range test at a 95% confidence level.

3.2.7.1. Effect of the position in stacking on the package permeance

Containers were stored in plastic boxes commonly used in supermarkets, perforated to permit air flow, but without impacting directly on perforations. The containers and boxes were kept in a walk-in room at 5ºC, placed inside two stacked boxes and stacked in the box, in four different positions: i) in a box on the top of another box, ii) in a box under another box, iii) on the top of another container in a same box and iv) under another container in a same box.

3.2.7.2. Effect of the position of the perforation on the package permeance

Containers were laid out in different positions to determine the influence of the direction of flow relative to the perforation. Some containers were placed with the perforation perpendicular to the air movement (facing the front of the fan), others also perpendicular but hidden from the fan by another container, and others parallel to the air direction (top, right and left).

3.2.8. Determination of film permeance

The convection mass transfer coefficients (k) were obtained by least squares regression of the model predictions obtained by solving the mass balance with Newton's convection equation.

The mass balance to the container in unsteady state is:

$$V\frac{dC}{dt} = n \qquad (3.1)$$

where C is the gas concentration, n is the molar flow rate of gas through the package and V the volume of the container. The flow is proportional to the concentration gradient and area of the film (A), with the apparent permeance of the perforated film being the proportionality constant:

$$n = \mathrm{P}_a \, \mathrm{A} \, (C_e - C_i) \tag{3.2}$$

where P_a is the apparent permeance of the film.

Using the ideal gas law, C = yP/RT with y being the molar (or volumetric) fraction of gas, P the pressure, R the ideal gas constant and T the absolute temperature, and developing the equations:

$$y_t = y_e - (y_e - y_0) \cdot e^{-\frac{\mathrm{P}_a \, \mathrm{A}}{V} \cdot t} \tag{3.3}$$

where y_t is the molar fraction inside the container at any given time t, y_e the outer atmosphere and y_0 the value of y_t at time t=0.

The apparent permeance is the result of the flow through the perforations and through the film itself. Equation 3.2 can be decomposed in these 2 flows:

$$n = n_{perf} + n_{film} \tag{3.4}$$

The flow through the perforations (n_{perf}) is a convective flow which can be quantified by Newton’s convection mass transfer law, whereas the flow through the film (n_{film}) is quantified by its permeance. Hence:

$$n = KA_p(C_e - C_i) + P_{film}\left(A - A_p\right)(C_e - C_i) \qquad (3.5)$$

where K is the overall convection mass transfer coefficient through the perforations, P_{film} the permeance of the film itself and A_p the area of the n perforations ($n \cdot \pi/4 \cdot d_p^2$). Combining eq. 3.5 with 3.2 gives:

$$K = \mathrm{P}_a \frac{A}{A_p} + \mathrm{P}_{film}\left(\frac{A}{A_p} - 1\right) \qquad (3.6)$$

The effective permeance of the film was determined experimentally with unperforated films, which means that if the crimping or sealing would not be perfect, this would be accounted for in this experimental value anyway.

3.3. RESULTS AND DISCUSSION

3.3.1. Effect of different parameters on the mass transfer coefficient

Data for the unperforated film at 10°C showed that the effective permeance of the OPP film with this type of sealing was $1.11 \cdot 10^{-6}$ cm/s, which was similar to the permeance of $1.6 \cdot 10^{-6}$ cm/s reported by Sandhya (2010), much lower than the $3.60 \cdot 10^{-4}$ cm/s provided by Weng, Osako, and Tanaka (2009) for OPP at 20°C and a relative humidity of 50% , but greater than the value of 4.06·10^{-7} cm/s obtained by Rubino et al. (2001) at 25°C and relative humidity of 80%.

Films were single-perforated and the effect of the air velocity, diameter of perforation and distance of perforation from the edge was studied. The results are shown in Table 3.1.

Table 3.1– Mass Transfer Coefficients (K, in m·s^{-1}; average of 2 repeats) of Perforated Films with different perforation diameters (in μm), air velocities (in m·s^{-1}) and distances from edge (in cm), and with P_{film} = 1.11·10^{-8} cm/s

	Diameter	Air Velocity	Distance	$P_a \cdot 10^7$	$K \cdot 10^2$
1	270	0	2.5	3.90	5.20
2	270	0	5	4.30	5.75
3	270	0	7.5	4.10	5.47
4	270	2.7	2.5	5.50	7.39
5	270	2.7	5	4.10	5.47
6	270	2.7	7.5	3.50	4.65
7	270	4	2.5	4.60	6.16
8	270	4	5	3.50	4.65
9	270	4	7.5	5.50	7.39
10	450	0	2.5	4.40	2.12
11	450	0	5	5.10	2.46
12	450	0	7.5	9.10	4.44
13	450	2.7	2.5	7.80	3.80
14	450	2.7	5	7.10	3.45
15	450	2.7	7.5	7.20	3.50
16	450	4	2.5	7.00	3.40
17	450	4	5	8.50	4.14
18	450	4	7.5	14.60	7.12
19	750	0	2.5	7.48	1.31
20	750	0	5	9.40	1.65
21	750	0	7.5	5.67	9.89
22	750	2.7	2.5	11.90	2.10
23	750	2.7	5	8.40	1.47
24	750	2.7	7.5	10.40	1.83
25	750	4	2.5	16.10	2.85
26	750	4	5	10.90	1.92
27	750	4	7.5	9.25	1.62
28	450	2.7	5	7.80	3.80
29	450	2.7	5	6.20	3.01
30	450	2.7	5	5.60	2.71

Figure 3.2 shows the Analysis of Variance results for the mass transfer coefficient K ($R^2 = 0.94$) in a visual manner, with the raw sums of squares represented in a pie chart. Diameter was clearly the most important parameter, having a negative effect on K. Air velocity was also statistically significant, with a positive effect on K. The interactive effects Diameter^2 x Distance and Air Velocity^2 x Distance also presented significant effect on K, as shown in Fig. 3.2. The distance from the edge was not significant but some interaction effects were statistical significant, which means that its effect depends on the levels of air velocity and diameter of perforation.

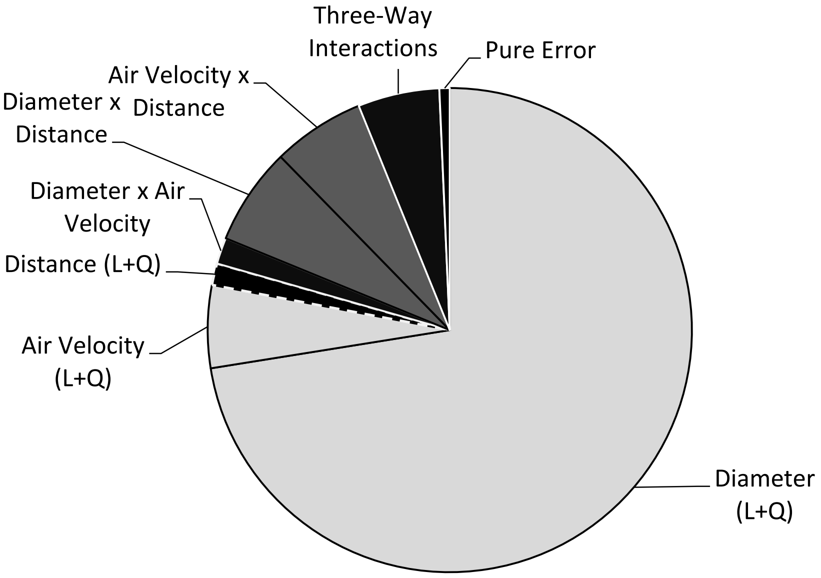

Figure 3.2– Result of the Analysis of Variance of the mass transfer coefficient for diameter, distance and air velocity for a single perforation at 10°C, showing the portions of the raw sums of squares explained by each effect (total number of points = 30, total SS = 0.0103), where light grey denotes statistically significant effects ($p < 0.05$), dark grey marginally significant effects ($0.1 > p > 0.05$) and black non-significant effects ($p > 0.1$)

It is important to note that while an increase in the diameter resulted in a decrease on the mass transfer flow rate through the perforation, it represented an increase in the apparent permeance, due to the relation between both K and P_a and the total area of the film and the area of perforation (see Eq. 3.6). This effect on the overall permeance was also observed by Mastromatteo et al. (2012) and was related to the fact that the perforation offers much less resistance to the flux than the film. Results obtained by Techavises and Hikida (2008) also indicate greater permeances on wider openings, and they proposed a mathematical model that relates diameter and permeability. At the same time, it is expected that smaller openings present greater K, as it is possible to associate mass transfer to velocity as it is described by distance of flow per time (Cussler 2009).

The air velocity might create a small difference of pressure across the perforation, and a viscous flow component that increases with the air velocity (Ghosh and Anantheswaran 2001). The increase in air velocity affects the flow at the film that tends to pass from laminar to turbulent leading to an unstable pattern (Bird, Stewart, and Lightfoot 2007). The influence of the air velocity on the oxygen transport through perforated packaging was observed also by Allan-Wojtas et al. (2008) and Montanez et al. (2010b) in different conditions.

As the diameter of perforation had the greatest effect on the mass transfer (within the ranges of values assessed), the effect of number of perforations and temperature on the mass transfer were studied with air ventilation fixed at 2.7 m/s and films single-perforated were pierced at 5 cm from the edge. The mass transfer coefficients obtained are shown in Table 3.2.

Table 3.2– Mass Transfer Coefficient (K, $m^2 \cdot s^{-1}$, average of 2 repeats) of Perforated Films with different number of holes (X_1) and diameter of perforations (X_2, in μm), air velocity of 2.7 m/s at 5, 10 and 15ºC.

	Holes	Diameter	K_5	K_{10}	K_{15}
1	1	270	$8.62 \cdot 10^{-2}$	$5.06 \cdot 10^{-2}$	$7.26 \cdot 10^{-2}$
2	1	450	$4.02 \cdot 10^{-2}$	$2.57 \cdot 10^{-2}$	$6.02 \cdot 10^{-2}$
3	1	750	$2.07 \cdot 10^{-2}$	$1.65 \cdot 10^{-2}$	$2.59 \cdot 10^{-2}$
4	3	270	$7.78 \cdot 10^{-2}$	$4.83 \cdot 10^{-2}$	$7.65 \cdot 10^{-2}$
5	3	450	$2.94 \cdot 10^{-2}$	$4.18 \cdot 10^{-2}$	$4.12 \cdot 10^{-2}$
6	3	750	$1.96 \cdot 10^{-2}$	$2.05 \cdot 10^{-2}$	$2.99 \cdot 10^{-2}$
7	5	270	$6.06 \cdot 10^{-2}$	$5.31 \cdot 10^{-2}$	$5.88 \cdot 10^{-2}$
8	5	450	$3.17 \cdot 10^{-2}$	$3.14 \cdot 10^{-2}$	$6.56 \cdot 10^{-2}$
9	5	750	$2.13 \cdot 10^{-2}$	$1.81 \cdot 10^{-2}$	$1.71 \cdot 10^{-2}$

K_5, K_{10}, and K_{15} are values of mass transfer coefficient at 5, 10 and 15ºC, respectively.

The Analysis of Variance results showed that the diameter of perforation was again the parameter with the most significant effect on the mass transfer coefficient. The quadratic term of temperature also presented a negative effect on K.

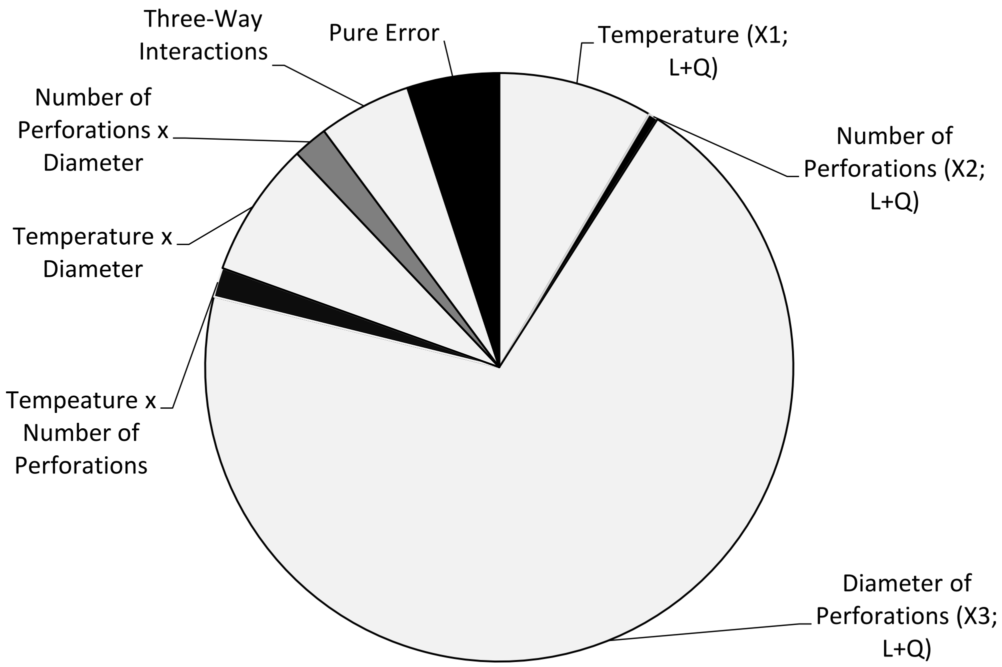

Figure 3.3– Result of the Analysis of Variance of the mass transfer coefficient for diameter, temperature and number of perforations, with 2.7 m/s air velocity, showing the portions of the raw sums of squares explained by each effect (total number of points = 54, total SS = 2.4483), where light grey denotes statistically significant effects ($p < 0.05$), dark grey marginally significant effects ($0.1 > p > 0.05$) and black non-significant effects ($p > 0.1$)

The interactions between temperature and diameter of perforation (Temperature x Diameter and Temperature x Diameter), the linear effect of temperature and the interaction between temperature and number of perforations (Temperature x Number of perforations^2) all had significant, and positive, effect on K. The interaction between number and diameter of perforations (Number of perforations x Diameter of Perforations) also presented a significant, but negative, effect.

Storage temperature influences some air properties such as density, viscosity and diffusion, which affects the air flow and the transport through the perforations.

Diameter of perforation was the most influential variable on the mass transfer coefficient, which decreased with an increase in the diameter, same tendency observed by Montanez et al. (2010b) and generally found in the meta-study shown in Chapter 2. As the perforation diameter narrows turbulence increases due to the higher resistance to the flow and higher velocities, thus an increase in the mass transfer coefficient (Javaherdeh, Mirzaei Nejad, and Moslemi 2015).

González et al. (2008), however, associated oxygen transmission rate with area of perforation, but considered that diameter of perforation did not affect the oxygen permeability. They affirmed that with diameters in a range between 96 and 118 μm the oxygen transmission rate increased only by 30% according to the mathematical model that they proposed relating area of perforation and oxygen transmission rate, while Ghosh and Anantheswaran (2001) observed an increase of almost 300% on the oxygen flux.

In order to study the role of area, Table 3.3 shows the comparison between total area and diameter of perforations. These results help to determine whether the total area of perforation or diameter of perforation affects k. Perforated films with different number and diameter of perforations, but similar areas of perforation (0.0016, 0.003 and 0.008 cm^2), and with different areas but similar diameter of perforation (260, 270, 450, 600 and 700 μm) were analysed.

The results indicated that the diameter is the most important parameter; films with same or similar diameter of perforation presented the same K, despite the fact they had different numbers of perforations (and therefore different total area of perforation).

Table 3.3- Mass Transfer Coefficient (K, in $\cdot m^{-2} \cdot s^{-1}$, average of 3 replicates) of Perforated Films with different number of perforations, diameter (in μm) and area of perforation (in cm^2), with air velocity of 2.7 m/s

Row	Perforations	Diameter	Area	K
1	1	270	0.00057	$5.70 \cdot 10^{-2}$ a
2	3	260	0.00159	$5.11 \cdot 10^{-2}$ a,b
3	1	450	0.00159	$4.08 \cdot 10^{-2}$ a,b,c
4	3	270	0.00172	$5.79 \cdot 10^{-2}$ a
5	1	600	0.00283	$2.99 \cdot 10^{-2}$ c
6	5	270	0.00286	$5.19 \cdot 10^{-2}$ a,b
7	1	750	0.00442	$1.99 \cdot 10^{-2}$ c
8	3	450	0.00477	$4.04 \cdot 10^{-2}$ a,b,c
9	2	700	0.0077	$2.15 \cdot 10^{-2}$ c
10	5	450	0.00795	$3.12 \cdot 10^{-2}$ b,c

K values followed by different letters are significantly different ($p < 0.05$).

Experiments 2 and 3, 7 and 8, and 9 and 10 had same or similar total area of perforation and their results were statistically equal ($p > 0.05$), but experiments 5 and 6 had the same area and yet different results. At the same time, experiments with similar diameter of perforation had K statistically equal, independent of the number of perforations, i.e. despite of the fact that they had different areas. Experiments 2 and 3 had the same area of perforation and were statistically equal, but they were also equal to experiments 6 and 1, which have areas of perforation 75% bigger and 65% smaller, respectively. They were also statistically equal to experiments 3 and 8, with 450 μm of diameter, same observed on experiments 10, 9, 7 and 5, suggesting that the total perforated area did not influence the mass transfer coefficient of the perforated films.

Techavises and Hikida (2008) observed that the total permeability of their films did not vary linearly with the total area of perforations, but did not investigate the causes, and just associated it to the fact that the effective thickness might be greater than the real value, as other authors have also suggested.

Films with 260, 270, and 450 μm of hole diameter had the same mass transfer coefficient, as well as films perforated with 450, 600, 700 and 750 μm. It is possible that the perforations did not present a diameter exactly equal to the diameter of the needle. As pinpointed by Allan-Wojtas et al. (2008), perforations made by cold needles can be partially covered by the remained material, affecting the effective perforation size.

Measurements using image software showed that perforations presented a real diameter of 746 ± 87 μm, which means that diameter variated from 659 to 833 μm. Perforations with a needle of 450 μm diameter resulted in holes of 418 ± 78 μm (340 to 496 μm). Greatest variations were observed on perforations made by needles of 270 μm diameter, whose average effective diameter was 350 ± 124.

González et al. (2008) calculated the exact area of each perforation obtained and suggested the use of small perforations assuming that the effect of imprecise perforations of small holes on the mass transfer would be lower. However, the results of this present work lead to the opposite conclusion, because the smallest perforation presented greatest variation on diameter.

These results can justify the similar results observed for 270 and 450 μm and then amongst 600, 700 and 750 μm.

Meidner and Mansfield (1968) proposed that the explanation for the mass transfer coefficient depending only on diameter and not on area lies in Stefan's Law, as illustrated in Fig. 3.4. When the pore diameter increases by a factor f, its area increases by f square, but the length of a diffusion path increases by f; rephrasing: "the rate of diffusion is proportional to the diameter of the surface, and not its area".

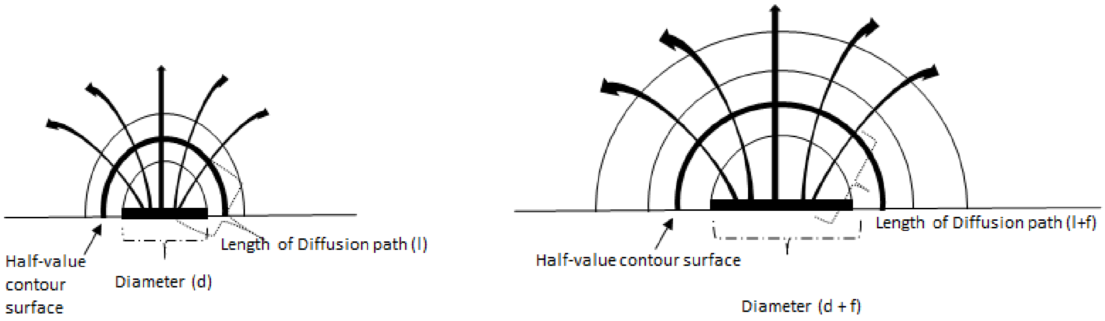
Half-value contour surface
Diameter (d)
Length of Diffusion path (l)
Half-value contour surface
Length of Diffusion path (l+f)
Diameter (d + f)

Figure 3.4 - Representation of flow path through a pore. Adapted from Meidner and Mansfield (1968).

3.3.2. Influence of the distance between perforations

The distance between perforations could affect the mass transfer coefficient due to synergistic effects when perforations are close, The greater the distance between pores, the smaller the effect of the flux path through one pore into the other (Meidner and Mansfield 1968). In order to assess the relevance of this issue, films with two perforations with different distances between them were analysed.

Table 3.4– Mass Transfer Coefficient (K) of Perforated Films with different distances between two perforations (average of 3 replicates)

Distance	$K \cdot 10^2$ (m/s)
0.1	1.56 ± 0.38 [a]
0.2	1.43 ± 0.21 [a]
0.3	1.49 ± 0.17 [a]
0.5	1.86 ± 0.42 [a]
1.0	1.59 ± 0.15 [a]
1.5	1.95 ± 0.17 [a]
2.5	2.05 ± 0.37 [a]
5.0	2.07 ± 0.13 [a]

While there seems to be some increase of the mass transfer coefficient with the distance, there were no statistically significant differences between all values (10ºC, air velocity: 2.7 m/s, diameter of perforation: 750 μm), and thus this effect may exist but it does not have a significant impact to merit being considered further in the design of MAP, even with small distances between perforations.

3.3.3. Effect of storage conditions during storage on mass transfer coefficient

3.3.3.1. Effect of the position in stacking on the package permeance

Results showed statistically significant differences between the permeance of packages at the top (iii) and at the bottom (iv) of a two layer stacking in a same box (Table 3.5, positions iii and iv).

Table 3.5- Permeance (Pa) and Mass Transfer Coefficient (K) through microperforated films at different positions of the stacking

Position	$K \cdot 10^2$ (m/s)
i (box above)	1.554 ± 0.2^{a}
ii (box below)	1.364 ± $0.1^{a,b}$
iii (container on top)	1.806 ± 0.3^{a}
iv (container below)	1.038 ± 0.1^{b}

K values followed by different letters are statistically different ($p < 0.05$) according to a Tukey-HSD test.

Perforated packages stacked under other packages were found to have lower mass transfer coefficients due to the more stagnated conditions caused by the proximity between perforation on top of one package and the bottom of the one above. It is noted that the perforation of the container at the bottom was not covered by the one at the top due to the geometry of the containers; however, trays normally used for food packaging could fit better one above the other and the perforations of packages placed underneath others could be even more covered, moreover there is an even greater danger of loss of permeance if handling movements cause the perforations to be covered.

K values of perforated packages stacked in boxes did not show statistically significant differences, indicating that the openings of the boxes were enough to keep the air circulating around the perforations in a relatively homogenous manner.

3.3.3.2. Effect of the position of the perforation on the package permeance

It was found that perforated containers underneath others have a significantly lower K (Table 3.5, positions iv and iii, respectively). Unfortunately, trays are stacked in storage rooms in order to optimize space, and given the low margins of commodity businesses, not stacking or leaving too much space in between is not a financially feasible option.

A simple solution could be to perforate the films on the sides of the container, instead of the top. Table 3.6 shows the mass transfer coefficients of films perforated in different sides of the container. There were no statistically significant differences between the K values of the perforated films in any of the positions, meaning that the packaging could be pierced in any side without altering the mass transfer and in such case, the position of the perforation relative to the direction of the air flow did not influence the result.

Hence, package trays placed into boxes could be perforated on the sides rather than on the top, thus avoiding the stacking effect found earlier, where packages under other packages have a significantly hindered K. It is noted that the trays had slanted sides, which is common in trays, that is, even when a package is placed just next to another, there is a sufficient free space in between the sides.

Table 3.6- Mass Transfer Coefficient through films perforated in different positions

	K x 10^2 (m/s)
Front	2.055 ± 0.09^a
Back	2.068 ± 0.12^a
Right	1.997 ± 0.28^a
Left	1.859 ± 0.03^a
Top	1.894 ± 0.08^a

K values followed by different letters are statistically different ($p < 0.05$) according to a Tukey-HSD test.

3.3.4. Effect of atmosphere composition on mass transfer coefficient

The results for different atmosphere compositions shown in table 3.7 indicate that the movement of the water vapour through the perforation affected the oxygen mass transfer coefficient. This result is important because it shows that it is an effect that should be considered in the design of modified atmosphere packaging.

Fresh produce release water during storage due to respiration, and their RH of storage is always recommended to be high, normally higher than 75% (Tumwesigye et al. 2017). It leads to the conclusion that is it very likely that during storage there will be a relative humidity gradient, and the experimental conditions to determine K through the perforation should be chosen accordingly. The conditions expected in a normal package are water vapour and carbon dioxide moving out and oxygen coming in, so the comparable situation of table 1.7 is row 5, where the lowest mass transfer coefficient was obtained. The two conditions with reversed water vapour direction of flow (1 and 2), with water vapour moving in the same direction as oxygen, gave significantly different (higher) mass transfer coefficients. The 3 cases where there was no movement of water vapour (3, 5 and 6), but nitrogen moved differently also provided different results. When nitrogen (nor water) moved (row 3) the mass transfer coefficient was significantly higher, so the counter movement of water vapour (relative to oxygen) hinders oxygen permeance significantly. When nitrogen also moved in the same direction as oxygen (row 6) the mass transfer coefficient duly increased significantly, although when it moved against oxygen (row 5), the effect was not statistically significant.

Table 3.7- Mass Transfer Coefficient of oxygen through microperforated films flushed with different atmosphere compositions

Row	N_2 (%)	CO_2 (%)	O_2 (%)	RH_{inside} (%)	$K \times 10^2$ (m/s)
1	80	20	0	0	1.84 ± 0.09^{a}
2	80	20	0	52.9	2.50 ± 0.1^{b}
3	80	20	0	Ambient*	1.49 ± 0.07^{c}
4	80	20	0	100	1.10 ± 0.1^{d}
5	100	0	0	Ambient*	$1.27 \pm 0.1^{c,d}$
6	60	40	0	Ambient*	2.27 ± 0.06^{b}

*Ambient Relative Humidity (RH of the cold room during the storage) was 80±3.
K values followed by different letters are statistically different ($p < 0.05$).

3.4. CONCLUSION

This work studied different potentially relevant factors that may affect the permeance of perforated films: diameter, location, position and number of perforations, area of perforation, temperature, and air velocity. It was shown that although the diameter of perforation has the greatest impact on K, air velocity and temperature also have a significant influence on mass transfer and show significant interactive effects, which implies that a model able to predict the permeance due to perforations should not be additive. Analysis comparing films with same total area but different diameter with films with same diameter but different total perforated area confirmed that the diameter is the relevant effect on the mass transfer coefficient (or permeance), not the total area (the total area obviously affects the total flow rate, but not the permeance or mass transfer coefficient). It is also shown that it is important to recommend that packages should be perforated on their sides, not only on the top, to maximise the robustness of the package performance to maintain the optimum atmosphere with a well-designed permeance. It was also observed that the distance between two perforations did not affect the mass transfer, but the gas composition does, and therefore the relative movements of other gases, and namely water vapour, need to be considered.

4. DIMENSIONLESS CORRELATIONS FOR ESTIMATING THE PERMEABILITY OF PERFORATED PACKAGING FILMS TO OXYGEN

ABSTRACT

The permeance of a perforated package is controlled largely by the dimensions of the perforations, although also influenced by the surrounding air velocity and temperature. It is argued that the most robust, yet simple, approach to determine the permeance due to perforations is to avail of dimensionless correlations that relate the mass transfer coefficient with all relevant factors. The Π-Buckingham Method was applied to this situation yielding a generic correlation that obeys the principles of dynamic similarity. Experimental results were obtained in the ranges of temperatures 5 to 15°C, perforation diameters 270 to 750 μm and air velocity 0.76 to 4 m/s. The resulting correlation with least squares regression of the model fit provided a good adjustment of the experimental data (R^2= 92%) and was further validated with an additional set of experiments, with a 0.96 correlation coefficient between the model predictions and the independent experimental data set. This correlation proposes a power relation between the ratio of the mass transfer coefficient and air velocity (ratio of convection to drag forces) as a function of the Schmidt and Peclet numbers. It is shown that correlations with the Sherwood number are not appropriate because this number actually varied very little in this range of conditions, typical of

real packaging conditions. It is further shown that the influence of the perforation diameter is so dominant that within the experimental variability the model can be simplified to an inverse proportionality between the mass transfer coefficient and the perforation diameter. This agrees with two models proposed in literature, although many others provided very poor predictions for this set of experimental data.

4.1. INTRODUCTION

Modified atmosphere packaging (MAP) prolongs shelf-life of fresh and minimally processed produce. It ensures a protective gas composition inside the package as a result of the interplay between product respiration and package permeability. Virtually all packaging films, of which Oriented PolyPropylene (OPP) is a very common choice, are too impermeable to gases for successful MAP of products with medium to high respiration rates. In order to design the perforation profile to ensure MAP targets for extended shelf life (avoiding anoxia conditions), it is necessary to describe appropriately the contribution of perforations to the package permeance.

There are different approaches in literature to describe the phenomena, such as Fick's law (González-Buesa et al. 2009), an adaptation of it considering an "end effect of perforation" (Ghosh and Anantheswaran 2001), and a model that correlates area of perforation with mass transfer coefficient (González et al. 2008). These were reviewed in Chapter 2, where it was shown that the lack of consideration for the application of dynamic similarity principles may justify a variety of models proposed in literature, and that a better generic model able to describe a wide variety of situations and not just one single set of data might be achieved by developing dimensionless correlations that obey these principles, which are commonly used in chemical engineering to describe mass transfer. The Π-Buckingham theorem is widely applied in mechanics, heat and mass transfer problems (Yarin 2012) and has been successfully used in other areas such as management (Miragliotta 2011) and microrobotics (Behkam and Sitti 2004).

Dimensionless correlations are commonly used in engineering to predict the behaviour of complex systems. They are built with dimensionless numbers, which are groups of variables that are combined in such a way that the dimension results in a unity. Sherwood and Stanton numbers involves mass transfer coefficient, Schmidt, Lewis and Prandtl numbers are different comparisons of diffusion, and Reynolds, Grashof and Peclet numbers describe flow (Ruzicka 2008, Cussler 2009). Correlations for the Sherwood number as a function of others can be applied when there is flow over a flat surface (Oliveira and Oliveira 2010, Metz et al. 2005). The Buckingham π- Method can be applied to determine which dimensionless numbers are describe better a specific phenomenon (Curtis, Logan, and Parker 1982, Reddy and Reddy 2014) (See also Chapter 1).

The most common correlations proposed in literature relate the Sherwood number with Schmidt and Reynolds numbers, applicable to convection for flow over a flat surface (Oliveira and Oliveira 2010, Metz et al. 2005), and has the form:

$$Sh = \beta_1 + \beta_2 \cdot Re^{\beta_3} \cdot Sc^{\beta_4} \tag{4.1}$$

where β are the model parameters determined by fitting experimental data and vary with the range of dimensionless numbers and geometric and hydrodynamic specifics of the situation and the dimensionless numbers are given by:

$$Sh = \frac{K\alpha}{D}$$

$$Re = \frac{\rho v\alpha}{\mu}$$

$$Sc = \frac{\mu}{\rho D} \qquad (4.2)$$

where K is the convection mass transfer coefficient, D the gas diffusivity, ρ the density, μ the viscosity and α the characteristic dimension of the geometry of the problem. In the case of perforations, this could be the diameter, while there are situations where it could be a length or a distance, depending on the problem geometry. It has been successfully used in literature to predict the mass transfer coefficient through membranes (Lee, Amy, and Cho 2004, Metz 2003, Park et al. 2009) and also appears in studies involving transpiration and air-film mass transport coefficient (Becker and Fricke 2015, Xanthopoulos, Koronaki, and Boudouvis 2012). However, there are no studies using dimensionless correlations to describe mass transfer through packaging films.

The purpose of this work was to establish a dimensionless correlation to predict the permeance to oxygen provided by perforations in plastic films that obeys the dynamic similarity principles defined by the Π-Bukingham theorem, supported by experimental data. The results would be compared to other literature data and proposed models.

4.2. MATERIALS AND METHODS

4.2.1. Experimental procedure

Hermetic containers with an open top where a $7.85 \cdot 10^{-3}$ m^2 oriented polypropylene (OPP) film could be hermetically crimped were used. The containers were flushed with 20-23% v/v of CO_2 and the balance with N_2 and kept in a walk-in controlled temperature cold room maintained within 1°C of the set temperature.

The O_2 concentration inside the containers was measured using a Fiber Optic Oxygen Transmitter (Presens, Germany). This device uses an optical probe to determine the inner concentrations without disturbing the inner atmosphere, from colorimetric changes in spots glued to the inner surface of the film, across its transparency.

The films were perforated with a needle making one single perforation of the defined diameter (270, 450 or 750 μm diameter), at 2.5, 5 or 7.5 cm from the edge of the container. A fan located next to the packages was set at different speeds and the average air velocity over the package surface measured, giving 3 different conditions: 0.76, 2.7 and 4 m/s Two experimental designs were completed: a full factorial design at 3 levels for diameter, distance from edge and air velocity, all at 10°C, and with repeats of the centre point (30 combinations), and a full factorial design at 3 levels for diameter and temperature (5, 10 and 15°C), all with 2.7 m/s air velocity and 5 cm from the edge plus some repeats (16 combinations), totalling 46 experiments. It is noted that the distance from the edge was previously found to have a negligible effect within this range (see chapter 3) and is not a parameter considered for the correlations, it is introduced in the experimental tests as a noise factor (providing for repeats with experimental variability).

The 46 data points were used to determine the parameters of the correlations predicting the mass transfer coefficient and an extra set of experiments were then performed for model validation. A total of 10 experiments were run with 10 random combinations of 1, 2, 3 or 5 perforations of 270, 450, 560, 600, 700 or 750 μm of diameter, with 0.76 or 2.7 m/s of air velocity and at 5 or 10°C.

4.2.2. Determination of Mass Transfer Coefficient

The apparent permeance of the film (P_a) and the convection mass transfer coefficients (K) were obtained by least squares regression of the model predictions obtained by solving the mass balance with Newton's convection equation, as described in chapter 3:

$$y_t = y_e - (y_e - y_0) \cdot e^{-\frac{\mathrm{P}_a \mathrm{A}}{V} \cdot t} \qquad (4.3)$$

where y are the molar (same as volumetric) fractions of oxygen with the subscripts t for the value at time t, e for the external atmosphere and 0 for the initial container atmosphere at time 0, A ($7.85 \cdot 10^{-3}$ m^2) is the area of the film and V the container volume (1559.7 mL).

The apparent permeance is the result of the flow through the perforations and through the film itself and thus the relation between the mass transfer coefficient through the perforation and the apparent permeance of the film is given by (see chapter 3):

$$K = \mathrm{P}_a \frac{A}{A_p} + \mathrm{P}_{film} \left(\frac{A}{A_p} - 1 \right) \qquad (4.4)$$

The permeance of the unperforated film itself (P_{film}) was determined experimentally, thus incorporating the effective permeance under real conditions of use (relevant due to the influence of temperature and potentially of humidity in the permeance of a polymeric film, as well as eventual imperfections of the seal and consequent leakage flow. This ensures that the values of K calculated were entirely due just to the gas flow across the perforations.

4.2.3. Dimensionless Correlations

Based on the previous work from chapter 3, the parameters that were considered more influential in the mass transfer process through the perforations were mass transfer coefficient (K), density of air (ρ), air velocity (v), Diffusivity through stagnated air (D), diameter of perforation (d_{perf}) and viscosity of air (μ). These are 6 parameters that involve only 3 fundamental dimensions (length, mass and time) and therefore the Π-Buckingham theorem states that 3 dimensionless groups (6-3 = 3) are needed to describe the situation. The three parameters chosen as primary factors to obtain these 3 groups (to appear in all groups, each raised to a specific exponent) were ρ, v and D. Each of the other 3 is then added at a time to generate each of the 3 dimensionless groups, with the exponents of the primary factors being determined as needed to make each group dimensionless (an exponent of 0 eliminates that factor from the group). The three dimensionless numbers (or Π's) thus obtained are:

$$\Pi_1 = \frac{K}{v}$$

$$\Pi_2 = \frac{vd_{perf}}{D}$$

$$\Pi_3 = \frac{\mu}{\rho D} \qquad (4.5)$$

These numbers represent ratios between different forces, in the case of Π_1 it is the ratio between convective and drag forces ($k \cdot v^{-1}$), for which there is no specially named number. Π_2 is the Schmidt number (Sc), which quantifies the ratio between viscous and diffusional forces. Finally, Π_3 is the Peclet number (Pe) defined for the perforation diameter as characteristic dimension, quantifying the ratio between drag and molecular forces, that is, advective transport and diffusive transport. Thus, a dimensionless correlation obeying the dynamic similarity principles will be of the form:

$$\frac{K}{v} = \beta_1 + \beta_2 \cdot Sc^{\beta_3} \cdot Pe^{\beta_4} \tag{4.6}$$

There is no selection of 3 primary factors according to Π-Buckingham principles that would result in a correlation like eq. 4.1. Therefore, such correlation even though it is applicable to many comparable scenarios involving mass transfer, does not actually comply with the principles of dynamic similarity for this specific case. Notwithstanding, due to its familiarity, it was decide to test this model as well. It is noted that the ratio K/v is equal to the product between the Sherwood and Peclet numbers. A correlation of Sherwood number as a function of Peclet and Schmidt numbers is therefore also possible, and is indeed obtained if choosing ρ, d_{perf} and D as the 3 primary factors. Eq. 4.6 was however preferred for reasons that will become clear in the results and discussion.

.The physical properties of air were considered for ρ and μ varying with temperature (Geankoplis 1993). The diffusivity of oxygen through stagnated air, D was calculated as (in SI units for T in Kelvin):

$$D = 1.13 \times 10^{-9} T^{1.724} \tag{4.7}$$

4.3. RESULTS AND DISCUSSION

The dimensionless correlations of equations 4.1 and 4.6 were fitted to the 46 experimental data, giving the results shown in table 4.1.

Table 4.1– Parameters of the dimensionless correlations

	β_1	β_2	β_3	β_4	R^2
Eq. 4.1	79.57	-12.54	-0.00033	-5.98	0.731
Eq. 4.6	-0.00208	0.0252	-11.01	-0.921	0.924

It is important to assess the statistical significance of the model parameters. In the case of eq. 4.6, β_1 has no statistical significance and in fact neither does β_3 because while temperature influences the physical properties, their combination in the Schmidt number gives almost no change between the temperatures of 5 and 15°C (Sc varied between 0.725238 and 0.725661). Therefore, the true meaningful parameter for this fit is $\beta_2 \cdot Sc^{\beta_3}$ multiplying the term with the Pe number and its exponent. This results in the following model, with a R^2 value of 0.923:

$$\frac{K}{v} = 0.856 \cdot Pe^{-0.986} \tag{4.8}$$

It is further noted that the exponent of the Peclet number is not statistically different from 1 (which is within the margin defined by the 95% confidence interval), and therefore a simpler model provides an indistinguishable model fit, with $R^2 = 0.923$:

$$\frac{K}{v} \approx 0.893 \cdot Pe^{-1} \tag{4.9}$$

This simplification while being statistically acceptable within the margin of error, eliminates in fact the influence of the air velocity, as replacing Pe by its definition leads to

$$K \approx \frac{0.893 \cdot D}{d_{perf}} \tag{4.10}$$

This correlation suggests that the influence of air velocity in this range of values is indistinguishable compared to experimental variability and model lack of fit, whereas temperature has a small influence due to its effect on the diffusivity, and the mass transfer coefficient varies proportionally with the reciprocal of the diameter of the perforation. It is also noted that this simple model of equation 4.10 suggests that the Sherwood number is approximately constant and equal to 0.893 for this set of data. It was found in chapter 3 that velocity has a statistically significant effect, although it can be seen that the value obtained in the Analysis of Variance is just slightly above the 95% limit of significance, so the influence is small. When developing a correlation there are two sources of error, the experimental variability and the lack of fit of the model. It is therefore not surprising that the influence of velocity is now within the error.

Figure 4.1 shows the model fit diagnosis plots, where it can be seen that the model predictions of eq. 4.10 are well within the margin of error compared to the predictions with the full eq. 4.6 and parameters of table 4.1. It can also be noted that the correlation for eq. 4.1 is not only poor, but even predicts that the Sherwood number for 15°C would be significantly higher than those at 5 and 10°C, as the former are the data points in fig. 4.1b well above Sh=1 in the y-axis, an effect that the experimental data (x-axis) do not show at all. This common correlation is therefore totally inappropriate in this situation, which can be due to the fact that it does not obey the Π-Buckingham principles, or simply that the Sherwood number in this case varies less than the experimental error. In fact. Equation 4.10 predicts Sh=0.893. A correlation between the Sherwood number and the Peclet and Schmidt numbers was also tried, with equally poor results, and therefore this a sufficient justification.

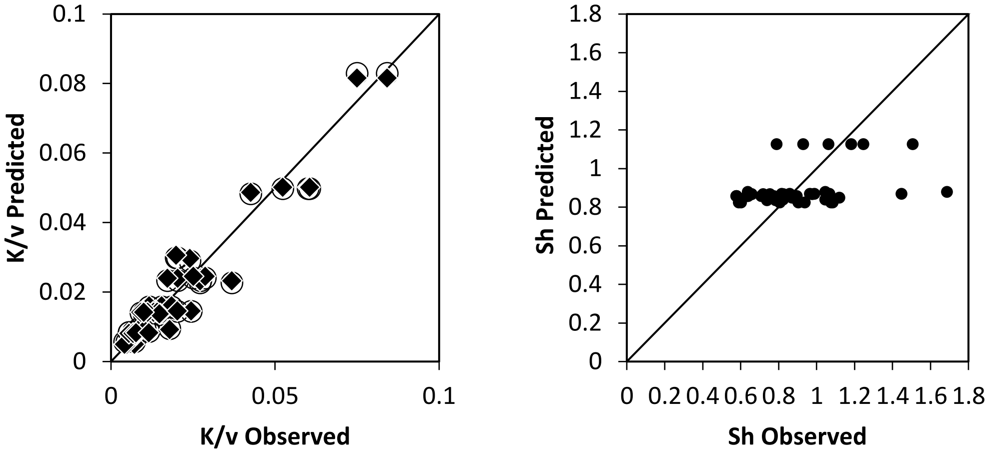

Figure 4.1- Observed versus predicted values of the mass transfer coefficient determined by Buckingham π- Method (a) and Sherwood Correlation (b).

The correlations were validated with the additional set of 10 experimental data points. Fig. 4.2 shows the experimental results obtained for the mass transfer coefficient experimentally, and from the predictions of eq. 4.7 (which includes effects for both temperature and air velocity, in addition to perforation diameter) and 4.9 (which gives no influence to velocity). It is noted that the set of validation experiments includes more diameters than those used, as well as more than one perforation - it is reminded from chapter 3 that it was concluded that the total area of perforations does not affect the mass transfer coefficient. The validation conditions were therefore more challenging than the range of conditions used to produce the model. It can be seen that the model provided by the simple equation 4.9 overestimates slightly the mass transfer coefficient compared to the experimental values, although it does so within the experimental variability of the first set of data (see fig. 4.1a) and with a correlation coefficient predictions vs. observed values of 0.96 for the model of eq. 4.9.

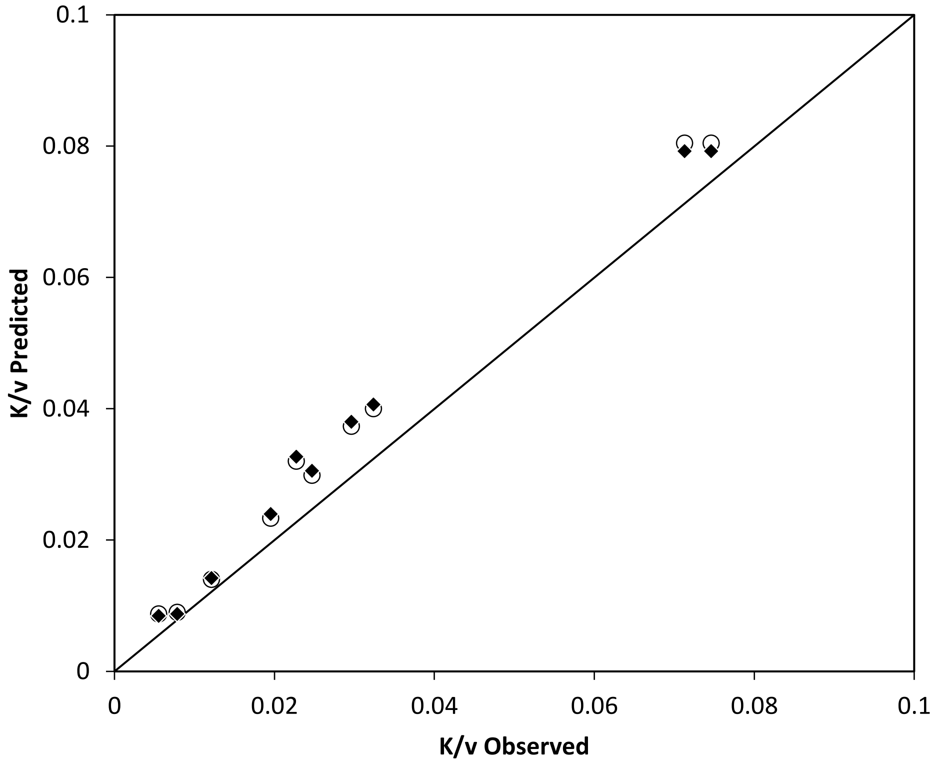

Figure 4.2- Comparison of the predictions of eq. 4.7 (open symbols) and eq. 4.9 (closed symbols) with the experimental values obtained in the validation trial

These results were compared with the predictions that would be made by other models proposed in literature (see chapter 2) for this same set of experiments.

Fick's law of diffusion has been used to describe the transmission rate of perforated packaging (González et al. 2008, González-Buesa et al. 2009, Larsen and Liland 2013). However, the results predicted are generally higher than the effective gas transfer through perforations (Ghosh and Anantheswaran 2001, Lange et al. 2000). The mass transfer coefficient thus estimated (K_F) would just be equal to:

$$K_F = \frac{D}{L} \tag{4.11}$$

with L being the film thickness (length of the diffusional path).

The mass transfer coefficients predicted from eq. 4.11 would be 10 to 40 times bigger than those obtained experimentally. Hence, it is clear that the process cannot be described by diffusion. In fact, Cussler (2009) emphasises that it might be difficult to establish whether a phenomenon should be treated as diffusion or convection but suggests that fluxes across a surface are likely to be the latter. Fonseca et al. (2000) observed that their results were on the same order of magnitude of gas diffusion through air, but the perforations used were actually small tubes, of a much bigger length than diameter. When the L/d ratios are high the resistance to mass transfer is dominated by the diffusion along the tube, hence the mass flux is mainly due to the diffusion.

In order to adapt Fick's diffusional model, the mass flux through perforated films has been related to a rate between the gas diffusion in air across an apparent length, higher than the length of the film perforation, defined as the sum of the effects of the thickness of the perforation and the diameter of the perforation corrected by a characteristic factor of the end effects of the perforations (Ghosh and Anantheswaran 2001, Briassoulis et al. 2013). This implies that the mass transfer coefficient would be equal to:

$$K = \frac{D}{L + \varepsilon d_{perf}} \tag{4.12}$$

where ε is the characteristic factor of the end effect. It is noted that in the case of perforations, as L is much smaller than d_{perf}, this model will be approximately equal to eq. 10, predicting that K is inversely proportional to the perforation diameter.

In their work, Ghosh and Anantheswaran (2001) concluded that this model presented the best fitting for the experimental results, with $\varepsilon = 0.5$, same value adopted by Fishman, Rodov, and BenYehoshua (1996) - predictions with equation 4.12 for this value of ε will be denoted as K_{GA}.

On the other hand, Lee and Renault (1998) used data for nitrogen transport through perforations and obtained $\varepsilon = 1.1$ and Paul and Clarke (2002) obtained $\varepsilon = 7/6$ (app. 1.2) calculating it in terms of geometrical parameters. Predictions made with eq. 4.12 for these two values of ε will be denoted as K_{LR} and K_{PC}, respectively. Briassoulis et al. (2013) used the same model without, however, identifying the ε value considered. Lange et al. (2000) adopted $\varepsilon = 5/6$ or 3/7 under stagnated or moving air, respectively.

González et al. (2008) proposed an empirical relation between transmission rates (TR) and the area of perforation ($TR = 0.880 \cdot {A_p}^{0.577}$). Fick's law was then used for modelling the transmission rate, which leads to the following model for the mass transfer coefficient (K_G):

$$K_G = \left(\frac{4}{\pi}\right)^{1-a_2} \cdot \frac{a_1 \cdot 10^4}{d^{(2-2a_2)} \cdot 864} \tag{4.13}$$

with d_p in μm and K_G in m/s

It is noted that these authors considered perforations with an area of perforation smaller than most experiments presented in table 4.2. Also, the experiments used to develop the model were performed at 23°C, which has little practical interest as the storage temperature of fresh produce should generally be low, within the range used in the present work.

Techavises and Hikida (2008) obtained an empirical equation relating what the authors called effective permeability to the diameter of perforation. The mass transfer coefficient (K_T) would be given by:

$$K_T = \frac{(2.98 \cdot 10^{-2} \cdot d^2 + 5.37 \cdot 10^{-1} \cdot d + 8.22 \cdot 10^{-1}) \cdot 0.101325 \cdot 10^{-3}}{A_p \cdot 3600} \tag{4.14}$$

The constants given are valid for K_G in m /s, the area of perforation A_p in m^2 and the diameter d in mm.

There is a significant limitation in the use of this model, which is that that the authors calculated what they called permeability in units of flux, thus incorporating the area within the results, which means that their data are specific of the area of their perforations. This is the same problem that would occur with Emond et al. (1991) and Fonseca et al. (2000) models. Table 4.2 shows the capacity of these models to predict the experimental data.

Table 4.2– Mass Transfer Coefficient (K) obtained by applying different mathematical models

Equation	ε	E (%)	Validation R^2	Total R^2
Fick's Law	0	2396.99	-1446.64	-855.30
Ghosh and Anantheswaran (2001)	0.5	146.26	-6.51	-2.75
Lee and Renault (1998)	1.1	19.28	0.91	0.70
Paul and Clarke (2002)	7/6	14.08	0.95	0.66
Lange et al. (2000)	5/6	54.68	0.08	0.53
	3/7	189.10	-11.68	-5.62
González et al. (2008)	-	116.38	-3.50	-1.06
Techavises and Hikida (2008)	-	244.15	-21.11	-109.06

It can be seen that the models described by eq. 4.12 with the values of ε proposed by Lee and Renault (1998) and Paul and Clarke (2002) of 1.1 and 7/6, respectively, provided quite good estimates for the 10 cases of the validation set of experiments, while all others overestimated the mass transfer coefficients quite significantly, but were not able to estimate the overall data with the same accuracy.

4.4. CONCLUSION

Applying the principles of dynamic similarity with the Π-Buckingham method provided a good correlation to estimate the mass transfer coefficient through perforations, which is equal to the permeance provided by the perforation. Within the experimental variability, the correlation can be reduced to the ratio between the mass transfer coefficient and the air velocity being inversely proportional to the Peclet number, defined with the perforation diameter. This shows also that the Sherwood number is approximately constant and that dimensionless correlations with it would not be appropriate for this situation. This result explains why various models proposed in literature that can be reduced to the permeance due to a perforation being inversely proportional to the diameter have been widely reported in literature, but also show that not all such correlations use parameters that are acceptable.

5. ANALYSIS OF THE INFLUENCE OF THE OXYGEN CONCENTRATION GRADIENT ON THE PERMEANCE OF PERFORATED PACKAGING FILMS

ABSTRACT

The permeance due to perforations in packaging films has been estimated considering various geometric and process factors (e.g. perforation diameter, temperature, air velocity) that influence the hydrodynamic conditions surrounding the perforations and hence the mass transfer process. The dominant influence of the perforation diameter that has been widely proven shows that the average velocity of the flow through the perforation itself is a very important effect. This is influenced by the concentration gradient between the inside and the outside of the package, but this effect has not been assessed and the concentration gradient is not part of any proposed model of the mass transfer coefficients (or permeance due to perforations). The objective of this work was to determine the mass transfer coefficient as a function of concentration gradients and develop a dimensionless correlation for oxygen permeance applying the Π-Buckingham method to ensure the principles of dynamic similarity and based on experimental data, collected in the range of values of air velocity 0.76 to 4 m/s, temperature 5 to 10°C perforation diameters 270 to 750 μm and oxygen concentration gradients 3 to 20 %. Mass transfer coefficients were obtained from the unsteady state measurements of oxygen

concentration in a container initiated with low oxygen concentration, allowed to equilibrate to outside air. Average mass transfer coefficients from time 0 to time t were obtained and related to the instantaneous value at time t with Leibniz rule. The dimensionless correlation obtained fitted the experimental data well (R^2=0.95). A further set of independent validation experiments was performed, with the model providing predictions with a correlation coefficient of 0.97 with the experimental values. However, results showed that the mass transfer coefficient is in fact approximately constant in the range of concentration gradients 5 to 20%, and therefore the predictive ability achieved by considering a constant mass transfer coefficient equal to the average was not significantly lower (correlation coefficient with the experimental data of the validation trials of 0.96). This implies that for food packaging applications,the relevance of the oxygen concentration gradient in the permeance due to perforations is only important if desired to model the earlier times of atmosphere modification when the gradient is building up to at least 5% (internal oxygen concentration above 15%) .

5.1. INTRODUCTION

The oxygen concentration in a food package is modified from atmospheric due to the continuous metabolic activity of respiration, which oxidises nutrients (mainly glucose) to provide energy as adenosine triphosphate (ATP) (Sousa, Oliveira, and Sousa-Gallagher 2017). A package therefore needs to be sufficiently permeable to oxygen to allow it to enter the package and replace the consumption, otherwise dangerous anoxia would eventually set in. Products with medium to high respiration rates typically require packaging films to be perforated as the package would be too impermeable otherwise. If the perforation profile is appropriate, it may restrict the influx of oxygen to a point of equilibrium between oxygen permeance and consumption by respiration, with low oxygen and high carbon dioxide and relative humidity, which will extend the product shelf-life by retarding respiration rates - the modified atmosphere packaging (MAP) concept (Mistriotis et al., 2016; Oliveira et al., 2012).

Normal atmosphere contains approximately 78% of Nitrogen, 20.9% Oxygen, and small percentages of other gases, including water vapour. Due to respiration, CO_2 is produced inside the package and flows out through the perforation in the opposite direction of oxygen. Experimental analyses performed to study the permeability of perforated packages often try to mimic these conditions as much as possible, as this counter flow will certainly influence the rate of oxygen intake.

In experimental tests of film permeance, carbon dioxide is normally used to replace oxygen and an atmosphere of 20% CO_2 and 80% N_2 is generated inside the package (Mastromatteo et al. 2012, Montanez et al. 2010b), which is then allowed to equilibrate to normal atmosphere (about 0.1% of CO_2). The permeance of the film is then calculated by this rate, which is an exponential evolution as given by the mass balance. Other scenarios have been used to create different concentration gradients between inside and outside of a test cell, such as 100% N_2 (Ghosh and Anantheswaran 2001), 10% O_2 – 10% CO_2 (Moyls et al. 1998, Allan-Wojtas et al. 2008) and 5% O_2 and 15% CO_2 (Montanez et al. 2010a), balance with N_2.

Notwithstanding, in all cases the internal O_2 concentration is constantly changing during the experiment, until equilibrium. The concentration gradient is linearly related to the average velocity of the gas fluxes into/out of the container through the perforation, which will affect the hydrodynamic conditions on the 2 sides of the package, especially the outside where there can be convective flow of air interacting with it (for instance, from cold room fans). Previous work (see chapters 2, 3 and 4) has shown that the most dominant effect in the permeance due to a perforation is its diameter, with much higher mass transfer coefficients as the diameter reduces size. The effect of the diameter in the gas fluxes is to increase the average velocity of the cross-perforation flow, thus showing that the greater this velocity the higher the permeance. Therefore, the permeance should also be influenced by the concentration gradient, and be higher the greater the gradient. However, there have been no quantitative studies or analysis that would allow assess whether this is the case, and if so, to what extent.

Ghosh and Anantheswaran (2001) observed an increase of the oxygen transmission rate due to an increase of the flow rate and associated it with an increase in the concentration gradient. However, mathematical models proposed to date have been considered independent of the gas concentration gradient in the various different approaches that have been used to quantify this phenomenon (Emond 1992, Lange et al. 2000, González-Buesa et al. 2009), chapter 2, 3 and 4.

The objective of this study was to evaluate the effect of the concentration gradient of oxygen on its mass transfer coefficient (permeance) due to perforations, and develop a mathematical model to incorporate it using dimensionless correlations obeying the principles of dynamic similarity using the Π-Buckingham method..

5.2. MATERIALS AND METHODS

5.2.1. Experimental Procedure

Hermetic containers with an open top where a $7.85\cdot10^{-3}$ m^2 oriented polypropylene (OPP) film could be hermetically crimped were used. The containers were flushed with 20-23% v/v of CO_2 and the balance with N_2

and kept in a walk-in controlled temperature cold room maintained within 1°C of the set temperature (5, 10 and 15° C were used).

The O_2 concentration inside the containers was measured using a Fiber Optic Oxygen Transmitter (Presens, Germany). This device uses an optical probe to determine the inner concentrations without disturbing the inner atmosphere, from colorimetric changes in spots glued to the inner surface of the film, across its transparency.

The films were perforated with a needle making one single perforation of the defined diameter (270, 450 or 750 μm diameter). A fan located next to the packages was set at different speeds and the average air velocity over the package surface measured, using 3 different conditions: 0.76, 2.7 and 4 m/s. A total of 47 experiments with all combinations of the 3 values of temperature, air velocity and perforation diameter, including replicates, were performed.

In order to validate the model, an additional set of 10 different experiments were performed, with 10 random combinations of 1, 2, 3 or 5 perforations of 270, 450, 560, 600, 700 or 750 μm of diameter, with 0.76 or 2.7 m/s of air velocity and at 5 or 10ºC.

These two sets of experimental data, one for model development and another for model validation, are the same as in chapter 4.

5.2.2. Determination of average and variable permeances

The apparent permeance of the perforated film is obtained from a mass balance to the container:

$$V\frac{dC}{dt} = n \tag{5.1}$$

where C is the oxygen concentration (moles/m^3), n is the molar flow rate of oxygen through the package (moles/s) and V the volume of the container (m^3). The flow is proportional to the concentration gradient and area of the film (A), with the apparent permeance (Pa) of the perforated film being the proportionality constant:

$$n = \mathrm{P}_a\ \mathrm{A}\ (C_e - C_t) \tag{5.2}$$

with the C subscripts e and t denoting external and at time t, respectively. C can be obtained by the ideal gas law, being equal to yp/RT where y is the molar (same as volumetric) fraction of oxygen, p the pressure, R the ideal gas constant and T the absolute temperature. If the permeance is constant, replacing eq. 5.2 in 5.1 and integrating gives:

$$y_t = y_e - (y_e - y_0) \cdot e^{-\frac{\mathrm{P}_a\,\mathrm{A}}{V} \cdot t} \tag{5.3}$$

where the subscripts t, e and O denote at time t, on the external side and at time 0, respectively.

If the permeance is not constant, then the P_a value in equation 5.3 is the average permeance from time 0 to time t, which will be denoted by $\overline{\mathrm{P}_a}$, that is:

$$\overline{\mathrm{P}_a} = \frac{\int_0^t \mathrm{P}_{a,(\mathrm{t})}\mathrm{dt}}{t} \tag{5.4}$$

where $P_{a,(t)}$ is the function providing the change of permeance with time. With a small manipulation of eq. 5.4, taking then the derivative and using Leibniz rule, gives:

$$\mathrm{P}_{a,(\mathrm{t})}\mathrm{dt} = \frac{d(t\overline{\mathrm{P}_a})}{dt} \tag{5.5}$$

Leibniz's rule is frequently applied in the study of variable mass or heat diffusivity (Ahmed 1999, Voller 2001, Nottale 2005). Equation 5.5 states that the value of the permeance at instant t can be found by plotting the product between time and the average permeance from time 0 to that instant t, for several instants of time, and then taking the slope of the resulting line at that instant, as this is the graphical meaning of a derivative. If the only cause of variation of the permeance with time is the concentration gradient (as all other factors in an experiment are rigorously constant), then $P_a(t)$ is the value of the permeance for the concentration gradient that occurred at that time t. This converts from the $P_{a,(t)}$ function to the $P_{a,(yt-ye)}$ function.

The apparent permeance is the result of the flow through the perforations and through the film itself and thus the relation between the mass transfer coefficient through the perforation and the apparent permeance of the film is given by (see chapter 3):

$$K = \mathrm{P}_a \frac{A}{A_p} + \mathrm{P}_{film} \left(\frac{A}{A_p} - 1 \right) \tag{5.6}$$

The permeance of the unperforated film itself (P_{film}) was determined experimentally, thus incorporating the effective permeance under real conditions of use (relevant due to the influence of temperature and potentially of humidity in the permeance of a polymeric film, as well as eventual imperfections of the seal. This ensures that the values of K calculated were entirely due just to the gas flow across the perforations. This permeance of the polymeric film (plus any eventual leakage effects if the seal is not perfect) was not considered to vary with time (or concentration gradient) because the flux through the entire surface of the film is very mild compared to what occurs in a perforation, and is in fact dominated by diffusion through the polymeric film itself, so convection currents at the surfaces have a negligible effect in this permeance.

Data from an experiment where the concentration of oxygen varies from 0 to atmospheric over time were therefore handled as follows: for each instant of time for which there was an experimental data point, the average permeance from time 0 to time t was calculated with eq. 5.3. These average permeances multiplied by the respective time were then plotted against time. These data points were fitted to a polynomial function to determine the derivatives of the curves for each experimental sampling time, which gives the value of the permeance at that time. These values were then plotted against the respective gradients to reveal the $P_{a,(yt-ye)}$ function. Equation 5.4 was then used to determine the respective mass transfer coefficients for each of the experimentally measured gradients ($K_{(ye-yt)}$).

To obtain predictions of the evolution of oxygen concentration with time, the mass balance can be solved numerically:

$$V\frac{dy_t}{dt} = \left[K_{(y_e-y_t)}\frac{A_p}{A} + \mathrm{P}_{film}\left(1-\frac{A_p}{A}\right)\right] \mathrm{A}\,(y_e - y_t) \qquad (5.7)$$

5.2.3. Dimensionless Correlations

Dimensionless numbers relevant to a specific phenomenon can be obtained by the Π-Buckingham theorem (Geankoplis 2003), following the principles of dynamic similarity. This is important to be able to compare different situations and even scale up, as this principle ensures that, provided that the dimensionless numbers are the same, their relationship is the same regardless of the individual values of the various parameters (Grimvall 1999, Geankoplis 1993, Delaplace et al. 2015b). For packages all of the same thickness, the physical parameters that may influence the permeability according to the results of chapters 3 and 4 are:

$$K = f\,(\rho, v, D, \Delta\chi, d_{perf}, \mu) \tag{5.8}$$

where K is the mass transfer coefficient that quantifies the permeance to a gas provided by one perforation of diameter d_{perf} for a concentration gradient across the perforation $\Delta\chi$, with viscosity μ and density ρ of air flowing over the surface at a velocity v and with D being the gas diffusivity through normal stagnated air. The total number of parameters is 7, adding the gas concentration gradient to those considered in chapter 4. The concentration gradient is expressed with mass concentrations, otherwise it would be the only parameter with molar dimensions, thus the fundamental dimensions are kept at 3, which implies from Π-Buckingham theorem that the dimensionless correlation will involve 4 dimensionless numbers (or Π's).

If the volumetric concentration inside is C_{in} and outside is C_{out} of a gas of molecular weight M_w, and with the molar gradient being equal to the volumetric gradient:

$$\Delta\chi = |C_{in} - C_{out}| \cdot M_w \tag{5.9}$$

$\Delta\chi$ therefore has units of mass per volume. Choosing for primary factors the same 3 as in chapter 4 (ρ, v and D) and using the Π-Buckingham method (see chapter 1) gives the following dimensionless groups (the first 3 being obviously the same 3 as in the previous chapter):

$$\Pi_1 = \frac{K}{v}$$

$$\Pi_2 = \frac{v d_{perf}}{D} = Pe$$

$$\Pi_3 = \frac{\mu}{\rho D} = Sc$$

$$\Pi_4 = \frac{\Delta\chi}{\rho} \tag{5.10}$$

A dimensionless correlation including the effect of the concentration gradient obeying the dynamic similarity principles will thus be given by:

$$\frac{K}{v} = \beta_1 + \beta_2 \cdot \ Sc^{\beta_3} \cdot Pe^{\beta_4} \cdot \left(\frac{\Delta\chi}{\rho}\right)^{\beta_5} \tag{5.11}$$

There is no specific name for the ratio between the concentration gradient and the density of air (Δχ/ρ). These quantities are not involved in existing dimensionless numbers exactly, but they are similar to the buoyancy term in natural convection, except that instead of a gradient of densities due to differences in temperature between a surface and the bulk of the fluid, in this case there is a concentration gradient across a package.

The Archimedes number quantifies the ratio between buoyancy and viscous forces and is obtained by multiplying the Galileo number by a buoyant correction $\Delta\rho \cdot \rho$ (Ruzicka 2008). As $\Delta\rho$ is equal to $M_w \cdot \Delta C$, $\frac{M_w}{\rho}\Delta C$ is precisely the buoyancy correction term, and therefore, it can be said that $\Delta\chi/\rho$ quantifies the enhanced buoyancy due to the flux caused by the concentration gradient across the package, over the perforation

5.3. RESULTS AND DISCUSSION

The 46 model development experiments provided $t \times \overline{\mathrm{P}_a}$ vs. t plots that were all approximately straight lines up to 15% oxygen concentration at least (that is, concentration gradients of 5% or less), which means that the permeance is in fact constant until the concentration gradient becomes quite small. All data points in these graphs could be approximated by a 2nd order polynomial with R^2 values over 0.999 and therefore these polynomials were used to fit the $t \times \overline{\mathrm{P}_a}$ vs. t, with the derivatives giving $P_{a,(t)}$ (eq. 5.5).

Figure 5.1 shows examples for the 3 diameter sizes, the 2 replicate experiments with the lowest air velocity (0.76 m/s) and 10°C. It can be seen that while there are some slight differences between a constant permeance (straight line) and a 2nd order polynomial, these are far less than the difference between repeats. The same was verified in all other cases.

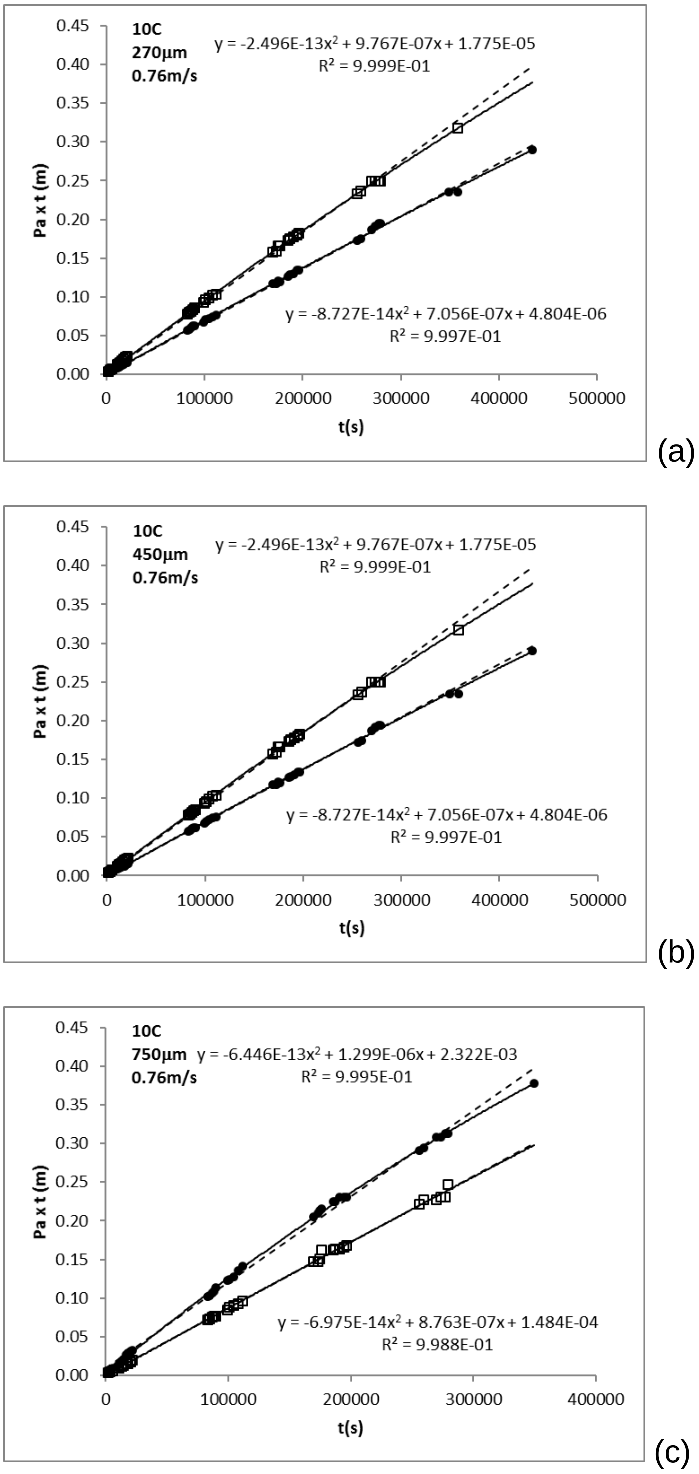

Figure 5.1 - Plots to obtain instant values of the permeance for the 2 replicates at 10°C with 0.76 m/s air velocity for perforations of (a) 270 µm, (b) 450 µm and (c) 750 µm. Polynomial fits (equations and R^2 indicated next to the lines) are shown in full lines, with the dotted lines showing the best straight line (the slope of which is the average permeance)

The values of permeance for each experimental data point were converted to the respective mass transfer coefficients with eq. 5.6, and eq. 5.11 was then fitted to the experimental data with least squares regression. The parameters obtained are shown in table 5.1.

Table 5.1 – Model fitting results with least squares regression

	β_1	β_2	β_3	β_4	β_5	R^2
Eq. 5.11	-0.00265	4.37×10^5	42.47	-0.916	0.123	0.952

Similarly to chapter 4, parameter β_1 does not have statistical significance, nor does β_2 and β_3 independently because of the very small variation of the Sc number in the range of values of interest to food packaging. Simplifying the model gave the following result, with R^2=0.951

$$\frac{K}{v} = 1.1003 \cdot Pe^{-0.994} \left(\frac{\Delta\chi}{\rho}\right)^{0.130} \tag{5.12}$$

It is further noted that the exponent of the Peclet number is not statistically different from 1 and therefore a simpler model provides an indistinguishable model fit, with R^2=0.951:

$$\frac{K}{v} \approx \frac{1.120}{Pe} \cdot \left(\frac{\Delta\chi}{\rho}\right)^{0.129} \tag{5.13}$$

The goodness of fit is shown in fig. 5.2, the predicted data points from eq. 5.11 with the parameters of table 5.1 are almost indistinguishable from those of eq. 5.13. It is noted that many data points fall on top of others, the total number of data points in fig. 5.2 is 952. Similarly to chapter 4, this simplified model actually predicts no influence of the air velocity, with the mass transfer coefficient being inversely proportional to the perforation diameter:

$$K \approx \frac{1.120 \times D}{d} \cdot \left(\frac{\Delta\chi}{\rho}\right)^{0.129} \tag{5.14}$$

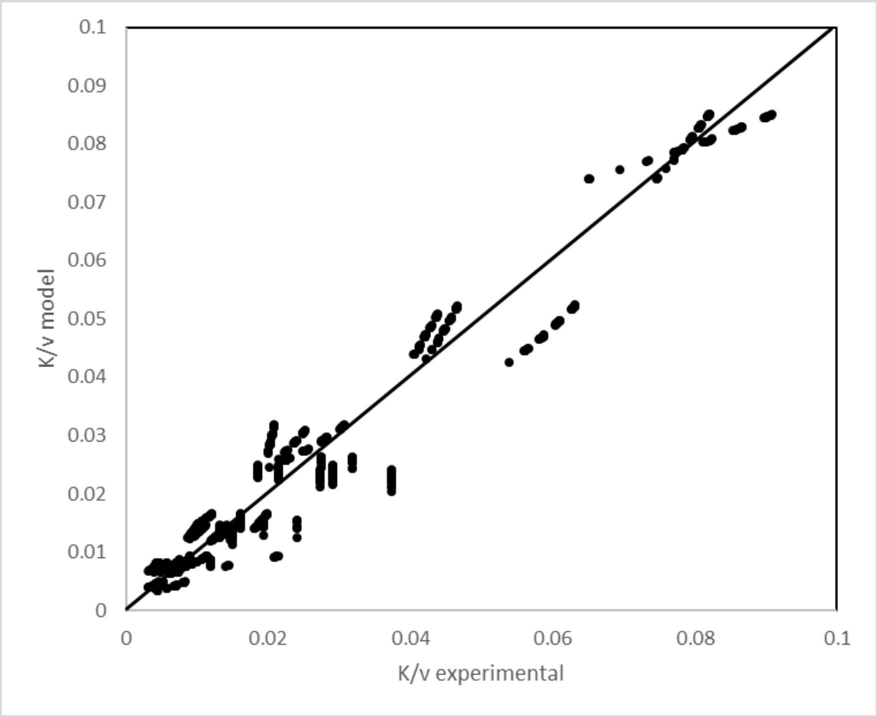

Figure 5.2 - Diagnosis plot of the dimensionless correlation of eq. 5.11 with the parameters of table 5.1.

The main cause of spread in fig. 5.2 is the difference between repeats. The influence of the concentration gradient is small, as noted in fig.

5.1. Fig. 5.3 shows an example, with the corresponding variations of the mass transfer coefficient with the concentration gradient for the experimental data points of fig. 5.1, together with the values predicted by eq. 5.11 and the average mass transfer coefficient in each case. The increase of permeance with the gradient was also observed by Javaherdeh, Mirzaei Nejad, and Moslemi (2015) studying mass transfer through porous medium. Notwithstanding, in the present case the difference between the 2 replicates is very clear in fig. 5.3, and the influence of diameter is sufficiently dominant for the sets with each perforation to be also clearly separated. It is evident that differences between considering the concentration gradient effect or neglecting it (dotted lines and full lines) are less than differences between replicates. Similar results were found in all other cases.

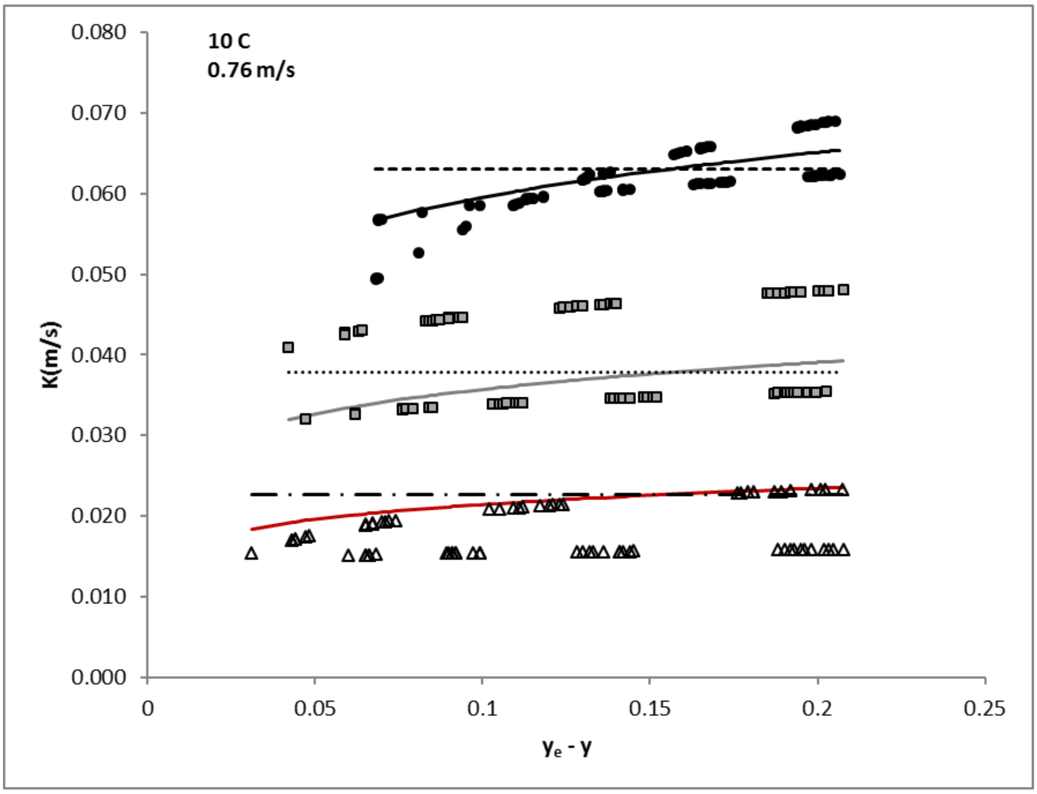

Figure 5.3 - Influence of the concentration gradient on the mass transfer coefficient in two replicate experiments at 10ºC and 0.76 m/s air velocity for perforations of 270 μm (filled spheres), 450 μm (shaded squares) and 750 μm (open triangles). The horizontal dotted lines indicate the average mass transfer coefficient and the full lines the model predictions of eq. 5.11.

The predictive ability of the model was studied independently with the set of 10 validation experiments, validating the very good ability of the model to predict various situations. The correlation coefficient between eq. 5.13 predictions and the experimental data was 0.968. Fig. 5.3a shows the diagnosis plot. It is noted that considering a constant mass transfer coefficient throughout does not have statistically significant differences (fig. 5.3b), where the model predictions have a slightly lower correlation coefficient of 0.961.

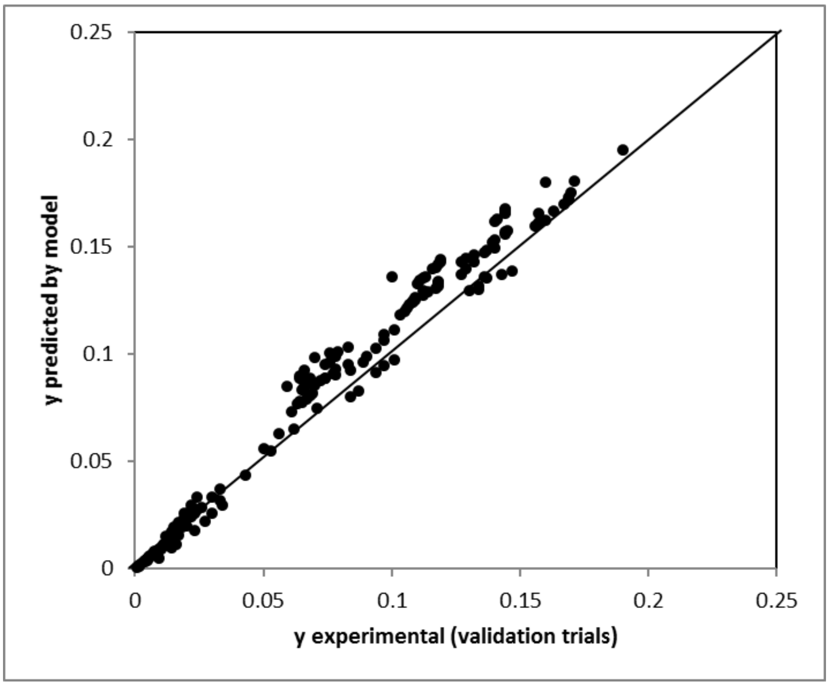

(a)

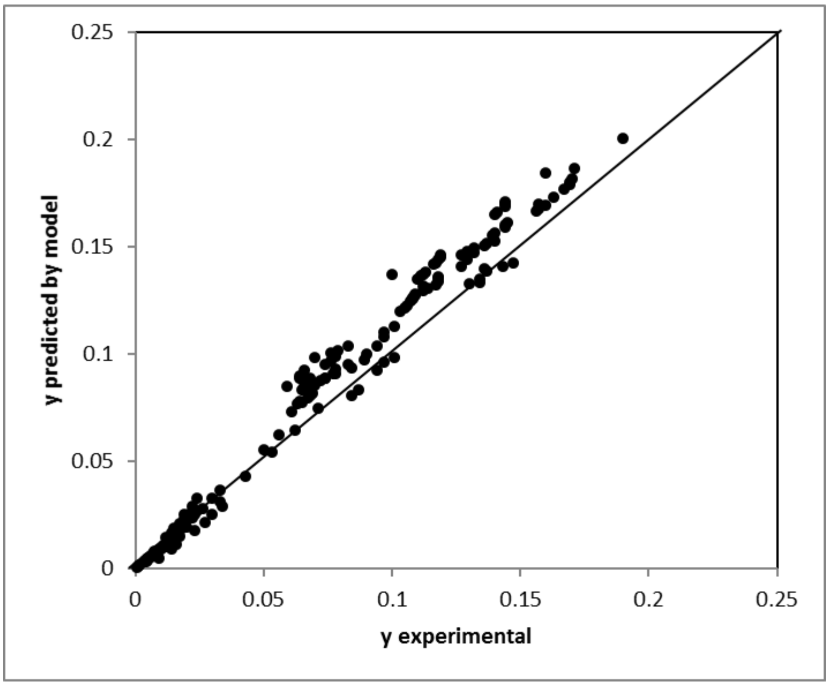

(b)

Fig. 5.3 - Comparison of the experimental values obtained in the validation trial with (a) eq. 5.13 predictions and (b) eq. 4.8 of chapter 4 (no influence of the concentration gradient).

The accuracy in predicting the independent set of experiments is particularly good given that the original set of data has a fair variability between repeats. This is most likely due to the natural variability of obtaining perforations of an exact dimension using a needle, because diameter has such a strong influence on the mass transfer coefficient. It was shown in chapter 3 that needles with a diameter of 270 μm presented an average effective diameter of 350 ± 124, needles with 450 μm diameter resulted in holes of 418 ± 78 μm and 750 μm in perforations of 746 ± 87 μm. This variability is however a problem that will occur in practical applications anyway.

5.4. CONCLUSION

The oxygen concentration gradient has a small influence on the permeance due to perforations. For gradients of 5% or less the permeance is slightly lower, but increases rapidly as the gradient builds up, being approximately constant for gradients above 5% (internal oxygen concentrations of 15% or less). For practical applications in food packaging, this means that calculations of modified atmospheres at equilibrium do not require to consider the effect of the concentration gradient, as all cases of interest will have much higher gradients (typical oxygen concentrations being 3 to 10% at most). However, if it is desired to model the evolution of the internal atmosphere of the package from the beginning, the earlier times will be better predicted with a model that considers the effect of the concentration gradient, as the dimensionless correlation proposed here.

6. DETERMINATION OF THE MASS TRANSFER OF WATER VAPOUR THROUGH MICROPERFORATED PACKAGING FILMS

ABSTRACT

Modified atmosphere packaging (MAP) is a technology that allows to extend shelf-life of perishable produce by controlling the gas atmosphere inside the packaging. Products with medium to high respiration rates typically require perforations to avoid anoxia and reach a protective atmosphere. One of the critical components of a protective atmosphere is humidity, which should not be too high to avoid condensation and mould growth, nor too low to avoid drying and weight loss. Therefore, quantifying the water vapour transfer through perforations is critical to be able to design optimum packaging systems. The objective of this work was to analyse the mathematical models proposed in literature to describe the mass transfer of water vapour through perforations and propose models that benefit from the principle of dynamic similarity by developing dimensionless correlations using the Π-Buckingham method. The results obtained showed that none of the mathematical models previously proposed was able to provide good predictions. A dimensionless correlation relating the mass transfer coefficient of the water vapour to Schmidt and Peclet numbers provided a good fit to the data and was also able to then predict correctly the results of an additional set of validation experiments. It was found that despite the fact

that the proposed correlation provided good predictions when the conditions of relative humidity inside the package was different from 0%, by adding a term for the concentration gradient it was possible to obtain a more robust dimensionless correlation.

6.1. INTRODUCTION

Modified atmosphere packaging (MAP) ensures a protective gas composition inside the package as a joint result of the respiration of the product itself and the permeability of the package (Spencer 2005). Fruits and vegetables are perishable products that maintain their metabolic activities, such as respiration, after harvesting and consequently during storage. As a result, air circulation around the products is crucial to remove the respiration heat and maintain the integrity and quality of the produce during storage (Rao 2015).

Perforated films have been suggested for Modified Atmosphere Packaging (MAP) to reach appropriate permeances for highly respiring products that would otherwise reach anoxia conditions; however, the effect of hydrodynamic conditions has not received due attention, in spite of being a critical control factor of the effective permeability of such packages. The permeance of a perforated package is quantified by the convection mass transfer coefficient of the perforation(s), and this will be influenced by the surrounding air flows.

Most literature data concerning microperforations for MAP consider the fluxes of oxygen, and some of carbon dioxide as well, but permeance to water vapour is equally critical: too high and the produce dries and loses weight, thus quality, and too low and there is condensation inside the package, which stimulates mould growth, again loss of quality (Ben-

Yehoshua, Rodov, and Perzelan 2009, Fishman, Rodov, and BenYehoshua 1996, Mastromatteo et al. 2012). Yet, few studies have explored the water transport through perforations, and none of them considered the impact of air movement surrounding the perforations, or the influence of the humidity gradient itself. The influence of external hydrodynamic conditions on the permeance to oxygen has been discussed by some authors (Montanez et al. 2010b, Rao 2015), chapters 2, 3 and 4.

The purpose of this work was to analyse the mathematical models proposed in literature for water vapour transport through perforated films, and as these have significant inaccuracies, propose a dimensionless correlation able to explain various situations appropriately. In order to design the perforation profile to ensure MAP targets for extended shelf life, it is necessary to describe appropriately the mass transfer through a perforated package. The simplest, yet effective, best practice in mass transfer analysis is to determine the convection mass transfer coefficient, which due to the principle of dynamic similarity might be best described with dimensionless correlations.

6.2. EXPERIMENTAL SET UP

Oriented Poly-Propylene (OPP) was supplied by Huhtamaki (Forchheim, Germany). Permeation cells specially designed for the analysis were filled with $CaCl_2$ to create an internal atmosphere of 0% relative humidity. Films were fitted to the cells with a 5 cm diameter exposed area to the outside atmosphere. The cells were kept in a walk-in cold room and the films were single-perforated with a surgical needle, of one of 3 different sizes (0.270, 0.450 or 0.750 mm diameter), at 5 or 10°C. A fan was used to provide an air flow over the cells at set velocities between 0.75 and 4.5 m/s.

Two sets of experiments were performed, one set for model developed (used to obtain model parameters for new models or to adjust empirical models used in literature) and another independent set for model validation, with random combinations of different conditions (some different from those of the other set, but within the same range). For the model development set, experiments were replicated at least once for all combinations of the different values of perforation diameter, temperature and air velocity, in a total of 94 experiments. Relative humidity (RH) inside the cold room was 80% at 5°C and 85% at 10°C. For the validation set, additional experiments were performed using 10 random combinations of perforations of 360, 430, 580 or 730 μm diameter, temperature of either 5 or 10°C, and air velocity between 0.8 to 3 m/s, in a total of 13 runs. For this second set the relative humidity (RH) inside the cold room was 95.5% at 5°C and 95.8% at 10°C.

An extra set of experiments was also performed to study the mass transfer coefficient of perforations exposed to smaller relative humidity gradients. Perforations of 270, 360, 450, 680, 730 and 750 μm diameter were used, and the relative humidity gradients were 16.6, 21.6, 52.6, 61.6

and 68.6 %. Containers were stored at 5°C and a total of 12 experiments was performed. The RH in the cold room was 96.6% and the internal RH was created by using saturated solutions as suggested by Stokes and Robinson (1949), The RH of the ambient created by the saturated solutions at 5°C was verified with Escort iMini Temperature and Humidity data logger (Cryopak, France). Air velocity was set with a fan blowing air over the packages at average velocities between 0.8 and 4 m/s.

The water vapour flow rate was measured by the weight gain of the $CaCl_2$ salt for 0% RH (or respective solution for other internal relative humidities). Assuming that water vapour permeance is constant, the mass balance gives a linear variation of the weight with time, with the slope being equal to the permeance multiplied by the area of the film and the partial pressure gradient. As OPP is quite impermeable to water vapour, this permeance is due to the convection mass flow through the perforation, giving the mass transfer coefficient (K) from Newton's convection law, which is equal to the permeance multiplied by the ratio between the area of the film and that of the perforation. This was validated by determining the permeance of non-perforated films with the same system (that would therefore also account for any imperfections of the sealing), which yielded values of permeance to water vapour 5 orders of magnitude lower than those of the microperforated films.

6.3. RESULTS AND DISCUSSION USING MODELS FOR WATER VAPOUR FLUXES THROUGH PACKAGING PERFORATIONS SUGGESTED IN LITERATURE

One of the most common approaches to quantify the gas exchange through pores is Fick's Law (Han 2014). However, when the average gas diffusivity in air is considered in the calculations, the results obtained are far from the reality.

$$\dot{n}_{perf} = D \cdot A_p \cdot \frac{\Delta C}{L} \tag{6.1}$$

In order to correct the calculations, some authors have proposed modifications to the model, and the concepts of end effect (or end correction) and effective opening depth were introduced. The "end correction" to account for convective effects at the interface with circulating air was suggested by Meidner and Mansfield (1968), working on diffusion through stomata. They proposed an end effect of $\pi/8 \cdot d$, where d is the pore diameter. This would lead to a mass transfer coefficient K equal to the diffusivity of water vapour through air divided by the sum of the film's thickness to this end effect, as follows:

$$n_{perf} = \frac{D \cdot A_p}{L + \frac{\pi}{8} \cdot d} \cdot \Delta C \tag{6.2}$$

As a result, the mass transfer coefficient thought perforations could be simplified as follows:

$$K_{MM} = \frac{D}{L + \frac{\pi}{8} \cdot \mathrm{d}} \tag{6.3}$$

Nobel (1974) applied a similar concept, named “effective opening depth” of stomata on leaves, where the end effect would be equal to the radius of the pore, i.e. d/2. As 8/π is slightly over 2.5, this implies a 25% bigger end effect compared to Meidner and Mansfield (1968).

Nobel (1974) claimed that small pores (in the order of microns) are subjected to molecular interactions with the sides of the opening that affect the mass transfer and this geometrical correction is suitable. K is calculated as:

$$K_N = \frac{D}{L + \frac{d}{2}} \tag{6.4}$$

More recently, authors working with food packages have suggested the end effect concept to calculate the gas exchange through perforated films. Fishman, Rodov, and BenYehoshua (1996) adopted Nobel’s effective opening depth, while Lee, Kang, and Renault (2000) considered an end correction of 1.1 · d, which is an end effect more than twice as big as Nobel’s.

Mastromatteo et al. (2012) put forward an empiric model for the permeability instead, as follows:

$$WVP_{tot} = WVP_{film} + \beta_1 \cdot \frac{n}{A} \cdot e^{\beta_2 \cdot d^2} \tag{6.5}$$

Knowing that the permeance Pa is equal to the ratio between the water vapour permeability WVP_{tot} and the film thickness, the mass transfer coefficient could be calculated as:

$$K = \mathrm{P}_{a,f} + \frac{\beta_1 \cdot R \cdot T \cdot e^{(\beta_2 \cdot (d \times 10^6)^2)}}{162 \cdot \pi \cdot d^2 \cdot L} \tag{6.6}$$

Where $P_{a,f}$ is the permeance through the film, R is the universal constant of gases in $m^3 \cdot atm \cdot K^{-1} \cdot mol^{-1}$, T in K, d in m, and K in $m \cdot s^{-1}$. β_1 and β_2 are constants proposed by the authors considering the experimental results obtained on their research; β_1 is $1.0015 \cdot 10^{-9}$ $g \cdot cm \cdot m^2 \cdot cm^{-2} \cdot h^{-1} \cdot atm^{-1}$ and β_2 is $4.4585 \cdot 10^{-5}$ μm^{-2}.

Techavises and Hikida (2008) obtained an empiric equation relating what the authors called effective permeability to the diameter of perforation. The mass transfer coefficient could be calculated as follows:

$$K = \frac{(2.98 \cdot 10^{-2} \cdot d^2 + 5.37 \cdot 10^{-1} \cdot d + 8.22 \cdot 10^{-1}) \cdot 0.101325 \cdot 10^{-3}}{3600 \times A_p} \tag{6.7}$$

K is obtained in $m \cdot s^{-1}$ when area of perforation A_p is given in m^2 and diameter d in mm.

A set of 13 experiments were performed with different combinations of air velocity, perforation diameter and temperature and the models cited above were used to test the predictive ability of all models.

The results are shown in Fig. 6.1 and it can be seen that all these end effect models underestimated the mass transfer coefficient very significantly. End effects of π/8 or half of the perforation diameter provided estimates that were between 3 and 10 times lower than the experimental results, while an end effect of 1.1 underestimated by a factor of 7 to 20 times the real values.

The model proposed by Techavises and Hikida (2008) predicted results 25 to 60 % smaller than those obtained experimentally. Authors claimed that their prediction is valid for films less thick than 0.025 mm and the films used were 0.30 mm thick. However, this difference is probably not sufficient to justify such differences in the mass transfer coefficients. The authors described the mass transport through the perforations in terms of flux per unit of pressure and their data are dependent on the area used in their experiments. As they used perforations much larger than the diameters used in this work, this is a more likely justification for the mass transfer coefficient being predicted poorly by this model.

Due to the fact that the Mastromatteo et al. (2012) model with the parameters suggested in the original paper provided estimates with completely different orders of magnitude, this model was re-fitted to a set of 94 other experimental data points (used for model development) to ensure the best parameters for the system being analysed. This fit yielded 5.56x10^{-8} for β_1 and 4.10x10^{-7} for β_2 in the units used by the original authors ($g.cm.m^2.cm^{-2}.h^{-1}.atm^{-1}$ and mm^{-2} respectively). However, this fit was poor, with a R^2 of just 0.73, and as shown in the diagnosis plot in Fig. 6.2, illustrating the almost obvious reason that it does not account for the influence of the different air velocities. During storage, fresh fruits and vegetables are exposed to air movement in cold rooms and fridges, and so the effect of the air movement on the mass transfer needs to be considered (Montanez et al. 2010b).

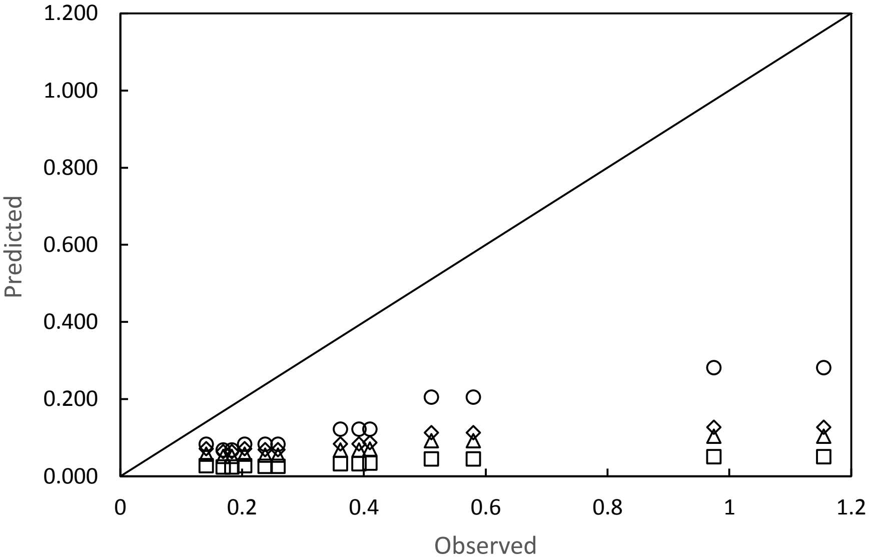

Figure 6.1 –Mass Transfer Coefficient (K) predicted by the 6 models compared to the experimental results in the validation set of experiments. Legend: (◊) Eq. 6.3, (Δ) Eq. 6.4, (□) using the end correction proposed by Lee et al. (2000),.

Notwithstanding, this model with re-calculated parameters was used to predict the results of the 10 validation experiments, shown in figure 6.1 as well. Although the performance of this equation was not as bad as the other 5 models, it was not robust enough to provide satisfactory predictions. Its correlation coefficient was 0.81 and some points were overestimated by 40%.

6.4. DEVELOPMENT OF NEW MODELS USING DIMENSIONLESS NUMBERS

Regretfully, none of these models obeys the principle of dynamic similarity, with the mass transfer coefficient being given in all cases by expressions that are not dimensionless. This means that there is a high probability that parameters determined with a given set of data under given system characteristics might not predict well other scenarios, and this is what likely happened. It is therefore very important to obtain models that have a generic applicability, otherwise there would be one model for each set of data, which explains why different authors proposed different models and in each case they validate their models with their set of data.

Furthermore, the end effect concept may make sense in the original stomata work, where the pores are much longer than wide and therefore most gas flow occurs by fully developed diffusional flow along the pore, which is disturbed at the interface by the convection movements. In the case of perforated packages however, the situation is totally the reverse, so there is in fact virtually no fully developed diffusion flow.

Therefore, two dimensionless correlations were developed to estimate the mass transfer coefficient, to be determined by fitting the correlations to the set of data obtained experimentally, as these could benefit from the principle of dynamic similarity and therefore be more widely applicable to different scenarios, provided that the dimensions numbers are the same. First, a usual model, with the Sherwood number being a function of the Reynolds and Schmidt numbers, was tried:

$$Sh = \beta_1 + \beta_2 \cdot \; Re^{\beta_3} \cdot Sc^{\beta_4} \left(\frac{L}{d_p}\right)^{\beta_5} \tag{6.8}$$

Then, the Π-Buckingham theorem was applied to determine a set of dimensionless numbers that would fulfil the requirements of dynamic similarity. This resulted in the dimensionless number obtained by dividing the mass transfer coefficient by the air velocity, being a function of the Schmidt and Peclet numbers, $\frac{K}{v}\;(Sc, Pe)$, as follows (see chapter 4):

$$\frac{K}{v} = \beta_1 + \beta_2 \cdot \; Sc^{\beta_3} \cdot Pe^{\beta_4} \tag{6.9}$$

The Sherwood correlation has been used to describe mass transfer caused by convection widely for various situations, such as mass transfer through membranes, determining the external resistance to heat transfer in processes where the diffusional resistance through a medium is the dominant phenomenon, and convection quantifies the conditions at the boundary (Karode and Kumar 2001, Lipnizki and Jonsson 2002, Cussler 2009, Raisi, Aroujalian, and Kaghazchi 2008, Oliveira and Oliveira 2010).

The models in equations 6.8 and 6.9 were fitted to the set of 92 experiments of the model development set with least squares regression, giving the results shown in Table 6.1 and diagnosis plots in fig. 6.3. The Sherwood correlation (eq.6.8) was able to explain only 78% of the variance, which is a better result than observed with Mastromatteo's equation but still poor.

Table 6.1- Goodness of fit (coefficient of determination) of 3 empirical models for the convection mass transfer coefficient in microperforations obtained with the 94 experimental data points

Model	β_1	β_2	β_3	β_4	β_5	R^2
(Mastromatteo et al. 2012)	5.56E-08**	4.10E-07***	-	-	-	0.73
Sh (Re, Sc)	133.010	95.941	-0.261	11.05	2.059	0.78
K/v (Sc, Pe)	0.078	5.34E09	36.819	-2.0	-	0.90

*v is the average air velocity; **in $g \cdot cm \cdot m^2 \cdot cm^{-2} \cdot h^{-1} \cdot atm^{-1}$; *** in mm^{-2}

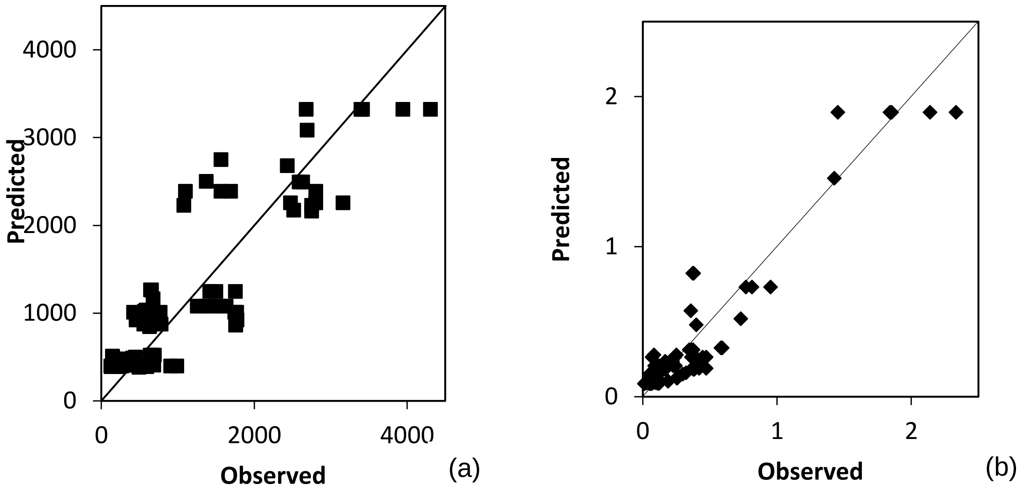

Figure 6.2 –Diagnosis plots of the Sherwood correlation (a) and K/v (b) fitting

As the variability of the Schmidt number is very little, equation 6.9 can be simplified to a model without β_3. The mathematical model obtained gave a good fit to the data, with a R^2 value of 0.892. Unlike the results observed in chapter 4, the mass transfer coefficient of water vapour is dependent on the air velocity.

$$\frac{K}{v} = 0.070 + 174.407 \cdot Pe^{-2} \tag{6.10}$$

Figure 6.3 shows the comparison between the predictions of the resulting models and the experimental data of the independent set of 13 experiments (same as those in fig. 6.1), where it can be seen that the model of eq. 6.9 with the parameters of table 6.1 predicted the validation trial values very well and observed of 0.96, which indicates that this model works very well for predicting results different from those initially used to establish the parameters. The predictions of the Sherwood correlation still presented a better ability than the literature models, with a correlation coefficient of 0.87. Results obtained with equation 6.10 presented a performance that does not distinguish much from equation 6.9, with a correlation coefficient of 0.95.

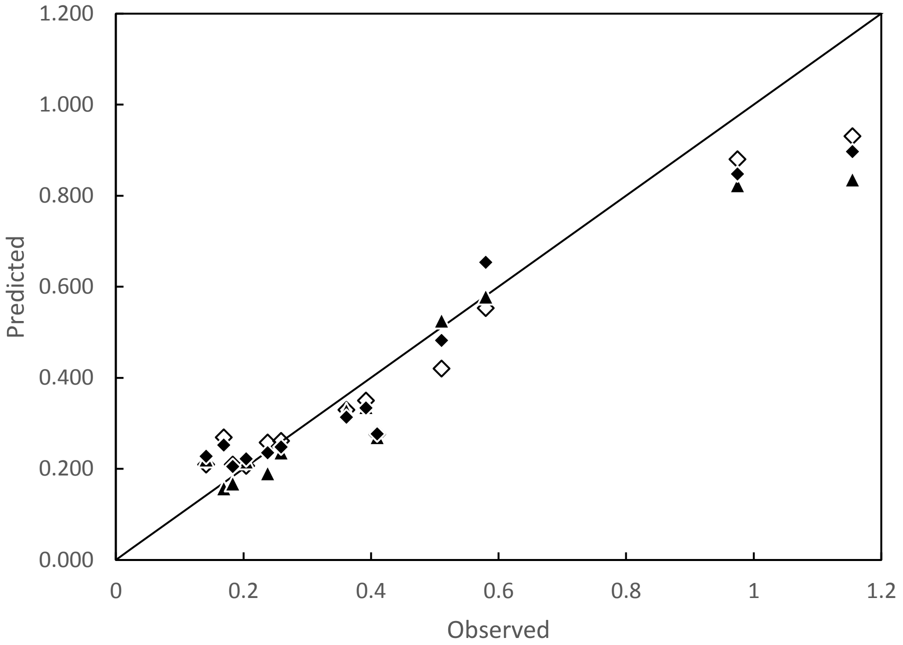

Figure 6.3 –Mass Transfer Coefficient (K) of the validation set of experiments predicted by the proposed models. Legend: (▲) Eq. 6.8, (◊) Eq. 6.9, (♦) Eq. 6.10.

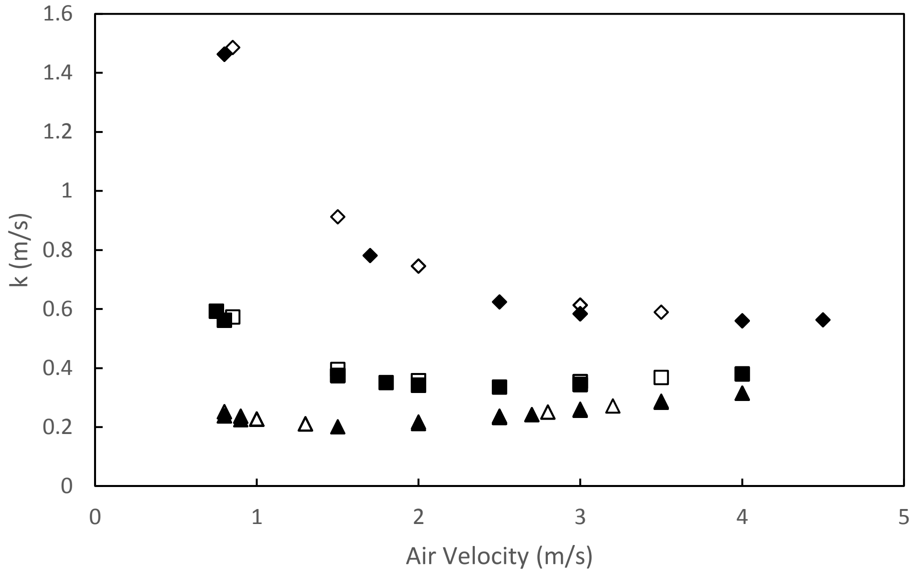

Figure 6.4– K values obtained by the proposed dimensionless correlations (♦) 270 μm at 5ºC, (◊) 270 μm at 10ºC, (■) 450 μm at 5ºC, (□) 450 μm at 10ºC, (▲) 750 μm at 5ºC, (∆) 750 μm at 10ºC.

Figure 6.4 shows the values predicted for some conditions using the dimensionless correlation model of eq. 6.10, showing both the very significant influence of the perforation diameter, and also a relevant impact of the air velocity. Techavises and Hikida (2008) also reported the effect of perforation diameter, with smaller perforations presenting higher K values, but did not assess the influence of air velocity.

The influence of air velocity shown in fig. 6.5 is much more significant than that found in chapter 4 for oxygen, and seems somewhat complex. A slight to negligible influence of air velocity (similar to chapter 4 results for oxygen) is seen for air velocities above 2 m/s only, with the mass transfer coefficient increasing quite sharply when lowering velocity. It seems difficult to explain physically why decreasing convection currents would increase the mass transfer coefficient, so there must be an effect other than average air velocity to explain this effect.

When air velocity was lower than 1.5 m/s the flow over the film is laminar and therefore one would expect a decrease in K with lower velocities, not an increase, so flow effects do not justify the results. However, in the case of water vapour there is an important effect to bear in mind, which is that there is a maximum water content in air, which is defined by the point of saturation, and this depends on pressure and on temperature. Flow causes a decrease on the water retention capacity of the air and a drop of vapour pressure (Rao 2015) or a cooling effect and therefore the water vapour gradient may be affected by this.

It is possible to assess the effect of the velocity on temperature and pressure. The relation between pressure and velocity of a gas is given by Euler's equation (not Bernouilli's equation, which is the integrated form but only valid for incompressible fluids (Bird, Stewart, and Lightfoot 2007). For a same height from the ground and assuming no head losses (in reality they may be relevant and are likely to be proportional to the square of the rotational velocity of the fan):

$$\frac{dp}{\rho} + v \cdot dv = 0 \tag{6.11}$$

For air at normal pressures the ideal gas law is valid, so ρ is the ratio between the product between p and molar mass of air M_{air} and the product between the ideal constant of gases R and temperature T. Also from the ideal gas law, the ratio p - T can be assumed constant (= n·R/V) by attributing all cooling to the pressure difference (no expansion nor contraction of the volume), in which case applying Euler's equation between a point moving at a velocity v_1 and another at velocity v_2 gives indeed Bernouilli's equation.

$$\frac{p-p}{\rho} = \frac{{v_2}^2-{v_1}^2}{2} \tag{6.12}$$

If point 2 is static and point 1 is moving at the circulation speed induced by the fan:

$$p_{at\ v} = p_{static} - \frac{\rho_{static} \cdot v^2}{2} \tag{6.13}$$

Using the ideal gas law (and T in Kelvin):

$$T_{air\ moving\ at\ v} = T_{static} \cdot \frac{p_{at\ v}}{p_{static}} = T_{static} \frac{p_{static} - \frac{\rho_{static} v^2}{2}}{p_{static}} \tag{6.14}$$

Therefore:

$$T_{air\ moving\ at\ v} = T_{static} - \frac{M_{air} v^2}{2R} = T_{static} - 1.732 \times v^2 \tag{6.15}$$

Similarly

$$p_{at\ v} = p - \frac{\rho_{static} v^2}{2} = p \cdot \left(1 - 1.732 \frac{v^2}{T_{at\ v}}\right) \tag{6.16}$$

Hence, the humidity in air might be affected by the air velocity, as it is dependent on both pressure and temperature. To consider the effect of the moisture present in air on K, one might adopt the absolute humidity h_{abs}. In this case, the molar mass fraction can assume one of two values:

i) $y_w = \frac{h_{abs}}{1 + h_{abs}}$, when h_{abs} is smaller than the humidity of saturation of the moving air;

ii) $y_w = y_{s\ at\ v}$, when the air in movement reaches its saturation. $y_{s\ at\ v}$ is calculated considering $p_{at\ v}$ and $T_{air\ moving\ at\ v}$.

The results on Fig. 6.5 show the effect of velocity on K corrected to consider its impact on the humidity. The molar mass fraction of the humid air was determined not by the relation between relative humidity and mass fraction of saturation of the stagnant air but according to the real amount of water in air, i.e. the mass fraction of the saturated air in movement or determined by its relation to the absolute humidity of air. The increase in K due to the velocity now becomes evident. This shows that an even mild effect in temperature and/or pressure affecting the saturation point, while in some cases too small to be relevant for temperature itself, (the difference between the experimental temperature (5 or 10°C) and the temperature of the air moving at the defined air velocity varies from 1.10 to 27.7 K), is sufficient to cause significant differences in the concentration gradient and thus in the calculation of K.

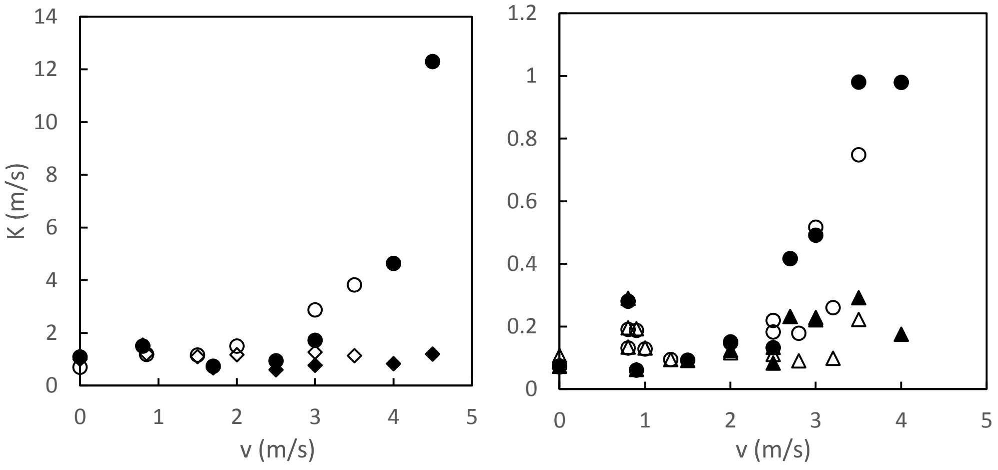

Figure 6.5– Mass transfer coefficients obtained initially ignoring the effect of velocity on the saturation point at (♦) 270 μm at 5°C, (◊) 270 μm at 10ºC, (▲) 750 μm at 5°C, (Δ) 750 μm at 10°C, and obtained with the correction of the saturation point from the cooling effect of velocity denoted by (●) and (○) on both graphs for 5 and 10°C, respectively.

It can be seen that the mass transfer coefficients now have a far greater influence of the air velocity, increasing significantly with it, a very different result from that of oxygen.

Increase in air velocity leads to turbulence around the perforation. At high air velocity, the flow is turbulent, and according to McCabe, Smith, and Harriott (2005) turbulence leads to an increase in the rate of transfer per area and probably facilitated the movement of water molecules from one side to the other. However, comparing with the results for oxygen and the difference between fig. 6.4 and fig. 6.5, it can be said that the most significant effect of air velocity is due to the difference that it causes in the saturation point of the air that surrounds the perforations and hence on the effective concentration gradient.

Fig. 6.5 also shows a relevant interactive effect between air velocity and diameter, as the curves for different diameters are not parallel. It suggests that air velocity and diameter act synergistically on the mass transfer coefficient. It is possible to identify this interaction clearly by observing that the increase on K due to the air velocity is more significant on 270 μm perforations that on 750 μm (Fig. 6.5.a and b, respectively). Moreover, if there were more K values at higher air velocities the curves would probably cross each other as a result of the interaction effect between air velocity and diameter (Calado and Montgomery 2003).

It seems that K decreased slightly with the increase of temperature from 5 to 10°C, but its effect was smaller than the effect of perforation diameter and air velocity as it is barely observable in the curves. This behaviour was also found for oxygen transport through perforated films (see chapter 4) and is attributed to thermodynamic and transport properties of the gases such as viscosity, diffusivity and density. As there is very little change on these properties from 5 to 10ºC, it is reasonable that temperature presents a small effect on K (Techavises and Hikida 2008).

A more accurate correction of K would require the determination of the head losses, because they might be also relevant and are likely to be proportional to the square of the rotational velocity of the fan; however, its determination is more complex than that and demands numerical calculations. Hence, the results of Fig. 6.5 do not intend to be the corrected results of K, but only serve as means to evaluate the effect of air velocity on humidity, and therefore on K, and justify the shape of the curves of fig. 6.4. That said, Eq. 6.9 using the parameters of Table 6.1 incorporates the effect of air movement on the ambient humidity and therefore is enough to analyse the problem.

In summary, high air velocities culminate in a drop on air moisture that reflected a smaller humidity gradient and consequent decrease of K. Unfortunately it also indicates that this model might not predict data with the same accuracy when the air circulation occurs on the side where the relative humidity is lower, because then it would increase the gradient and create the inverse effect, i.e. greater K values at high velocities. As this dimensionless correlation was successfully applied on this situation, it is very likely that a simple re-fit of data generated from containers with higher relative humidity on the inside might be enough to have good prediction on both situations. However, it must be cautioned that dimensionless correlations for water vapour transport may therefore be very different depending on the direction of the flow. In the case of oxygen or carbon dioxide, this direction is always the same while in the case of water vapour it may depend on what the relative humidity of the storage atmosphere is.

A small gradient of relative humidity is recommended for fresh produce in order to avoid drying during storage, and to achieve that, it is important to keep the relative humidity high outside the package. The air velocity during storage is important to remove the respiration heat but is this limited by the maximum dryness that the product can tolerate.

The parameters in Table 6.1 were obtained for mass transfer coefficients through perforations exposed to only two relative humidity gradients, 0.8 and 0.85, in the model development set of experiments and the relative humidity inside the cells was always 0%. Results obtained in the validation set of experiments (Figs. 6.1 and 6.3) were performed with an external atmosphere of 95.5 and 95.8% RH and were successfully calculated using Eq. 6.9 with the parameters from the previous fitting. At the same time, both sets of data presented an internal RH of 0%, and it is necessary to verify if the same correlation is valid under different RH gradients.

Another set of data obtained from 12 experiments with relative humidity gradients varying from 16.6 to 68.6% was performed and the results obtained experimentally compared with the predictions obtained from eq. 6.10 with the parameters in table 6.1. The correlation coefficient was 0.93, indicating that the model predicted very well also these totally different set of results. Figure 6.6 shows the comparison between K values obtained in this set of data and the model predictions (open symbols).

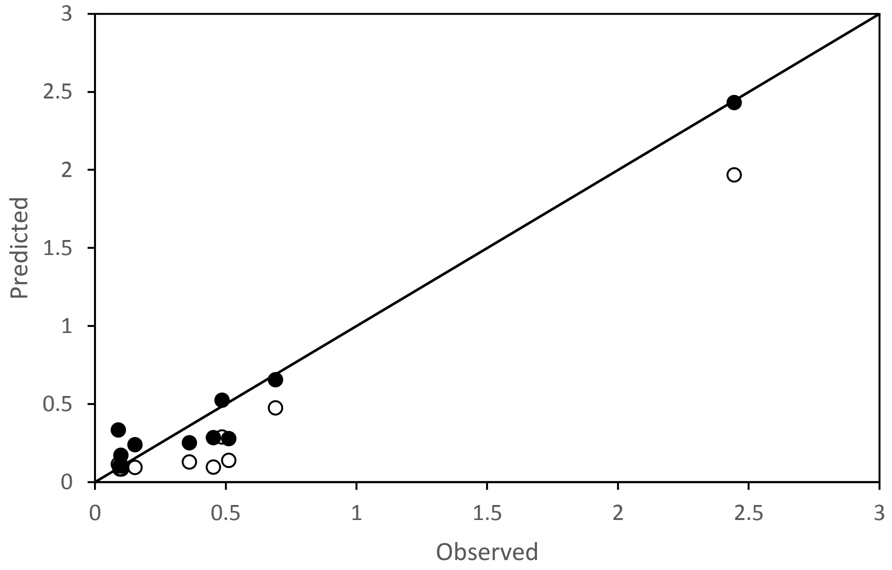

Figure 6.6 – Diagnosis plot of experimental data obtained in the 3rd set of experiments with different internal humidities and the predictions made with eq. 6.10 (●) and with eq. 6.17 (○)

However, a better fit was obtained with a variation of Eq. 6.9 that considers the effect of the concentration gradient $\Delta\chi$ across the perforation (similar to chapter 5 for oxygen):

$$\frac{K}{v} = \beta_1 + \beta_2 \cdot \ Sc^{\beta_3} \cdot \left(\frac{v \cdot d_{perf}}{D}\right)^{\beta_4} \cdot \left(\frac{\Delta\chi}{\rho}\right)^{\beta_5} \tag{6.17}$$

The density used in the calculations was the density of humid air inside the cell, which varied with the internal relative humidity. In order to provide parameters that could be applied to the largest range of RH possible, results used on Fig. 6.6 were added of 6 experimental points with a gradient of RH of 80% (2 results for each diameter).

The parameters obtained by fitting eq. 6.17 to this set of experiments with different internal humidities were β_1 = -0.047, β_2 = 1.134, β_3 = 0, β_4 = -1.00 and β_5 = -0.4657. Eq. 6.17 was able to explain 96.6% of the variance. The predictions are also shown in fig. 6.6. Although they are slightly better that those with eq. 6.9 and table 6.1 parameters, it must be noted that eq. 6.17 is giving a model fit of this set of data and therefore it would inevitably have a better correlation.

Films highly permeable to water may rely very little on the mass transfer of water vapour through the perforations because the film can be responsible for great part of the transport; however, perforations are the only path water vapour can take through films with low permeability to water, and therefore it is crucial to calculate properly how much water is passing through the perforations in order to avoid condensation inside the package. Besides, even films more permeable to water that are used to pack produce with a high respiration rate that releases a great amount of water or demand many perforations can be affected by the mass transfer through the perforations.

Data given by Mistriotis et al. (2016) was used as an example. The authors provided the permeance of PLA at 20ºC and the rate of water loss for tomatoes and peaches. Some assumptions were necessary so that it was possible to study the application of the proposed dimensionless correlation to the design of perforated packaging for these commodities. As the authors do not provide any data for air velocity surrounding the packages, 0.75 was assumed due to the fact that was the smallest value used in the present research. It was also assumed that Eq. 6.17 can be applied to situations where the smaller relative humidity is inside the package. Besides, despite the fact that the parameters of Eq. 6.17 were obtained with data at 5ºC, it is possible that the predictions for 20ºC will not be far from the real values because temperature has a small effect on K. Moreover, this example just intends to illustrate the impact of the mass transfer through the perforation on the permeability of the film and does not intend to provide exact results.

The total permeance can be obtained as follows:

$$P_a = \frac{K \cdot A_p + P_{a,f} \cdot (A - \mathrm{A}_p)}{A} \tag{6.18}$$

Where A is the area of the film, A_p is the area of perforation and $P_{a,f}$ the permeance of the film (as obtained by Auras et al. (2003) for PLA films at 20°) .

In order to avoid condensation, the total flux through the film (unperforated film + perforations), calculated by the product of total permeance, area of the film and concentration gradient should be equal to the product between the transpiration rate and the mass of produce.

The authors used the permeability to CO_2 to establish the number of perforations; they relied on the fact that water vapour permeability of PLA is much higher than its barrier to CO_2. Hence, in order to design the area of film necessary to avoid condensation due to the water release, they used only the WVP of PLA films, and disregarded the mass flux through the holes. However, as already shown in chapter 1 (see table 1.5), the perforations can be responsible for a great amount of the mass flux.

Table 6.2– Design of PLA packages for tomatoes and peaches

	Tomato		Peach
n	5	5	100
d (μm)	200	200	200
Area (cm^2)	650	400	900
RHi	80	90	85
K (m/s)	2.11	1.65	1.84
Pa (m/s)	9.04E-05	9.18E-05	1.49E-04
$\dot{n}_{perf}/\dot{n}_{total}$ (%)	5.64	7.04	42.90
Area (cm^2) considering K	607.26	358.95	465.69

Where n is number of perforations, d is the diameter of perforation, K is the mass transfer coefficient, $\dot{n}$ is the mass flux through the perforations (subscript perf) or through both film and perforations (subscript total)

Results in Table 6.2 confirmed that the flux through the perforations play an important role on the total mass flux, representing 5.64, 7.04 or 42.90% depending on the number of perforations, produce and relative humidity outside the package. If the mass transfer coefficient of water vapour were considered, the reduction in material consumption could reach 48% depending on the number of perforations. Although the K obtained may be considered only as an approximation, these results show the applicability of the proposed dimensionless correlation and the importance of considering not only the film material but also the characteristics of the perforation on the design of MAP.

6.5. CONCLUSIONS

The permeance of microperforated packages to water vapour was not estimated properly by any of the end effects models suggested in literature, which significantly underestimated the convection mass transfer coefficient. This is likely due to the fact that the thickness of a package is very small and therefore the diffusional component of a model composed by diffusion mass transfer plus end effects correction is negligible and therefore in practice those models applied to this situation estimate that permeance is due to end effects only. Also, the models do not consider the effect of air movement around the packaging, which is common in food storage and should be considered in the design of MAP using perforated films.

The application of a dimensionless correlation, developed from independent experimental data, provided good estimates, especially when the model complied with the dynamic similarity principles of the Π-Buckingham theorem.

The correlation proposed predicts a fall of the mass transfer coefficient with air velocity up to a point, followed by a slight increase. However, this may be justified by the effect of velocity on the real saturation point of air and hence on the effective gradient. Considering a cooling effect the corrected mass transfer coefficients would show a significant increase with air velocity, shaper the higher the velocity.

Air velocity therefore has a much more significant effect on the permeance of a package to water vapour than it does to oxygen, and this is likely to be due to this thermodynamic impact on the saturation point then it is to convection and turbulence itself.

7. ANALYSIS OF PLASTICIZING AND ANTIPLASTICIZING EFFECTS OF HUMIDITY ON THE PERMEABILITY OF BIOBASED FILMS TO WATER VAPOUR

ABSTRACT

Biobased films have generally high affinities with water, which may imply significant effects of humidity on their water vapour permeability. The effect of the water content corresponding to equilibrium with atmospheres of different relative humidities was studied for two biobased films, poly-lactic acid (PLA) and NatureFlex^{TM} NVS, a cellulose-based film. Water Vapour Permeance (WVP) was divided in its two components, phase equilibrium (characterised by adsorption and desorption isotherms) and molecular diffusion of the dissolved water (with diffusivity depending on water content). NVS showed a typical plasticizing effect of water content on the permeance, which was well described by applying the WLF equation to quantify molecular diffusion as a function of glass transition temperature, in turn related to water content by Gordon-Taylor equation, and with Park's model for the sorption isotherms. Qualitatively, this corresponds to a behaviour where the higher the atmospheric humidity, the higher the permeance of the film to water vapour. The model and additional experiments with various humidity gradients show very clearly that WVP values obtained with ASTM methods with 0% RH on one side of the film and a high RH on the other

underestimate 2 to 6 times the WVP in conditions of practical interest for food packaging. The PLA film studied showed a different behaviour, with anti-plasticizing effects that could be related to a rearrangement of the molecular structure of the polymer, increasing its crystallinity, at higher water contents. This led to a lower permeance of the films when exposed to very high relative humidities.

7.1. INTRODUCTION

Eco-friendly plastic materials made of biopolymers are frequently proposed as an alternative to synthetic polymers for environmental and sustainability reasons, minimising the need for non-renewable materials (oil derivatives). However, they often present poor mechanical and barrier properties and are usually highly hydrophilic; normally these characteristics are considered as flaws of biobased materials (Azeredo 2009, Magalhães and Andrade 2009, Nascimento, Calado, and Carvalho 2012). Improvements have been suggested with the addition of different types of fillers, such as clay minerals (Choudalakis and Gotsis 2009), cellulose nanowhiskers (Sanchez-Garcia and Lagaron 2010) and starch nanocrystals (Calado and Ramos 2016).

High permeabiltty to water vapour is not necessarily a hinderance, depending on the product being packed. Highly respiring products such as fresh-cut fruits and salads, for instance, will release significant amounts of water due to respiration (for instance, for sugar substrates like glucose and fructose, one mole of water vapour is produced for each mole of carbon dioxide equally produced). If these significant quantities of water vapour are not released through the package to the outside atmosphere, the internal atmosphere will quickly reach saturation resulting in significant condensation of water. This is visible for consumers in inappropriate packages with water droplets all over the internal film and accumulation of liquid water at the bottom of the package. In turn, this leads to mould growth and/or fermentation, with fast deterioration of quality.

Conventional synthetic films used for packing fresh and minimally processed fruits and vegetables have been perforated to achieve a desired atmosphere inside the package, increasing permeability both to oxygen and water vapour to the level required for products with medium to high respiration rate. Properly designed perforation profiles allow to ensure a favourable atmosphere inside the package by controlling the gas exchange through the perforations (Hussein, Caleb, and Opara 2015).

Highly hydrophilic biobased materials can therefore be an alternative to perforations for Modified Atmosphere Packaging, with their high WVP allowing the release of the produced water vapour without requiring perforations. However, high hydrophilic behaviour typically means higher quantities of dissolved water in the polymeric structure, which can be a problem as it may imply significant variation with the humidity of the atmospheres that the package is subjected to. Water equilibrium polymer-atmosphere in hydrophobic polymers usually obeys Henry's Law and just a small amount of water is absorbed (Van Krevelen and Te Nijenhuis 2009). For hydrophillic polymers the relation is much more complex, with the isotherms showing a sigmoidal shape defined as type II in the BET classification. This corresponds to increasingly sharp variations in water content of the film as the relative humidity (water activity) approaches saturation.

Water is the most important plasticizer in biological systems, affecting the thermophysical properties of hydrophilic materials. However, polymers may also show antiplasticizing effects, whether for water or other plasticizers, such as glycerol, that are often used in polymeric matrices to improve physical properties and manufacturing processes such as extrusion (Chang, Abd Karim, and Seow 2006).

Water molecules tend to form hydrogen bonds originating water-water or water-polymer interactions through polar groups on the polymeric chain. The latter is normally observed in hydrophilic polymers, where each polar group connects to one water molecule. The polymer hydrophilicity will depend on the amount of polar groups, the intensity of water-water versus water-polymer interactions and the effect of water on the crystallinity of the material.

Therefore, it may be critical to quantify the effect of humidity on water content and the resulting permeability of films in order to design and assess the performance of packaging films sensitive to water under various conditions of use. Due to the resistance of the film to gas transfer, the internal atmosphere of packages will be high - this is good to avoid excessive water loss with transpiration, but up to the point where the atmosphere does not reach saturation. The outside of the package may be exposed to atmospheres of quite variable relative humidities, though typically around 70 to 80%. This depends not only on environments, which means variations in geographic locations and time of the year, but also on the storage conditions. Usually cold rooms are used to extend shelf life and at low temperatures high relative humidities are reached more easily. Thus, most food packages will be exposed to high relative humidities, precisely the conditions where their WVP might therefore vary the most due to variations in the corresponding water content of the polymer and its impact on molecular mobility.

Material data sheets shed no light on this issue. ASTM 96 (1995) methods involve the determination of WVP at temperatures between 21 and 36°C (when extreme conditions, also denoted as tropical, are desired) with films exposed to close to 0% and 100% RH on each side. This implies a gradient of water content in the film from 0 to its maximum and therefore WVP values thus obtained are averages of the specific condition chosen and resulting concentration profile, which cannot thus be related with any other conditions, and hence is an insufficient data to predict how WVP will be affected by exposition to different atmospheric humidities.

The objective of this work was to assess the influence of relative humidity on the WVP of two biobased films (examples of films showing anti-plasticizing and plasticizing water effects) and the ability of polymer science models that quantify plasticising effects to predict accurately this influence. Poly lactic acid (PLA) and NatureFlex^{TM} NVS were used. PLA is a biobased material that has been produced in commercial scale since the 1990s. (Auras et al. 2010). NatureFlex^{TM} NVS (NVS) film is a metalized heat-sealable cellulose-based compostable film. It is semi-permeable to moisture, presents good barrier to water and aroma and was designed to keep its integrity at humid storage conditions (Innovia 2015, Dukalska et al. 2013).

7.2. MATERIALS AND METHODS

7.2.1. Mathematical methods

7.2.1.1. Quantification of WVP

WVP measures the rate of transfer of water vapour from the atmosphere on one side of the film to the other, which is the net effect of possibly 5 phenomena: hydrodynamic movement of water vapour within the atmosphere on one side up to the surface of the film, polymer-atmosphere phase equilibrium on that surface, movement of the dissolved water from one side of the film to the other, phase equilibrium on that other side, and hydrodynamic movement of the surrounding gas. With the molecular diffusion of the dissolved water through the film being a slow process, the hydrodynamic movements on the two sides (boundary mass transfer resistances) can be neglected and thus two phenomena need to be described to provide a proper quantitative analysis of WVP: phase equilibrium (which will occur on the two sides at different points of the equilibrium relation) and molecular diffusion of dissolved water through the polymer. If a packaging film is composed of more than one material (layers), it is assumed that one of them controls the diffusion rate (this being a case of resistances in series), and unit partition coefficients for equilibrium between different layers are considered.

The complexity of these phenomena needs to be noted. In relation to phase equilibrium, sorption may show hysteresis, which means that the phase equilibrium on the side that is adsorbing water molecules may be different from that on the side where they desorb, and the point of equilibrium depends on whether the film was previously dried or wetted (Piringer 2000). In the case of molecular mobility through the polymer, water content may influence diffusivity significantly, and to interpret data from close to 0 to 100% RH through the film requires a good model to account for this influence over significant gradients.

If the only effect of water is plasticizing the polymer structure, then there is a well established way of describing molecular diffusivity in polymer science:

- Mass transfer of the dissolved molecules in the polymer structure occurs by diffusion, which is quantified by Fick's laws. In steady state, and as water content is necessarily small, true and pure diffusion are the same and Fick's 1st law can be written as:

$$m = DA\rho_f \frac{dx}{dl} \tag{7.1}$$

where m is the mass flow rate of water through the polymer (e.g., g/s), D the diffusion coefficient of water in the polymer (cm^2/s), A the area perpendicular to the movement (cm^2), l the distance from the wetter surface in the direction of the movement, ρ_f the density of the film (g/cm^3) and x the mass fraction of water in the film (g water / g film). If the diffusion coefficient was constant, then:

$$m = \frac{\bar{D} A \rho_f}{\delta}(x_1 - x_2) \tag{7.2}$$

where δ is the film thickness and the subscripts 1 and 2 refer to the 2 sides of the film, the former being the wetter side. If the diffusion coefficient is not constant, then eq. 7.2 gives the average coefficient for the particular concentration profile, denoted by $\bar{D}$, that is:

$$\bar{D} = \frac{\int_{x_2}^{x_1} D_{(x)} dx}{x_1 - x_2} \tag{7.3}$$

where the subscript (x) in D is used just to stress that D is the concentration-dependent value of diffusion for a specific location of the film with its corresponding water content.

- The diffusion coefficient is directly related to molecular mobility and relaxation times and thus varies with the glass transition temperature according to the WLF (Williams, Landell and Ferry) model (Williams, Landell and Ferry) model, which can be written as (Roos and Karel 1991):

$$D_{(x)} = D_g 10^{\pm\frac{C_1(T-T_g)}{C_2+(T-T_g)}} \tag{7.4}$$

with the + sign below glass transition and the - sign above, T being the temperature of the medium, T_g the glass transition temperature of the polymer, which depends on its water content, and D_g the diffusion coefficient at glass transition T_g. The model constants C_1 and C_2 are physical properties of the polymer to be determined experimentally and that are different above and below glass transition. For a wide variety of polymers, the original authors reported average values above glass transition of 17.44 (dimensionless) and 51°C (Williams, Landel, and Ferry 1955), respectively.

- The influence of water content on the glass transition temperature of a polymer is generally well described by the Gordon-Taylor equation (Gordon and Taylor 1952):

$$T_g = \frac{xT_{g,w}+k(1-x)T_{g,s}}{1+k(1-x)} \tag{7.5}$$

where k is the Gordon-Taylor constant, to be determined experimentally for the specific polymer, and the subscripts w and s for T_g

denote the glass transition temperatures of water and the totally dry polymer solid, respectively. The latter needs to be determined experimentally, while $T_{g,w}$ is given the theoretical value of 138 °C (Levine and Slade 1986).

For phase equilibrium, it is necessary to determine experimentally the isotherms for films from totally dry to saturation (adsorption) and then from saturated to dry (desorption). Different empirical and semi-empirical models have been used to describe polymer-gas equilibrium. The following were considered in this work, to select a best one from the experimental data:

GAB (van den Berg 1985):

$$X = \frac{X_{mono} \cdot C_G \cdot K_G \cdot a_w}{(1 - K_G \cdot a_w) \cdot (1 - K_G \cdot a_w + C_G \cdot K_G \cdot a_w)} \tag{7.6}$$

Oswin (1946):

$$X = c_{O,1} \left(\frac{a_w}{1 - a_w} \right)^{c_{O,2}} \tag{7.7}$$

Peleg (1993):

$$X = K_{P,1} {a_w}^{n_{P,1}} + K_{P,2} {a_w}^{n_{P,2}} \tag{7.8}$$

Viollaz and Rovedo (1999):

$$X = \frac{x_{mono} \cdot C_V \cdot K_V \cdot a_w}{(1 - K_V \cdot a_w) \cdot (1 - K_V \cdot a_w + \cdot C_V \cdot K_V \cdot a_w)} + \frac{\cdot C_V \cdot K_V \cdot k_{V,2} \cdot {a_w}^2}{(1 - K_V \cdot a_w) \cdot (1 - a_w)} \tag{7.9}$$

Park (1986):

$$X = \frac{A_{P,L} \cdot b_{P,L} \cdot a_w}{1 + b_{P,L} \cdot a_w} + K_{P,H} \cdot a_w + K_{P,a} \cdot {a_w}^{n_P} \tag{7.10}$$

where a_w, the water activity, is equal to the relative humidity of the air at equilibrium with the film and X is the mass fraction in dry basis (e.g. g water / g dry film). The relationship between dry basis and normal (wet) basis is:

$$X = \frac{x}{1-x} \tag{7.11}$$

The relationship between sorption - diffusion and WVP is easier to see when one of the sides is kept totally dry (0% RH, a_w=0), that is, x_2=0, whatever the sorption model. WVP is determined simply from the measurements of water flow rate across the polymer and the humidity gradient. ASTM methods and material data sheets often use WVTR (water vapour transmission rate), which simply incorporates the vapour pressure:

$$m = WVP \cdot p_v \cdot A \cdot \left(h_{r,1} - h_{r,2}\right) = WVTR \cdot A \cdot (h_{r,1} - h_{r,2}) \tag{7.12}$$

where p_v is the vapour pressure at the particular temperature and the relative humities h_r are equal to the water activities in the film a_w. Thus, when $h_{r,2} = a_{w,2} = x_2 = 0$:

$$\overline{D} = \frac{WVTR \cdot \delta \cdot a_{w,1}}{\rho_f \cdot x_1}$$

Hence, comparing with eq. 7.2:

$$\overline{D} = \frac{WVP \cdot p_v \cdot \delta \cdot a_{w,1}}{\rho_f \cdot x_1} \tag{7.13}$$

with the ratio $a_{w,1}/x_1$ being given by the chosen adsorption isotherm (as water is adsorbing into the wetter surface).

Note however eq. 7.3 giving the $\overline{D}$ dependent on the whole concentration profile from 0 to x_1, not only the point for x_1.

7.2.1.2. Data analysis to determine variable diffusion coefficients

Values of the diffusion coefficient for different water contents are easily determined from experimental data with 0% relative humidity on one side and various relative humidities on the other. In these case eq. 7.3 becomes:

$$\overline{D} = \frac{1}{x_1}\int_0^{x_1} D_{(x)}dx \tag{7.14}$$

Thus, using Leibinz's rule of derivation of integrals:

$$D_{(x)} = \frac{d(x_1\overline{D})}{dx_1} \tag{7.15}$$

Hence, determining values of $\overline{D}$ for various x_1 allows building a plot $x_1 \times \overline{D}$ versus x_1 and the values of $D_{(x)}$ are the tangents of the resulting curve at the respective x point. In general cases for concentration dependent diffusion coefficients (Crank 1975), the easiest is to fit a simple mathematical expression to $x_1 \times \overline{D}$ versus x_1 data and obtain $D_{(x)}$ from the derivatives of that model. A straight line (or parts of the plot well described by straight lines) corresponds to constant diffusion coefficients.

In the present case, there is actually a model for this variation. From equations 7.4 and 7.5, and noting that the glass transition temperature of a usable packaging film should be above its operating temperature:

$$D_{(x)} = D_g 10^{\frac{C_1\left(T-\frac{xT_{g,w}+k(1-x)T_{g,s}}{1+k(1-x)}\right)}{C_2+\left(T-\frac{xT_{g,w}+k(1-x)T_{g,s}}{1+k(1-x)}\right)}} \tag{7.16}$$

Replacing this model in eq. 7.3 (x_2=0) and then solving the integral numerically gives $\overline{D}$ model predictions. Experimental data determining water vapour mass flow rates give experimental values of $\overline{D}$ model, from combining eqs. 7.11 and 7.12:

$$\overline{D}_{exp,0-x_1} = \frac{m_{exp,0-a_{w,1}} \cdot \delta}{A \cdot \rho_f \cdot x_1} \tag{7.17}$$

where the subscripts exp,0-x_1 and exp,0-$a_{w,1}$ are used just to stress that these quantities refer to experimental values determined with no humidity (water content) on one side, and x_1,$a_{w,1}$ (point of an adsorption isotherm) on the other.

Fitting the WLF + Gordon-Taylor model predictions of $\overline{D}$ from the numerical integration of eq. 7.14 with eq. 7.16 giving $D_{(x)}$ to the experimental values for each data point with least squares regression at a constant temperature T provides the 4 parameters of this model, C_1, C_2, k and $T_{g,s}$.

7.2.2. Experimental methods

7.2.2.1. Materials

PLA (poly-lactic acid polymer) was supplied by Huhtamaki (Forchheim, Germany), and NatureFlex^{TM} NVS by Innovia Packaging Group

(Wigton, UK). NVS is a compostable cellulose-based film developed by this company.

7.2.2.2. Experimental procedures

Differential scanning calorimetry (DSC) measurements were performed with a NETZSCH DSC 200 F3 calorimeter (from NETZSCH-Gerätebau GmbH, Germany) equipped with a thermal analysis data station (NETZSCH Proteus® 6.0, Germany).

The glass transition temperature (T_g) was characterized as the midpoint of the inflexion on the baseline in a differential calorimetry scan due to a discontinuity on heat capacity. At temperatures below the T_g, the rearrangements on the backbones of polymeric chains are very slow (Ghanbarzadeh and Oromiehi 2008, Ferry 1980). The T_g was determined on a second heating after one heating and cooling cycle in order to eliminate effects of sample history (Gontard and Ring 1996, Tumwesigye et al. 2016). The melting temperature (T_m), observed as an endothermic peak, and the associated enthalpy (ΔH_m) were also determined (and expressed as $J \cdot g^{-1}$). Each sample was heated at a rate of $10°C \cdot min^{-1}$, from 5 to 250°C, under an inert atmosphere (N_2). The experiments were performed at least in duplicate, using aluminium DSC pans containing 10 mg of sample. An empty pan was used as reference.

X-ray diffraction (XRD) measurements were performed on a D2-Phaser diffractometer (Bruker, Karlsruhe, Germany) with a CuKα radiation (λ = 1.5418 Å), at 30 kV and 10 mA. Films were scanned over the range of diffraction angle $2\theta = 2 – 45°(2\Theta)$, at a rate of 0.15°/min, a step size of 0.02°, a divergence slit width of 0.6 mm, a scatter slit width of 0.6 mm and a receiving slit width of 0.2 mm.

For the determination of water sorption and mass flow rates through films the temperature of 5°C was chosen, being a typical average temperature of storage for fresh packed products.

Water sorption isotherms were obtained by maintaining the films under different relative humidities from 0 to 100% at 5°C and calculating the moisture absorbed by weight difference from a fully dried film. To obtain fully dried samples, films cut into 75 x 15 mm strips were dried at 35°C until reaching constant weight and kept at 0% RH. Such films were then placed in environments kept at 5˚C under different relative humidities, up to fully saturated air for the adsorption isotherm. For the desorption isotherm fully wet films equilibrated with saturated atmospheres were then placed in environments at different, and lower, relative humidites. Water and anhydrous calcium chloride were used to maintain relative humidity at (close to) 100% and 0%, respectively. Other relative humidities were obtained with glycerol solutions, as proposed by Wheeler et al. (2012), or saturated solutions (Stokes and Robinson 1949, Winston and Bates 1960): 0.16, 0.28, 0.5, 0.57, 0.65, 0.7, 0.8, 0.85, 0.9, 0.95. The weights of the samples were checked for 3 weeks, and equilibrium was judged to have been attained when the difference between consecutive sample weightings was less than 1mg/g dry solid.

The water vapour transmission rate through the film was determined by a gravimetric method based on ASTM E96/95 with modifications (ASTM 96 1995). Permeation cells were kept at 5°C in enclosed in humidity-controlled containers stored in temperature controlled incubators, and the water vapour gradient was obtained by creating different atmospheres inside and outside the cell, which were equilibrated with solutions similar to the determination of isotherms. Relative humidity outside the cells was controlled by using a Temperature and Humidity Data Logger (Cryopak, France). The measurements were performed over 48 h. The variation in weight of the solutions inside the cell provided the measurements of the mass flow rate of water, with WVP then given by eq. 7.12.

Models were developed from data with 0% RH inside the container and various RH outside. For model validation and analysis of the practical implications of the findings, an additional set of data was obtained with different internal RH as well.

It is important to note that the drier side must be the inside of the container. It was verified experimentally that if water vapour moves from the inside out, there is a decrease in pressure because the film is much more impermeable to other gases and thus the loss of water vapour molecules from the internal atmosphere is not compensated fast enough by an influx of nitrogen and oxygen. Furthermore, there should also be a cooling effect due to the latent heat of evaporation of water given the small volume of the container. Both effects, even if very small in absolute terms for temperature and pressure themselves, have a significant impact in increasing the relative humidity inside the container from the assumed conditions of temperature and pressure outside it. For instance, WVTR measurements with 90% RH inside and 50% outside were 64% higher than those determined with 50% RH inside and 90% outside, which due to the influence of relative humidity on the permeance that will be shown in the results section is explained by an increase in the real internal relative humidity from 90% to closer to saturation due to the pressure loss resulting from the uncompensated outward flow rate of water and to evaporative cooling.

7.3. RESULTS AND DISCUSSION

7.3.1. Sorption isotherms at 5°C

The adsorption and desorption isotherms of PLA and NVS are shown in figure 7.1. Adsorption and desorption data for PLA did not vary more than experimental error and thus a single sorption curve was considered. The same occurred with NVS but only up to 95% relative humidity, with significant hysteresis for higher water activities, thus leading to different adsorption and desorption curves, even though the predictions are indistinguishable between the 2 within experimental error up to a_w=0.95.

The parameters obtained with least squares regression for the various models and the goodness of fit statistics are shown in table 7.1.

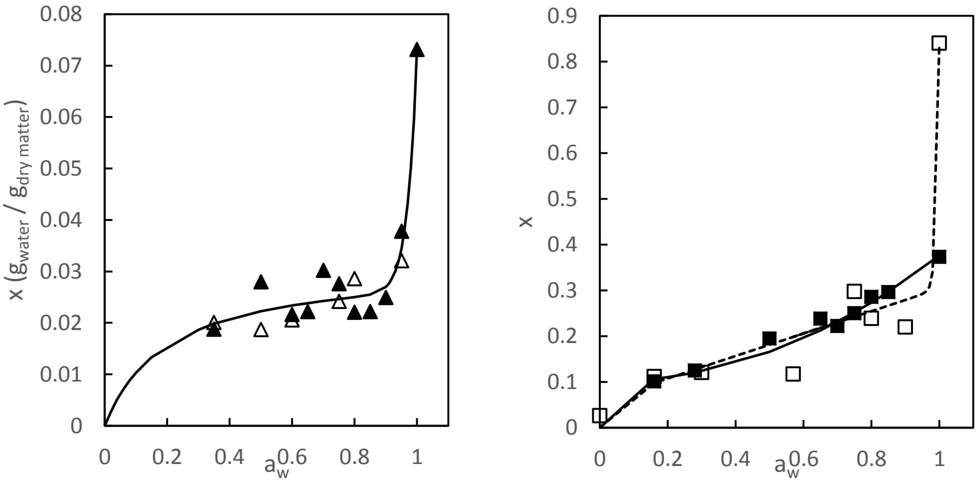

(a) (b)

Figure 7.1 - Sorption isotherms of (a) PLA (▲) and (b) NVS (■) films at 5°C. Open symbols are experimental data for desorption and full symbols for adsorption; the lines show fits of Park's model (joint adsorption-desorption for PLA and for NVS, solid line for adsorption and dashed line for desorption).

Table 7.1– Model parameters and goodness of fit of the sorption curves of PLA and NVS at 5 ºC

Model	Parameter	PLA	NVS	
			Sorption	Desorption
GAB	q_{mono}	0.009	0.131	0.071
	C	9484946.6	17.011	47584.5
	K	0.832	0.667	0.912
	R^2	0.578	0.911	0.894
	E(%)	23.218	17.027	26.680
Oswin	c_1	0.021	0.172	0.176
	c_2	0.142	0.330	0.247
	R^2	0.924	0.846	0.689
	E(%)	11.380	11.315	16.447
Peleg	k_1	0.047	0.275	0.548
	k_2	33.730	2.088	139.047
	n_1	0.027	0.101	0.293
	n_2	0.266	0	0.646
	R^2	0.938	0.919	0.964
	E(%)	10.133	15.936	19.271
Viollaz e Rovedo	q_{mono}	0.027	0.109	0.139
	C	87657.526	36.290	30.000
	K	0.000	0.761	0.503
	k_2	0.000	0.000	0.000
	R^2	0.593	0.888	0.128
	E(%)	11.097	17.227	22.163
Park	A_L	0.031	0.101002	0.059
	b_L	4.931	1496.942	1496.941
	K_h	0	0	0.245
	K_a	0.047	0.275139	0.537
	n	32.973	2.092132	126.108
	R^2	0.939	0.919	0.966
	E(%)	10.175	15.935	18.191

For this set of data Park's model provided the best results, requiring only 4 parameters for PLA and NVS adsorption, although Peleg's model would provide indistinguishably good fits.

Park’s model parameters have a semi-empirical meaning, as the equations can be seen to be a composition of different elements. It incorporates Henry's law or Flory-Huggins-type sorption, Langmuir-type sorption on internal pore surfaces and the formation of clusters; and as a consequence, it is useful to predict the water sorption of not only hydrophilic materials but also hydrophobic ones (Park 1986). The parameters of Park’s model have a physical meaning, which is interesting to evaluate the water-related behaviour of the materials. $A_{P,L}$ is the monolayer capacity, $b_{P,L}$ the Langmuir affinity constant, $k_{P,H}$ Henry’s solubility coefficient, $K_{P,a}$ the equilibrium constant for the clustering reaction and n_P the mean number of water molecules per cluster. The first term is a Langmuir’s isotherm and thus provides the fit for low water activities, giving a portion of the curve that tends to the monolayer value (water content of the first molecular layer of water, strongly adsorbed physically and chemically to the polymer surface), which is thus the meaning of parameter $A_{P,L}$. It provides a measure of the extent of the internal pore surfaces per unit volume of membrane while $b_{P,L}$ is the Langmuir sorption (or affinity) parameter quantifying the curvature (the higher its value, the lower the a_w at which the monolayer is reached). Both had smaller values for PLA films than NVS and the difference was very pronounced for b_L. This suggests that NVS films had greater surface solubility than PLA films, indicating more capacity to form bonds with the water molecules (Alix et al. 2009, Wolf et al. 2016). The much higher value of $A_{P,L}$ of NVS compared to PLA quantifies the much higher solubility of water in this material, about 10 times more than PLA.

$K_{P,H}$ would be Henry's constant (if $A_{P,L} = K_{P,A} = 0$, Parks' model gives the linear isotherm corresponding to Henry's law), and could be used for very low water activities (there being no experimental data at low a_w it is thus not surprising that this parameter is not statistically significant in this data regression; it is noted that low ranges are not relevant in practical applications of food packaging). This implies that the relevant part of the sorption behaviour is driven by water aggregation, or cluster formation, following the initial adsorption into the micro-porosities of the polymer explained by the Langmuir relationship (1st term of Park's model, Park, 1986).

The 3rd term provides the sigmoidal part of the curve, rising rapidly from the monolayer value for higher water activities, with n_P quantifying the curvature. It can be seen in figure 7.1 that with the exception of adsorption in NVS the curvature is only sharp at quite high values of a_w, which numerically corresponds to high values of n_P in table 7.1. This means that clustering of water molecules occurs only for high relative humidities (this will have particular relevance for PLA, as will be discussed later). This desorption behaviour is similar to those observed by other authors in polymers such as polyester filled with flax fibre (Alix et al. 2009), cellulose whiskers and microfibrils films (Belbekhouche et al. 2011) and sodium caseinate films (Colak et al. 2015).

7.3.2. Water diffusivity through the polymers at 5°C

The glass transition temperatures of fully dried films determined by DSC, as described in the methods section, were 125°C for NVS and 40°C for PLA. NVS actually showed 2 T_g points, 95°C being the other, as it is a multilayer material with the cellulose composite covered on both sides by a proprietary material to provide printability and sealability (the coating may vary depending on client’s specifications). As mentioned in the introduction, it is assumed that one of the layers (with higher T_g) is the dominant resistance to water vapour (as it would be the purpose of that layer in the film) and that the partition coefficient of water between the two polymeric materials is 1.

7.3.2.1. Results for NVS

For model development, the water vapour flow rate through the films was determined with internal atmospheres of 0% RH and external of 50, 65, 70, 75, 80, 85, 90 and 100% (the latter was confirmed with a humidity meter) for NVS, with 3 replicates in each case. Least squares regression of the average diffusivities calculated numerically with eq. 7.14 (with individual diffusivities given by eq. 7.16) and obtained experimentally (eq. 7.17) yielded the parameters shown in table 7.2. The plot can be seen in fig. 7.2, which also shows the diagnosis plot for the ability of the WLF and Gordon-Taylor combination, with table 7.2 parameters, to describe the variation of diffusivity with water content. Fig. 7.2b shows the $x_1 \times \bar{D}$ versus x_1 plot used to determine variable diffusion coefficients generically. The model predictions have a 0.989 correlation coefficient with the experimental values in this plot, a much better fit than any empirical model would provide (exponential, power, polynomial, etc.), even though the model parameters were not obtained with this regression, but with the average diffusivities themselves (fig. 7.2a). The individual values of diffusivity for each water content are the tangents of the curve in fig. 7.1b. Fig. 7.2c shows how these individual coefficients, the average from 0 to the specific water content, and the glass transition temperature vary with the water content of the film.

Table 7.2 - WLF and Gordon-Taylor parameters obtained by least squares regression of average diffusivities of water through NVS and PLA at 5°C

Parameter	NVS	PLA **	units
D_g	8.270×10^{-14}	9.38×10^{-12}	cm^2/s
C_1	2.86	2.07	dimensionless
C_2	23.9	7.78	°C
k	1.20	0.738	dimensionless
$T_{g,s}$ *	125	40	°C
R^2	93.1%	13.7%	

* determined experimentally with DSC, ** for a_w<0.95 only

The C_1 and C_2 parameters are different from the universal constants 17.44 and 51.6, but as affirmed by Ferry (1980), the differences from one polymer to another may be significant. Paz et al. (2005), for example, studied the permeability to ethylene of wheat gluten films and obtained values of C_1 and C_2 very different from the universal values (28.2 and 360.2, respectively). It should also be noted that table 7.2 parameters refer to conditions below T_g. It has been shown that C_1 and C_2 depend not only on the material but also on the property evaluated and on the temperature used as reference, and consequently those parameters should not be generalised to all cases as they can assume significantly different values (Peleg 1992, Roos 2000). Notwithstanding, the values obtained in table 7.2 for the permeability of NVS to water vapour are of the usual order of magnitude and well within typical values.

The use of a single Tg in a film with 2 different materials is questionable, but it has been applied to copolymers that also presented two T_g (Kumins and Roteman 1961). The justification in this case, as already noted, is that it is assumed that one of the materials dominates the resistance to water diffusion and hence diffusivity depends only on the T_g of that material (which is likely to be the one with highest T_g).

Values of the parameter k are obtained from fitting the mathematical model to the data and reflect the strength of interaction between compounds and the plasticization effect; for instance, the effect of triacetin glycerin and polyglycidyl ether as plasticisers on cellulose diacetate based biocomposites (Phuong and Lazzeri 2012) and the compatibility of cellulose acetate hydrogen phthalate and poly methyl methacrylate (Rao, Ashokan, and Shridhar 1999).

The results in this work suggests that water content has a mild plasticiser effect on NVS because the value of k is relatively low (Arvanitoyannis and Biliaderis 1998, Chaudhary, Adhikari, and Kasapis 2011). High values of k are associated with highly hydrophilic materials, very susceptible to water (Gontard and Ring 1996). It must be noted that table 7.2 data are for 5˚C, which is a typical storage temperature for fresh foods, but it is not surprising that plasticising effects are milder under these conditions.

It can be concluded that the WLF and Gordon-Taylor models provide an excellent description of the influence of water content (and humidity) on the diffusion coefficient, showing a typical plasticizing effect in the whole range of humidities 50 of 100 % of interest to food packaging. WLF and Gordon-Taylor equations are often used to study T_g and its effect on different material properties, but it is not common to find literature references connecting both models to study the influence of water content in molecular mobility in a polymer. Räderer, Besson, and Sommer (2002) successfully applied both models to describe the drying kinetics of a shrinking film and its dependence on glass transition temperature and hence on the water content.

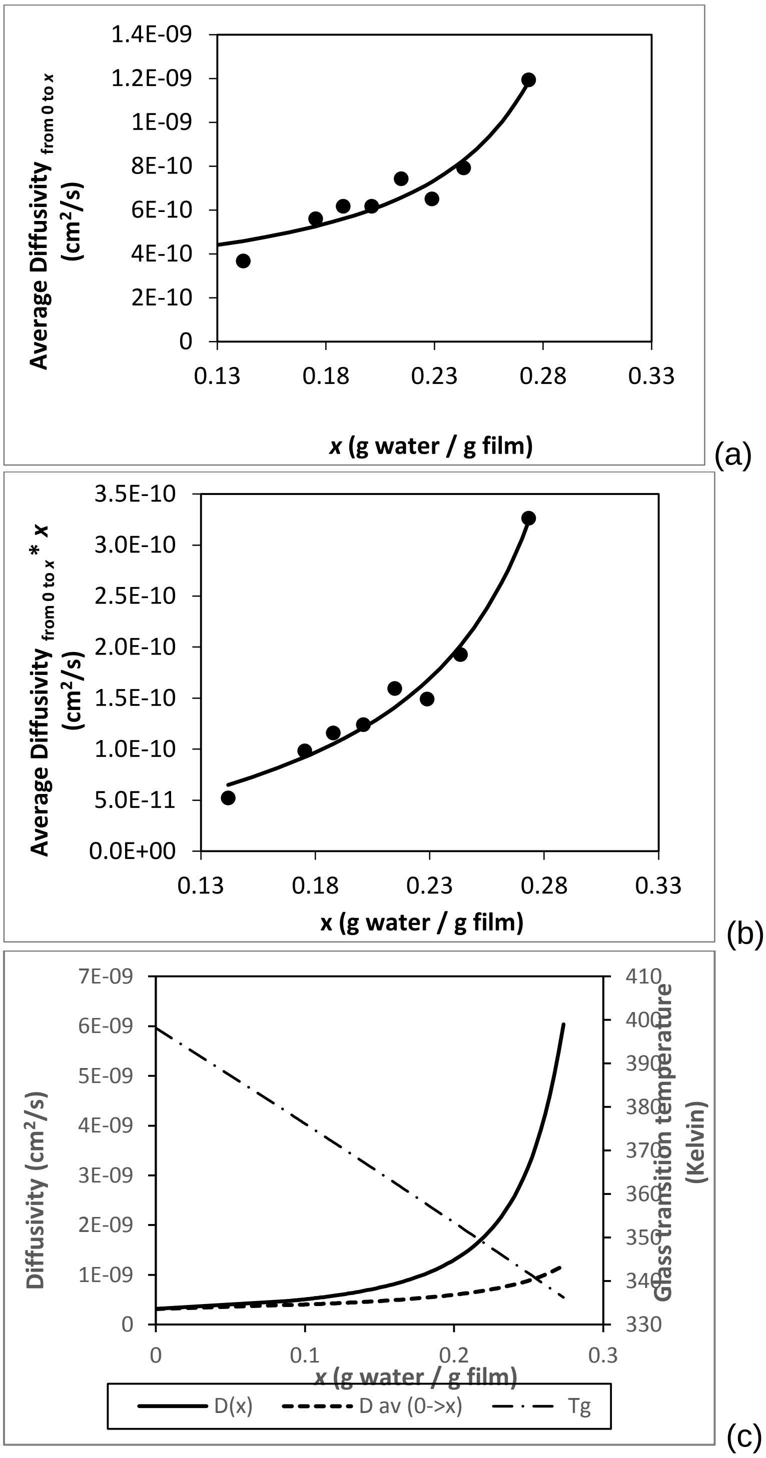

Figure 7.2 - Experimental average diffusivities (symbols) of water through NVS at 5°C and model predictions (lines). (a) average diffusivities; (b) variable diffusivity diagnosis plot; (c) variation of individual and average (from 0) diffusivities (full and dashed lines, respectively, on the left y-axis) and glass transition temperature (dash-dot line, on the right y-axis) with the water content of NVS.

7.3.2.2. Results for PLA

For model development, the water vapour flow rate through the films was determined with internal atmospheres of 0% RH and external of 35, 50, 60, 75, 80, 95 and 100% (the latter was confirmed with a humidity meter) for PLA, with 3 replicates in each case. The model fitting results are shown in table 7.2 and the plots in fig. 7.3.

There are two anomalies in these results: (i) the value for 100% RH is two orders of magnitude smaller than all the others, showing a drastic fall of the water vapour permeability for the fully wetted film and hence cannot be added to the model fitting; (ii) although the concentration dependence of diffusivity in the diagnosis plot (fig. 7.3b) is well described by the WLF and Gordon-Taylor models with the parameters of table 7.2 for the data points up to 95% RH, it is not statistically different from a simple straight line, that is, the diffusion coefficient could be considered constant within the margin of error. Fig. 7.3a indeed shows that a constant average diffusivity would fit the data points equally well, hence the R^2 in table 7.2 is very poor.

Therefore, PLA shows a negligible plasticization effect from the water contents at equilibrium with relative humidity in the 35 to 95% range, but at higher relative humidites the diffusion coefficient was 100 times lower than with the other water contents.

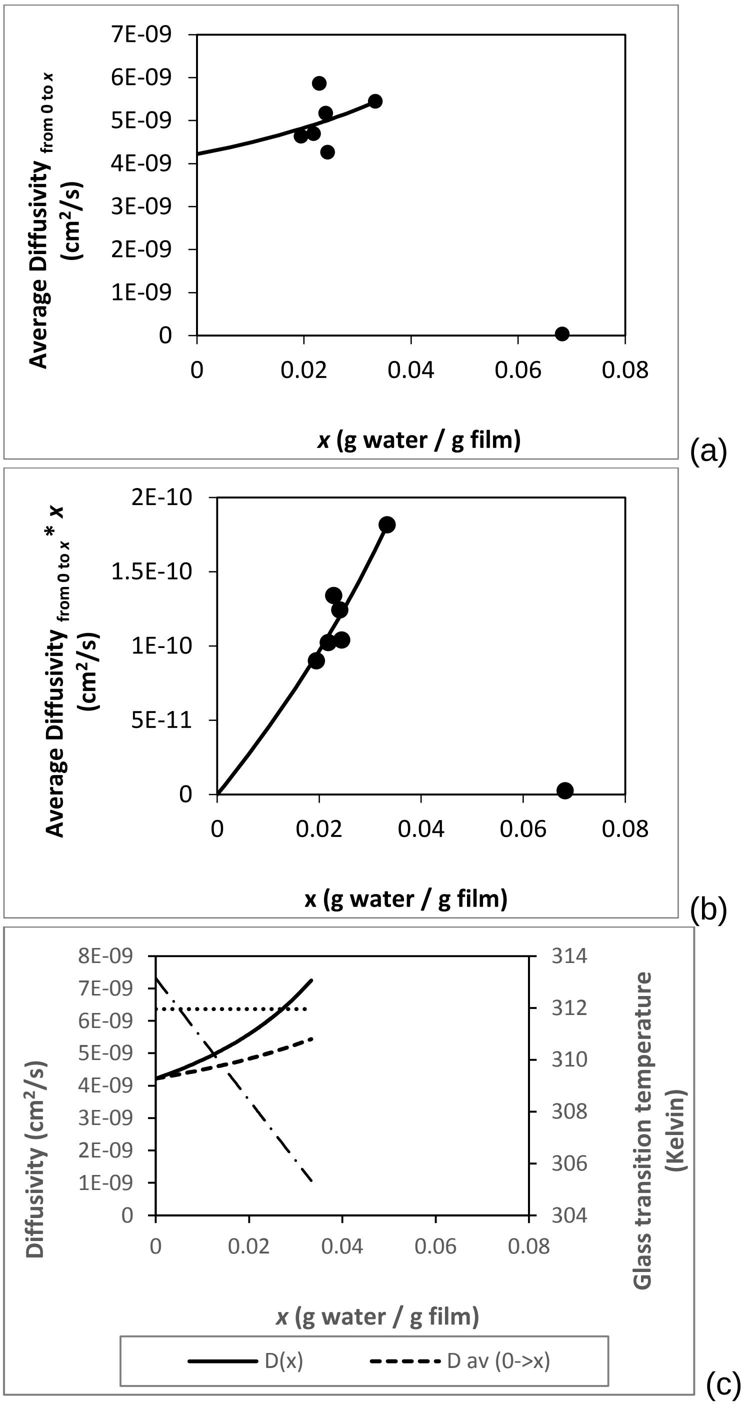

Figure 7.3 - Experimental average diffusivities (symbols) of water through PLA at 5 ^{o}C and model predictions (lines) for $a_w \leq 0.95$. (a) average diffusivities; (b) variable diffusivity diagnosis plot; (c) variation of average and individual diffusivities (full and dashed lines, respectively, on the left y-axis) and glass transition temperature (dash-dot line, on the right y-axis) with the water content of PLA; the constant diffusivity for this range of water contents is also shown as a dotted line.

It is reminded that the adsorption isotherm of PLA shows a very sharp curvature, with the water content at 100% RH being more than twice the amount at equilibrium with 95% RH (fig. 7.1a). It is also noted that the glass transition temperature of the fully dry PLA was fairly low, just about 40°C. Therefore, it is quite possible that the glass transition temperature of the wetted film approaches the environment temperature (5°C), even possibly becoming lower, and thus the molecular mobility of the structure with these higher water contents increases very significantly. This would allow the polymer to recrystallize to some extent. As diffusion through crystalline polymer is much slower than through amorphous, an increase in the crystallinity of the PLA enabled by the high water contents would justify the fall in water vapour permeability. A similar effect was observed by Colak et al. (2015) with sodium caseinate films, where diffusivities decreased with increased relative humidity when the films were subjected to RH over 50%.

Another factor that might compromise the water diffusivity is that water adsorption might be led by hydrolytical degradation. As observed by Holm, Ndoni, and Risbo (2006) the amount of water on PLA films might not be entirely transported through the film, but could react with the membrane on its way.

Auras et al. (2003) observed similar results for WVP of PLA films, which, according to those authors, make PLA films an interesting choice to form multilayer structures with other polymers more susceptible to moisture. However, for food packaging this is a detrimental effect. The packed fruits or vegetables will produce significant quantities of water vapour due to respiration, even if the internal package environment is sufficiently humid to limit transpiration. Therefore, in most cases it is important that the released water vapour is allowed to escape the package at an appropriate rate to prevent condensation. This rate is proportional to the permeance of the film and the gradient of relative humidities. The internal atmosphere will always be humid due to respiration, so if the external atmosphere is also relatively humid, the film has a high water content throughout and a low gradient, so the permeance needs to be higher the more humid the outside environment. Thus, anti-plasticizing effects will denote films that are much more likely to lead to internal condensation the higher the storage humidity.

WVP of PLA films has been described as driven by the water cluster model rather than the solution diffusion model. The water-water interactions are probably stronger than the water-polymer interactions, which is typical of polymers that are not very hydrophilic and do not have many polar groups (Almenar and Auras 2010, Van Krevelen and Te Nijenhuis 2009, Siparsky et al. 1997). These results also concur with the findings of Du et al. (2012), who investigated the clustering of water molecules into PLA matrix by evaluating the enthalpy of water sorption and observed a strong indicative of clustering in PLA films. As fig. 7.1a and table 7.1 parameters show, water clustering on the PLA film tested at 5°C occurs only at very high humidities, above a_w 0.95 (sharp curvature of the sorption isotherm; high value of n_P); above these conditions polymer restructuring and/or clustering effects are more important than plasticization, whereas below this the balance between different effects leads to a roughly constant rate of diffusion.

T_g is a secondary order transition corresponding to the point that the polymer becomes rubbery with a liquid-like mobility. The increase in the chain mobility demands more molecular space for the long-range movement. Plasticisers intentionally added or absorbed by the polymer tend to lodge among the polymeric chains, moving them apart from each other. This separation of the chains reduces the intermolecular interaction forces, increasing the chain mobility of the amorphous phase. The molecular lubrication promoted by the plasticizer decreases the energy necessary to give mobility to the chains (Canevarolo 2006). The anti-plasticization effect of water molecules in a polymer has been attributed to water molecules occupying the intermolecular spaces, filling the polymer free volume. Consequently, the molecular mobility decreases due to the increase of water molecules into the polymeric matrix, which is reflected as a raise in T_g (Robeson 1969). Water might appear as an anti-plasticizer of polymers commonly used at temperatures above Tg (Pittia and Sacchetti 2008). According to Guo (1993), when molecules of plasticizer interact with the polymer the molecular mobility decreases, which is likely to happen in systems with low content of plasticizer. It was also observed by Liu et al. (1990) studying films of glassy polycarbonate containing relatively low concentration of the diluent di-n-butyl phthalate. It is noted from fig. 7.1 and table 7.1 parameters that the water content of PLA was particularly low compared to NVS.

Notwithstanding the physical justifications, these results indicated the necessity of studying the effect of the water content on the crystallinity of PLA in order to validate the causes of the structural effect of water.

First, a simple experiment was performed in order to observe the effect of the water molecules on the structure of the matrix. PLA films were stored at 50% RH for 15 days and the WVP determined at 5ºC as in the previous set of experiments, with 0% RH inside and 50% outside. Results are shown in Table 7.3, row I. After that, these films were stored at 75% RH for 15 days and again the WVP was determined at 5ºC, in this case with 75% RH outside, giving the results in Table 7.3, row II. Finally, the same samples were stored at 50% RH for another 15 days and the WVP was again determined at 5°C with 50 % RH outside, giving the results in Table 7.5, row III.

Table 7.3 – Water Vapour Permeability of PLA previously stored at different Relative Humidity (RH) conditions at 5˚C (in g · m^{-2} · day^{-1}, average of 3 replicates)

	storage prior to testing	RH outside	WVP *
I	15 days at 50% RH	50%	23.437 ^{a}
II	+ 15 days at 75% RH	75%	58.805 ^{b}
III	+ 15 days at 50% RH	50%	66.018 ^{c}

* different letters refer to different homogenous groups according to a Tukey HSD test at 95% confidence level

It can be seen that the water vapour transmission rates of the 3 samples were statistically different, according to a Tukey HSD test at 95%

confidence level. The difference between I and II can be due to the plasticising effect of water between 50 and 75% and not to changes during storage, although the previous results did not suggest a significant difference of the average diffusivities. However, the very significant difference between I and III can only be explained by the film having changed irreversibly as a result of the previous storage. Issues related to water-water versus water-polymer interactions, clustering effects, etc., would not justify that the previous storage history of a film would affect its permeability.

To investigate the changes that occur with high humidities in the PLA film, X-ray diffraction was used. The X-ray patterns of PLA films are shown in Figure 7.4 and two peaks were observed in all samples. Films stored at 0% RH presented peaks at $2\theta = 16.56$ and 29.9°. These peaks were slightly displaced on other films due to the water content. A decrease of the peak intensity is noticeable from the film stored at 0% RH to 50% RH, with the reduction of peak width and height. This is expectable in a plasticizing effect. The peak at 75% recovered somewhat compared to 0 RH, but still shows a plasticizing effect compared to the dried film, but not to 50%. Films stored at 100% RH presented a much sharper peak, higher and wider than the others. This suggests that at 100% RH recrystallization of the polymeric matrix occurred to a significant extent.

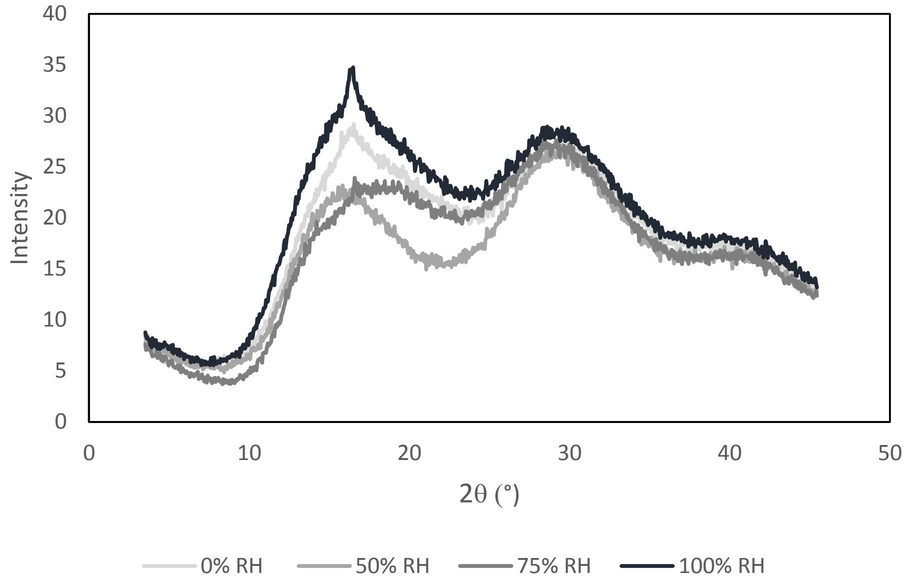

Figure 7.4– X-ray pattern of PLA films conditioned to different relative humidity conditions by storage over 15 days

Crystallization in films due to the presence of water molecules can happen due to the structural effect of the water. The presence of the plasticiser in low concentration gives enough molecular mobility that it allows the molecules to reorganize, hence improving the crystallinity (Lourdin, Bizot, and Colonna 1997).

Cairncross et al. (2006) pinpointed that results in literature concerning PLA films were inconsistent and contradictory. They also observed in their work that the crystallinity of the polymer did not affect the water sorption, that had been dismissed *a priory* by the authors, but the present work shows that it does indeed influence water sorption. Despite the fact that well-defined crystallites are not subjected to the effect of water, polar groups on their surface may react with water (Van Krevelen and Te

Nijenhuis 2009). The presence of the plasticizer might also increase crystallinity by increasing the number of cross-links on the polymeric chain, increasing the rigidity of the polymer (Lourdin, Bizot, and Colonna 1997).

A justification for anti-plasticizing effects can be that the reality is a structural change from amorphous to crystalline in polyvinyl chloride (PVC) materials seems the most appropriate in the present case also. It has been observed that the presence of small quantities of plasticizer increases the chain mobility allowing the polymeric chain to reorganize, and the materials can reach the same crystallinity of unplasticized polymers (Guerrero 1989), which was exactly what was observed in this work for PLA films. The decrease of chain mobility due to the presence of plasticiser was also identified by Sun et al. (2013); and its effect on mechanical properties of films were observed by Suppakul et al. (2013) and Chang, Cheah, and Seow (2000).

Considering the results in Table 7.5, it is possible that the inconsistency in published literature reported by Cairncross et al. (2006) may be due to the fact that the properties of PLA may be strongly dependent on the storage conditions, which means that sorption, WVP and Diffusion may vary with the history of the polymer. This implies that for practical applications the WVP of PLA must be determined at the time of usage, and repeated over storage periods, with the standard values of the material data sheets providing, at best, a rough indication of what to expect.

7.3.3. Water vapour permeance under different conditions of use

The previous results and eqs. 7.2 and 7.12 clearly show that the WVP of a film will depend on the actual humidities on both sides of the film. Thus, standard measurements of WVP may give very inaccurate predictions of the effective capacity of a film to be permeated by water vapour (typical ASTM conditions being 0% relative humidity on one side of the film and 100%, or another very high value, on the other). Literature suggests predicting the flow rate of water through a film by multiplying the standard WVTR by the humidity gradient (of the WVP by the vapour pressure and the humidity gradient). However, the models show very clearly that a same gradient will give significantly different results depending on the absolute values.

A series of experiments were performed to validate the models and prove this point, with various internal and external atmospheres. For NVS, WLF and Gordon-Taylor models can be used, whereas for PLA the result was a constant diffusivity up to 95% RH and a sharp fall above that, so NVS was chosen.

From eqs. 7.2 and 7.12, the WVTR that should be measured in a particular test with different relative humidities inside and outside the film is related to diffusivity by:

$$WVTR = \frac{\bar{D} \cdot \rho_f \cdot (x_1 - x_2)}{\delta \cdot (h_{r,1} - h_{r,2})} \qquad (7.18)$$

where $h_{r,2}$ is the relative humidity of the drier side and x_2 the point for $a_w=h_{r,2}$ of the isotherm and $h_{r,1}$ is the relative humidity of the more humid side and x_1 the point for $a_w=h_{r,1}$ of the isotherm. Whether the adsorption or desorption isotherm need to be used depends on the history of the film; in the case of films used from the roll and hence dry, it is the adsorption isotherm that applies to both sides. The value of $\overline{D}$ is given by eq. 7.3 with the diffusivity following WLF and Gordon-Taylor models as in eq. 7.16, that is, by solving numerically the integral:

$$\overline{D} = \frac{D_g}{x_1-x_2}\int_{x_2}^{x_1} 10^{\frac{C_1\left(T-\frac{xT_{g,w}+k(1-x)T_{g,s}}{1+k(1-x)}\right)}{C_2+\left(T-\frac{xT_{g,w}+k(1-x)T_{g,s}}{1+k(1-x)}\right)}}dx \qquad (7.19)$$

Tests were performed in triplicate with two pairs of internal and external relative humidities in the range of interest to food packaging conditions: 50 and 90% in 3 experiments and 75% and 100% in 3 others.

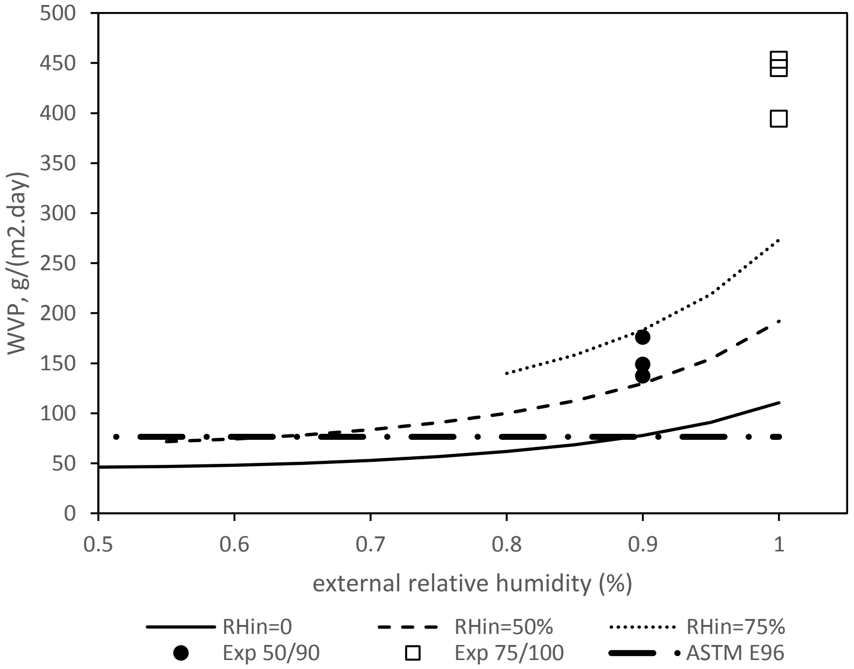

Figure 7.5 - Water Vapour Transmission Rates of NVS at 5˚C obtained experimentally (full spheres for 50%-90% humidity gradient and open squares for 75%-100%), predicted by the model for the dryer side at 0% RH (full line), 50% RH (dashed line) and 75% RH (dotted line), with wetter side on the x-axis, and obtained with ASTM E36 method at 5°C (dash-dot line).

Figure 7.5 shows how the WVTR measured depends on the relative humidity gradient according to the model predictions. Three lines are shown for 3 different dryer environments: 0%, 50% and 75% RH (solid, dashed and dotted, respectively). The ASTM E96 value is also shown as a dotted-dashed line, this being the method used in the material datasheets of NVS. This method measures WVTR at 100°F with 0% RH on one side and 90% on the other; at that temperature the material data sheets correspond to WVTR = 556.6 g/(m^2.day). These experimental conditions for the temperature of 5°C used in this work were part of the model development data set, so the value obtained in those 3 replicates of WVTR = 76.45 g/(m^2.day) is the ASTM E96 value shown here. The points obtained experimentally are also shown, with full circles for 50%-90% gradient (which thus compares with predictions of the dashed line) and open squares for 75%-100% gradient (which compares with the dotted line).

The relevance of the actual relative humidities is very clear in figure 7.5. For instance, for 0-50% (in the full line) WVTR predicted by the model is 46.2 g/(m^2.day) whereas for 50%-100% (in the dashed line) it is 192 g/(m^2.day), which is around 4 times higher, even though the gradient itself is 50% in both cases. The 3 experimental points obtained with the 50%-90% conditions are slightly under predicted by the model (149, 176 and 137, experimental values compared to 130 g/(m^2.day) of the model), still within the margin of error though. However, the model underpredicts significantly the WVTR obtained with 75%-100% (445, 453 and 395 experimental values, compared to 273 g/(m^2.day) of the model). This is however within the margin of error of the isotherm, as there were no points between a_w=0.95 and a_w=1 in the adsorption isotherm determination, which is where the isotherm curves vary significantly. A small error in the isotherm model results in a very significant difference in water content, as can be seen in fig. 7.1b. However, the main point is that the ASTM values would be totally inappropriate, the more so the higher the relative humidities of the two sides. The 50%-90% conditions show an experimental WVTR that is twice the ASTM value.

This is extremely relevant to food packaging, because the real conditions of use are a high internal relative humidity and an external that depends on storage conditions, but is usually high (excessively dry storage atmospheres would cause too much water loss due to transpiration/drying). 90%-50% would be underestimating likely atmospheres in practical applications, and the real WVTR at 5°C is already more than twice the ASTM value. For a package near saturation inside and with 75% RH outside, a not too unusual situation, the model predicts a WVTR that is 3 times the ASTM value (and experimentally, values 6 times higher were found).

7.4. CONCLUSION

Water content showed a very significant effect on the water vapour permeance of PLA and NVS. In the latter case this could be described well by applying WLF and Gordon-Taylor equations to quantify the diffusion of water molecules through the polymer and Park's equation for the sorption isotherms. PLA showed an approximately constant WVP up to 95% RH but a very significant loss of permeance for 100% RH, to just 1% of the 50-95% RH value.

In practical conditions of food packaging internal atmospheres are humid and storage atmospheres should be too, implying that the values determined with ASTM methods may underestimate WVP significantly. It is therefore important to determine the WVP of a packaging film in the real conditions of use, and to understand and describe appropriately the effect of humidity and water content on the effective WVP.

Plasticising effects, like those found for NVS, are beneficial for food packaging because higher humidities will typically occur with lower gradients between inside and outside of the package, and therefore it is beneficial that WVP increases with lower gradients. The internal atmosphere will always be humid due to respiration, so high gradients would imply a dryer storage environment, and the decrease of WVP resulting from that effect thus compensates somewhat to minimise the loss of water and potential drying and consequent loss of quality.

Structural effects, like those found in PLA are detrimental because if a package is subjected to relative humidities close to saturation (for instance, if the high respiration rate of the product on packaging is high, which is likely due to temperature and the mechanical stresses of handling and processing) the film will irreversibly lose permeance, thus becoming even more likely to cause internal condensation and loss of quality.

8. MAXIMISING THE CONFORMITY OF THE EFFECT OF SEAL LEAKAGE IN THE EFFECTIVE PERMEANCE OF PACKAGES

ABSTRACT

The contribution of seal leakage to the oxygen permeability of packages was analysed using APET trays sealed with NatureFlex NVS films. The influence of 3 sealing factors, sealing temperature, time and compression force, on the seal leakage and on its variability was assessed on a small sealing machine. The Taguchi method for robust engineering design was applied using an experimental design with a 5-times replicated L-8 orthogonal array (full factorial design). In spite of differences due to the sealing factors being generally of the order of magnitude as variabilities between repeats, sealing temperature had a significant effect on the effective oxygen permeability of the sealed package at 95% confidence level and was also the most influential factor on the variability, quantified by the signal-to-noise ratio. Sealing time had a marginal impact on repeatability (with an interaction with temperature for the effective permeance, but not for its variability) while compression force did not show significant effects. Adding a 4-times replicated centre point to the design and assessing the dispersion effects indicated however that compression force may have relevant interactions with both temperature and time, and also indicated that the centre point provided the sealing settings with greatest consistency. This

approach illustrates the relevance of sealing in the effective permeability of packages, the importance of ensuring its consistency to design optimum packages for maximum shelf life, and a simple methodology based on Taguchi concepts to establish optimum settings for that objective.

8.1. INTRODUCTION

Food packaging is an extensive research field that covers many areas, from packaging materials related to polymer science and technology to aspects connected to other areas such as cold chain management and post-harvest physiology. For fresh and minimally processed fruits and vegetables the main purpose is to design packaging systems that maximise their protection value to quality and thus maximise the shelf life, reducing losses and ensuring quality of the produce to the consumer.

For packed products, protection means a protective atmosphere with low oxygen and high carbon dioxide and humidity, specific values depending on the actual commodity, and so a major concern for food packaging is the package barrier against gases. Excessive permeance offers no added protective effect to normal atmosphere, whereas excessive barrier can be very detrimental and even a health hazard if anoxia conditions set in as a result of the product’s respiration consumption of oxygen not being compensated by the influx from the atmosphere through the package. Several authors in literature have worked on oxygen, carbon dioxide and water vapour permeability, either trying to improve barrier properties of permeable films (Calado and Ramos 2016, Azeredo 2009) or perforating films in order to achieve a desired permeance (Hussein, Caleb, and Opara 2015, Fonseca et al. 2000). Achieving maximum shelf life therefore requires an accurate determination of both respiration rates and effective permeability of the package.

Perforated packaging films are used for designing modified atmosphere packaging (MAP), which is a technique that relies on the proper calculation of the permeabilities through both film and perforations. However, the contribution of package seals lacks proper attention. It has been argued that leaks on the packaging may spoil MAP’s performance by increasing the effective permeability (Tumwesigye et al. 2017). There are many registered patents of sealing systems trying to improve the sealing and ensure reliability (Pfaffmann 1992, Douglas 2004, Massey et al. 2002, Ishikawa et al. 2014).

However, whether a package leaks through seals or not is in fact a secondary issue, it may even be beneficial to have sealing leakage providing an appropriate permeance instead of perforations. Perforations remove a physical barrier to microbial (and even insect) contamination and if covered inadvertently will then cause anoxia in the package. A somewhat permeable seal could be a better choice to achieve appropriate permeabilities for products with medium to high respiration rates. Seals can be responsible for the effective permeance of a package being significantly higher than that of the film itself, for instance, Reinas et al. (2016) reported that 25% of the total mass transfer through the package was due to sealing leakage.

Thus, the critical issue about seals in MAP is not necessarily to ensure that they are truly hermetic, the problem of seal leakage for successful MAP is inconsistency in the effect. The permeability of a film may vary somewhat with operating conditions but it is a fairly well controlled property of the material. Likewise, if perforation sizes are accurately controlled, so is the variability of the permeance they cause. The problem of sealing leakage is whether it can be controlled within accepted variability. This is the type of problem that is often addressed industrially by applying the Taguchi method of robust engineering design (Rekab and Muzaffar 2005, Myers, Montgomery, and Anderson-Cook 2016), the objective of which is to establish the process settings that result in maximum conformity of performance. In this particular case, it does not actually matter too much what the permeance contribution of seals is, what matters most is that it is a consistent contribution that does not vary excessively from package to package. A package can be designed for any condition, it is possible to incorporate the effect of the seal in the permeance (material, product weight, film area, perforation profile, etc.), the critical issue is repeatability. This problem has not been analysed to date.

Seals are made by heating two thermoplastic materials under pressure during sufficient time to promote the necessary melting of the surfaces that are weld together as the material cools (Yam 2010). Often, one or both surfaces are coated with an adhesive material to improve sealability, but not necessarily, especially if the two surfaces are actually the same polymer.

The objective of this work was to assess the influence of sealing parameters on the effective permeability of a package (due to the packaging materials and the seal) and on its variability between repeats. Taguchi and statistical methods were intended to illustrate an approach to establish the sealing parameters that would ensure maximum repeatability.

8.2. MATERIALS AND METHODS

8.2.1. Experimental procedure

APET/RPET (Amorphous Polyethylene Terephthalate/ Recycled Polyethylene Terephthalate) Trays (607 B, Avoncourt, Ireland) with an open top were used, to be sealed with a 226.77 m^2 NatureFlex^{TM} NVS film (Innovia Packaging Group, Wigton, UK). A small pilot sealing machine (VS 300, Maple, United Kingdom) was used. Slotted weights (100, 120 or 140 N) were used to exert different compression forces on the sealing machine. Sealing was carried out at 8, 12 or 16 seconds, and the temperature was controlled to settings 3, 3.5 or 4 on the sealing machine, which correspond to approx. 115, 145 and 185°C, respectively. The containers were flushed with 20-23% v/v of CO_2 and the balance with N_2 and kept in a walk-in controlled temperature cold room maintained at 10°C.

A full factorial design at 2 levels with the extreme settings of each factor was used first, with 5 replicates for each combination, totalling 40 trials. Four replicates of the centre point were then also performed.

The O_2 concentration inside the containers was measured using a Fiber Optic Oxygen Transmitter (Presens, Germany). This device uses an optical probe to determine the inner concentrations through the transparent film, without piercing nor disturbing the inner atmosphere.

The apparent permeance of the perforated film is obtained from a mass balance to the container:

$$V\frac{dC}{dt} = n \tag{8.1}$$

where C is the oxygen concentration (moles/m^3), n is the molar flow rate of oxygen through the package (moles/s) and V the volume of the container. The flow is proportional to the concentration gradient and area of the film (A), with the apparent permeance (Pa) of the perforated film being the proportionality constant:

$$n = \mathrm{P}_a\,\mathrm{A}\,(C_e - C_i) \tag{8.2}$$

C can be obtained by the ideal gas law, and is equal to yp/RT where y is the volumetric fraction of oxygen, p the pressure, R the ideal gas constant and T the absolute temperature, and developing the equations:

$$V\frac{dy}{dt} = \mathrm{P}_a\,\mathrm{A}\,(y_e - y_t) \qquad (8.3)$$

where y_t is the molar fraction inside the container at any given time t, y_e the outer atmosphere and y_0 the value of y_t at time t=0.

The apparent permeance is due to two possible fluxes: through the film itself and through the seal.

8.2.2. Statistical analysis

The results were analyzed using Statistica software for Windows v. 7.1 (Tulsa, USA). In order to avoid the elimination of some results that could be important to explain some observed phenomena, results with $0.05 < p < 0.1$ were called marginally significant, and also considered in the analysis (Montgomery 2013).

Repeatability was assessed by the standard deviation determined with replicates of a same set of operating conditions (σ) and wit the Signal-to-Noise ratio used in the Taguchi method, for 2 possible targets: the highest possible permeance (SNR_{max}) and the lowest (SNR_{min}):

$$\sigma_j = \sqrt{\frac{\sum_{i=1}^{n_{r,j}}\left(P_{a,i,j}-\overline{P_{a,J}}\right)^2}{n_{r,j}-1}}$$

$$SNR_{min,j} = -10 \times log_{10}\left[\frac{\sum_{i=1}^{n_{r,j}}\left(\frac{1}{P_{a,i,j}}\right)^2}{n_{r,j}}\right]$$

$$SNR_{max,j} = -10 \times log_{10}\left[\frac{\sum_{i=1}^{n_{r,j}} P_{a,i,j}{}^2}{n_{r,j}}\right] \tag{8.4}$$

where the subscript j denotes values obtained with combination j of the sealing parameter settings and i is the counting variable of replicated values obtained at the respective set of conditions. $n_{r,j}$ is therefore the number of repeated values of combination j and $P_{a,i,j}$ the values of P_a obtained experimentally.

8.3. RESULTS AND DISCUSSION

Results obtained are summarised in table 8.1.

Table 8.1 Effective permeance (Pa) of sealed packages with different sealing conditions.

	Temp (^oC)	Force (N)	Time (s)	average P_a 10^6(cm/s)	σ	SNR_{min}	SNR_{max}
2 level design	115	100	8	5.047	5.776	-118.57	95.84
	185	100	8	1.790	0.771	-126.03	107.35
	115	140	8	6.018	8.968	-120.35	92.99
	185	140	8	1.832	0.748	-125.01	107.21
	115	100	16	16.279	30.226	-118.11	83.03
	185	100	16	2.751	2.344	-123.73	102.23
	115	140	16	15.181	29.394	-120.27	83.36
	185	140	16	2.075	0.785	-123.88	106.20
centre point	145	120	12	1.459	0.706	-126.96	108.98

The permeance of OPP itself (determined as described in Chapter 3) was $1.11 \cdot 10^{-6}$ cm/s, thus showing that depending on the sealing conditions permeances could be otained between 30% and 14 times the permeance of a truly perfectly hermetic seal.

The analysis of variance of the 2-level full factorial design with all 8 combinations of the 2 extreme values of each factor is given in table 8.2. For the SNR, as the method eliminates degrees of freedom due to data except for the 3-level interaction, effects that are not significant are pooled with the error until only statistically significant effects at 90% confidence level are left, i order to improve the estimate of the error.

It can be seen that within the margin of variability of the repeats sealing temperature has a marginally significant effect (significant at 90% confidence level, but not at 95%) on the effective permeance whereas the compression force has no influence at all. Sealing time and its interaction with temperature may however be relevant for repeatability, as they affect the SNR should the objective be a sealing as perfect as possible. Only temperature is relevant for conformity if the objective would be a higher permeance of the seal.

Table 8.2 - Analysis of variance of the effective permeances of the 2-level design. Raw sums of squares (SS) and probability of the null hypothesis are shown (p<0.1 is significant at a 90% confidence level. Statistically significant effects at 90% confidence level are highlighted in bold

Factors	P_a		SNR $_{\text{min}}$		SNR $_{\text{max}}$	
	SS	p	SS	p	SS	p
time (t)	291.55	0.276	**101.96**	**0.0043**	pooled	
force (F)	0.3617	0.9691	pooled		pooled	
t x w	4.8581	0.8871	pooled		pooled	
Temperature (T)	**725.77**	**0.0899**	**574.18**	**0.0002**	**56.933**	**0.0005**
1 x T	230.15	0.3321	**33.21**	**0.0292**	pooled	
F x T	0.1604	0.9794	pooled		pooled	
t x F x T	1.1393	0.9452	pooled		pooled	
error	7594.7		12		7.4502	
Total	8848.7		721.34		64.383	

Therefore, the best option for consistency is to target a minimum permeance, where using the highest temperature rather than the lowest is the key factor.

The effect of temperature in plastics is related to the properties of the polymer, and heat sealing is associated to the melting temperature (Yam 2010, Tongnuanchan et al. 2016). NVS films presented a melting temperature between 188.7 and 215.1, depending on the water content in the film. It might explain the dependence of temperature effect on force, as the temperature of the sealing machine was lower than the minimum required to melt the film, but as this is coated with an adhesive it may explain the sealing at the lower temperatures. Besides, temperature helps smooth the surface area and the pressure acts improving the contact between the thermoplastic materials (Yam 2010).

The effect of temperature on sealing was observed by Leminen et al. (2015) , but the melting temperature of their film was lower than the sealing temperature. The authors also identified empirically a dependence between temperature and sealing pressure, and concluded that the sealing pressure was the most important aspect with influence on the leakage, which corresponds to the compression force in the present work (pressure is the ratio between force and area).

The 2-level design has the advantage of allowing to test all interactions, but does not allow to analyse curvatures, that is, a point of optimum may exist within the solution space defined by the extremes. Adding the centre point to the analysis allows to assess this effect, albeit requiring now the use of a model to obtain the ANoVA results.

It is common to find in literature research involving a design of experiments without replicates, such as on the barrier properties of films (Tihminlioglu, Atik, and Özen 2010, Mali et al. 2004), other properties such as tensile strength and solubility (Tapia-Blácido, Sobral, and Menegalli 2005, Tao et al. 2007). Unreplicated 2^k design is perhaps the most used design, and by adding central replicates the results provide some assessment of the effect of curvature and an independent estimation of the error may be obtained (Montgomery 2013). Notwithstanding, unreplicated designs would be pointless for the purpose of this work where repeatability is the most important issue.

Full results are not shown, but they would indicate a negligible curvature (p=0.48), and similarly to table 8.2 results, temperature is the only significant effect with p between 0.05 and 0.1. Notwithstanding, table 1 shows that the middle point would be slightly better than combination 2 for lower permeance, lower standard deviation and higher SNR_{min}.

A more thorough assessment of variability is therefore needed. Dispersion effects F_i are those that affect the replication variance and exert a significant effect on the mean (or location) effect (Myers, Montgomery, and Anderson-Cook 2016). F_i may be calculated as the ratio between the average variance when factor i is positive and negative. A log transformation is recommended due to its efficiency in stabilizing variability (Montgomery 2013).

$$F_i = ln \left| \frac{\overline{s^2{}_{\imath+}}}{\overline{s^2{}_{\imath-}}} \right| \qquad (8.5)$$

where i is the number of effects and s^2 the variance.

An approximate normal distribution would result in both variances being equal and F_i close to zero suggests a variance that is not significant. The dispersion effects can be used to create normal plots and their normality evaluated. Points far from the straight line are the effects that are important to the dispersion of the variance (Montgomery 2013). The use of normal plots as a graphical valuable technique was suggested by Daniel (1976) and George and Meyer (1986) successfully applied it to study the dispersion effect by using the residuals of unreplicated experiments. Myers, Montgomery, and Anderson-Cook (2016) pinpointed that the dispersion effect could be analysed for both replicated and unreplicated data graphically via normal plots.

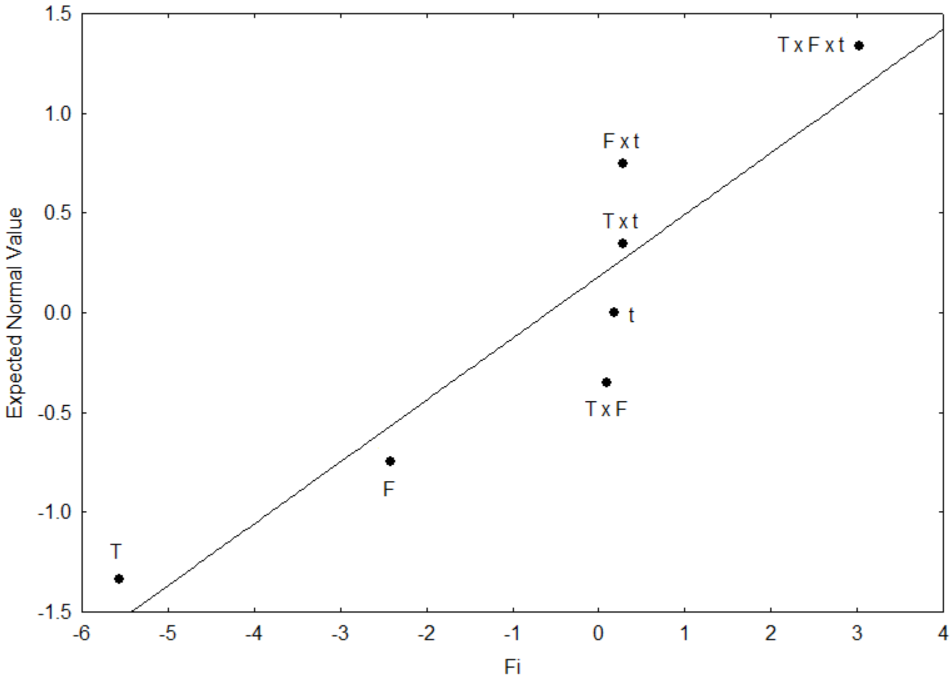

Figure 8.1- Normal plots of dispersion effects Fi, where T is the Temperature, F is Force and t is the time.

Fig. 8.3 indicates that the interactive effects between Temperature and Force (T x F) and Force and time (F x t) had the greatest effect on variability. The fact that the main effects had a lower influence on the variance, but the interaction effects were important, suggests that the effects of time, force and temperature are not independently additive and interactions would need to be considered. When the interaction is large, the main effects have less importance. In practice, it means that the effect of temperature tends to be dependent on the applied force (and vice versa), and force and time also depend on each other (Montgomery, Runger, and Hubele 2010). On the other hand, the interaction time-temperature was almost normal, and therefore did not have effect on the variance. The sealing time was high compared to the approx. 2 seconds recommended by the manufacturer, the 1 or 1.5 seconds used by Tongnuanchan et al. (2016) or the 2.5 seconds adopted by Leminen et al. (2015); however, it was not possible to seal the packages at a setting temperature of 3 in less than 8 seconds. In fact, at a setting temperature of 4, the minimum time required to seal a tray was 5 seconds. In high speed machineries, the sealing time tends to be around 1 second, and it is likely that force and temperature become even more relevant than time in these processes.

Therefore, even though the addition of the centre point gives negligible quadratic effects, it brings in a possible relevance of interactive effects within the solution space that the 2-level design (working only with points from the boundary of the solution space) did not identify.

8.4. CONCLUSION

The results indicated that in order to obtain reliable results of permeance of sealed packages, replicates are important to establish the variance and determine the settings that provide greater consistency. In the case studied, greater consistency was obtained with the lowest permeance. Although it is possible to seal the package with a permeance up to 3 times higher with some consistency, those conditions show a greater variability. The most influential factor was the sealing temperature, with the lowest temperature giving higher permeances and higher variability. The sealing leakage represented an increase of between 30% to 14 times the permeability of OPP itself, which emphasises the importance of establishing operating conditions that result in less variability in the sealing.

9. CONCLUSIONS AND RECOMMENDATIONS

9.1. GENERAL CONCLUSIONS

The research carried out in this three year-study showed that it is very important to design a package with a proper understanding of the effect of the storage conditions on its performance in the modulation of a protective environment, able to extend shelf life with security.

Perforated packages are frequently stacked, which tends to cover the perforation and compromise the packaging performance. Also, there is air movement surrounding the packaging either caused by the refrigeration system or simply from natural convection currents. This work provided data showing that air movement has significant impact on mass transfer coefficients, and therefore on the effective permeances of perforated packages. It was observed that the diameter of perforation has the greatest impact on the mass transfer coefficient, and temperature has a significant, but smaller effect. In addition, it was shown that a robust model developed in terms of dimensionless numbers can be constructed by applying the Buckingham$-\Pi$ Theorem and it was also shown that establishing other empirical relations can lead to overspecific or even inaccurate results. Ensuring that the Buckingham$-\Pi$ Theorem conditions are verified is therefore very important. The mathematical model obtained on this analysis was:

$$\frac{K}{v} = \beta_1 + \beta_2 \cdot Sc^{\beta_3} \cdot Pe^{\beta_4} \cdot \left(\frac{\Delta\chi}{\rho}\right)^{\beta_5}$$

Where Sc is the Schmidt number, Pe is the Peclet number, K is the mass transfer coefficient, v is the air velocity, $\Delta\chi$ is the concentration gradient across the perforation and ρ the density of the air. β_i are the i parameters obtained from the adjustment of the curve to the mass transfer coefficient obtained experimentally for oxygen and for water vapour. The Schmidt number varied very little and for the range of conditions tested the models could be simplified to, within the margin of variability between repeats and model lack of fit:

oxygen: $\frac{K}{v} = \frac{0.893}{Pe}$

water vapour: $\frac{K}{v} = 0.070 + \frac{174.407}{Pe^2}$

Relative humidity and actual gas composition also affected both O_2 and water vapour permeability and thus design of packaging of products that are subjected to different conditions should not rely on data obtained under standard conditions. This is especially dramatic for water transport through biobased materials, where temperature and water concentration exert great impact on the polymer properties. It is shown that in this case the most appropriate is to provide complete information on the water adsorption-desorption profile and dependence of Diffusion and Permeability on the water content. for water plasticizing effects, an appropriate description of water vapour permeance was obtained for NVS films combining sorption isotherms with Gordon-Taylor and WLF equations. At 5 ^{o}C the adsorption isotherm of NVS films was well described by Park's model with A_L = 0.10, b_L = 1496.942, K_H = 0, K_a = 0.275 and n = 2.09 for adsoprtion and: A_L =0.059, b_L = 1496.941, K_H = 0, K_a = 0.537 and n = 126.108 for desorption. The parameters obtained for WLF and Gordon-Taylor equations were C_1 = 2.86, K = 1.20, C_2 = 23.9and Dwg = $8.27 \cdot 10^{-14}$ cm^2/s, with the T_g of the dry polymer determined experimetnally at 125 ^{o}C.

Finally, it was also illustrated how the operating parameters of a packaging sealing machine can be tuned to provide the most consistent effective permeability, that is, attempting to have seals as providing some contribution to the permeance that is as consistent as possible. It is better to have a somewhat permeable seal provided that the permeability it gives is consistent, as then the package can be properly designed accounting for the seal, this will be a more robust system, with less losses.

9.2. FUTURE WORK

Results of this work indicate that it is highly recommended that research on hydrophilic films presents data of isotherms of sorption-desorption, and data on the integrated model of WLF and G-T equations, as presented in this research. Predicting WVP implies describing Diffusion and phase equilibrium in the films at any desired condition of analysis. Hence, it is imperative that the WVP obtained under a specific condition of relative humidity (internal and external) not be used to predict behaviour under different conditions, as WVP can be highly dependent on water content. More word is therefore needed regarding the influence of humidity and water content on permeability.

The next step in the study of Mass Transport in Food Packaging should definitely be to include ethylene in the analysis. It may affect respiration rates substantially in ways that have not been properly quantified yet with appropriate models. Furthermore, ts presence might affect the mass transport of the other gases through perforations, and as ethylene is an organic gas, it is possible that it would also affect the diffusion through the polymer. Therefore, an accurate design of MAP for climacteric produce should take into account the effect of ethylene.

Water vapour transport through perforations were analysed under a higher relative humidity outside than inside the package. It is likely that the effect of air velocity on the mass transfer coefficient when the gradient is the other way around will be different, due to the vapour pressure reduction due to the air movement and consequent influence on the actual relative humidity in contact with the package surface. If the relative humidity on the outside is smaller than inside, and the air velocity is likely to decrease the vapour pressure even more, the relative humidity gradient will tend to be greater in practice than if the relative humidity outside was the highest. Therefore, the mass transfer coefficient of water vapour through perforations is likely to be different in both cases. As fruits and vegetables tend to be stored at an ambient relative humidity lower than inside the packaging, there is a chance that the model proposed in this work will not cover properly a scenario more similar to a real condition of storage. Hence, it might be necessary to investigate the mass transfer coefficient of water vapour through perforations with relative humidity gradients more similar to real conditions of storage, and obtain the parameters that apply to this situation.

REFERENCES

Abdillahi, H., E. Chabrat, A. Rouilly, and L. Rigal. 2013. "Influence of citric acid on thermoplastic wheat flour/poly(lactic acid) blends. II. Barrier properties and water vapor sorption isotherms." *Industrial Crops and Products* no. 50:104-111. doi: http://dx.doi.org/10.1016/j.indcrop.2013.06.028.

Aguirre-Loredo, Rocio Yaneli, Adriana Inés Rodriguez-Hernandez, and Gonzalo Velazquez. 2017. "Modelling the effect of temperature on the water sorption isotherms of chitosan films." *Food Science and Technology (Campinas)* no. 37:112-118.

Ahmed, S.G. 1999. "An approximate method for oxygen diffusion in a sphere with simultaneous absorption." *International Journal of Numerical Methods for Heat & Fluid Flow* no. 9 (6):631-643. doi: doi:10.1108/09615539910276115.

Akanbi, Charles Taiwo, Remi Sikiru Adeyemi, and Ademola Ojo. 2006. "Drying characteristics and sorption isotherm of tomato slices." *Journal of Food Engineering* no. 73 (2):157-163. doi: http://dx.doi.org/10.1016/j.jfoodeng.2005.01.015.

Al-Muhtaseb, A. H., W. A. M. McMinn, and T. R. A. Magee. 2002. "Moisture Sorption Isotherm Characteristics of Food Products: A Review." *Food and Bioproducts Processing* no. 80 (2):118-128. doi: http://dx.doi.org/10.1205/09603080252938753.

Alix, S., E. Philippe, A. Bessadok, L. Lebrun, C. Morvan, and S. Marais. 2009. "Effect of chemical treatments on water sorption and mechanical properties of flax fibres." *Bioresource Technology* no. 100 (20):4742-4749. doi: https://doi.org/10.1016/j.biortech.2009.04.067.

Allan-Wojtas, P., C. F. Forney, L. Moyls, and D. L. Moreau. 2008. "Structure and gas transmission characteristics of microperforations in plastic films." *Packaging Technology and Science* no. 21 (4):217-229. doi: 10.1002/pts.804.

Almenar, Eva, and Rafael Auras. 2010. "Permeation, Sorption, and Diffusion in Poly(Lactic Acid)." In *Poly(Lactic Acid)*, 155-179. John Wiley & Sons, Inc.

Amorós, A., M. T. Pretel, P. J. Zapata, M. A. Botella, F. Romojaro, and M. Serrano. 2008. "Use of Modified Atmosphere Packaging with

Microperforated Polypropylene Films to Maintain Postharvest Loquat Fruit Quality." *Revista de Agaroquimica y Tecnologia de Alimentos* no. 14 (1):95-103. doi: 10.1177/1082013208089985.

Arvanitoyannis, Ioannis, and Costas G. Biliaderis. 1998. "Physical properties of polyol-plasticized edible films made from sodium caseinate and soluble starch blends." *Food Chemistry* no. 62 (3):333-342. doi: http://dx.doi.org/10.1016/S0308-8146(97)00230-6.

Astarita, Gianni. 1997. "Dimensional analysis, scaling, and orders of magnitude." *Chemical Engineering Science* no. 52 (24):4681-4698. doi: http://dx.doi.org/10.1016/S0009-2509(97)85420-6.

ASTM 96. 1995. ASTM 96: Standard Test Methods for Water Vapor Transmission of Materials. In *Annual Book of ASTM Standards*. Conshohocken, PA: ASTM.

Auras, R.A., L.T. Lim, S.E.M. Selke, and H. Tsuji. 2010. *Poly(lactic acid): Synthesis, Structures, Properties, Processing, and Applications*: Wiley.

Auras, Rafael A., Bruce Harte, Susan Selke, and Ruben Hernandez. 2003. "Mechanical, Physical, and Barrier Properties of Poly(Lactide) Films." *Journal of Plastic Film & Sheeting* no. 19 (2):123-135. doi: doi:10.1177/8756087903039702.

Auras, Rafael, Bruce Harte, and Susan Selke. 2004. "Effect of water on the oxygen barrier properties of poly(ethylene terephthalate) and polylactide films." *Journal of Applied Polymer Science* no. 92 (3):1790-1803. doi: 10.1002/app.20148.

Azeredo, Henriette M. C. de. 2009. "Nanocomposites for food packaging applications." *Food Research International* no. 42 (9):1240-1253. doi: http://dx.doi.org/10.1016/j.foodres.2009.03.019.

Baehr, H.D., and K. Stephan. 2006. *Heat and Mass Transfer*: Springer Berlin Heidelberg.

Ballantyne, A., R. Stark, and J. D. Selman. 1988. "Modified atmosphere packaging of shredded lettuce." *International Journal of Food Science & Technology* no. 23 (3):267-274. doi: 10.1111/j.1365-2621.1988.tb00578.x.

Basu, Santanu, U. S. Shivhare, and A. S. Mujumdar. 2006. "Models for Sorption Isotherms for Foods: A Review." *Drying Technology* no. 24 (8):917-930. doi: 10.1080/07373930600775979.

Beaudry, R. M. 1999. "Effect of O2 and CO2 partial pressure on selected phenomena affecting fruit and vegetable quality." *Postharvest Biology and Technology* no. 15 (3):293-303. doi: http://dx.doi.org/10.1016/S0925-5214(98)00092-1.

Becker, B. B., and B. A. Fricke. 1996. "Transpiration and respiration of fruits and vegetables." *New Developments in Refrigeration for Food Safety and Quality.*

Becker, Bryan R. , and Brian A. Fricke. 2015. *Transpiration and Respiration of Fruits and Vegetables* 2015 [cited July 17th 2015]. Available from b.web.umkc.edu/beckerb/publications/chapters/trans_resp.pdf.

Becker, Bryan R., Anil Misra, and Brian A. Fricke. 1996. "Bulk Refrigeration of Fruits and Vegetables Part I: Theoretical Considerations of Heat and Mass Transfer." *HVAC&R Research* no. 2 (2):122-134. doi: 10.1080/10789669.1996.10391338.

Behkam, Bahareh, and Metin Sitti. 2004. "E. Coli Inspired Propulsion for Swimming Microrobots." (47063):1037-1041. doi: 10.1115/IMECE2004-59621.

Belbekhouche, Sabrina, Julien Bras, Gilberto Siqueira, Corinne Chappey, Laurent Lebrun, Bertine Khelifi, Stéphane Marais, and Alain Dufresne. 2011. "Water sorption behavior and gas barrier properties of cellulose whiskers and microfibrils films." *Carbohydrate Polymers* no. 83 (4):1740-1748. doi: http://dx.doi.org/10.1016/j.carbpol.2010.10.036.

Ben-Yehoshua, S., and A. C. Cameron. 1989. "Exchange Determination of Water Vapor, Carbon Dioxide, Oxygen, Ethylene, and Other Gases of Fruits and Vegetables." In *Gases in Plant and Microbial Cells*, edited by Hans-Ferdinand Linskens and John F. Jackson, 177-193. Berlin, Heidelberg: Springer Berlin Heidelberg.

Ben-Yehoshua, Shimshon, Stanley P. Burg, and Roger Young. 1985. "Resistance of Citrus Fruit to Mass Transport of Water Vapor and Other Gases." *Plant Physiology* no. 79 (4):1048-1053. doi: 10.1104/pp.79.4.1048.

Ben-Yehoshua, Shimshon, and Victor Rodov. 2002. "Transpiration and Water Stress." In *Postharvest Physiology and Pathology of Vegetables*. CRC Press.

Ben-Yehoshua, Shimshon, Victor Rodov, and Jacob Perzelan. 2009. Control of water condensation and effects of perforation of the plastic film of the sealed. Paper read at 10th International Controlled & Modified Atmosphere Research Conference,, at Antalya, Turkey.

Bilck, Ana Paula, Maria V. E. Grossmann, and Fabio Yamashita. 2010. "Biodegradable mulch films for strawberry production." *Polymer Testing* no. 29 (4):471-476. doi: http://dx.doi.org/10.1016/j.polymertesting.2010.02.007.

Biliaderis, C. G., A. Lazaridou, and I. Arvanitoyannis. 1999. "Glass transition and physical properties of polyol-plasticised pullulan–starch blends at low moisture." *Carbohydrate Polymers* no. 40 (1):29-47. doi: http://dx.doi.org/10.1016/S0144-8617(99)00026-0.

Bird, R. B., W. E. Stewart, and E. N. Lightfoot. 2007. *Transport phenomena, Inc.* 2nd. Edition ed, *AIChE Journal*. New York - USA: John Wiley and Sons Inc.

Blaney, C.A., W.F. Cartwright, and D.C. Strack. 2000. Microporous film containing a microbial adsorbent. Google Patents.

Bovi, Graziele G., Oluwafemi J. Caleb, Manfred Linke, Cornelia Rauh, and Pramod V. Mahajan. 2016. "Transpiration and moisture evolution in packaged fresh horticultural produce and the role of integrated mathematical models: A review." *Biosystems Engineering* no. 150:24-39. doi: http://dx.doi.org/10.1016/j.biosystemseng.2016.07.013.

Brandelero, Renata P. Herrera, Maria Victória Grossmann, and Fabio Yamashita. 2013. "Hidrofilicidade de filmes de amido/poli(butileno adipato co-tereftalato) (Pbat) adicionados de tween 80 e óleo de soja." *Polímeros* no. 23:270-275.

Briassoulis, Demetrios, Antonios Mistriotis, Anastasios Giannoulis, and Dimitrios Giannopoulos. 2013. "Optimized PLA-based EMAP systems for horticultural produce designed to regulate the targeted in-package atmosphere." *Industrial Crops and Products* no. 48 (0):68-80. doi: http://dx.doi.org/10.1016/j.indcrop.2013.03.017.

Brunauer, Stephen, Lola S. Deming, W. Edwards Deming, and Edward Teller. 1940. "On a Theory of the van der Waals Adsorption of Gases." *Journal of the American Chemical Society* no. 62 (7):1723-1732. doi: 10.1021/ja01864a025.

Brunauer, Stephen, P. H. Emmett, and Edward Teller. 1938. "Adsorption of Gases in Multimolecular Layers." *Journal of the American Chemical Society* no. 60 (2):309-319. doi: 10.1021/ja01269a023.

Buckingham, E. 1914. "On physically similar systems." *Phys. Rev.* no. 4 (2):345.

Cairncross, Richard A., Jeffrey G. Becker, Shri Ramaswamy, and Ryan O’Connor. 2006. "Moisture Sorption, Transport, and Hydrolytic Degradation in Polylactide." In *Twenty-Seventh Symposium on Biotechnology for Fuels and Chemicals*, edited by James D. McMillan, William S. Adney, Jonathan R. Mielenz and K. Thomas Klasson, 774-785. Totowa, NJ: Humana Press.

Calado, V., and D.C. Montgomery. 2003. *Planejamento de Experimentos usando o Statistica*: E-Papers Serviços Editoriais.

Calado, Veronica M. A., and Andresa Ramos. 2016. "Applications of Starch Nanocrystal-based Blends, Composites and Nanocomposites." In *Starch-based Blends, Composites and Nanocomposites*, 143-216. The Royal Society of Chemistry.

Caleb, Oluwafemi J., Kathrin Ilte, Antje Fröhling, Martin Geyer, and Pramod V. Mahajan. 2016. "Integrated modified atmosphere and humidity package design for minimally processed Broccoli (Brassica oleracea L. var. italica)." *Postharvest Biology and Technology* no. 121:87-100. doi: http://dx.doi.org/10.1016/j.postharvbio.2016.07.016.

Caner, C., P. J. Vergano, and J. L. Wiles. 1998. "Chitosan Film Mechanical and Permeation Properties as Affected by Acid, Plasticizer, and Storage." *Journal of Food Science* no. 63 (6):1049-1053. doi: 10.1111/j.1365-2621.1998.tb15852.x.

Canevarolo, S. V. 2006. *Ciencia de Polímeros: um texto básico para tecnólogos e engenheiros*. São Paulo: Artliber Editora.

Cantwell, Marita I., and Michael S. Reid. 1993. "Postharvest Physiology and Handling of Fresh Culinary Herbs." *Journal of Herbs, Spices & Medicinal Plants* no. 1 (3):93-127. doi: 10.1300/J044v01n03_09.

Cassini, A. S., L. D. F. Marczak, and C. P. Z. Noreña. 2006. "Water adsorption isotherms of texturized soy protein." *Journal of Food Engineering* no. 77 (1):194-199. doi: http://dx.doi.org/10.1016/j.jfoodeng.2005.05.059.

Cerqueira, Miguel A., Bartolomeu W. S. Souza, José A. Teixeira, and António A. Vicente. 2012. "Effects of Interactions between the Constituents of Chitosan-Edible Films on Their Physical Properties." *Food and Bioprocess Technology* no. 5 (8):3181-3192. doi: 10.1007/s11947-011-0663-y.

Chang, Y. P., A. Abd Karim, and C. C. Seow. 2006. "Interactive plasticizing–antiplasticizing effects of water and glycerol on the tensile properties of tapioca starch films." *Food Hydrocolloids* no. 20 (1):1-8. doi: http://dx.doi.org/10.1016/j.foodhyd.2005.02.004.

Chang, Y. P., P. B. Cheah, and C. C. Seow. 2000. "Plasticizing—Antiplasticizing Effects of Water on Physical Properties of Tapioca Starch Films in the Glassy State." *Journal of Food Science* no. 65 (3):445-451. doi: 10.1111/j.1365-2621.2000.tb16025.x.

Charlon, Sébastien, Nadège Follain, Jérémie Soulestin, Michel Sclavons, and Stéphane Marais. 2017. "Water Transport Properties of Poly(butylene succinate) and Poly[(butylene succinate)-co-(butylene adipate)] Nanocomposite Films: Influence of the Water-Assisted Extrusion Process." *The Journal of Physical Chemistry C* no. 121 (1):918-930. doi: 10.1021/acs.jpcc.6b11077.

Chaudhary, Deeptangshu S., Benu P. Adhikari, and Stefan Kasapis. 2011. "Glass-transition behaviour of plasticized starch biopolymer system – A modified Gordon–Taylor approach." *Food Hydrocolloids* no. 25 (1):114-121. doi: https://doi.org/10.1016/j.foodhyd.2010.06.002.

Cheng, Hongyuan, and Alan Friis. 2010. "Modelling extrudate expansion in a twin-screw food extrusion cooking process through dimensional analysis methodology." *Food and Bioproducts Processing* no. 88 (2–3):188-194. doi: https://doi.org/10.1016/j.fbp.2010.01.001.

Chitarra, A. B., and R. E Alves. 2001. *Tecnologia de Pós Colheita para Frutas Tropicais*. Fortaleza, CE: FRUTAL'2001.

Chitarra, M. I. F., and A. B. Chitarra. 2005. *Pós-Colheita de Frutas e Hortaliças: Fisiologia e Manuseio*. 2 ed. Lavras (MG) - Brazil.

Choudalakis, G., and A. D. Gotsis. 2009. "Permeability of polymer/clay nanocomposites: A review." *European Polymer Journal* no. 45 (4):967-984. doi: http://dx.doi.org/10.1016/j.eurpolymj.2009.01.027.

Chung, Donghwan, Spyridon E. Papadakis, and Kit L. Yam. 2003. "Simple models for evaluating effects of small leaks on the gas barrier properties of food packages." *Packaging Technology and Science* no. 16 (2):77-86. doi: 10.1002/pts.616.

Cliffe-Byrnes, V., C. P. Mc Laughlin, and D. O'Beirne. 2003. "The effects of packaging film and storage temperature on the quality of a dry coleslaw mix packaged in a modified atmosphere." *International Journal of Food Science & Technology* no. 38 (2):187-199. doi: 10.1046/j.1365-2621.2003.00658.x.

Colak, Basak Yilin, Fabrice Gouanve, Pascal Degraeve, Eliane Espuche, and Frédéric Prochazka. 2015. "Study of the influences of film processing conditions and glycerol amount on the water sorption and gas barrier properties of novel sodium caseinate films." *Journal of Membrane Science* no. 478:1-11. doi: http://dx.doi.org/10.1016/j.memsci.2014.12.027.

Crank, J. 1975. *The Mathematics of Diffusion*. 2nd ed. Bristol, England: Oxford University Press.

Curtis, W. D., J. David Logan, and W. A. Parker. 1982. "Dimensional analysis and the pi theorem." *Linear Algebra and its Applications* no. 47 (0):117-126. doi: http://dx.doi.org/10.1016/0024-3795(82)90229-4.

Cussler, E. L. 2009. *Diffusion: Mass Transfer in Fluid Systems*. Third Ed. ed: Cambridge University Press.

Damodaran, S., K.L. Parkin, and O.R. Fennema. 2007. *Fennema's Food Chemistry, Fourth Edition*: Taylor & Francis.

Daniel, C. 1976. *Applications of Statistics to Industrial Experimentation*: Wiley.

de la Cruz, G. Velázquez, J. A. Torres, and M. O. Martín-Polo. 2001. "Temperature effect on the moisture sorption isotherms for methylcellulose and ethylcellulose films." *Journal of Food Engineering* no. 48 (1):91-94. doi: http://dx.doi.org/10.1016/S0260-8774(00)00143-6.

de Souza Mendes, Paulo R. 2007. "Dimensionless non-Newtonian fluid mechanics." *Journal of Non-Newtonian Fluid Mechanics* no. 147 (1–2):109-116. doi: http://dx.doi.org/10.1016/j.jnnfm.2007.07.010.

Debongnie, Jean-François. 2016. Sur le théorème de Vaschy-Buckingham. ULg/LMF.

DeELL, Jennifer R. , Robert K. Prange, and Herman W. Peppelenbos. 2003. "Postharvest Physiology of Fresh Fruits and Vegetables." In *Handbook of Postharvest Technology: Cereals, Fruits, Vegetables, Tea, and Spices.* , edited by Amalendu Chakraverty, Arun S. Mujumdar, G. S. Vijaya-Raghavan and Hosahalli S. Ramaswamy, 455-483. New York, USA: Marcel Dekker.

Del-Valle, V., E. Almenar, J. M. Lagarón, R. Catalá, and R. Gavara. 2003. "Modelling permeation through porous polymeric films for modified atmosphere packaging." *Food Additives & Contaminants* no. 20 (2):170-179. doi: 10.1080/0265203021000042869.

Delaplace, G., K. Loubière, F. Ducept, and R. Jeantet. 2015a. "Appendix 2 - Physical Meaning of Dimensionless Numbers Commonly Used in Process Engineering A2 - Delaplace, Guillaume." In *Dimensional Analysis of Food Process*, edited by Karine Loubière, Fabrice Ducept and Romain Jeantet, 279-293. Elsevier.

Delaplace, Guillaume, Karine Loubière, Fabrice Ducept, and Romain Jeantet. 2015b. "1 - Objectives and Value of Dimensional Analysis." In *Dimensional Analysis of Food Process*, 1-11. Elsevier.

Delaplace, Guillaume, Karine Loubière, Fabrice Ducept, and Romain Jeantet. 2015c. "2 - Dimensional Analysis: Principles and Methodology." In *Dimensional Analysis of Food Process*, 13-59. Elsevier.

Detallante, Virginie, Dominique Langevin, Corinne Chappey, Michel Métayer, Régis Mercier, and Michel Pinéri. 2001. "Water vapor sorption in naphthalenic sulfonated polyimide membranes." *Journal of Membrane Science* no. 190 (2):227-241. doi: http://dx.doi.org/10.1016/S0376-7388(01)00437-9.

Doty, Paul M., Captain Wm H. Aiken, and Hermann Mark. 1944. "Water Vapor Permeability of Organic Films." *Industrial & Engineering Chemistry Analytical Edition* no. 16 (11):686-690. doi: 10.1021/i560135a007.

Douglas, B. 2004. Packaging machine for producing reclosable packages. Google Patents.

Du, An, Donghun Koo, Grayce Theryo, Marc A. Hillmyer, and Richard A. Cairncross. 2012. "Water transport and clustering behavior in homopolymer and graft copolymer polylactide." *Journal of Membrane Science* no. 396:50-56. doi: http://dx.doi.org/10.1016/j.memsci.2011.12.030.

Dukalska, Lija, Eva Ungure, Ingrida Augspole, Sandra Muizniece-Brasava, Vita Levkane, Rakcejeva Tatjana, and Inta Krasnova. 2013. Evaluation of the Influence of Various Biodegradable Packaging Materials on the Quality and Shelf Life of Different Food Products. In *Proceedings of the Latvia University of Agriculture*.

Emond, J. P., F. Castaigne, C. J. Toupin, and D. Desilets. 1991. "Mathematical modeling of gas exchange in modified atmosphere packaging." no. 34 (1). doi: 10.13031/2013.31652.

Emond, J. P., K. V. Chau, J. K. Brecht, and M. O. Ngadi. 1998. "MATHEMATICAL MODELING OF GAS CONCENTRATION PROFILES IN MODIFIED ATMOSPHERE BULK PACKAGES." no. 41 (4). doi: 10.13031/2013.17236.

Emond, Jean Pierre. 1992. *Mathematical modeling of gas concentration profiles in perforation-generated modified atmosphere bulk packaging*, University of Florida.

Eskin, N. A. Michael, and Ernst Hoehn. 2013. "Chapter 2 - Fruits and Vegetables." In *Biochemistry of Foods (Third Edition)*, 49-126. San Diego: Academic Press.

Exama, A., J. Arul, R. W. Lencki, L. Z. Lee, and C. Toupin. 1993. "Suitability of Plastic Films for Modified Atmosphere Packaging of Fruits and Vegetables." *Journal of Food Science* no. 58 (6):1365-1370. doi: 10.1111/j.1365-2621.1993.tb06184.x.

Fajardo, P., J. T. Martins, C. Fuciños, L. Pastrana, J. A. Teixeira, and A. A. Vicente. 2010. "Evaluation of a chitosan-based edible film as carrier of natamycin to improve the storability of Saloio cheese." *Journal of Food Engineering* no. 101 (4):349-356. doi: http://dx.doi.org/10.1016/j.jfoodeng.2010.06.029.

Fellows, P. J. 2009. "Packaging." In *Food Processing Technology: Principles and Practice*, edited by P. J. Fellows, 713-781. CRC Press.

Ferreira, Ana R. V., Cristiana A. V. Torres, Filomena Freitas, Chantal Sevrin, Christian Grandfils, Maria A. M. Reis, Vítor D. Alves, and Isabel M. Coelhoso. 2016. "Development and characterization of bilayer films of FucoPol and chitosan." *Carbohydrate Polymers* no. 147:8-15. doi: http://dx.doi.org/10.1016/j.carbpol.2016.03.089.

Ferry, J.D. 1980. *Viscoelastic Properties of Polymers*: Wiley.

Finnegan, Elizabeth M. 2014. *Technology and raw material quality to underpin the Irish fresh-cut fruit industry* Department of Life Sciences, Faculty of Science and Engineering, University of Limerick, Ireland.

Finnigan, Bradley. 2009. "Barrier Polymers." In *The Wiley Encyclopedia of Packaging Technology*, edited by K.L. Yam. Hoboken NJ, USA: J. WIley & Sons.

Fishman, S., V. Rodov, and S. BenYehoshua. 1996. "Mathematical model for perforation effect on oxygen and water vapor dynamics in modified-atmosphere packages." *Journal of Food Science* no. 61 (5):956-961. doi: 10.1111/j.1365-2621.1996.tb10910.x.

Follain, N., B. Alexandre, C. Chappey, L. Colasse, P. Médéric, and S. Marais. 2016. "Barrier properties of polyamide 12/montmorillonite nanocomposites: Effect of clay structure and mixing conditions." *Composites Science and Technology* no. 136:18-28. doi: http://dx.doi.org/10.1016/j.compscitech.2016.09.023.

Fonseca, Susana C., Fernanda A. R. Oliveira, Isabel B. M. Lino, Jeffrey K. Brecht, and Khe V. Chau. 2000. "Modelling O2 and CO2 exchange for development of perforation-mediated modified atmosphere packaging." *Journal of Food Engineering* no. 43 (1):9-15. doi: http://dx.doi.org/10.1016/S0260-8774(99)00122-3.

Foo, K. Y., and B. H. Hameed. 2010. "Insights into the modeling of adsorption isotherm systems." *Chemical Engineering Journal* no. 156 (1):2-10. doi: http://dx.doi.org/10.1016/j.cej.2009.09.013.

Foust, A.S. 1980. *Principles of unit operations*: Wiley.

Galus, Sabina, and Andrzej Lenart. 2013. "Development and characterization of composite edible films based on sodium alginate and pectin." *Journal of Food Engineering* no. 115 (4):459-465. doi: http://dx.doi.org/10.1016/j.jfoodeng.2012.03.006.

Geankoplis, C.J. 1993. *Transport Processes and Unit Operations*: PTR Prentice Hall.

Geankoplis, Christie John. 2003. *Transport Processes and Separation Process Principles*. Edited by Inc. Pearson Education. Forth Edition ed. New Jersey - USA: Bernard goodwin.

Gekas, Vassilis, and Bengt Hallström. 1987. "Mass transfer in the membrane concentration polarization layer under turbulent cross flow : I. Critical literature review and adaptation of existing sherwood correlations to membrane operations." *Journal of Membrane Science* no. 30 (2):153-170. doi: http://dx.doi.org/10.1016/S0376-7388(00)81349-6.

George, E. P. Box, and R. Daniel Meyer. 1986. "An Analysis for Unreplicated Fractional Factorials." *Technometrics* no. 28 (1):11-18. doi: 10.2307/1269599.

Ghanbarzadeh, Babak, and A. R. Oromiehi. 2008. "Studies on glass transition temperature of mono and bilayer protein films plasticized by glycerol and olive oil." *Journal of Applied Polymer Science* no. 109 (5):2848-2854. doi: 10.1002/app.28289.

Ghosh, V., and R. C. Anantheswaran. 2001. "Oxygen transmission rate through micro-perforated films: Measurement and model comparison." *Journal of Food Process Engineering* no. 24 (2):113-133. doi: 10.1111/j.1745-4530.2001.tb00535.x.

Giles, Charles H., David Smith, and Alan Huitson. 1974. "A general treatment and classification of the solute adsorption isotherm. I. Theoretical." *Journal of Colloid and Interface Science* no. 47 (3):755-765. doi: http://dx.doi.org/10.1016/0021-9797(74)90252-5.

Goldstein, Martin. 1985. "Glass temperature mixing relations and thermodynamics." *Macromolecules* no. 18 (2):277-280.

Gontard, N., and S. Ring. 1996. "Edible Wheat Gluten Film: Influence of Water Content on Glass Transition Temperature." *Journal of Agricultural and Food Chemistry* no. 44 (11):3474-3478. doi: 10.1021/jf960230q.

Gontard, Nathalie, Christophe Duchez, Jean-Louis Cuq, and StÉPhane Guilbert. 1994. "Edible composite films of wheat gluten and lipids: water vapour permeability and other physical properties." *International Journal of Food Science & Technology* no. 29 (1):39-50. doi: 10.1111/j.1365-2621.1994.tb02045.x.

González-Buesa, Jaime, Ana Ferrer-Mairal, Rosa Oria, and María L. Salvador. 2009. "A mathematical model for packaging with microperforated films of fresh-cut fruits and vegetables." *Journal of Food Engineering* no. 95 (1):158-165. doi: http://dx.doi.org/10.1016/j.jfoodeng.2009.04.025.

González-Buesa, Jaime, Ana Ferrer-Mairal, Rosa Oria, and María L. Salvador. 2013. "Alternative Method for Determining O2 and CO2 Transmission Rates Through Microperforated Films for Modified Atmosphere Packs." *Packaging Technology and Science* no. 26 (7):413-421. doi: 10.1002/pts.1988.

González, Jaime, Ana Ferrer, Rosa Oria, and Maria L. Salvador. 2008. "Determination of O2 and CO2 transmission rates through microperforated films for modified atmosphere packaging of fresh fruits and vegetables." *Journal of Food Engineering* no. 86 (2):194-201. doi: http://dx.doi.org/10.1016/j.jfoodeng.2007.09.023.

Gordon, Manfred, and James S. Taylor. 1952. "Ideal copolymers and the second-order transitions of synthetic rubbers. i. non-crystalline copolymers." *Journal of Applied Chemistry* no. 2 (9):493-500. doi: 10.1002/jctb.5010020901.

Gouanvé, F., S. Marais, A. Bessadok, D. Langevin, C. Morvan, and M. Métayer. 2006. "Study of water sorption in modified flax fibers." *Journal of Applied Polymer Science* no. 101 (6):4281-4289. doi: 10.1002/app.23661.

Gregg, SJ, and Kenneth SW Sing. 1983. "Adsorption, surface area, and porosity."

Grimvall, Göran. 1999. "Appendix A - Buckingham's Π-theorem." In *Thermophysical Properties of Materials*, edited by Göran Grimvall, 353-355. Amsterdam: Elsevier Science B.V.

Guerrero, Saul J. 1989. "Antiplasticization and crystallinity in poly(vinyl chloride)." *Macromolecules* no. 22 (8):3480-3485. doi: 10.1021/ma00198a046.

Guillaume, Carole, Valérie Guillard, and Nathalie Gontard. 2010. "Modified Atmosphere Packaging of Fruits and Vegetables." In *Advances in Fresh-Cut Fruits and Vegetables Processing*, 255-284. CRC Press.

Guo, Jian-Hwa. 1993. "Effects of Plasticizers on Water Permeation and Mechanical Properties of Cellulose Acetate: Antiplasticization in Slightly Plasticized Polymer Film." *Drug Development and Industrial Pharmacy* no. 19 (13):1541-1555. doi: 10.3109/03639049309069325.

Han, J.H. 2014. *Innovations in Food Packaging*: Elsevier Science.

Han, Jung H., and Martin G. Scanlon. 2014. "Chapter 3 - Mass Transfer of Gas and Solute Through Packaging Materials." In *Innovations in Food Packaging (Second Edition)*, 37-49. San Diego: Academic Press.

Hauser, Paul M., and A. Douglas McLaren. 1948. "Permeation through and Sorption of Water Vapor by High Polymers." *Industrial & Engineering Chemistry* no. 40 (1):112-117. doi: 10.1021/ie50457a032.

Heiss, Rudolf. 1949. "Die Verpackung feuchtigkeitsemphndlicher Lebensmittel." *Zeitschrift für Lebensmittel-Untersuchung und Forschung* no. 89 (2):173-183. doi: 10.1007/BF00705049.

Hertog, M. L. A. T. M., H. A. M. Boerrigter, G. J. P. M. van den Boogaard, L. M. M. Tijskens, and A. C. R. van Schaik. 1999. "Predicting keeping quality of strawberries (cv. `Elsanta') packed under modified atmospheres: an integrated model approach." *Postharvest Biology and Technology* no. 15 (1):1-12. doi: http://dx.doi.org/10.1016/S0925-5214(98)00061-1.

Holm, Vibeke K., Sokol Ndoni, and Jens Risbo. 2006. "The Stability of Poly(lactic acid) Packaging Films as Influenced by Humidity and Temperature." *Journal of Food Science* no. 71 (2):E40-E44. doi: 10.1111/j.1365-2621.2006.tb08895.x.

Hong, S. I., and J. M. Krochta. 2003. "Oxygen Barrier Properties of Whey Protein Isolate Coatings on Polypropylene Films." *Journal of Food Science* no. 68 (1):224-228. doi: 10.1111/j.1365-2621.2003.tb14143.x.

Hussein, Zaharan, Oluwafemi J. Caleb, and Umezuruike Linus Opara. 2015. "Perforation-mediated modified atmosphere packaging of fresh and minimally processed produce—A review." *Food Packaging and Shelf Life* no. 6:7-20. doi: http://dx.doi.org/10.1016/j.fpsl.2015.08.003.

Ignacio, Lira. 2013. "Dimensional analysis made simple." *European Journal of Physics* no. 34 (6):1391.

Innovia. 2016. *NatureFlex^{TM} NVS - Data*. Innovia Films Company 2015 [cited 20/01/2016 2016]. Available from http://www.innoviafilms.com/Our-Products/Packaging/NatureFlex%E2%84%A2-NVS.aspx.

Ishikawa, D., T. Shinohara, Y. Kobayashi, H. Tanaka, T. Maru, H. Kohno, and M. Akamatsu. 2014. Heat-insulating packaging film, packaging bag, and packaging bag having opening member. Google Patents.

James, C.W. 2007. *Gas Transport in Proton Exchange Membranes for Use in Fuel Cell Applications* Chemical Engineering, Faculty of the Virginia Polytechnic Institute and State University, Blacksburg, VA , USA.

Jangchud, A., and M. S. Chinnan. 1999. "Properties of Peanut Protein Film: Sorption Isotherm and Plasticizer Effect." *LWT - Food Science and Technology* no. 32 (2):89-94. doi: http://dx.doi.org/10.1006/fstl.1998.0498.

Javaherdeh, K., Mehrzad Mirzaei Nejad, and M. Moslemi. 2015. "Natural convection heat and mass transfer in MHD fluid flow past a moving vertical plate with variable surface temperature and concentration in a porous medium." *Engineering Science and Technology, an*

International Journal no. 18 (3):423-431. doi: http://dx.doi.org/10.1016/j.jestch.2015.03.001.

Jenckel, Ernst, and Rudolf Heusch. 1953. "Die Erniedrigung der Einfriertemperatur organischer Gläser durch Lösungsmittel." *Kolloid-Zeitschrift* no. 130 (2):89-105. doi: 10.1007/BF01519799.

Karode, Sandeep K., and Ashwani Kumar. 2001. "Flow visualization through spacer filled channels by computational fluid dynamics I.: Pressure drop and shear rate calculations for flat sheet geometry." *Journal of Membrane Science* no. 193 (1):69-84. doi: http://dx.doi.org/10.1016/S0376-7388(01)00494-X.

Kartal, Serkan, Mehmet Seckin Aday, and Cengiz Caner. 2012. "Use of microperforated films and oxygen scavengers to maintain storage stability of fresh strawberries." *Postharvest Biology and Technology* no. 71:32-40. doi: http://dx.doi.org/10.1016/j.postharvbio.2012.04.009.

Kirkland, B. S., R. Clarke, and D. R. Paul. 2008. "A versatile membrane system for bulk storage and shipping of produce in a modified atmosphere." *Journal of Membrane Science* no. 324 (1–2):119-127. doi: http://dx.doi.org/10.1016/j.memsci.2008.07.001.

Kristo, Eleana, and Costas G. Biliaderis. 2006. "Water sorption and thermo-mechanical properties of water/sorbitol-plasticized composite biopolymer films: Caseinate–pullulan bilayers and blends." *Food Hydrocolloids* no. 20 (7):1057-1071. doi: http://doi.org/10.1016/j.foodhyd.2005.11.008.

Kumins, C. A., and J. Roteman. 1961. "Diffusion of gases and vapors through polyvinyl chloride-polyvinyl acetate copolymer films I. Glass transition effect." *Journal of Polymer Science* no. 55 (162):683-698. doi: 10.1002/pol.1961.1205516222.

Kwei, T. K. 1984. "The effect of hydrogen bonding on the glass transition temperatures of polymer mixtures." *Journal of Polymer Science: Polymer Letters Edition* no. 22 (6):307-313. doi: 10.1002/pol.1984.130220603.

Labuza, To P. 1968. "Sorption phenomena in foods." *Food technology* no. 22 (3):15-&.

Lange, J., B. Büsing, J. Hertlein, and S. Hediger. 2000. "Water vapour transport through large defects in flexible packaging: modeling, gravimetric measurement and magnetic resonance imaging."

Packaging Technology and Science no. 13 (4):139-147. doi: 10.1002/1099-1522(200007)13:4<139::AID-PTS507>3.0.CO;2-E.

Langmuir, Irving. 1918. "The adsorption of gases on plane surfaces of glass, mica and platinum." *Journal of the American Chemical Society* no. 40 (9):1361-1403. doi: 10.1021/ja02242a004.

Larotonda, F. D. S., K. N. Matsui, P. J. A. Sobral, and J. B. Laurindo. 2005. "Hygroscopicity and water vapor permeability of Kraft paper impregnated with starch acetate." *Journal of Food Engineering* no. 71 (4):394-402. doi: http://dx.doi.org/10.1016/j.jfoodeng.2004.11.002.

Larsen, Hanne, and Kristian Hovde Liland. 2013. "Determination of O2 and CO2 transmission rate of whole packages and single perforations in micro-perforated packages for fruit and vegetables." *Journal of Food Engineering* no. 119 (2):271-276. doi: http://dx.doi.org/10.1016/j.jfoodeng.2013.05.035.

Laufer, Galina, Christopher Kirkland, Amanda A. Cain, and Jaime C. Grunlan. 2013. "Oxygen barrier of multilayer thin films comprised of polysaccharides and clay." *Carbohydrate Polymers* no. 95 (1):299-302. doi: http://dx.doi.org/10.1016/j.carbpol.2013.02.048.

Lazaridou, Athina, and Costas G. Biliaderis. 2002. "Thermophysical properties of chitosan, chitosan–starch and chitosan–pullulan films near the glass transition." *Carbohydrate Polymers* no. 48 (2):179-190. doi: http://dx.doi.org/10.1016/S0144-8617(01)00261-2.

Lee, Dong Sun, Jun Soo Kang, and Pierre Renault. 2000. "Dynamics of internal atmosphere and humidity in perforated packages of peeled garlic cloves." *International Journal of Food Science & Technology* no. 35 (5):455-464. doi: 10.1046/j.1365-2621.2000.00397.x.

Lee, Dong Sun, and Pierre Renault. 1998. "Using pinholes as tools to attain optimum modified atmospheres in packages of fresh produce." *Packaging Technology and Science* no. 11 (3):119-130. doi: 10.1002/(SICI)1099-1522(199805/06)11:3<119::AID-PTS421>3.0.CO;2-N.

Lee, Sangyoup, Gary Amy, and Jaeweon Cho. 2004. "Applicability of Sherwood correlations for natural organic matter (NOM) transport in nanofiltration (NF) membranes." *Journal of Membrane Science* no. 240 (1–2):49-65. doi: http://dx.doi.org/10.1016/j.memsci.2004.04.011.

Lei, Qiao, Jiazhen Pan, Jianqiang Bao, Zhiying Huang, and Yuting Zhang. 2014. "Analysis and modeling of moisture sorption behavior for antimicrobial composite protein films." *Bio-medical materials and engineering* no. 24 (6):1969-1978.

Leminen, Ville, Petri Mäkelä, Panu Tanninen, and Juha Varis. 2015. *Leakproof Heat Sealing of Paperboard Trays - Effect of Sealing Pressure and Crease Geometry*. Vol. 10, *2015*.

Leonardi, C., A. Baille, and S. Guichard. 2000. "Predicting transpiration of shaded and non-shaded tomato fruits under greenhouse environments." *Scientia Horticulturae* no. 84 (3):297-307. doi: http://dx.doi.org/10.1016/S0304-4238(99)00130-2.

Levine, Harry, and Louise Slade. 1986. "A polymer physico-chemical approach to the study of commercial starch hydrolysis products (SHPs)." *Carbohydrate Polymers* no. 6 (3):213-244. doi: http://dx.doi.org/10.1016/0144-8617(86)90021-4.

Lewicki, Piotr P. 1998. "A three parameter equation for food moisture sorption isotherms." *Journal of Food Process Engineering* no. 21 (2):127-144. doi: 10.1111/j.1745-4530.1998.tb00444.x.

Lewicki, Piotr P. 2000. "Raoult’s law based food water sorption isotherm." *Journal of Food Engineering* no. 43 (1):31-40. doi: http://dx.doi.org/10.1016/S0260-8774(99)00130-2.

Lipnizki, Jens, and Gunnar Jonsson. 2002. "Flow dynamics and concentration polarisation in spacer-filled channels." *Desalination* no. 146 (1):213-217. doi: http://dx.doi.org/10.1016/S0011-9164(02)00474-5.

Liu, Y., A. K. Roy, A. A. Jones, P. T. Inglefield, and P. Ogden. 1990. "An NMR study of plasticization and antiplasticization of a polymeric glass." *Macromolecules* no. 23 (4):968-977. doi: 10.1021/ma00206a013.

Lourdin, D., H. Bizot, and P. Colonna. 1997. "“Antiplasticization” in starch-glycerol films?" *Journal of Applied Polymer Science* no. 63 (8):1047-1053. doi: 10.1002/(SICI)1097-4628(19970222)63:8<1047::AID-APP11>3.0.CO;2-3.

Lucas, Susana, Mª José Cocero, Carsten Zetzl, and Gerd Brunner. 2004. "Adsorption isotherms for ethylacetate and furfural on activated carbon from supercritical carbon dioxide." *Fluid Phase Equilibria* no. 219 (2):171-179. doi: http://dx.doi.org/10.1016/j.fluid.2004.01.034.

Lundberg, J. L. 1972. Molecular clustering and segregation in sorption systems. In *Pure and Applied Chemistry*.

Magalhães, N. F., and C. T. Andrade. 2009. "Thermoplastic corn starch/clay hybrids: Effect of clay type and content on physical properties." *Carbohydrate Polymers* no. 75 (4):712-718. doi: http://dx.doi.org/10.1016/j.carbpol.2008.09.020.

Mahajan, P. V., F. A. R. Oliveira, M. J. Sousa, S. C. Fonseca, and L. M. Cunha. 2005. "An Interactive Design of MA-Packaging for Fresh Produce." In *Handbook of Food Science, Technology, and Engineering - 4 Volume Set*. CRC Press.

Mahajan, P. V., F. A. S. Rodrigues, and E. Leflaive. 2008. "Analysis of water vapour transmission rate of perforation-mediated modified atmosphere packaging (PM-MAP)." *Biosystems Engineering* no. 100 (4):555-561. doi: http://dx.doi.org/10.1016/j.biosystemseng.2008.05.008.

Mali, Suzana, Maria Victória E. Grossmann, Maria A. García, Miriam N. Martino, and Noemi E. Zaritzky. 2004. "Barrier, mechanical and optical properties of plasticized yam starch films." *Carbohydrate Polymers* no. 56 (2):129-135. doi: http://dx.doi.org/10.1016/j.carbpol.2004.01.004.

Mannapperuma, Jatal D, Devon Zagory, R Paul Singh, and AA Kader. 1989. Design of polymeric packages for modified atmosphere storage of fresh produce. Paper read at Proceedings of the 5th international controlled atmosphere research conference.

Marrero, T. R., and E. A. Mason. 1972. "Gaseous Diffusion Coefficients." *Journal of Physical and Chemical Reference Data* no. 1 (1):3-118. doi: doi:http://dx.doi.org/10.1063/1.3253094.

Martelli, Sílvia Maria , Geovana Moore, Sabrina Silva Paes, Cristhiane Gandolfo, and João Borges Laurindo. 2006. "Influence of plasticizers on the water sorption isotherms and water vapor permeability of chicken feather keratin films." *LWT - Food Science and Technology* no. 39 (3):292-301. doi: http://dx.doi.org/10.1016/j.lwt.2004.12.014.

Mascia, L. 1978. "Antiplasticization of poly (vinyl chloride) in relation to thermal ageing and non-linear viscoelastic behaviour." *Polymer* no. 19 (3):325-328. doi: http://dx.doi.org/10.1016/0032-3861(78)90226-4.

Massey, L.K. 2003. *Permeability Properties of Plastics and Elastomers: A Guide to Packaging and Barrier Materials*: Elsevier Science.

Massey, S.M., R. Phillips, V.J. Jodts, and T.A. Lord. 2002. Container with improved lid seal and lid sealing method. Google Patents.

Mastromatteo, Marcella, Annalisa Lucera, Vincenzo Lampignano, and Matteo Alessandro Del Nobile. 2012. "A new approach to predict the mass transport properties of micro-perforated films intended for food packaging applications." *Journal of Food Engineering* no. 113 (1):41-46. doi: http://dx.doi.org/10.1016/j.jfoodeng.2012.05.029.

Mc, Millan Wg, and E. Teller. 1951. "The assumptions of the B.E.T. theory." *J Phys Colloid Chem* no. 55 (1):17-20.

McCabe, W., J. Smith, and P. Harriott. 2005. *Unit Operations of Chemical Engineering*: McGraw-Hill Education.

Meidner, H., and T.A. Mansfield. 1968. *Physiology of stomata*: McGraw-Hill.

Merenga, A. S., and G. A. Katana. 2010. "Dynamic Mechanical Analysis of PMMA-Cellulose Blends." *International Journal of Polymeric Materials and Polymeric Biomaterials* no. 60 (2):115-123. doi: 10.1080/00914030903538553.

Metz, S. J. 2003. *Water vapor and gas transport through polymeric membranes*, Enschede.

Metz, S. J., W. J. C. van de Ven, J. Potreck, M. H. V. Mulder, and M. Wessling. 2005. "Transport of water vapor and inert gas mixtures through highly selective and highly permeable polymer membranes." *Journal of Membrane Science* no. 251 (1):29-41. doi: http://dx.doi.org/10.1016/j.memsci.2004.08.036.

Mir, Nazir , and Randolph M. Beaudry. 2016. "Modified Atmosphere Packaging." In *The commercial storage of fruits, vegetables, and florist and nursery stocks*, edited by Kenneth C. Gross, Chieng Yi Wang and Mikal Salveit, 42-53. U.S. Dept. of Agriculture; [for sale by the Supt. of Docs., U.S. Govt. Print. Off.

Miragliotta, Giovanni. 2011. "The power of dimensional analysis in production systems design." *International Journal of Production Economics* no. 131 (1):175-182. doi: http://dx.doi.org/10.1016/j.ijpe.2010.08.009.

Mistriotis, Antonis, Demetrios Briassoulis, Anastasios Giannoulis, and Salvatore D'Aquino. 2016. "Design of biodegradable bio-based equilibrium modified atmosphere packaging (EMAP) for fresh fruits and vegetables by using micro-perforated poly-lactic acid (PLA) films." *Postharvest Biology and Technology* no. 111:380-389. doi: http://dx.doi.org/10.1016/j.postharvbio.2015.09.022.

Montanez, Julio C., Fernanda A. S. Rodríguez, Pramod V. Mahajan, and Jesús M. Frías. 2010a. "Modelling the effect of gas composition on the gas exchange rate in Perforation-Mediated Modified Atmosphere Packaging." *Journal of Food Engineering* no. 96 (3):348-355. doi: http://dx.doi.org/10.1016/j.jfoodeng.2009.08.007.

Montanez, Julio C., Fernanda A. S. Rodríguez, Pramod V. Mahajan, and Jesús M. Frías. 2010b. "Modelling the gas exchange rate in perforation-mediated modified atmosphere packaging: Effect of the external air movement and tube dimensions." *Journal of Food Engineering* no. 97 (1):79-86. doi: http://dx.doi.org/10.1016/j.jfoodeng.2009.09.018.

Montgomery, D.C. 2013. *Design and Analysis of Experiments, 8th Edition*: John Wiley & Sons, Incorporated.

Montgomery, D.C., G.C. Runger, and N.F. Hubele. 2010. *Engineering Statistics, 5th Edition*: John Wiley & Sons, Incorporated.

Moreno, Olga, Lorena Atarés, and Amparo Chiralt. 2015. "Effect of the incorporation of antimicrobial/antioxidant proteins on the properties of potato starch films." *Carbohydrate Polymers* no. 133:353-364. doi: http://dx.doi.org/10.1016/j.carbpol.2015.07.047.

Moyls, A. L., D. L. McKenzie, R. P. Hocking, P. M. A. Toivonen, P. Delaquis, B. Girard, and G. Mazza. 1998. "Variability in O_2, CO_2, and H_2O Transmission Rates Among Commercial Polyethylene Films for Modified Atmosphere Packaging." no. 41 (5). doi: 10.13031/2013.17279.

Muraille, L., M. Pernes, A. Habrant, R. Serimaa, M. Molinari, V. Aguié-Béghin, and B. Chabbert. 2015. "Impact of lignin on water sorption properties of bioinspired self-assemblies of lignocellulosic polymers." *European Polymer Journal* no. 64:21-35. doi: http://dx.doi.org/10.1016/j.eurpolymj.2014.11.040.

Myers, R.H., D.C. Montgomery, and C.M. Anderson-Cook. 2016. *Response Surface Methodology: Process and Product Optimization Using Designed Experiments*: Wiley.

Nascimento, T. A., V. Calado, and C. W. P. Carvalho. 2012. "Development and characterization of flexible film based on starch and passion fruit mesocarp flour with nanoparticles." *Food Research International* no. 49 (1):588-595. doi: http://dx.doi.org/10.1016/j.foodres.2012.07.051.

Nelson, D.L., and M.M. Cox. 2013. *Lehninger Principles of Biochemistry*: W.H. Freeman.

Nobel, P.S. 1974. *Introduction to Biophysical Plant Physiology*: W. H. Freeman.

Nottale, L. 2005. "On the transition from the classical to the quantum regime in fractal space–time theory." *Chaos, Solitons & Fractals* no. 25 (4):797-803. doi: http://dx.doi.org/10.1016/j.chaos.2004.11.071.

Oliveira, Fernanda A. R. , and Jorge C. Oliveira. 2010. "Sherwood Number." In *Encyclopedia of Agricultural, Food, and Biological Engineering, Second Edition*, 1545-1550. Taylor & Francis.

Oliveira, N. S., C. M. Gonçalves, J. A. P. Coutinho, A. Ferreira, J. Dorgan, and I. M. Marrucho. 2006. "Carbon dioxide, ethylene and water vapor sorption in poly(lactic acid)." *Fluid Phase Equilibria* no. 250 (1):116-124. doi: http://dx.doi.org/10.1016/j.fluid.2006.10.009.

Oswin, C. R. 1946. "The kinetics of package life. III. The isotherm." *Journal of the Society of Chemical Industry* no. 65 (12):419-421. doi: 10.1002/jctb.5000651216.

Pantastico, E.B. 1975. *Postharvest physiology, handling, and utilization of tropical and subtropical fruits and vegetables*: Avi Pub. Co.

Park, Geoffrey S. 1986. "Transport Principles—Solution, Diffusion and Permeation in Polymer Membranes." In *Synthetic Membranes: Science, Engineering and Applications*, edited by P. M. Bungay, H. K. Lonsdale and M. N. de Pinho, 57-107. Dordrecht: Springer Netherlands.

Park, Noeon, Sangyoup Lee, Seung-Hyun Lee, Sang Don Kim, and Jaeweon Cho. 2009. "Mass transfer of bacterial by-products (BBP) during nanofiltration: characterizations, transport, and sherwood relationships." *Desalination* no. 247 (1–3):623-635. doi: http://dx.doi.org/10.1016/j.desal.2008.07.022.

Paul, D. R., and R. Clarke. 2002. "Modeling of modified atmosphere packaging based on designs with a membrane and perforations." *Journal of Membrane Science* no. 208 (1–2):269-283. doi: http://dx.doi.org/10.1016/S0376-7388(02)00303-4.

Paz, H. Mujica, V. Guillard, M. Reynes, and N. Gontard. 2005. "Ethylene permeability of wheat gluten film as a function of temperature and relative humidity." *Journal of Membrane Science* no. 256 (1–2):108-115. doi: http://dx.doi.org/10.1016/j.memsci.2005.02.011.

Peleg, M. 1992. "On the use of the WLF model in polymers and foods." *Crit Rev Food Sci Nutr* no. 32 (1):59-66. doi: 10.1080/10408399209527580.

Peleg, Micha. 1993. "ASSESSMENT of A SEMI-EMPIRICAL FOUR PARAMETER GENERAL MODEL FOR SIGMOID MOISTURE SORPTION ISOTHERMS1." *Journal of Food Process Engineering* no. 16 (1):21-37. doi: 10.1111/j.1745-4530.1993.tb00160.x.

Pfaffmann, G.D. 1992. Induction heating and package sealing system and method. Google Patents.

Phuong, Vu Thanh, and Andrea Lazzeri. 2012. "“Green” biocomposites based on cellulose diacetate and regenerated cellulose microfibers: Effect of plasticizer content on morphology and mechanical properties." *Composites Part A: Applied Science and Manufacturing* no. 43 (12):2256-2268. doi: https://doi.org/10.1016/j.compositesa.2012.08.008.

Piringer, Otto. 2000. "Permeation of gases, water vapor and volatile organic compounds." In *Plastic Packaging Materials for Food*, 239-285. Wiley-VCH Verlag GmbH.

Pittia, Paola, and Giampiero Sacchetti. 2008. "Antiplasticization effect of water in amorphous foods. A review." *Food Chemistry* no. 106 (4):1417-1427. doi: http://dx.doi.org/10.1016/j.foodchem.2007.03.077.

Räderer, Marc, Alain Besson, and Karl Sommer. 2002. "A thin film dryer approach for the determination of water diffusion coefficients in viscous products." *Chemical Engineering Journal* no. 86 (1–2):185-191. doi: http://doi.org/10.1016/S1385-8947(01)00288-1.

Raisi, Ahmadreza, Abdolreza Aroujalian, and Tahereh Kaghazchi. 2008. "Multicomponent pervaporation process for volatile aroma compounds recovery from pomegranate juice." *Journal of Membrane Science* no. 322 (2):339-348. doi: http://dx.doi.org/10.1016/j.memsci.2008.06.001.

Ramin, AA, and D Khoshbakhat. 2008. "Effects of microperforated polyethylene bags and temperatures on the storage quality of acid lime fruits." *American–Eurasian Journal of Agriculture and Environmental Science* no. 3:590-594.

Ramos, A. V., C. W. P Carvalho, and V. M. A. Calado. 2014. Permeabilidade ao vapor de água de filmes de farinha de mandioca e de farinha de taro incorporados de zeólita modificada. *WORKSHOP DA REDE DE NANOTECNOLOGIA APLICADA AO AGRONEGÓCIO*, September, 2014, 208-211.

Rao, C.G. 2015. *Engineering for Storage of Fruits and Vegetables: Cold Storage, Controlled Atmosphere Storage, Modified Atmosphere Storage*: Elsevier Science.

Rao, V., P. V. Ashokan, and M. H. Shridhar. 1999. "Studies on the compatibility and specific interaction in cellulose acetate hydrogen phthalate (CAP) and poly methyl methacrylate (PMMA) blend." *Polymer* no. 40 (25):7167-7171. doi: https://doi.org/10.1016/S0032-3861(99)00311-0.

Reddy, G. Maheedhara, and V. Diwakar Reddy. 2014. "Theoretical Investigations on Dimensional Analysis of Ball Bearing Parameters by Using Buckingham Pi-Theorem." *Procedia Engineering* no. 97 (0):1305-1311. doi: http://dx.doi.org/10.1016/j.proeng.2014.12.410.

Reinas, Isabel, Jorge Oliveira, Joel Pereira, Pramod Mahajan, and Fátima Poças. 2016. "A quantitative approach to assess the contribution of seals to the permeability of water vapour and oxygen in thermosealed packages." *Food Packaging and Shelf Life* no. 7:34-40. doi: http://dx.doi.org/10.1016/j.fpsl.2016.01.003.

Rekab, Kamel, and Shaikh Muzaffar. 2005. "Taguchi's Approach to the Design of Experiments." In *Statistical Design of Experiments with Engineering Applications*, 97-120. CRC Press.

Renault, Pierre, Lydie Houal, G. U. Y. Jacquemin, and Yves Chambroy. 1994. "Gas exchange in modified atmosphere packaging. 2: Experimental results with strawberries." *International Journal of Food Science & Technology* no. 29 (4):379-394. doi: 10.1111/j.1365-2621.1994.tb02080.x.

Renault, Pierre, Michel Souty, and Yves Chambroy. 1994. "Gas exchange in modified atmosphere packaging. 1: A new theoretical approach for micro-perforated packs." *International Journal of Food Science & Technology* no. 29 (4):365-378. doi: 10.1111/j.1365-2621.1994.tb02079.x.

Rennie, T. J., and S. Tavoularis. 2009. "Perforation-mediated modified atmosphere packaging: Part I. Development of a mathematical model." *Postharvest Biology and Technology* no. 51 (1):1-9. doi: http://dx.doi.org/10.1016/j.postharvbio.2008.06.007.

Robeson, L. M. 1969. "The effect of antiplasticization on secondary loss transitions and permeability of polymers." *Polymer Engineering & Science* no. 9 (4):277-281. doi: 10.1002/pen.760090407.

Rodov, Victor, Shimshon Ben-Yehoshua, Nehemia Aharoni, and Shabtai Cohen. 2010. "Modified Humidity Packaging of Fresh Produce." In *Horticultural Reviews, Volume 37*, 281-329. John Wiley & Sons, Inc.

Rodriguez-Aguilera, Rocio, Jorge C. Oliveira, Julio C. Montanez, and Pramod V. Mahajan. 2009. "Mathematical modelling of the effect of gas composition and storage temperature on the gas exchange rate of soft cheese." *Journal of Food Engineering* no. 95 (1):82-89. doi: http://dx.doi.org/10.1016/j.jfoodeng.2009.04.010.

Rodriguez-Aguilera, Rocio, and JorgeC Oliveira. 2009. "Review of Design Engineering Methods and Applications of Active and Modified Atmosphere Packaging Systems." *Food Engineering Reviews* no. 1 (1):66-83. doi: 10.1007/s12393-009-9001-9.

Rojas-Graü, Maria A., Roberto J. Avena-Bustillos, Carl Olsen, Mendel Friedman, Philip R. Henika, Olga Martín-Belloso, Zhongli Pan, and Tara H. McHugh. 2007. "Effects of plant essential oils and oil compounds on mechanical, barrier and antimicrobial properties of alginate–apple puree edible films." *Journal of Food Engineering* no. 81 (3):634-641. doi: http://dx.doi.org/10.1016/j.jfoodeng.2007.01.007.

Roos, Yrjo H. 2000. "Water Activity and Plasticization." In *Food Shelf Life Stability*. CRC Press.

Roos, YrjÖ, and Marcus Karel. 1991. "Plasticizing Effect of Water on Thermal Behavior and Crystallization of Amorphous Food Models." *Journal of Food Science* no. 56 (1):38-43. doi: 10.1111/j.1365-2621.1991.tb07970.x.

Rosa, Gabriela S., Mariana A. Moraes, and Luiz A. A. Pinto. 2010. "Moisture sorption properties of chitosan." *LWT - Food Science and Technology* no. 43 (3):415-420. doi: http://dx.doi.org/10.1016/j.lwt.2009.09.003.

Rouquerol, J., F. Rouquerol, P. Llewellyn, G. Maurin, and K.S.W. Sing. 2013. *Adsorption by Powders and Porous Solids: Principles, Methodology and Applications*: Elsevier Science.

Roy, Soumya, Aristippos Gennadios, Curtis L. Weller, and Robert F. Testin. 2000. "Water vapor transport parameters of a cast wheat gluten film." *Industrial Crops and Products* no. 11 (1):43-50. doi: https://doi.org/10.1016/S0926-6690(99)00032-1.

Rubino, Maria, Marvin A. Tung, Sylvia Yada, and Ian J. Britt. 2001. "Permeation of Oxygen, Water Vapor, and Limonene through Printed and Unprinted Biaxially Oriented Polypropylene Films." *Journal of Agricultural and Food Chemistry* no. 49 (6):3041-3045. doi: 10.1021/jf001427s.

Ruzicka, M. C. 2008. "On dimensionless numbers." *Chemical Engineering Research and Design* no. 86 (8):835-868. doi: http://dx.doi.org/10.1016/j.cherd.2008.03.007.

Saberi, Bahareh, Quan Vuong, Suwimol Chockchaisawasdee, John Golding, Christopher Scarlett, and Costas Stathopoulos. 2016. "Water Sorption Isotherm of Pea Starch Edible Films and Prediction Models." *Foods* no. 5 (1):1.

Sanchez-Garcia, Maria D., and Jose M. Lagaron. 2010. "On the use of plant cellulose nanowhiskers to enhance the barrier properties of polylactic acid." *Cellulose* no. 17 (5):987-1004. doi: 10.1007/s10570-010-9430-x.

Sandhya. 2010. "Modified atmosphere packaging of fresh produce: Current status and future needs." *LWT - Food Science and Technology* no. 43 (3):381-392. doi: https://doi.org/10.1016/j.lwt.2009.05.018.

Schnell, Matthias, and Bernhard Anton Wolf. 2001. "Excess viscosity and glass transition." *Polymer* no. 42 (21):8599-8605. doi: http://doi.org/10.1016/S0032-3861(01)00372-X.

Schulze, E.-D., and A. E. Hall. 1982. "Stomatal Responses, Water Loss and CO2 Assimilation Rates of Plants in Contrasting Environments." In *Physiological Plant Ecology II: Water Relations and Carbon Assimilation*, edited by O. L. Lange, P. S. Nobel, C. B. Osmond and H. Ziegler, 181-230. Berlin, Heidelberg: Springer Berlin Heidelberg.

Silva, Filipa M., Khe V. Chau, Jeffrey K. Brecht, and Steven A. Sargent. 1999. "Modified atmosphere packaging for mixed loads of horticultural commodities exposed to two postharvest temperatures." *Postharvest Biology and Technology* no. 17 (1):1-9. doi: http://dx.doi.org/10.1016/S0925-5214(99)00026-5.

Silva, J. S., F. L. Finger, and P. C. Corrêa. 2000. "Armazenamento de frutas e hortaliças." In *Secagem e armazenagem de produtos agrícolas*, edited by J. S. Silva, 469-502. Viçosa- MG: Aprenda Fácil.

Sing, K. S. W., D. H. Everett, R. A. W. Haul, L. Moscou, R. A. Pierotti, J. Rouquerol, and T. Siemieniewska. 1985. Reporting Physisorption Data for Gas/Solid Systems With Special Reference to the Determination of Surface Area and Porosity.

Siparsky, Georgette L., Kent J. Voorhees, John R. Dorgan, and Kevin Schilling. 1997. "Water transport in polylactic acid (PLA), PLA/polycaprolactone copolymers, and PLA/polyethylene glycol blends." *Journal of environmental polymer degradation* no. 5 (3):125-136. doi: 10.1007/bf02763656.

Sivertsik, M., J. T. Rosnes, and H. Bergslien. 2002. "4 - Modified atmosphere packaging." In *Minimal Processing Technologies in the Food Industries*, 61-86. Woodhead Publishing.

Sothornvit, Rungsinee, and Natcharee Pitak. 2007. "Oxygen permeability and mechanical properties of banana films." *Food Research International* no. 40 (3):365-370. doi: http://dx.doi.org/10.1016/j.foodres.2006.10.010.

Sousa-Gallagher, Maria J., and Pramod V. Mahajan. 2013. "Integrative mathematical modelling for MAP design of fresh-produce: Theoretical analysis and experimental validation." *Food Control* no. 29 (2):444-450. doi: http://dx.doi.org/10.1016/j.foodcont.2012.05.072.

Sousa, A. R., J. C. Oliveira, and M. J. Sousa-Gallagher. 2017. "Determination of the respiration rate parameters of cherry tomatoes and their joint confidence regions using closed systems." *Journal of Food Engineering*. doi: http://dx.doi.org/10.1016/j.jfoodeng.2017.02.026.

Souza, A. C., R. Benze, E. S. Ferrão, C. Ditchfield, A. C. V. Coelho, and C. C. Tadini. 2012. "Cassava starch biodegradable films: Influence of glycerol and clay nanoparticles content on tensile and barrier properties and glass transition temperature." *LWT - Food Science and Technology* no. 46 (1):110-117. doi: http://dx.doi.org/10.1016/j.lwt.2011.10.018.

Spencer, Kevin C. 2005. "12 - Modified atmosphere packaging of ready-to-eat foods." In *Innovations in Food Packaging*, edited by Jung H. Han, 185-203. London: Academic Press.

Stokes, R. H., and R. A. Robinson. 1949. "Standard Solutions for Humidity Control at 25° C." *Industrial & Engineering Chemistry* no. 41 (9):2013-2013. doi: 10.1021/ie50477a041.

Sullof, E.C. . 2002. *Sorption Behavior Of An Aliphatic Series Of Aldehydes In The Presence Of Poly(Ethylene Terephthalate) Blends Containing Aldehyde Scavenging Agents* Virginia Polytechnic Institute and State University.

Sun, Bin, Wei Hong, Hany Aziz, Nasser Mohieddin Abukhdeir, and Yuning Li. 2013. "Dramatically enhanced molecular ordering and charge transport of a DPP-based polymer assisted by oligomers through antiplasticization." *Journal of Materials Chemistry C* no. 1 (29):4423-4426. doi: 10.1039/C3TC30667D.

Sun, Wendell Q. 1997. "Glassy State and Seed Storage Stability: The WLF Kinetics of Seed Viability Loss at T&gt;T g and the Plasticization Effect of Water on Storage Stability." *Annals of Botany* no. 79 (3):291-297. doi: 10.1006/anbo.1996.0346.

Suppakul, Panuwat, Buppa Chalernsook, Bhatama Ratisuthawat, Sakpipat Prapasitthi, and Natsaran Munchukangwan. 2013. "Empirical modeling of moisture sorption characteristics and mechanical and barrier properties of cassava flour film and their relation to plasticizing–antiplasticizing effects." *LWT - Food Science and Technology* no. 50 (1):290-297. doi: http://dx.doi.org/10.1016/j.lwt.2012.05.013.

Suriyatem, R., C. Rachtanapun, P. Raviyan, P. Intipunya, and P. Rachtanapun. 2015. "Investigation and modeling of moisture sorption behaviour of rice starch/carboxymethyl chitosan blend films." *IOP Conference Series: Materials Science and Engineering* no. 87 (1):012080.

Swain, Sarat K., Satyabrata Dash, Sudhir K. Kisku, and Rajesh K. Singh. 2014. "Thermal and Oxygen Barrier Properties of Chitosan Bionanocomposites by Reinforcement of Calcium Carbonate Nanopowder." *Journal of Materials Science & Technology* no. 30 (8):791-795. doi: http://dx.doi.org/10.1016/j.jmst.2013.12.017.

Tao, Yugui, Jun Pan, Shilei Yan, Bin Tang, and Longbao Zhu. 2007. "Tensile strength optimization and characterization of chitosan/TiO2 hybrid film." *Materials Science and Engineering: B* no. 138 (1):84-89. doi: http://dx.doi.org/10.1016/j.mseb.2006.12.013.

Tapia-Blácido, D. R., P. J. do Amaral Sobral, and F. C. Menegalli. 2013. "Effect of drying conditions and plasticizer type on some physical and mechanical properties of amaranth flour films." *LWT - Food Science and Technology* no. 50 (2):392-400. doi: http://dx.doi.org/10.1016/j.lwt.2012.09.008.

Tapia-Blácido, Delia, Paulo J. Sobral, and Florencia C. Menegalli. 2005. "Development and characterization of biofilms based on Amaranth flour (Amaranthus caudatus)." *Journal of Food Engineering* no. 67 (1–2):215-223. doi: http://dx.doi.org/10.1016/j.jfoodeng.2004.05.054.

Taylor, Ross, and R. Krishna. 1993. *Multicomponent Mass Transfer*. Hoboken, NJ, USA: J. Wiley & Sons.

Techavises, Nutakorn, and Yoshio Hikida. 2008. "Development of a mathematical model for simulating gas and water vapor exchanges in modified atmosphere packaging with macroscopic perforations." *Journal of Food Engineering* no. 85 (1):94-104. doi: http://dx.doi.org/10.1016/j.jfoodeng.2007.07.014.

Teixeira, Viviane Gomes, Fernanda M. B. Coutinho, and Ailton S. Gomes. 2001. "Principais métodos de caracterização da porosidade de resinas à base de divinilbenzeno." *Química Nova* no. 24:808-818.

Thommes, Matthias, Katsumi Kaneko, V. Neimark Alexander, P. Olivier James, Francisco Rodriguez-Reinoso, Jean Rouquerol, and S. W. Sing Kenneth. 2015. Physisorption of gases, with special reference to the evaluation of surface area and pore size distribution (IUPAC Technical Report). In *Pure and Applied Chemistry*.

Thomson-Reuters. 2017. Web of Science Core Collection. In *Web of Science*. Web of Science: Thomson-Reuters.

Tihminlioglu, Funda, İsa Doğan Atik, and Banu Özen. 2010. "Water vapor and oxygen-barrier performance of corn–zein coated polypropylene films." *Journal of Food Engineering* no. 96 (3):342-347. doi: http://dx.doi.org/10.1016/j.jfoodeng.2009.08.018.

Timmermann, E. O., J. Chirife, and H. A. Iglesias. 2001. "Water sorption isotherms of foods and foodstuffs: BET or GAB parameters?" *Journal of Food Engineering* no. 48 (1):19-31. doi: http://dx.doi.org/10.1016/S0260-8774(00)00139-4.

Timmermann, Ernesto O., and Jorge Chirife. 1991. "The physical state of water sorbed at high activities in starch in terms of the GAB sorption equation." *Journal of Food Engineering* no. 13 (3):171-179. doi: http://dx.doi.org/10.1016/0260-8774(91)90025-N.

Tongnuanchan, Phakawat, Soottawat Benjakul, Thummanoon Prodpran, Supachai Pisuchpen, and Kazufumi Osako. 2016. "Mechanical, thermal and heat sealing properties of fish skin gelatin film containing palm oil and basil essential oil with different surfactants." *Food Hydrocolloids* no. 56:93-107. doi: https://doi.org/10.1016/j.foodhyd.2015.12.005.

Tumwesigye, K. S., J. C. Oliveira, and M. J. Sousa-Gallagher. 2017. "Quantitative and mechanistic analysis of impact of novel cassava-assisted improved processing on fluid transport phenomenon in humidity-temperature-stressed bio-derived films." *European Polymer Journal*. doi: http://doi.org/10.1016/j.eurpolymj.2017.04.027.

Tumwesigye, K. S., A. R. Sousa, J. C. Oliveira, and M. J. Sousa-Gallagher. 2017. "Evaluation of novel bitter cassava film for equilibrium modified atmosphere packaging of cherry tomatoes." *Food Packaging and Shelf Life* no. 13:1-14. doi: https://doi.org/10.1016/j.fpsl.2017.04.007.

Tumwesigye, S. K., J. C. Montañez, J. C. Oliveira, and M. J. Sousa-Gallagher. 2016. "Novel Intact Bitter Cassava: Sustainable Development and Desirability Optimisation of Packaging Films." *Food and Bioprocess Technology*:1-12. doi: 10.1007/s11947-015-1665-y.

Ullsten, N. H., and M. S. Hedenqvist. 2003. "A new test method based on head space analysis to determine permeability to oxygen and carbon dioxide of flexible packaging." *Polymer Testing* no. 22 (3):291-295. doi: http://dx.doi.org/10.1016/S0142-9418(02)00101-0.

van den Berg, C. 1981. *Vapour sorption equilibria and other water-starch interactions : a physico-chemical approach*, Van den Berg, Wageningen.

van den Berg, C. 1985. "Development of B.E.T.-Like Models for Sorption of Water on Foods, Theory and Relevance." In *Properties of Water in Foods: in Relation to Quality and Stability*, edited by D. Simatos and J. L. Multon, 119-131. Dordrecht: Springer Netherlands.

van den Berg, C., and S. Bruin. 1981. "Water Activity And Its Estimation In Food Systems: Theoretical Aspects " In *Water Activity: Influences* *on Food Quality*, edited by George F. Stewart, 1-61. Academic Press.

Van Krevelen, D. W., and K. Te Nijenhuis. 2009. "Chapter 18 - Properties Determining Mass Transfer In Polymeric Systems." In *Properties of Polymers (Fourth Edition)*, 655-702. Amsterdam: Elsevier.

Vaschy, Aimé. 1892. Sur les lois de similitude en physique. Paper read at Annales télégraphiques.

Villalobos, Ricardo, Pilar Hernández-Muñoz, and Amparo Chiralt. 2006. "Effect of surfactants on water sorption and barrier properties of hydroxypropyl methylcellulose films." *Food Hydrocolloids* no. 20 (4):502-509. doi: http://dx.doi.org/10.1016/j.foodhyd.2005.04.006.

Viollaz, Pascual E., and Clara O. Rovedo. 1999. "Equilibrium sorption isotherms and thermodynamic properties of starch and gluten." *Journal of Food Engineering* no. 40 (4):287-292. doi: http://dx.doi.org/10.1016/S0260-8774(99)00066-7.

Voller, V. R. 2001. "Numerical treatment of rapidly changing and discontinuous conductivities." *International Journal of Heat and Mass Transfer* no. 44 (23):4553-4556. doi: https://doi.org/10.1016/S0017-9310(01)00089-8.

Wahid, A., S. Gelani, M. Ashraf, and M. R. Foolad. 2007. "Heat tolerance in plants: An overview." *Environmental and Experimental Botany* no. 61 (3):199-223. doi: http://dx.doi.org/10.1016/j.envexpbot.2007.05.011.

Weng, Wu Yin, Kazufumi Osako, and Munehiko Tanaka. 2009. "Oxygen permeability and antioxidative properties of edible surimi films." *Fisheries Science* no. 75 (1):233-240. doi: 10.1007/s12562-008-0024-6.

Wheeler, Matthew J., Silvia Russi, Michael G. Bowler, and Matthew W. Bowler. 2012. "Measurement of the equilibrium relative humidity for common precipitant concentrations: facilitating controlled dehydration experiments." *Acta Crystallographica Section F: Structural Biology and Crystallization Communications* no. 68 (Pt 1):111-114. doi: 10.1107/S1744309111054029.

Whitaker, Stephen. 2009. "Derivation and application of the Stefan-Maxwell equations." *Revista mexicana de ingeniería química* no. 8:213-243.

Wilke, C. R. 1950. "Diffusional properties of multicomponent gases." *Chemical Engineering Progress* no. 46:95-104.

Williams, Malcolm L., Robert F. Landel, and John D. Ferry. 1955. "The Temperature Dependence of Relaxation Mechanisms in Amorphous Polymers and Other Glass-forming Liquids." *Journal of the American Chemical Society* no. 77 (14):3701-3707. doi: 10.1021/ja01619a008.

Winston, Paul W., and Donald H. Bates. 1960. "Saturated Solutions For the Control of Humidity in Biological Research." *Ecology* no. 41 (1):232-237. doi: 10.2307/1931961.

Wolf, Caroline, Valérie Guillard, Hélène Angellier-Coussy, Gabriella Ghizzi D. Silva, and Nathalie Gontard. 2016. "Water vapor sorption and diffusion in wheat straw particles and their impact on the mass transfer properties of biocomposites." *Journal of Applied Polymer Science* no. 133 (16):n/a-n/a. doi: 10.1002/app.43329.

Wood, Lawrence A. 1958. "Glass transition temperatures of copolymers." *Journal of Polymer Science* no. 28 (117):319-330. doi: 10.1002/pol.1958.1202811707.

Xanthopoulos, G., E. D. Koronaki, and A. G. Boudouvis. 2012. "Mass transport analysis in perforation-mediated modified atmosphere packaging of strawberries." *Journal of Food Engineering* no. 111 (2):326-335. doi: http://dx.doi.org/10.1016/j.jfoodeng.2012.02.016.

Yam, K.L. 2010. *The Wiley Encyclopedia of Packaging Technology*: Wiley.

Yarin, L.P. 2012. *The Pi-Theorem: Applications to Fluid Mechanics and Heat and Mass Transfer*: Springer Berlin Heidelberg.

Zeller, B. L., F. Z. Saleeb, and R. D. Ludescher. 1998. "Trends in development of porous carbohydrate food ingredients for use in flavor encapsulation." *Trends in Food Science & Technology* no. 9 (11):389-394. doi: http://dx.doi.org/10.1016/S0924-2244(99)00007-2.

Żenkiewicz, Marian, and Józef Richert. 2008. "Permeability of polylactide nanocomposite films for water vapour, oxygen and carbon dioxide." *Polymer Testing* no. 27 (7):835-840. doi: http://dx.doi.org/10.1016/j.polymertesting.2008.06.005.

Zimm, Bruno H., and John L. Lundberg. 1956. "Sorption of Vapors by High Polymers." *The Journal of Physical Chemistry* no. 60 (4):425-428. doi: 10.1021/j150538a010.